PhD Program in Neurosciences
Institute of Neurosciences of Alicante
Miguel Hernandez University of Elche

GluN3A-NMDA receptors regulate protein synthesis by controlling the assembly of GIT1-mTORC1 complexes

Doctoral Thesis

María José Conde Dusman

Thesis Director: Isabel Pérez Otaño

2021

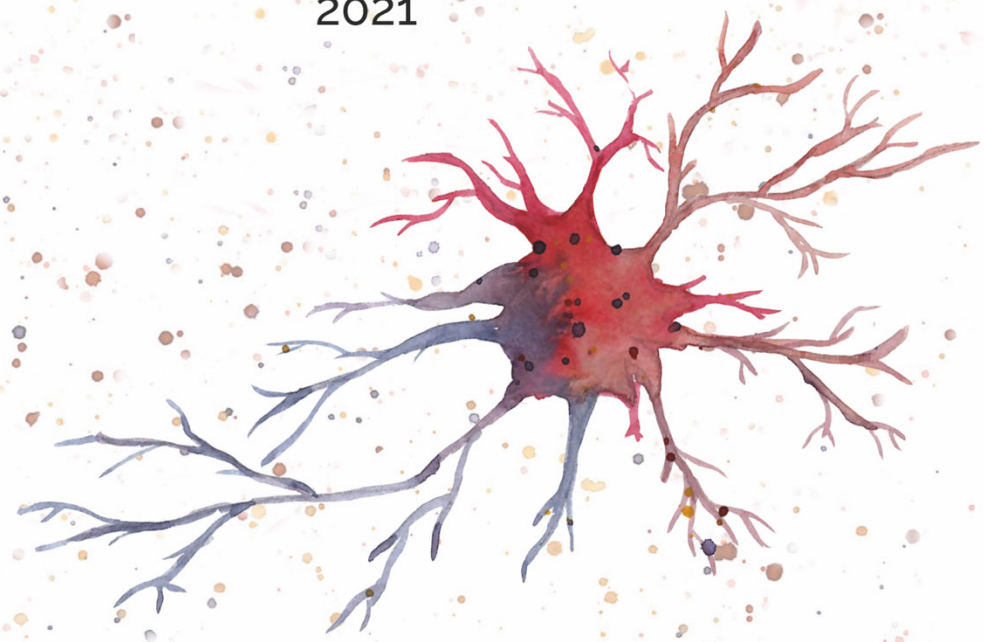

GluN3A-NMDA receptors regulate protein synthesis by controlling the assembly of GIT1-mTORC1 complexes

Doctoral Thesis presented by

María José Conde Dusman

Thesis Director:

Prof. Isabel Pérez Otaño, Full Professor, CSIC

PhD Program in Neurosciences

Institute of Neurosciences

Miguel Hernandez University of Elche

-2021-

This Doctoral Thesis, entitled "*GluN3A-NMDA receptors regulate protein synthesis by controlling the assembly of GIT1-mTORC1 complexes*", is presented under the conventional thesis form with the following quality indicators:

Crawley, O.*, Conde-Dusman, M. J.*, & Pérez-Otaño, I. (2021). GluN3A NMDA receptor subunits: more enigmatic than ever?. The Journal of Physiology, 10.1113/JP280879. Advance online publication. https://doi.org/10.1113/JP280879.

The results presented in this Doctoral Thesis, entitled "*GluN3A-NMDA receptors regulate protein synthesis by controlling the assembly of GIT1-mTORC1 complexes*", are part of the following work:

Conde-Dusman, M. J., Dey, P. N., Elía-Zudaire, Ó., G. Rabaneda, L., García-Lira, C., Grand, T., Briz, V., Velasco, E. R., Andero Galí, R., Niñerola, S., Barco, A., Paoletti, P., Wesseling, J. F., Gardoni, F., Tavalin, S. J., & Perez-Otaño, I. (2021). Control of protein synthesis and memory by GluN3A-NMDA receptors through inhibition of GIT1/mTORC1 assembly. *eLife 2021;10:e71575. https://doi.org/10.7554/eLife.71575* (Accepted for publication on October 13th 2021)

San Juan de Alicante, November 8th 2021

Dr. Ms. Isabel Pérez Otaño, Director of the doctoral thesis entitled "*GluN3A-NMDA receptors regulate protein synthesis by controlling the assembly of GIT1-mTORC1 complexes*",

CERTIFIES:

That Ms. María José Conde Dusman has carried out under my supervision the work entitled "*GluN3A-NMDA receptors regulate protein synthesis by controlling the assembly of GIT1-mTORC1 complexes*" in accordance with the terms and conditions defined in her Research Plan and in accordance with the Code of Good Practice of the Miguel Hernandez University of Elche, satisfactorily fulfilling the objectives foreseen for its public defence as a doctoral thesis.

Thesis Director

Dr. Ms. Isabel Pérez Otaño

San Juan de Alicante, November 8th 2021

Dr. Ms. Elvira de la Peña García, Coordinator of the PhD Program in Neurosciences at the Institute of Neurosciences in Alicante, a joint centre of the Miguel Hernandez University of Elche (UMH) and the Spanish National Research Council (CSIC),

INFORMS:

That Ms. María José Conde Dusman has carried out under the supervision of our PhD Program the work entitled "*GluN3A-NMDA receptors regulate protein synthesis by controlling the assembly of GIT1-mTORC1 complexes*" in accordance with the terms and conditions defined in its Research Plan and in accordance with the Code of Good Practice of the Miguel Hernandez University of Elche, fulfilling the objectives satisfactorily for its public defence as a doctoral thesis.

Which I sign for appropriate purposes, at San Juan de Alicante, November 8th 2021.

Coordinator of the PhD Program in Neurosciences

E-mail : elvirap@umh.es
Tel: +34 965 919533
www.in.umh.es
Fax: +34 965 919549
Av Ramón y Cajal s/n
CAMPUS DE SANT JOAN
03550 SANT JOAN D'ALACANT – ESPAÑA

This Doctoral Thesis entitled "*GluN3A-NMDA receptors regulate protein synthesis by controlling the assembly of GIT1-mTORC1 complexes*" has been supported by a predoctoral fellowship from Fundación Tatiana Pérez de Guzmán el Bueno and short-term stays fellowships from the International Brain Research Organization (IBRO) and the Federation of European Biochemical Societies (FEBS), all of them granted to María José Conde Dusman.

…Here is the deepest secret nobody knows

(here is the root of the root and the bud of the bud

and the sky of the sky of a tree called life; which grows

higher than the soul can hope or mind can hide)

and this is the wonder that's keeping the stars apart

i carry your heart (i carry it in my heart)…

E.E. Cummings

VII-IX

Table of Contents

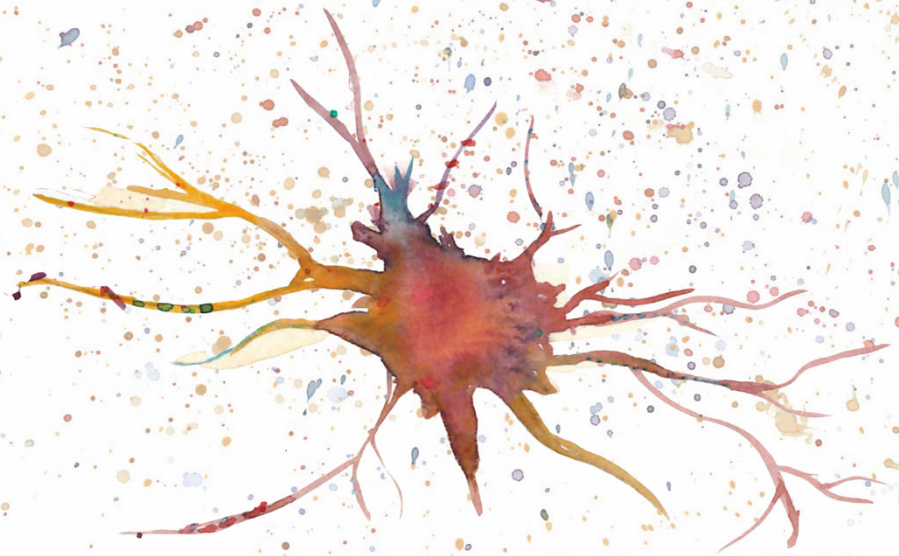

TABLE OF CONTENTS **19**

LIST OF ABBREVIATIONS **25**

LIST OF FIGURES **35**

LIST OF TABLES **41**

SUMMARY/ RESUMEN **45**

INTRODUCTION **51**

1. NMDA RECEPTORS DURING POSTNATAL DEVELOPMENT 53
   1.1. NMDARs' Structure and Function *54*
   1.2. Developmental Subunit Exchanges in NMDAR Subunit Composition *56*
   1.3. GluN3A-containing NMDARs: Gate-Keepers of Synapse Plasticity, Maturation and Cognition *58*
      1.3.1. Molecular biology of GluN3A subunits 58
      1.3.2. Receptor assembly and biophysical properties 60
      1.3.3. GluN3A-CTD interacts with a unique set of intracellular proteins 63
      1.3.4. Role of GluN3A-NMDARs in the refinement of neuronal circuits 67
      1.3.5. Signaling pathways mediating the effects of GluN3A-NMDARs 72
      1.3.6. GluN3A dysregulation is linked to CNS disorders 75
2. THE MTOR PATHWAY 78
   2.1. The mTOR Complexes *79*
   2.2. Upstream Activators of mTOR *80*
   2.3. Downstream Regulation of mTOR *82*
      2.3.1. mTORC1 and protein synthesis 82
      2.3.2. mTORC1 and autophagy 84
      2.3.3. mTORC2 and actin dynamics 84
   2.4. mTOR Regulates Brain Physiology and Function *85*
      2.4.1. mTOR localizes at synapses 86
      2.4.2. mTOR and synaptic plasticity, learning and memory; from activity to local protein synthesis 90
      2.4.3. mTOR signaling and local protein synthesis are regulated by NMDARs 94

2.5. Dysregulated mTOR and Neurodevelopmental and Neuropsychiatric Disorders *99*

OBJECTIVES **101**

MATERIALS AND METHODS **105**

1. ANIMALS 107
   - *1.1. Mouse Lines* *107*
   - *1.2. Brain Region Dissection* *108*
2. CELL CULTURE 108
   - *2.1. Cell Lines* *108*
   - *2.2. Primary Cultured Neurons* *109*
3. LENTIVIRAL PRODUCTION 110
   - *3.1. Recombinant Lentiviral System* *111*
     - 3.1.1. Transducing vector 111
     - 3.1.2. Packaging vector (pCMVΔR8.91) 111
     - 3.1.3. Envelope vector (pVSVg) 111
   - *3.2. Lentiviral Constructs* *112*
   - *3.3. Lentiviral Production* *113*
     - 3.3.1. Transfection of HEK293T/17 – calcium phosphate method 113
     - 3.3.2. Harvest and lentiviral purification 114
   - *3.4. Lentiviral Titration in Neuronal Cultures* *115*
     - 3.4.1. GFP and GluN3A immunoblot 115
     - 3.4.2. GFP immunofluorescence 115
     - 3.4.3. Biotinylation of Surface Proteins 116
4. NEURONAL CULTURE TREATMENTS 117
   - *4.1. BDNF Protocol Optimization* *119*
5. RNA PROFILING 120
   - *5.1. RNA Isolation* *120*
     - 5.1.1. RNA isolation from cell culture 120
     - 5.1.2. RNA isolation from tissue 120
   - *5.2. RNAseq* *121*
   - *5.3. cDNA Synthesis (Reverse-Transcription)* *121*
   - *5.4. qPCR* *122*
6. PROTEIN SAMPLE PREPARATION 123

6.1. Cell Culture Lysates *123*
6.2. Tissue Lysates *124*
6.3. Subcellular Fractionation *124*
7. CO-IMMUNOPRECIPITATION 125
8. WESTERN BLOTTING 126
8.1. SDS-PAGE electrophoresis *126*
8.2. Immunoblotting *127*
8.3. Immunodetection *128*
9. SURFACE SENSING OF TRANSLATION (SUNSET) 130
10. IMMUNOFLUORESCENCE STAINING OF TOTAL PROTEINS 130
11. PROXIMITY LIGATION ASSAY 131
12. ELECTROPHYSIOLOGY 132
13. BEHAVIOR 133
13.1. Conditioned Taste Aversion Test (CTA) *133*
14. STATISTICAL ANALYSIS 133

RESULTS 135

1. MODEL SYSTEM AND OTHER TOOLS 137
1.1. Lentiviral Manipulations of GluN3A Expression in Primary Neuronal Cultures *137*
1.2. Synaptic Stimulation Protocols *139*
2. GLUN3A INHIBITS THE INDUCTION OF PLASTICITY-RELATED PROTEINS AT THE POST-TRANSCRIPTIONAL LEVEL 139
3. POTENTIATED MTOR SIGNALING AND IEG PRODUCTION IN THE ABSENCE OF GLUN3A 144
4. GLUN3A PREVENTS THE DEPHOSPHORYLATION OF EEF2, KEY REGULATOR OF THE ELONGATION STEP OF PROTEIN SYNTHESIS 148
5. GLUN3A CONTROLS THE POSTNATAL EMERGENCE OF MTORC1-DEPENDENT PROTEIN SYNTHESIS 150
5.1. Lack of GluN3A Accelerates the Emergence of mTOR-Dependent Translation *151*
5.2. GluN3A Rescues Increased mTOR-Dependent Translation in Grin3a -/- Cortical Neurons *153*

6. mTOR INHIBITION REQUIRES GLUN3A C-TERMINAL DOMAIN INTERACTIONS154

6.1. GluN3A-CTD is Necessary to Decrease Enhanced Protein Synthesis Rates in Grin3a -/- Cortical Neurons 158

7. GLUN3A-CTD INTERACTIONS CONTROL THE ASSEMBLY OF SYNAPTIC GIT1-MTORC1 COMPLEXES 160

7.1. GIT1-mTORC1 complexes are synaptic and functional 161

7.2. GluN3A regulates the assembly of GIT1-mTORC1 complexes 165

7.3. GluN3A-CTD interactions are required for the modulation of GIT1-mTORC1 complex assembly 166

8. THE SYNAPTIC SCAFFOLDING PROTEIN GIT1 IS NECESSARY FOR MTORC1-DEPENDENT PROTEIN SYNTHESIS 167

9. GLUN3A CONSTRAINTS ON MTOR ACTIVATION FAVORS THE FORMATION OF ASSOCIATIVE MEMORIES 170

DISCUSSION 173

CONCLUSIONS/ CONCLUSIONE 183

REFERENCES 189

APPENDIX I: SCIENTIFIC PUBLICATIONS 219

1. GLUN3A NMDA RECEPTOR SUBUNITS: MORE ENIGMATIC THAN EVER? 221

2. CONTROL OF PROTEIN SYNTHESIS AND MEMORY BY GLUN3A-NMDA RECEPTORS THROUGH INHIBITION OF GIT1/MTORC1 ASSEMBLY 253

ACKNOWLEDGMENTS 305

List of Abbreviations

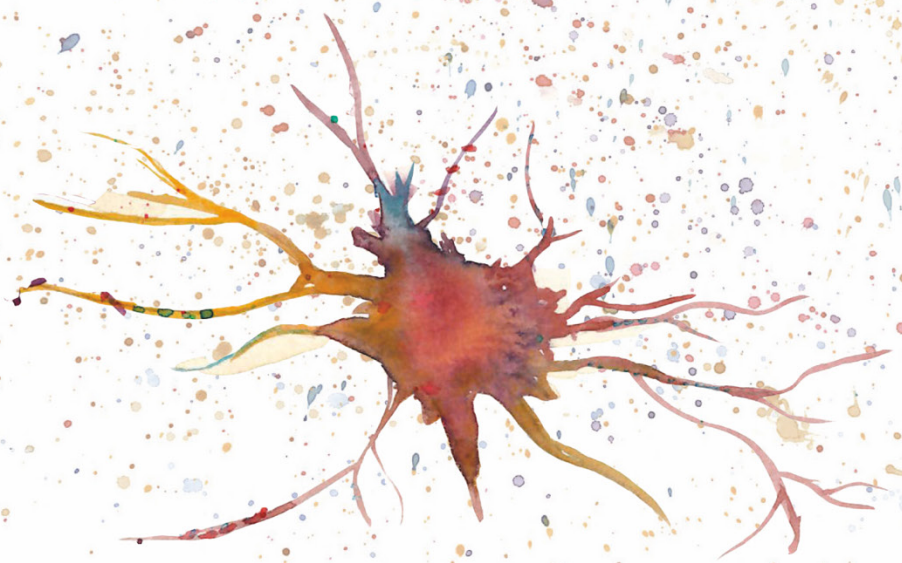

0-9

4E-BP	eIF4E-binding protein

A

Aa	Amino acid
ABD	Agonist Binding Domain
AD	Alzheimer's Disease
ANK	Ankyrin
AP2	Clathrin adaptor protein 2
APS	Ammonium persulfate
APV	D-2-amino-5-phosphonovaleric acid
Arf-GAP	ADP ribosylation factor-GAP domain
ASD	Autism Spectrum Disorder
ATCC	American Type Culture Collection

B

Bp	Base pair
BD	Bipolar Disorder
BDNF	Brain Derived Neurotrophic Factor
BSA	Bovine Serum Albumin

C

CaMKII	Calcium/ Calmodulin-dependent kinase II
CARP1	Cell cycle and apoptosis regulatory protein
CHX	Cycloheximide
CMVp	Cytomegalovirus promoter
CNS	Central Nervous System
Co-IP	Co-Immunoprecipitation
CREB	Cyclic AMP-responsive element-binding protein
CS	Conditioned stimulus
CST	Cell Signaling Technology
Ct	Cycle threshold

CTA	Conditioned Taste Aversion
CTD	C-terminal domain
CUMS	Chronic Unpredictable Mild Stress
CUS	Chronic Unpredictable Stress

D

D-MEM	Dulbecco's Modified Eagle Medium
DEPTOR	DEP-domain-containing mTOR-interacting protein
Disc1	Disrupted-in-schizophrenia-1 gene
DIV	Day(s) *in vitro*
DRG	Dorsal Root Ganglial neuron
dtGluN3A	double-transgenic GFP-GluN3A mouse model
DTT	(D,L) – Dithiothreitol

E

E-LTP	Early long-term potentiation
E. coli	*Escherichia coli*
ECL	Enhanced chemiluminescence western blotting detection reagent
eEF2	Eukaryotic elongation factor 2
eEF2K	Eukaryotic elongation factor 2 kinase
eIF	Eukaryotic initiation factor
ER	Endoplasmic reticulum
ERK1/2	Extracellular signal-regulated kinases 1 and 2

F

FBS	Fetal Bovine Serum
FDR	False Discovery Rate
fEPSP	Field excitatory postsynaptic potential
FKBP12	FK-binding protein 12
FMRP	Fragile X Mental Retardation Protein
FUDR	Anti-mitotic mix compound by uridine and 5-fluoro-2'-deoxyuridine
Fwd	Forward
FXS	Fragile X syndrome

G

GAP	GTPase Activating Protein
GC	Growth Cone
GEF	Guanine Exchange Factor
GFP	Green Fluorescent Protein
GIT1	G protein-coupled receptor kinase-interacting protein
GluN3A-NMDARs	GluN3A-containing NMDARs
Glyc	Glycosylation
GPS2	G-protein Pathway Suppressor 2
Grin3a -/-	GluN3A KO mouse model
GWAS	Genome-Wide Association Studies

H

H	Total homogenate
HBS	HEPES-buffered saline
HEPA	High-efficiency particulate
HD	Huntington's Disease
HEK293T/17	Human Embryonic Kidney cells constitutively expressing the simian virus 40 (SV40) large T antigen
HFS	High frequency stimulation
hSYNp	Human Synapsin 1 promoter

I

IB	Immunoblot
IEG	Immediate-early gen
IGF1	Insulin-like growth factor 1
iGluRs	Ionotropic Glutamate Receptors
IMDM	Iscove's Modified Dulbecco's Medium
I.p.	Intraperitoneal

K

KO	Knockout

L

L-LTP	Late long-term potentiation
LTD	Long-term depression
LOB	Lying On Belly
LTM	Long-term memory
LTP	Long-term potentiation
LTR	Long Terminal Repeat

M

MAP1S	Microtubule-associated protein 1S
MEM	Minimum Essential Media
mGluR	Metabotropic glutamate receptor
MHb	Medial habenula
mLST8	Mammalian lethal with SEC13 protein 8
Mo	Mouse
mPFC	Medial prefrontal cortex
mSIN1	Mammalian stress-activated MAPK-interacting protein 1
mTOR	Mechanistic target of rapamycin
mTORC	mTOR complex

N

NGS	Next-generation sequencing
NMDAR	N-methyl-D-aspartate-type glutamate receptor
NTD	N-terminal domain

O

o/n	Overnight
OFC	Orbitofrontal cortex

P

P2	Crude Membrane Fractions
p38MAPK	Mitogen-activated protein kinase p38

p70S6K	P70S6 kinases (also known as S6K)
PACSIN1	Protein kinase C and casein kinase substrate in neurons protein 1
PBD	Paxillin-binding domain
PBS	Phosphate Buffered Saline
PDK1	3-phosphoinositide-dependent protein kinase 1
PI3K	Phosphatidylinositol 3-kinase
PIP2	Phosphatidylinositol (3,4)-bis-phosphate
PIP3	Phosphatidylinositol (3,4,5)-trisphosphate
PFA	Paraformaldehyde
PFC	Prefrontal cortex
PLA	Proximity Ligation Assay
PNS (1)	Postnuclear Supernatant (also named P1)
PNS (2)	Peripheral Nervous System
PRAS40	Proline rich Akt substrate 40 kDa
Protor1/2	Protein observed with RICTOR 1 or 2
PRP	Plasticity-related protein
PSD	Post-synaptic density
PTEN	Phosphatase and tensin homolog
PVDF	Polyvinylidene difluoride
PP2A	Protein Phosphatase 2A

Q

qPCR	Quantitative Polymerase Chain Reaction

R

Raptor	Regulatory associated protein of mTOR
Rb	Rabbit
RBP	RNA-binding protein
RD	Royal Decree
RGC	Retinal Ganglion Cells
Rheb	Ras homologue enriched in brain
Rictor	Rapamycin-insensitive companion of mTOR
RIN	RNA Integrity Number

RNAseq	RNA sequencing
RT	Room temperature
Rv	Reverse

S

SCB	Santa Cruz Biotechnology
SDS	Sodium Dodecyl Sulfate
SDS-PAGE	Sodium Dodecyl Sulfate (SDS) – Polyacrylamide Gel Electrophoresis (PAGE)
SEM	Standard error of the mean
sh3A-GFP	shGluN3A1185-GFP
SHD	Spa2 homology domain
shRNA	Short hairpin RNA
SLD	Synaptic Localization Domain
SN	Sciatic Nerve
SP	Signal Peptide
SPF	Specific Pathogen-Free
SST	Somatostatin
SUnSET	Surface sensing of translation

T

TBS	Tris Buffer Saline
TBS-T	Tris Buffer Saline 0.05% Tween 20
TEMED	Tetramethylethylenediamine
Tg	Transgenic
THC	Tetrahydrocannabinol
TIF	Triton Insoluble Fractions
TMD	Transmembrane domain
TOP	Terminal oligopyrimidine motif
TOS	TOR signaling motif
TRAX1	Translin associated factor X1
TrkB	Tyrosine kinase receptor B
$tRNA_i^{Met}$	Initiator methionyl transfer RNA
TSC	Tuberous Sclerosis Complex
tTA	Tetracycline-controlled transactivator

TTX	Tetrodotoxin

U

ULK1	Unc-51–like autophagy-activating kinase 1
US	Unconditioned stimulus
UTR	Untranslated region

V

VSV	Vesicular Stomatitis Virus

W

WT	Wild-type

List of Figures

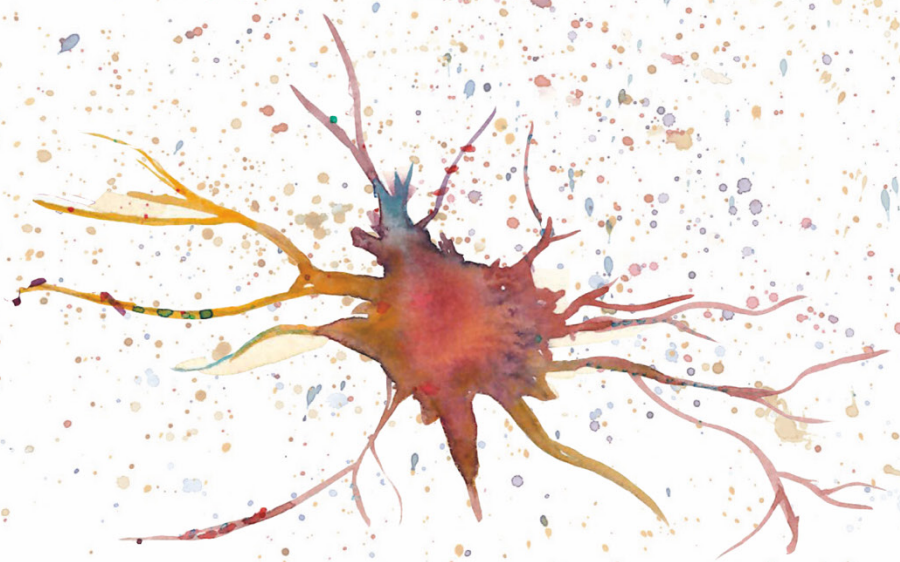

FIGURE 1. NMDAR SUBUNIT ARCHITECTURE. 55
FIGURE 2. DEVELOPMENTAL SUBUNIT EXCHANGE IN NMDAR SUBUNITS COMPOSITION. 57
FIGURE 3. GLUN3A SHARES THE MODULAR ARCHITECTURE AND TOPOLOGY OF ALL OTHER NMDAR SUBUNITS. 59
FIGURE 4. BIOPHYSICAL PROPERTIES OF NMDARS. 61
FIGURE 5. PROTEINS INTERACTING WITH GLUN3A-CTD. 64
FIGURE 6. GLUN3A DISPLAYS A UNIQUE EXPRESSION PATTERN. 69
FIGURE 7. GLUN3A-NMDARS IN SYNAPSE PLASTICITY AND MATURATION. 71
FIGURE 8. SIGNALING PATHWAYS MEDIATING PERSISTENT SYNAPSE AND SPINE ENLARGEMENT AND MEMORY CONSOLIDATION. 74
FIGURE 9. GLUN3A-NMDARS SELECTIVELY INHIBIT A SPECIFIC SUBSET OF SIGNALING PATHWAYS AND IEGS. 75
FIGURE 10. MTORC1 AND MTORC2. 79
FIGURE 11. THE MTOR SIGNALING PATHWAY IN NEURONS. 81
FIGURE 12. MTOR REGULATES BRAIN PHYSIOLOGY AND FUNCTION. 85
FIGURE 13. MTOR MACHINERY LOCALIZES AT POSTSYNAPTIC COMPARTMENTS. 88
FIGURE 14. MTOR MACHINERY LOCALIZES AT PRESYNAPTIC COMPARTMENTS. 90
FIGURE 15. MTOR IS A KEY REGULATOR OF SYNAPTIC PLASTICITY: FROM NMDARS TO LOCAL PROTEIN SYNTHESIS. 93
FIGURE 16. PRIMARY CORTICAL CULTURE. 110
FIGURE 17. SCHEMATIC REPRESENTATION OF GLUN3A'S LENTIVIRAL CONSTRUCTS. 113
FIGURE 18. CHARACTERIZATION OF TRANSDUCTION EFFICIENCY OF LENTIVIRAL GLUN3A. 116
FIGURE 19. CHARACTERIZATION OF SURFACE EXPRESSION OF LENTIVIRAL GLUN3A. 117
FIGURE 20. BDNF STIMULUS AS A NEW PROTOCOL FOR SYNAPTIC-ACTIVITY INDUCTION. 119
FIGURE 21. CYCLE PARAMETERS USED FOR AMPLIFICATION BY QPCR. 123
FIGURE 22. SCHEMATIC OF THE SUBCELLULAR FRACTIONATION PROTOCOL. 125
FIGURE 23. TIMINGS FOR LENTIVIRAL INFECTIONS. 138
FIGURE 24. TITRATION OF GLUN3A-GFP LENTIVIRUSES. 139
FIGURE 25. INHIBITION OF BICUCULLINE-DEPENDENT PROTEIN PRODUCTION OF IEGS BY GLUN3A. 141

FIGURE 26. GLUN3A DOES NOT ALTER BICUCULLINE-DEPENDENT IEGS' MRNA PRODUCTION. 141
FIGURE 27. INHIBITION OF BDNF-DEPENDENT PROTEIN PRODUCTION OF IEGS BY GLUN3A. 142
FIGURE 28. GLUN3A DOES NOT ALTER BDNF-DEPENDENT IEGS' MRNA PRODUCTION. 143
FIGURE 29. TRANSCRIPTOMIC PROFILE OF GFP AND GLUN3A-GFP NEURONS UPON BICUCULLINE AND BDNF STIMULI. 143
FIGURE 30. GENERAL BLOCKADE BY APV OF IEGS MRNA INDUCTION. 144
FIGURE 31. PROTEASOME BLOCKADE DID NOT RESCUE GLUN3A INHIBITION OF IEGS PROTEIN PRODUCTION. 144
FIGURE 32. TITRATION OF SH3A-GFP LENTIVIRUSES 145
FIGURE 33. GLUN3A KNOCKDOWN POTENTIATES BASAL MTOR ACTIVATION IN YOUNG NEURONS. 145
FIGURE 34. GLUN3A KNOCKDOWN POTENTIATES IEG INDUCTION IN YOUNG NEURONS. 146
FIGURE 35. MTOR AND ARC POTENTIATION IN GLUN3A KNOCKDOWN NEURONS IS RAPAMYCIN DEPENDENT. 147
FIGURE 36. POTENTIATION OF MTOR SIGNALING IN *GRIN3A -/-*. 148
FIGURE 37. GLUN3A MODULATES EEF2 PHOSPHORYLATION STATUS. 149
FIGURE 38. GLUN3A PREVENTS THE MTOR-DEPENDENT DEPHOSPHORYLATION OF EEF2. 150
FIGURE 39. SUNSET ASSAY 151
FIGURE 40. AGE-DEPENDENCE OF MTORC1-DEPENDENT PROTEIN SYNTHESIS. 152
FIGURE 41. GLUN3A KNOCKDOWN BOOSTS MTORC1-DEPENDENT PROTEIN SYNTHESIS. 153
FIGURE 42. GLUN3A RESCUES EXACERBATED MTOR-DEPENDENT PROTEIN SYNTHESIS. 154
FIGURE 43. INHIBITION OF MTOR REQUIRES GLUN3A-CTD INTERACTIONS. 156
FIGURE 44. GLUN3A AND GLUN3A1082Δ HAVE NO IONOTROPIC DIFFERENCES 157
FIGURE 45. GLUN1/ 3A AND GLUN1/ 3A1082Δ RECEPTORS GENERATE EQUALLY EVOKED GLYCINE CURRENTS. 158
FIGURE 46. GLUN3A RESCUES THE INCREASED MTOR-DEPENDENT PROTEIN SYNTHESIS IN *GRIN3A -/-* NEURONS. 159

FIGURE 47. GLUN3ACT2A MUTANT BOOSTS PROTEIN SYNTHESIS. 160
FIGURE 48. MTOR AND GIT1 INTERACTION IN MOUSE BRAIN. 161
FIGURE 49. FUNCTIONAL GIT1-MTORC1 COMPLEXES. 162
FIGURE 50. GIT1 CO-IMMUNOPRECIPITATES WITH MTOR IN SYNAPTIC TIF FRACTIONS. 163
FIGURE 51. MTOR AND GIT1 DIRECTLY INTERACT IN SYNAPTIC COMPARTMENTS..... 163
FIGURE 52. GIT1-MTORC1 COMPLEXES RESPOND TO ACTIVITY. 164
FIGURE 53. GIT1-MTORC1 COMPLEXES ARE REGULATED THROUGH POSTNATAL DEVELOPMENT. 165
FIGURE 54. GIT1-MTORC1 COMPLEX FORMATION IS ENHANCED IN P10 *GRIN3A-/-* HIPPOCAMPUS. 166
FIGURE 55. GLUN3A BUT NOT GLUN3A1082Δ DISRUPT GIT1-MTORC1 INTERACTIONS. 167
FIGURE 56. EXPERIMENTAL TIMING FOR GIT1 KNOCKDOWN. 167
FIGURE 57. GIT1 KNOCKDOWN REDUCES MTORC1 ACTIVATION BY BDNF AND RAPAMYCIN-SENSITIVE ARC TRANSLATION. 168
FIGURE 58. GIT1 KNOCKDOWN REDUCES PROTEIN SYNTHESIS IN A DOSE-DEPENDENT MANNER. 169
FIGURE 59. GIT1 KNOCKDOWN REDUCES MTORC1-DEPENDENT PROTEIN SYNTHESIS. 169
FIGURE 60. DTGLUN3A MICE, BUT NOT *GRIN3A-/-* MICE, EXHIBITED ABERRANT REGULAR ASSOCIATIVE MEMORIES. 171
FIGURE 61. RAPAMYCIN REVERSES ENHANCED ASSOCIATIVE MEMORY IN *GRIN3A-/-* MICE. 172
FIGURE 62. GIT1 BINDING DOMAINS. 178
FIGURE 63. MODEL FOR GIT1/ GLUN3A CONTROL OF MTORC1-DEPENDENT PROTEIN SYNTHESIS. 181

List of Tables

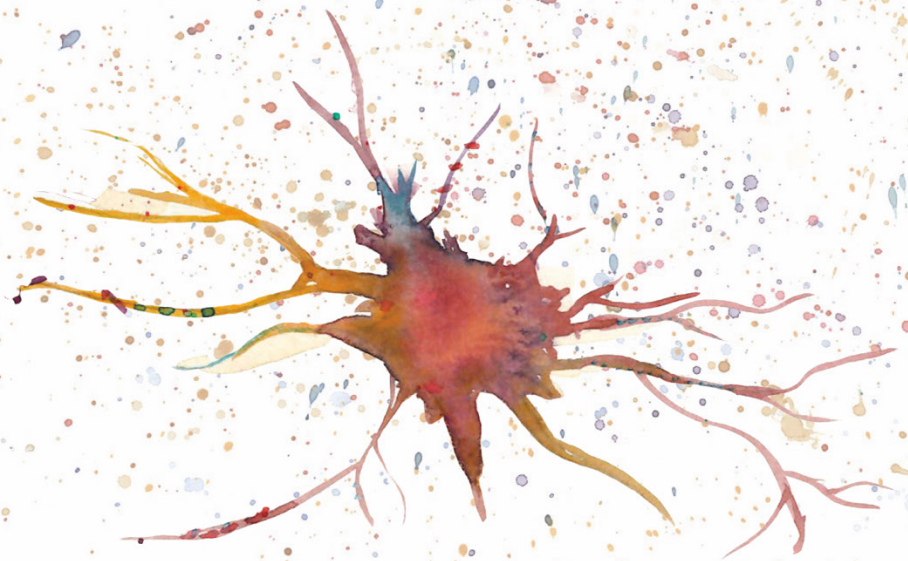

TABLE 1. NMDAR EFFECTS ON MTOR SIGNALING AND PROTEIN SYNTHESIS. 98
TABLE 2. LENTIVIRAL CONSTRUCTS 112
TABLE 3. DRUG TREATMENTS FOR CULTURED NEURONS. 118
TABLE 4. LIST OF PRIMERS USED IN QPCR ANALYSES. 123
TABLE 5. PRIMARY ANTIBODIES USED FOR CO-IP. 126
TABLE 6. PRIMARY ANTIBODIES USED FOR IMMUNOBLOTTING. 129
TABLE 7. SECONDARY ANTIBODIES USED FOR IMMUNOBLOTTING. 129
TABLE 8. PRIMARY ANTIBODIES USED FOR IMMUNOSTAINING. 130
TABLE 9. SECONDARY ANTIBODIES USED FOR IMMUNOSTAINING. 131
TABLE 10. PRIMARY ANTIBODIES USED FOR PLA. 132

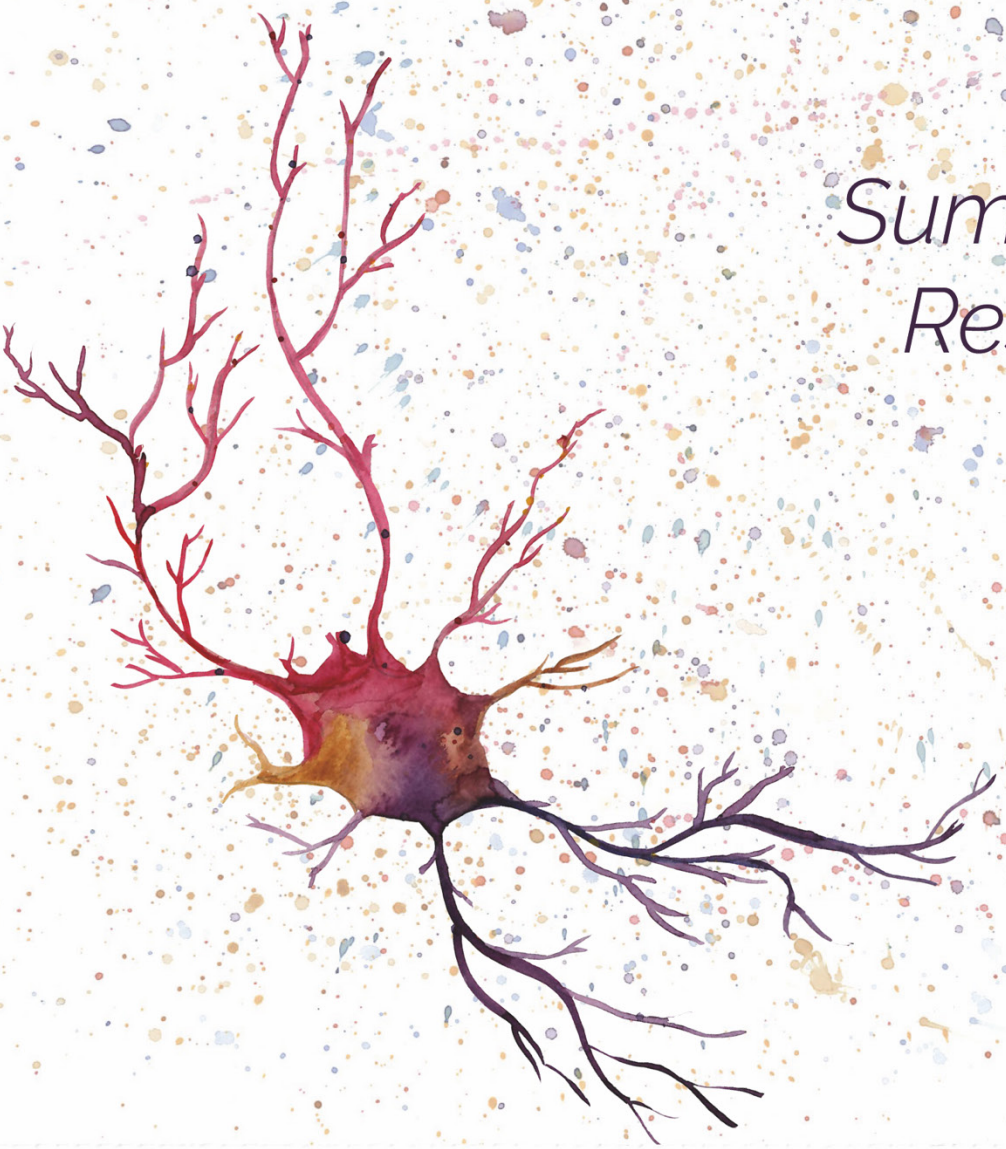

Summary/ Resumen

Early brain development is characterized by an overproduction of synapses which make weak functional connections between neurons. Neuronal activity later refines this basic circuitry by strengthening and maintaining subsets of connections but suppressing (or “pruning”) others, ultimately resulting in the formation of more precise and durable connections. Growing evidence links even subtle deficits in the balance between synapse maturation and pruning to a variety of severe brain disorders, ranging from autism, schizophrenia or bipolar disorder to neurodegenerative conditions that debut in the adult life. In an effort towards identifying the molecular underpinnings of this prevalent phenomenon of synaptic refinement, NMDA receptors containing GluN3A subunits (GluN3A-NMDARs) have emerged as key regulators. GluN3A-NMDARs are typically expressed before and during critical periods of postnatal development, prevent premature synapse maturation/ stabilization until the arrival of sensory experience, and later target less or non-used synapses for pruning. However, the cell biological and signaling mechanisms whereby GluN3A ensures correct synapse selection and its coupling to experience are yet poorly understood.

Previous work of our lab revealed that GluN3A-NMDARs sequester the scaffolding protein GIT1 and interfere with the restructuring of the actin cytoskeleton in spines. Moreover, GluN3A-NMDARs selectively inhibits the induction of a subset of activity- and NMDAR-regulated signaling pathways. The mTOR pathway, and specifically the multiprotein complex mTORC1, stands out within this group because of its central role in driving dendritic protein synthesis in response to synaptic signals. Both actin remodeling and protein synthesis are thought to be required for the conversion of relevant experiences into enduring memories by driving long-lasting structural changes that stabilize synaptic contacts.

Building on this work, here we investigate how GluN3A-NMDARs inhibit synaptic signaling to the multiprotein complex mTORC1 and evaluate its consequences on protein synthesis during postnatal development and memory encoding. We find that mTORC1 inhibition is mediated by direct binding of GluN3A to GIT1, which impedes the assembly of a new type of mTOR signaling complex composed of GIT1, mTOR and Raptor (termed GIT1-mTORC1). GIT1-mTORC1 complexes are located at or near synaptic sites and couple synaptic stimulation to mTORC1-dependent protein synthesis, providing a site for nucleating mTOR

responses at individual synapses. Loss of GluN3A during development or due to genetic manipulation enables GIT1-mTOR complex formation, potentiates mTORC1 signaling and enhances protein synthesis. Enhanced activity of the protein synthesis machinery correlates with enhanced long-term memory (LTM) formation in the conditioned taste aversion paradigm that is manifest after light training and reversed by the mTOR inhibitor rapamycin. Together, these findings uncover a major role of GIT1 and GluN3A-NMDARs in setting local modes of protein synthesis with implications for the development of precise neural circuits and adult cognitive processing.

El desarrollo temprano del cerebro se caracteriza por una sobreproducción de sinapsis que establecen conexiones funcionales débiles entre neuronas. La actividad neuronal refina después este circuito básico fortaleciendo y manteniendo subconjuntos de conexiones pero suprimiendo (o "podando") otras, lo que finalmente resulta en la formación de conexiones más precisas y duraderas. Evidencias recientes vinculan incluso sútiles déficits en el equilibrio entre la maduración y poda sináptica con una variedad de trastornos cerebrales graves, que van desde el autismo, la esquizofrenia o el trastorno bipolar hasta las afecciones neurodegenerativas que comienzan en la vida adulta. En un esfuerzo por identificar los fundamentos moleculares de este fenómeno prevalente de refinamiento sináptico, los receptores de NMDA que contienen subunidades GluN3A (GluN3A-NMDARs) han surgido como reguladores clave. Los GluN3A-NMDARs se expresan típicamente antes y durante los períodos críticos del desarrollo postnatal, previenen la maduración/ estabilización prematura de la sinapsis hasta la llegada de experiencia sensorial, y luego marcan las sinapsis menos o no utilizadas para su poda. Sin embargo, los mecanismos biológicos y de señalización celular por los que GluN3A asegura la correcta selección de dichas sinapsis y su acoplamiento a experiencia, son todavía poco conocidos.

En un trabajo anterior, nuestro laboratorio reveló que los GluN3A-NMDARs secuestran la proteína de andamiaje GIT1 e interfieren con la reestructuración del citoesqueleto de actina en las espinas. Además, los GluN3A-NMDARs inhiben selectivamente la inducción de un subconjunto de vías de señalización reguladas por actividad y NMDARs. La vía mTOR, y específicamente el complejo multiproteico mTORC1, destaca dentro de este grupo debido a su papel central en la regulación de la síntesis de proteínas dendríticas en respuesta a estímulos sinápticos. La remodelación del citoesqueleto de actina y la síntesis de proteínas son ambos considerados procesos necesarios para la conversión de experiencias relevantes en recuerdos duraderos al impulsar cambios estructurales perdurables que estabilizan los contactos sinápticos.

Sobre la base de este trabajo, aquí investigamos cómo los GluN3A-NMDARs inhiben la señalización sináptica al complejo multiproteico mTORC1 y evaluamos sus consecuencias en la síntesis de proteínas durante el desarrollo postnatal y la codificación de la memoria. Encontramos que la inhibición de mTORC1 está mediada por la unión directa de GluN3A a GIT1, lo que impide el

ensamblaje de un nuevo tipo de complejo de señalización de mTOR compuesto por GIT1, mTOR y Raptor (denominado GIT1-mTORC1). Los complejos GIT1-mTORC1 están ubicados en sitios sinápticos o cerca de ellos y acoplan la estimulación sináptica a la síntesis de proteínas dependiente de mTORC1, proporcionando un sitio para nuclear las respuestas de mTOR en sinapsis individuales. La pérdida de GluN3A durante el desarrollo o por manipulación genética permite la formación del complejo GIT1-mTOR, potencia la señalización de mTORC1 y aumenta la síntesis de proteínas. El aumento de actividad de la maquinaria de síntesis de proteínas correlaciona con un incremento en la formación de la memoria a largo plazo en el paradigma de aversión condicionado al sabor, el cual se manifiesta tras un entrenamiento ligero y es revertido por el inhibidor de mTOR rapamicina. Juntos, estos hallazgos revelan un papel importante de GIT1 y los GluN3A-NMDARs en el establecimiento de modos locales de síntesis de proteínas con implicaciones para el desarrollo de circuitos neuronales precisos y el procesamiento cognitivo adulto.

Introduction

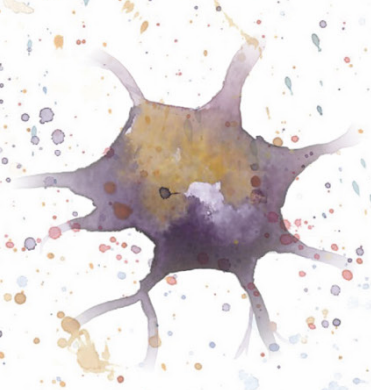

1. NMDA RECEPTORS DURING POSTNATAL DEVELOPMENT

During early brain development, massive synaptogenesis gives rise to immature neural circuits highly interconnected by weak synapses. Functional neural circuits with the capacity to support biological computation emerge later via coordinated refinement mechanisms that strengthen and stabilize some synapses but eliminate (or "prune") others (Katz and Shatz, 1996). The refinement mechanisms operate throughout the whole life of the individual but are unusually strong during "sensitive" or "critical" periods of postnatal development, when synapses are extremely plastic and can be potently remodelled by neuronal activity. For instance, in human and primate cortex, over 40% of the synapses initially formed are eliminated during this stage (Rakic et al., 1986; Zuo et al., 2005). Critical periods span the first couple of weeks in rodents, first years of life in humans, and the sensitivity of synapses to activity-dependent refinements diminishes as adult patterns of connectivity are established. This malleability is a fundamental property of the postnatal brain that allows early sensory experience to modify the architecture of neural circuits. As a result, it will shape, often permanently, the cognitive, social and emotional abilities so the individual can adapt to the environment at hand.

Accordingly, it is not surprising that growing evidence links defects in the balance between synapse maturation and pruning to a variety of brain disorders, ranging from autism, schizophrenia or bipolar disorder to neurodegenerative conditions that debut in adult life (Boksa, 2012; Kasai et al., 2021; Marco et al., 2013; Tsai et al., 2012a). The mechanisms that ensure correct synapse selection are not well understood, which has prevented the development of rationale-based interventions against validated targets. Whereas many high-profile studies have studied the reorganization of neural circuits by focusing on events that strengthen synapses and permit their maintenance for long periods, pruning is less understood at mechanistic and functional levels. One key event that determines whether individual synapses will be selected for stabilization versus pruning is the replacement of immature by mature forms of N-methyl-D-aspartate-type glutamate receptors (NMDARs) as a function of synapse use (Pérez-Otaño and Ehlers, 2004).

1.1. NMDARS' STRUCTURE AND FUNCTION

NMDARs are a functional class of ionotropic glutamate receptors (iGluRs) that mediate excitatory neurotransmission in the central nervous system (CNS). These glutamate-gated ion channels are widely distributed at all stages of development, and are critical mediators of functional and structural plasticity. The involvement in brain plasticity is supported by their unique properties, including: 1) voltage-dependent block by extracellular Mg^{2+}; 2) high permeability to Ca^{2+}; 3) requirement for both glutamate and a co-agonist (glycine or D-serine) for activation; and 4) the ability to sense the extracellular microenvironment via a wide range of modulatory sites (Hansen et al., 2017, 2018).

Functional NMDARs assemble as tetrameric complexes of an obligatory GluN1 subunit and various combinations of GluN2 and GluN3 subunits. Conventional NMDARs, majority in the CNS, are composed of two GluN1 subunits that bind glycine and two GluN2 subunits that bind glutamate (Hansen et al., 2018; Paoletti et al., 2013). In non-conventional NMDARs, the glycine-binding GluN3 subunits can also assemble with GluN1 and GluN2 subunits to form GluN1/ 2/ 3 receptors, or with GluN1 alone to form GluN1/ 3 excitatory glycine receptors (see below) (Cavara and Hollmann, 2008; Chatterton et al., 2002; Henson et al., 2010; Madry et al., 2007).

A total of seven NMDAR subunits, allocated in three different subfamilies, have been identified: the GluN1 subunit, including 8 functional splice variants; four distinct GluN2 subunits (GluN2A, GluN2B, GluN2C and GluN2D), encoded by four different genes; and two GluN3 subunits (GluN3A and GluN3B), encoded by two different genes as well. The sequences of NMDAR subunits range from 900 to 1480 amino acids (aa) in length. GluN1 was the first member of the family to be cloned and is the smallest NMDAR subunit, with approximately 938aa depending on the splice variant (Moriyoshi et al., 1991). GluN2 subunits show high homology (38-53% identity) but low compared to GluN1 (18-20% sequence identity), and have longer aa sequences than GluN1: 1464aa, 1482aa, 1250aa and 1356aa in GluN2A-D, respectively (Ishii et al., 1993; Monyer et al., 1992). The members of the GluN3 subfamily were the last ones to be cloned (Andersson et al., 2001; Ciabarra et al., 1995; Sucher et al., 1995).

Despite this diversity, all NMDAR subunits share a modular architecture with four discrete domains: an extracellular amino (N)-terminal domain (NTD); an agonist-binding domain (ABD), where the so-called S1 and S2 segments form a ligand binding pocket for glycine/ D-serine or glutamate depending on the subunit; a transmembrane domain (TMD) containing the ion channel pore; and an intracellular C-terminal domain (CTD) that couples receptors to signaling pathways. The CTD is the most divergent region among subunits in terms of aa sequence and length (Figure 1) (Paoletti et al., 2013; Traynelis et al., 2010). Combinatorial assembly of subunits confers distinct biophysical and pharmacological properties to NMDA receptors and enable various physiological roles at synaptic *vs* extrasynaptic sites, in diverse neuronal cell types and brain regions, or along neuronal development (Hansen et al., 2017).

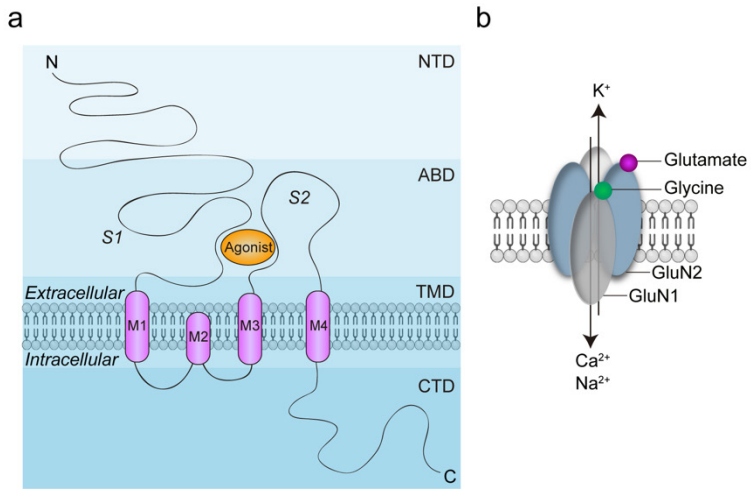

Figure 1. NMDAR subunit architecture.

(a) NMDAR subunits have a modular structure composed of two large extracellular domains, the NTD and the ABD, a TMD that forms part of the ion channel and an intracellular CTD. The ABD is defined by two segments of amino acids termed S1 and S2 and binds the agonist glycine or D-serine in GluN1 and GluN3 subunits or glutamate in GluN2 subunits. The TMD contains three membrane-spanning helices (M1, M3, and M4) and a membrane re-entrant loop (M2). *(b)* Model of tetrameric NMDAR. The majority of NMDARs in the CNS are composed of two GluN1 and two GluN2 subunits, which form a central cation-permeable channel pore.

1.2. DEVELOPMENTAL SUBUNIT EXCHANGES IN NMDAR SUBUNIT COMPOSITION

One prominent example of the functional relevance of NMDAR subunit diversity comes from examining changes in subunit composition during early postnatal brain development. During this period, the transition from juvenile to mature NMDAR subtypes is a key driver of the maturation and stabilization of excitatory synapses (Hansen et al., 2017; Paoletti et al., 2013). Soon after birth, synapses throughout the CNS are mainly composed of di-heteromeric GluN1/ 2B and tri-heteromeric GluN1/ 2B/ 3A NMDARs (Paoletti et al., 2013). These early subtypes are essentially required for postnatal cortical development (Hall et al., 2007), and are replaced in adults by mature di-heteromeric GluN1/ 2A or tri-heteromeric GluN1/ 2B/ 2A receptors in most brain regions (Sheng et al., 1994; Watanabe et al., 1992).

The GluN2B-to-GluN2A subunit exchange has been extensively studied: it is driven by synaptic activity and sensory experience (Barria and Malinow, 2002; Bellone and Nicoll, 2007; Philpot et al., 2001; Rodenas-Ruano et al., 2012), and correlates with the lasting stabilization of active synapses and associated dendritic spines (Gambrill and Barria, 2011; Holtmaat et al., 2005). The subunit exchange modifies the properties of NMDAR-mediated currents, the temporal integration of synaptic inputs and their plasticity properties. GluN2B-containing receptors (GluN2B-NMDARs) have slow kinetics and flux large amounts of calcium, enabling long-term potentiation (LTP) induction and plasticity-induced spine growth, and are thought to be responsible for heightened plasticity during sensitive periods (Gambrill and Barria, 2011; Lee et al., 2010b). Their replacement by GluN2A-containing subtypes (GluN2A-NMDARs) confers faster kinetics to NMDARs, shortening the duration of NMDAR-mediated synaptic currents and limiting calcium entry (Crair and Malenka, 1995; Hestrin, 1992; Tovar and Westbrook, 1999). The GluN2B-to-GluN2A subunit exchange is evident as changes in the pharmacology of synaptic currents: the sensitivity to the allosteric GluN2A-specific inhibitor Zn^{2+} increases in parallel with a decrease in the sensitivity to the GluN2B-specific antagonist ifenprodil (Figure 2) (Hatton and Paoletti, 2005; Karakas et al., 2011; Paoletti et al., 1997).

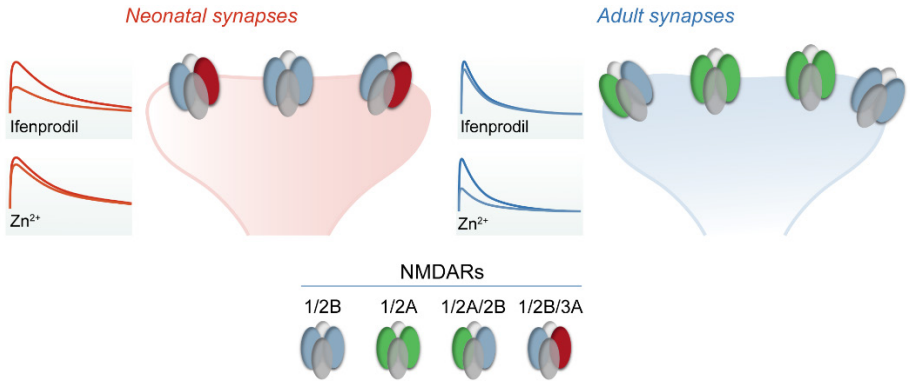

Figure 2. Developmental subunit exchange in NMDAR subunits composition.

Left, neonatal synapses are mainly composed of di-heteromeric GluN1/ 2B and tri-heteromeric GluN1/ 2B/ 3A receptors, leading to an increased sensitivity to GluN2B-specific antagonists as ifenprodil. *Right*, in adult synapses these receptors are replaced by di-heteromeric GluN1/ GluN2A and tri-heteromeric GluN1/ 2A/ 2B receptors in adults. The increased GluN2A-to-GluN2B ratio promotes an increased sensitivity to the GluN2A-specific antagonist Zn^{+2}. Figure adapted from (Paoletti et al., 2013).

In terms of subcellular localization, it has been widely accepted that GluN2A-NMDARs concentrate in postsynaptic densities (PSDs) whereas GluN2B-NMDARs can be also found at both peri- and extra-synaptic locations (Gladding and Raymond, 2011; Hardingham and Bading, 2010; Petralia et al., 2010). Therefore, the replacement of GluN2B- by GluN2A-NMDARs in the adult brain leads to stronger attachment of mature NMDARs to PSDs which might contribute to the kinetics change (Crair and Malenka, 1995; Stocca and Vicini, 1998; Tovar and Westbrook, 1999).

A second change in subunit composition involves the transition between GluN3A-containing to GluN3A-lacking NMDARs. As the GluN2B-to-GluN2A transition, this subunit exchange occurs postnatally, is controlled by synaptic activity and sensory experience, can be regulated locally at individual synapses, and plays a role in synapse selection during the postnatal refinement of neural circuits (see Role of GluN3A-NMDARs in the refinement of neuronal circuits). However, the mechanisms and functional implications are less understood.

1.3. GLUN3A-CONTAINING NMDARS: GATE-KEEPERS OF SYNAPSE PLASTICITY, MATURATION AND COGNITION

Along with GluN2B subunits, juvenile NMDARs often contain GluN3A subunits. GluN3A was cloned in 1995, lagging behind the identification of the other NMDAR subunits (Ciabarra et al., 1995; Sucher et al., 1995). It was initially termed χ-1 (chi-1, GenBank accession number L34938) or NMDAR-L (NMDAR-like, GenBank accession number U29873), later renamed NR3A, and then GluN3A (Das et al., 1998). In 2001, a new NMDAR subunit closely related to GluN3A was discovered: NR3B/ GluN3B (Andersson et al., 2001).

GluN3A and GluN3B exhibit high sequence homology (57.4% identity), but the temporal expression patterns and synaptic localizations are quite different (Pachernegg et al., 2012; Wee et al., 2016). GluN3A-NMDARs are more highly expressed and extensively studied, exhibit unique properties that allow them to behave as dominant-negative regulators of NMDAR activity (Das et al., 1998; Tong et al., 2008), and are key modulators of glutamatergic synapse maturation and synaptic plasticity (Fiuza et al., 2013; Henson et al., 2012; Kehoe et al., 2014; Larsen et al., 2011; Roberts et al., 2009).

1.3.1. Molecular biology of GluN3A subunits

The human gene encoding GluN3A, *GRIN3A,* is located on chromosome 9 (chromosome 4 in mice and 5 in rats) and encodes a protein of 1115aa with a molecular weight of approximately 125 kDa (Andersson et al., 2001). The rodent homologue, *Grin3a,* encodes two isoforms: a CTD-long isoform that includes a 20aa insertion (GluN3A-L) and a CTD-short isoform (GluN3A-S) (Andersson et al., 2001; Sun et al., 1998). The functional relevance or physiological impact of these isoforms is still lacking, but they display different temporal and regional expression patterns and humans only express the short version (Hansen et al., 2017).

GluN3A has relatively low sequence homology with GluN1 and GluN2 subunits (~27% identity) but shares the modular architecture and topology of all NMDAR subunits (Figure 3). Like GluN1, GluN3A subunits bind glycine and D-serine instead of glutamate in the pocket formed by the S1 and S2 segments. Nonetheless, GluN3A binds both agonists with much higher affinity than GluN1

(650-fold and more than 10-fold, respectively) (Yao and Mayer, 2006; Yao et al., 2008). The GluN3A CTD is shorter than GluN2 subunits and mediates interactions with different intracellular proteins that modulate a variety of cellular processes (Figure 3; see GluN3A-CTD interacts with a unique set of intracellular proteins). One other relevant feature of GluN3A subunits sequence is the presence of a 'GR' motif in the M2 helix loop. This motif differs from the 'QRN' site, which controls ion permeation in GluN1 and GluN2 subunits and may explain the singular channel-gating properties of GluN3A-containing NMDARs (Henson et al., 2010).

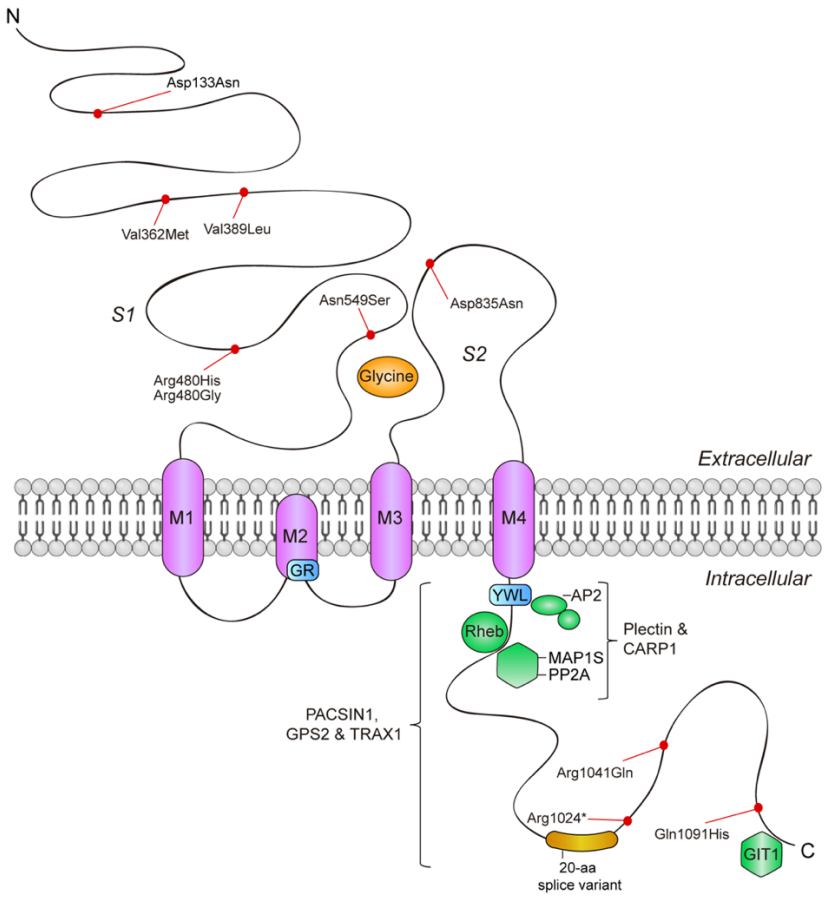

Figure 3. GluN3A shares the modular architecture and topology of all other NMDAR subunits.

Schematic showing, from top to bottom, the extended extracellular NTD; two extracellular aminoacidic segments, S1 and S2, that form the ABD site for glycine or D-serine; the TMD, composed of three membrane-spanning helices (M1, M3 and M4) and a membrane re-entrant loop (M2); and the intracellular CTD. Sequence motifs are indicated in blue: glycine–arginine residues (GR) that occupy key sites in the loop of M2 and determine ion permeation and a tyrosine-based internalization motif (YWL). Relevant binding sites of intracellular proteins are noted in green: clathrin adaptor protein 2

(AP2), Ras homologue enriched in brain (Rheb), protein phosphatase 2A (PP2A), microtubule-associated protein 1S (MAP1S) and G-protein-coupled receptor kinase interacting protein (GIT1). The predicted binding sites of interactors such as intermediate filaments (Plectin), a cell cycle and apoptosis regulatory protein (CARP1), protein kinase C and casein kinase substrate in neurons protein 1 (PACSIN1), G-protein pathway suppressor 2 (GPS2) and Translin associated factor X1 (TRAX1) are also shown. In orange is denoted the location of the 20-aminoacid insertion in the known GluN3A splice variant. In red, point mutations of GluN3A sequence linked to CNS diseases are indicated.

1.3.2. Receptor assembly and biophysical properties

Co-immunoprecipitation (co-IP) studies demonstrate that GluN3A subunits can form stable biochemical complexes with several NMDAR subunits in human embryonic kidney 293 (HEK293) and COS-7 cell lines (Chatterton et al., 2002; Matsuda et al., 2003; Nishi et al., 2001; Sasaki et al., 2002). However, the precise stoichiometry of GluN3A-NMDARs in the brain remains largely unexplored and could differ across brain regions, cell types and during development (Paoletti et al., 2013). For instance, GluN3A co-assembles with GluN2A and GluN2B in neurons (Das et al., 1998; Martínez-Turrillas et al., 2012; Nilsson et al., 2007) and with GluN2C in oligodendrocytes (Burzomato et al., 2010; Káradóttir et al., 2005).

Homomeric GluN3A or di-heteromeric GluN2A/ GluN3A complexes fail to exit the endoplasmic reticulum (ER). Co-assembly with GluN1 is required for these complexes to exit the ER and reach the cell surface (Perez-Otano et al., 2001), so only two types of functional GluN3A-containing receptors can be found in the surface: tri-heteromeric NMDARs (GluN1/ 2/ 3A) and di-heteromeric GluN3A-containing receptors (GluN1/ 3A) (Figure 4).

GluN3A-containing tri-heteromeric NMDARs

GluN3A-containing tri-heteromeric NMDARs (from now on referred to as GluN3A-NMDARs) respond to glutamate and NMDA. However, studies in heterologous cells and neurons have shown that GluN3A-NMDARs display atypical biophysical and trafficking properties relative to conventional NMDARs (Burzomato et al., 2010; Das et al., 1998; Matsuda et al., 2003; Perez-Otano et al., 2001; Roberts et al., 2009; Sasaki et al., 2002; Tong et al., 2008).

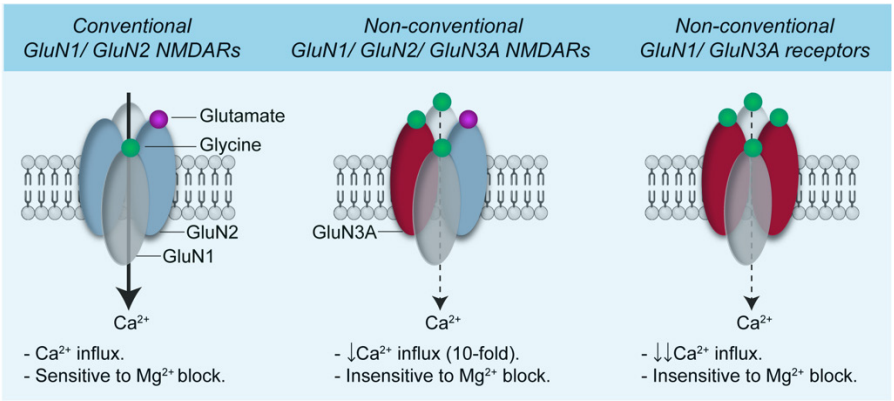

Figure 4. Biophysical properties of NMDARs.

Schematic illustrating the main channel properties of conventional NMDARs containing GluN1 and GluN2 subunits (left), non-conventional tri-heteromeric NMDARs containing GluN3A (middle) and the lately proven non-conventional GluN3A-containing di-heteromeric receptors (right). Tri-heteromeric NMDARs containing GluN3A exhibit reduced Ca^{2+} permeability and are less sensitive to voltage-dependent block by Mg^{2+} compared with conventional NMDARs. GluN3A-containing di-heteromeric receptors function as excitatory glycine receptors and display even lower Ca^{2+} permeability and are also insensitive to voltage-dependent Mg^{2+} block. Therefore, GluN3A expression leads a dominant-negative effect on conventional NMDARs properties.

Electrophysiological studies of pure populations of GluN3A-NMDARs were carried out using single-channel recordings upon co-expression of GluN1, GluN2A and GluN3A subunits in HEK293 cell lines and *Xenopus laevis* oocytes (Perez-Otano et al., 2001; Sasaki et al., 2002). Compared to conventional NMDARs, GluN3A-NMDARs were found to exhibit a smaller single-channel conductance (Perez-Otano et al., 2001; Sucher et al., 1995), a 10-times lower Ca^{2+} permeability (Sasaki et al., 2002), a lower open probability but longer mean open times (Perez-Otano et al., 2001), and a relative insensitivity to Mg^{2+} block at hyperpolarized potentials (Burzomato et al., 2010; Chatterton et al., 2002; McClymont et al., 2012; Roberts et al., 2009; Sasaki et al., 2002). Because of these properties, they were termed “non-conventional NMDARs”.

Importantly, single-channel recordings also provided evidence for the existence of endogenous GluN3A-NMDARs in cortical and hippocampal neurons (Sasaki et al., 2002). The channels displayed similar properties to recombinant GluN3A-NMDARs and were absent in *Grin3a -/-* mice (Das et al., 1998), but were a major component of the channel population in transgenic mice overexpressing GluN3A (Tong et al., 2008).

GluN3A-containing di-heteromeric receptors

Initial work in recombinant systems showed that GluN3A co-assembles with GluN1 to form excitatory glycine receptors (Chatterton et al., 2002; Das et al., 1998; Perez-Otano et al., 2001; Sucher et al., 1995). These complexes are: *1)* not activated by NMDA nor glutamate, *2)* insensitive to APV, a competitive antagonist at the glutamate binding site in GluN2 subunits, and *3)* relatively Ca^{2+}-impermeable (Chatterton et al., 2002; Madry et al., 2007) but see (Otsu et al., 2019). Studies with selective antagonists and site-directed mutagenesis revealed that glycine binding to the GluN3A ABD triggers channel opening and activation whereas binding to the GluN1 ABD causes rapid desensitization (Madry et al., 2007), a feature that was later used to unmask GluN1/ 3A currents *in vivo*.

Demonstrating the existence of GluN1/ 3A receptors *in vivo* proved difficult due to the rapid desensitization that derives from the GluN1 glycine binding site, combined with high levels of free glycine in brain slice preparations. Native GluN1/ 3A receptors were first observed in oligodendrocytes of mouse optic nerves rather than neurons, although their exact role is still a mystery (Piña-Crespo et al., 2010). Work on neuronal cultures later proposed a role in metaplasticity of excitatory hippocampal synapses by showing that, upon induction of chemical LTP, putative GluN1/ 3 receptors are recruited to enlarged synapses to facilitate depotentiation (Rozeboom et al., 2015).

Strong evidence has recently emerged thanks to the use of CGP-78608, a competitive antagonist with pronounced preference for the glycine-binding site of GluN1 over GluN3A, to unmask GluN1/ 3A responses (Grand et al., 2018; Yao and Mayer, 2006). Pre-incubation with CGP-78608 locks the GluN1 ABD, and prevents glycine binding to GluN1 that strongly desensitizes the receptor. Later application of saturating concentrations of glycine results in glycine binding to the GluN3A ABD and full activation of the receptor (Grand et al., 2018). Recordings of CA1 neurons in young (P8-P12) mouse hippocampal slices in the presence of CGP-78608 revealed a massive potentiation of glycine-induced inward currents in wild-type but not *Grin3a -/-* mice (Grand et al., 2018), clearly implicating GluN1/ 3A receptor function. GluN1/ 3 receptors were also found in the adult medial habenula (MHb) in adult mice In WT (but not *Grin3a -/-*) MHb neurons, glycine puffs increased firing rates and induced rapidly rising inward currents. Aptly, behavioral

tests suggested that MHb GluN1/ 3 receptors mediate conditioned place-aversion, a readout that depends on this region.

1.3.3. GluN3A-CTD interacts with a unique set of intracellular proteins

The CTD of GluN3A is different from that of GluN1 or GluN2 subunits and mediates interactions with a distinct set of intracellular proteins (Figure 3; more detailed in Figure 5), that regulate receptor signaling, trafficking and anchoring of the receptor to the plasma membrane.

GIT1

The G protein-coupled receptor kinase-interacting protein (GIT1) is a multifunctional scaffold that interacts with signaling molecules and regulates their localized activation.

In mature neurons, GIT1 is enriched in dendritic spines and postsynaptic sites. Spines are actin-rich and their structural remodeling relies on rearrangements of the actin cytoskeleton. Cytoskeletal rearrangements are regulated by the Rho family of small GTPases, molecular switches that cycle between an inactive GDP-bound and an active GTP-bound conformation. Two members of this family, Rac1 and RhoA, are major regulators of spine remodeling (Tashiro et al., 2000). Their activation state is controlled by guanine exchange factors (GEFs), which promote the exchange of GDP for GTP, and GTPase-activating proteins (GAPs), which catalyze GTP hydrolysis. GIT1 assembles with Rac1 and the Rac1-GEF β-PIX in spines, allowing the activation of the Rac1/ PAK signaling pathway and promoting synapse maturation (Zhang et al., 2003, 2005; Zhao et al., 2000).

NMDAR activation induces cytoskeletal and spine remodeling by activating Rac1-GEFs. Our lab previously reported that GluN3A has the opposite effect. GluN3A directly binds and sequesters GIT1 away from synaptic locations, impairing its ability to nucleate β-PIX and inhibiting Rac1/ PAK activation in dendritic spines (Fiuza et al., 2013). More specifically, this study revealed that GluN3A binds GIT1 through the distal 33aa of its CTD (Figure 5).

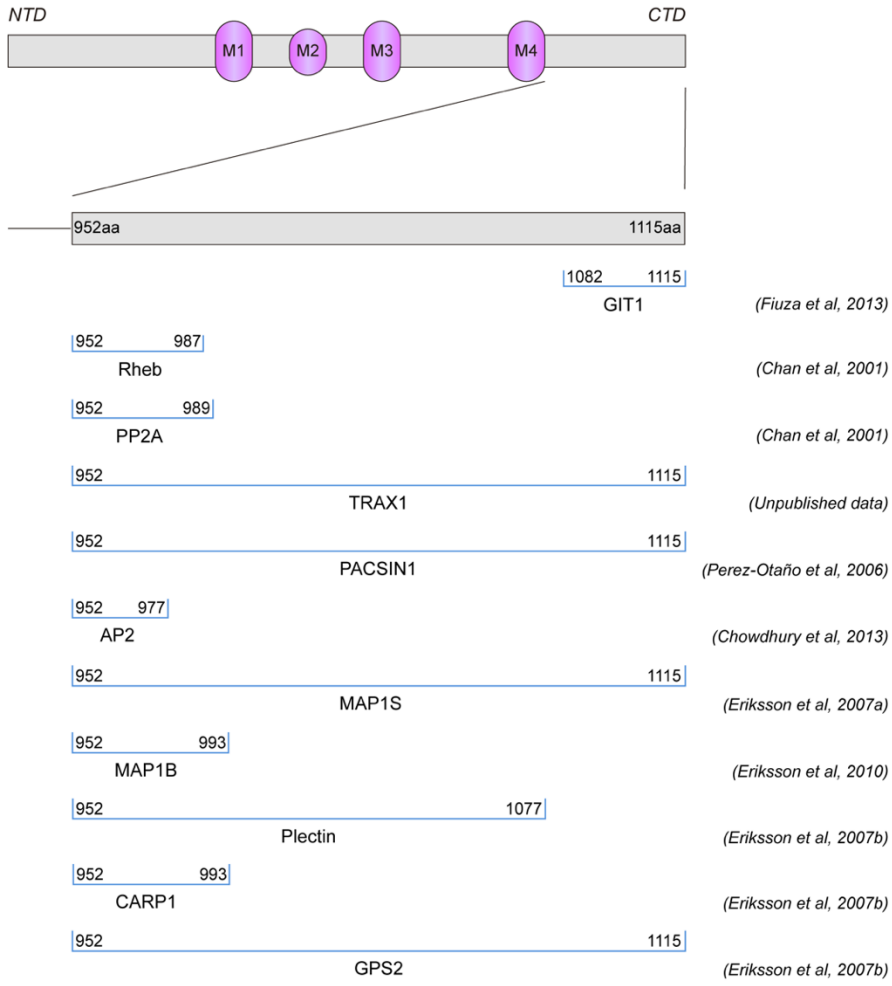

Figure 5. Proteins interacting with GluN3A-CTD.

Only proteins that directly interact with GluN3A are listed. Schematic representation of the specific domains of interaction within GluN3A-CTD.

Unbiased proteomic fishing for mTOR regulators in mouse astrocytes showed that GIT1 binds the serine/ threonine kinase mechanistic target of rapamycin (mTOR) (Smithson and Gutmann, 2016). Although the function of these complexes could not be established, it places GIT1 as a potential mechanism to coordinate actin rearrangements and mTOR activation in dendritic spines and ensure their long-term structural stabilization.

Rheb

The small GTPase Rheb (from Ras homologue enriched in brain) was originally detected as an immediate early response protein whose expression was induced by NMDAR-dependent synaptic activity in the brain (Yamagata et al., 1994). Rheb is a main activator of the mTOR pathway, and its activity is highly regulated by the Tuberous Sclerosis Complex (TSC), a GAP that stimulates the inhibition of Rheb by shifting its GTP-bound active conformation into the inactive GDP-bound one.

Rheb is enriched at synaptic membranes and appears to interact with the GluN3A CTD (Sucher et al., 2011) at sites overlapping with PP2A (Figure 5). Analogous to GIT1, we could hypothesize that GluN3A displaces Rheb from synapses and/ or inhibit its binding to mTOR and subsequent activation. This could have relevant physiological implications considering the crucial role of the mTOR pathway controlling spine maturation and stabilization as well as the establishment of long-term types of plasticity and learning and memory through protein synthesis (Costa-Mattioli and Monteggia, 2013).

TRAX1

Translin associated factor X1 (TRAX1) forms a complex with the RNA binding protein (RBP) Translin to regulate dendritic trafficking and translation of mRNAs (Park et al., 2017). Unpublished data from our group unveiled that TRAX1 interacts with GluN3A-CTD using a yeast two hybrid screening system. GluN3A binding to TRAX1 could thus promote an entirely different sort of mechanism to modulate protein synthesis similar to that of the RBP Fragile X Mental Retardation Protein (FMRP); upon nuclear export and transport to dendrites, mRNAs might remain translationally repressed at GluN3A-expressing non-activated synapses.

PP2A

Protein phosphatase 2A (PP2A) is one of the major serine-threonine phosphatases in the CNS and is responsible for controlling diverse cellular processes through the negative regulation of signaling pathways initiated by protein kinases. PP2A exists as a heterotrimeric enzyme complex consisting of a catalytic subunit, a structural subunit and a variable regulatory subunit (Strack et al., 1998). GluN3A interacts

with the catalytic subunit through the membrane-proximal 37aa CTD region (Figure 5) (Chan and Sucher, 2001; Ma and Sucher, 2004). This tight interaction is abolished upon NMDAR activation, which leads to the GluN1-Ser^{897} dephosphorylation and further attenuation of NMDAR channel currents (Chan and Sucher, 2001). Intriguingly, enhanced PP2A activity has been associated with downregulation of mTOR signaling (Liu et al., 2011). Postmortem examination of schizophrenia patients' brains have also revealed increased levels of GluN3A (Mueller and Meador-Woodruff, 2004) and enhanced PP2A activity, being the latter linked to decreased levels of phosphorylated GluN1-Ser^{897} (Emamian et al., 2004). Additionally, enhanced PP2A activity together with higher expression of GluN3A was found to contribute to the protective mechanism of Simvastatin in ischemic stroke (Zhu et al., 2012). Of note, PP2A expression, like GluN3A, is developmentally regulated, peaking around P8 and declining from P12 to a low level in adulthood (Chan and Sucher, 2001).

Other GluN3A-CTD interacting proteins

Other GluN3A binding partners include proteins involved in the trafficking or localization of the receptor. For instance, GluN3A endocytic removal is regulated through interaction with two different proteins. PACSIN1 (from protein kinase C and casein kinase substrate in neurons protein 1) is enriched at synapses and links the endocytic machinery with the actin cytoskeleton. Upon synaptic activity, PACSIN1 interacts with the GluN3A CTD promoting receptor internalization (Pérez-Otaño et al., 2006). The general clathrin adaptor protein 2 (AP2) binds the conserved 'YWL' motif within GluN3A-CTD and is also involved in endocytic removal of GluN3A from the cell surface (Chowdhury et al., 2013).

Other interactors are the microtubule-associated proteins (MAP1) MAP1S (Eriksson et al., 2007a) and MAP1B (Eriksson et al., 2010). MAP1 family proteins are important in the development of axon and dendrites, suggesting a potential role in transporting GluN3A-NMDARs through the dendritic shaft to their final location. However, their binding site on GluN3A-CTD overlaps with that of PP2A (Ma and Sucher, 2004), suggesting a potential competition or a reciprocal binding pattern.

GluN3A also interacts with the scaffolding protein Plectin, the cell-cycle and regulatory protein CARP1 and the G-protein signaling suppressor GPS2 (Eriksson et al., 2007b). However, little is known about these interactions and further study is required. Of note, GluN3A-CTDs lack PDZ domain-recognition motifs present in GluN2 subunits' CTDs. These motifs mediate the receptor binding to synaptic scaffolding proteins of the PSD-95 family and allow their anchoring and stabilization within the PSD (Bard et al., 2010; Eriksson et al., 2007b). The absence of PDZ-domain recognition motifs in GluN3A-CTD may explain the labile synaptic expression of GluN3A-NMDARs (see GluN3A-NMDARs display a unique expression pattern).

1.3.4. Role of GluN3A-NMDARs in the refinement of neuronal circuits

Extensive evidence now links juvenile NMDARs containing GluN3A subunits to the postnatal refinements that reconfigure neural circuits as a function of experience. First, GluN3A is highly expressed in the brain during the narrow temporal windows of postnatal development when massive synapse stabilization and elimination occur, and its expression drops markedly afterwards (Pérez-Otaño et al., 2006; Wong et al., 2002). Second, prolonging GluN3A expression beyond this time window inhibits synapse maturation and promotes pruning, whereas GluN3A removal is conversely associated with accelerated maturation (Henson et al., 2012; Kehoe et al., 2014; Roberts et al., 2009). Little is known about the downstream mechanisms by which GluN3A drives synapse dysfunction and pruning, but this information is critical to evaluate the potential of GluN3A or its downstream mechanisms as therapeutic targets.

GluN3A-NMDARs display a unique expression pattern

As mentioned, a unique feature of GluN3A is its prevalent expression during time windows of postnatal development that precede and overlap with critical periods of experience-dependent synaptic refinement. In rodents, GluN3A expression levels are low at embryonic stages, rise over the first postnatal week in most brain regions peaking around postnatal day 5 (P5) – P10, and then decrease into adulthood (Figure 6a) (Wong et al., 2002). Following the same pattern, GluN3A expression in humans surges soon after birth, peaks in the first year of life and gradually declines through adolescence (Henson et al., 2010).

Recent work from our lab mapped *Grin3a* mRNA expression in the mouse brain from embryonic to postnatal and adult stages (Murillo et al., 2021). GluN3A levels were found to be retained in areas of the adult mouse brain with high plasticity requirements or with a functional need for association of multiple inputs, i.e., the nuclei of the amygdala, MHb, association cortices, the olfactory system or the claustrum. This work complemented a prior study which identified *Grin3a* as one of the genes most strongly correlated with hierarchy gradients of functional integration across the neocortex, based on the MRI T1w:T2w ratio (Fulcher et al., 2019). High *Grin3a* expression and low T1w:T2w ratios were found in less differentiated association and transmodal cortical areas with strong needs for plasticity and functional integration throughout life such as the claustrum, rhinal, insular or prefrontal cortex. By contrast, low adult *Grin3a* expression was observed in primary sensorimotor unimodal cortices with highly consolidated circuitry and lower plasticity requirements. The match of GluN3A expression with sensory experience is remarkable. For instance, GluN3A's peak of expression is delayed in the mouse visual cortex, where synaptic rearrangements occur later, around P14, overlapping with eye opening (Figure 6a). Besides, mice deprived from visual experience sustained high levels of synaptic GluN3A expression for several weeks (Larsen et al., 2014).

At the ultrastructural level, the subcellular distribution of GluN3A-NMDARs differs from that of conventional NMDARs. Post-embedding immunogold electron microscopy (Pérez-Otaño et al., 2006) and biochemical fractionation (Martínez-Turrillas et al., 2012) demonstrate that GluN3A-NMDARs are found at PSDs but are specially enriched at perisynaptic (0–120nm from the edge of PSDs) and extrasynaptic (more than 120nm away from the PSDs) sites (Figure 6b). Within PSDs, GluN3A-NMDARs exhibit an inverse distribution gradient and concentrate at the edge of the postsynaptic specialization (Pérez-Otaño et al., 2006) instead of peaking at the centre like conventional NMDARs (Racca et al., 2000). This singular localization, together with the lack of PDZ-domain binding motifs and their rapid endocytic removal, prompted the idea that GluN3A-NMDARs form part of a mobile receptor pool and that inclusion of GluN3A within NMDAR complexes might affect their stabilization at synaptic sites. Of note, electron microscopy studies shown that large synapses (PSD length > 250nm) lack GluN3A expression at all (Roberts et al., 2009).

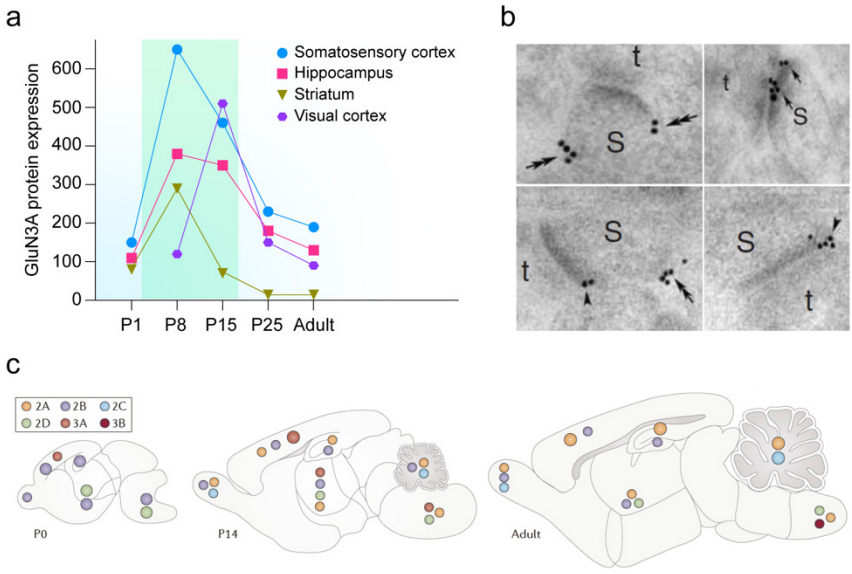

Figure 6. GluN3A displays a unique expression pattern.

(a) GluN3A protein expression in the rodent brain increases during the first postnatal week in most of the brain regions, peaks around P5-P10 (green shaded area) and sharply declines into adulthood. Schematic adapted from (Marco et al., 2013; Pérez-Otaño et al., 2016). *(b)* Ultrastructural localization of GluN3A at CA1 hippocampal synapses of adult rats using post-embedding immunogold electron microscopy. GluN3A predominantly localizes at perisynaptic (arrowheads) and extrasynaptic (double arrows) sites, although synaptic expression is also found (arrows). In the images, 't' indicates the position of presynaptic terminals, and 's' indicates the position of a dendritic spine. Image adapted from (Pérez-Otaño et al., 2006). *(c)* Schematic representing the developmental profile of NMDAR subunits in the mouse brain; GluN3A expression is highlighted in light red. Image taken from (Paoletti et al., 2013).

At the cellular level, neuronal cell types expressing GluN3A include excitatory pyramidal neurons in the cortex and hippocampus, retinal ganglion cells, cerebellar Purkinje neurons and inhibitory GABAergic interneurons (Henson et al., 2010; Pachernegg et al., 2012). Of note, GluN3A levels are particularly high in somatostatin (SST) interneurons of the neocortex and hippocampus (Murillo et al., 2021). This correlates with single-cell transcriptomic analyses of mouse somatosensory and visual cortex interneurons (Paul et al., 2017; Pfeffer et al., 2013) that identified *Grin3a* as a secondary molecular marker for SST interneurons. Besides, SST cell densities, as *Grin3a* levels, are negatively correlated with T1w:T2w ratios (Fulcher et al., 2019). Apart from neurons, GluN3A is also expressed in oligodendrocytes (Burzomato et al., 2010; Káradóttir et al.,

2005; Salter and Fern, 2005), astrocytes (Lee et al., 2010a; Palygin et al., 2011), microglia (Murugan et al., 2011) and brain endothelial cells (Mehra et al., 2020).

The spatiotemporal expression profile of GluN3A within the CNS is also strikingly unique (Figure 6c; GluN3A is referred as '3A' and denoted as light red dots). Early in development, GluN3A expression is widespread, with high levels found in the neocortex, hippocampal CA1 region, olfactory bulb, cerebellum, and nuclei of the amygdala, thalamus, hypothalamus and brainstem (Pachernegg et al., 2012).

GluN3A-NMDARs in synapse maturation, stabilization and plasticity

As introduced above, one molecular event required before synapses can be selected for stabilization *versus* pruning is the replacement of juvenile GluN3A-NMDARs with mature GluN1/ 2-containing conventional NMDARs (Pérez-Otaño et al., 2006). Much evidence comes from genetic studies (Figure 7). Initial work revealed that young (P19) *Grin3a -/-* mice exhibit a 2-3 fold increased spine density and stronger NMDA-induced currents in cortical pyramidal neurons; a difference that was less robust in adult mice (Das et al., 1998) (Figure 7b,c; left panels). Later studies using a double-transgenic GFP-GluN3A (dtGluN3A) mouse model revealed that enhancing GluN3A expression (Roberts et al., 2009) decreases spine density and yields a higher proportion of immature spines with smaller PSDs (Figure 7b,c; right panels). Hippocampal LTP was reduced in dtGluN3A mice, while *Grin3a -/-* mice showed an acceleration of the developmental onset of LTP (Figure 7d) (Roberts et al., 2009) and earlier expression of synaptic maturation markers (Henson et al., 2012).

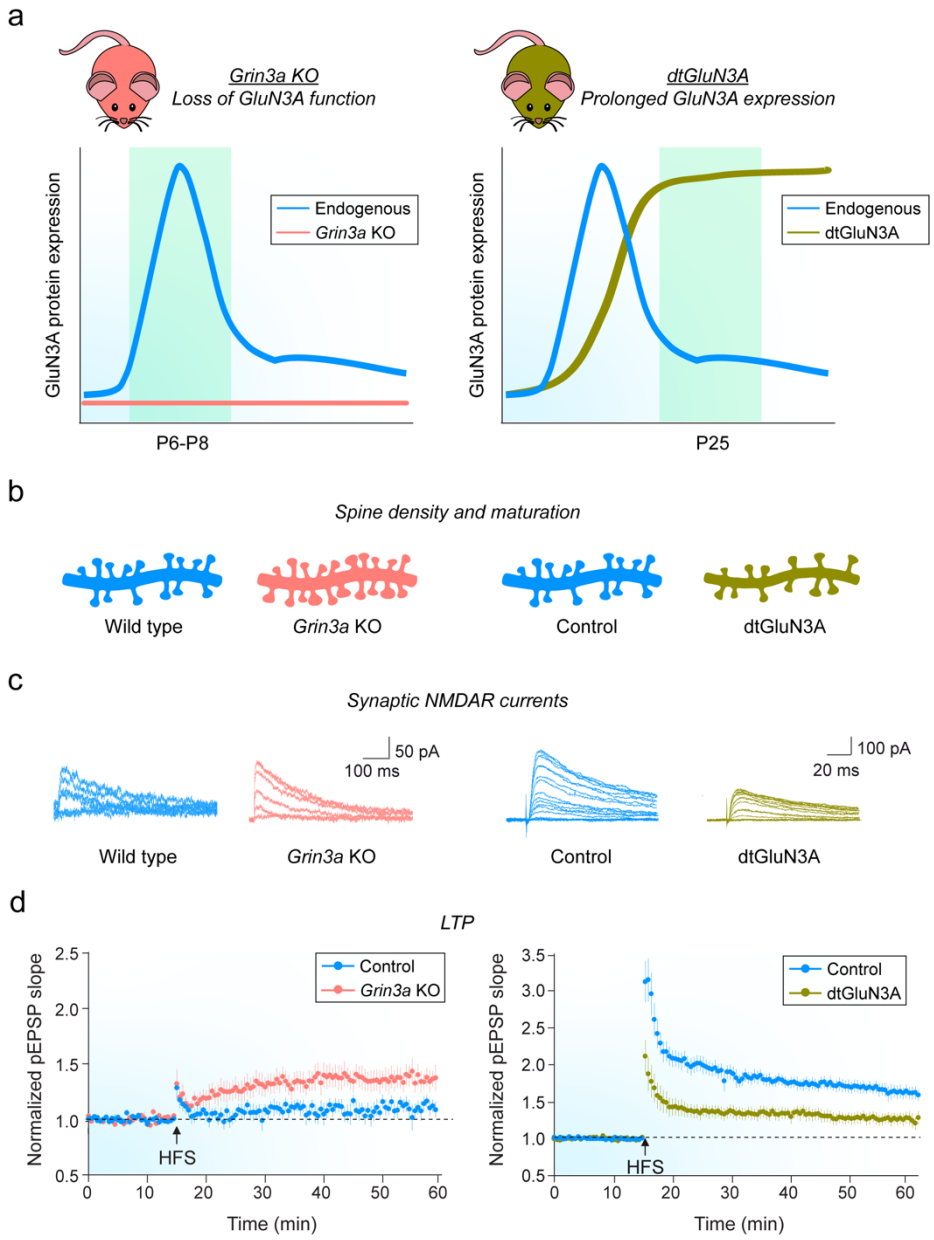

Figure 7. GluN3A-NMDARs in synapse plasticity and maturation.

(a) Effects of loss (*Grin3a -/-* mouse model; red) and prolonged (dtGluN3A mouse model; green) GluN3A protein expression were analyzed at the postnatal stages indicated by the green shaded areas: P6 - P8, peak of endogenous GluN3A protein expression, and P25, when endogenous GluN3A is down-regulated. *(b)* Left, cortical neurons from *Grin3a -/-* mice have increased density of dendritic spines with large spine heads, denoting mature morphology. Right, dendritic spine density and size are conversely reduced in dtGluN3A mice. *(c)* Left, genetic deletion of GluN3A accelerates the development of strong synaptic NMDAR currents in hippocampal CA1 pyramidal neurons (red). Right, on the other hand, prolonging GluN3A expression into later development stages reduces synaptic

NMDAR currents (green). *(d)* Left, genetic deletion of GluN3A increases LTP evoked by high-frequency stimulation (HFS) of Schaffer collaterals (100 Hz for 1s, repeated three times); measured in hippocampal CA1 region at early developmental stages. Right, prolonging GluN3A expression until P25 reduces the magnitude of hippocampal LTP. fEPSP, field excitatory postsynaptic potential. Figure adapted from (Pérez-Otaño et al., 2016).

GluN3A-NMDARs impact in behavior

Recent studies have started to unravel potential behavioral consequences of GluN3A-NMDARs alteration in plasticity. Young (3-4 week-old) *Grin3a -/-* mice exhibit increased pre-pulse inhibition, an indicator of sensorimotor gating, that is normalized in adulthood (Brody et al., 2005). Yu and colleagues described enhanced object recognition, spatial memory and learning in adult *Grin3a -/-* mice (Mohamad et al., 2013), but it is unclear whether this is a consequence of GluN3A absence during early postnatal life or in the adult brain. Memory acquisition is intact in adult dtGluN3A mice, but memory consolidation is disrupted (Roberts et al., 2009). Both Pérez-Otaño and Yu groups found that absence of GluN3A reduces locomotor activity in mice subjected to the open field test, although results from other locomotor tasks such as the rotarod were less clear (Marco et al., 2013; Mohamad et al., 2013). Further studies reported that *Grin3a -/-* mice display increased pain sensation (Mohamad et al., 2013), lowered odor distinguishable abilities (Lee et al., 2016) and impaired social behavior (Lee et al., 2018). More-extensive behavioral profiling should be performed using transgenic mice in which GluN3A expression could be turned off at specific developmental times and controlled genetic backgrounds. This would allow us to distinguish defects caused by altered development from those caused by normal GluN3A function in the adult brain.

1.3.5. Signaling pathways mediating the effects of GluN3A-NMDARs

Conventional NMDARs act as coincident detectors of presynaptic glutamate release and postsynaptic depolarization that drives the induction of LTP and LTD of AMPAR-mediated transmission (Lüscher and Malenka, 2012) and the resulting synaptic structural plasticity (Matsuzaki et al., 2004; Nicoll and Malenka, 1999). LTP has two phases, early (E-LTP) and late (L-LTP), with independent mechanisms regulating the duration of the enhancement of synaptic transmission. While E-LTP lasts 1 to 3 hours, L-LTP can last 24 hours or even longer and

requires the synthesis of new proteins (Huang and Kandel, 1994). Calcium entry via synaptic NMDARs couples this pre- and post-synaptic synergy to intracellular signaling pathways that phosphorylate transcription factors and activate gene expression to support the plastic changes and long-term maintenance of synapses (a phenomenon known as “structural plasticity”) (Hardingham, 2019; Matsuzaki et al., 2004). Some of these pathways are linked to persistent synapse remodeling as well as memory consolidation: *1)* the RAC1–GIT1–β-PIX pathway that controls actin rearrangements (Zhang et al., 2003); *2)* the cyclic AMP-responsive element-binding protein (CREB), that regulates transcription (Atkins et al., 1998; Sheng et al., 1994; Wu et al., 2001); or *3)* the mTOR-dependent mRNA translation, that determines the expression of plasticity-related proteins (PRPs) (see mTORC1 and protein synthesis) (Buffington et al., 2014; Costa-Mattioli and Monteggia, 2013) (Figure 8).

Lower calcium influx through GluN3A-NMDARs could be expected to decrease activity-dependent signaling and gene expression, and might underlie GluN3A effects on LTP and structural plasticity in neurons. To address this, Partha N. Dey (a former PhD student of the lab) performed a screening to test if GluN3A has a global inhibitory effect on NMDAR signaling or selectively inhibits pathways involved in lasting synapse remodeling and stabilization (Dey, 2017). Using primary cortical neurons as a model (Figure 9a), he found that enhancing GluN3A expression attenuated the induction of a subset of NMDAR-dependent signaling pathways, namely phosphorylation of Calcium/ Calmodulin-dependent kinase II (CaMKII), mitogen-activated protein kinase p38 (p38MAPK) and mTOR while pathways controlling activity-dependent transcription such as the extracellular signal-regulated kinases 1 and 2 (ERK1/2) or CREB were unaffected (Figure 9b; up).

Along with the rapid activation of phosphorylation cascades, NMDARs induce de novo expression of PRPs that mediate structural and functional changes in the network (Guzowski et al., 2001; Morgan et al., 1987; Rao et al., 2006; Saha et al., 2011), including the immediate-early genes (IEGs) Arc, c-Fos and Zif268 (also known as Egr1). The induction of Arc and c-Fos proteins was significantly reduced in GluN3A-infected neurons while Zif268 induction was unaffected, indicating that GluN3A does not cause a global inhibition of gene expression programs but targets a different mechanism (Figure 9b; down).

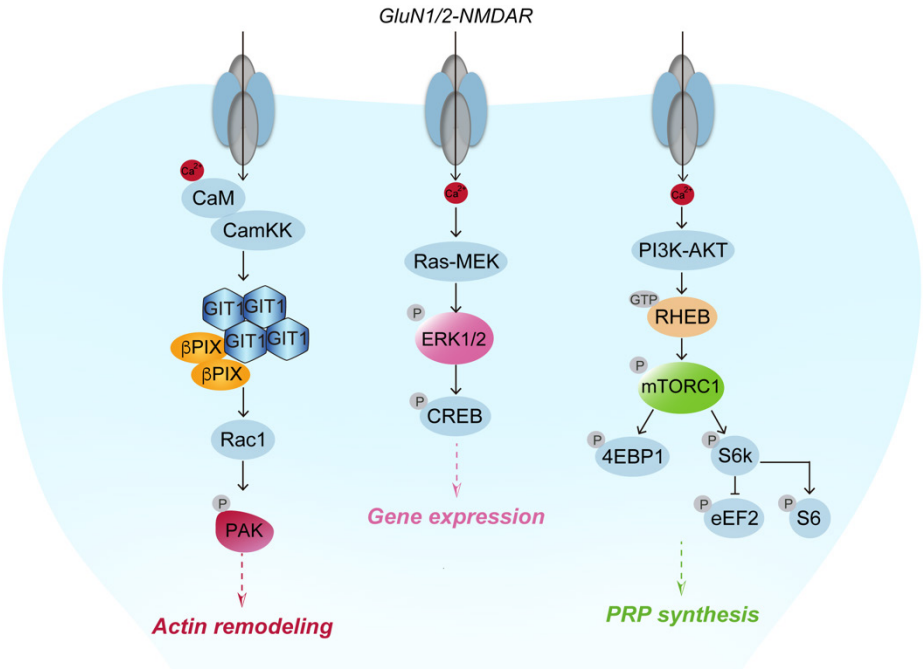

Figure 8. Signaling pathways mediating persistent synapse and spine enlargement and memory consolidation.

Schematic of signaling pathways downstream synaptic NMDARs that support the plastic changes and long-term maintenance of synapses as well as LTM storage upon calcium influx. From left to right: the RAC1–GIT1–β-PIX pathway controls the actin remodeling, the ERK1/2-CREB pathway mediates gene transcription and the mTOR pathway is involved in PRPs synthesis.

Considering the key position of mTOR controlling protein synthesis, a feasible scenario would be that mTOR and PRPs inhibition were related. Two set of experiments linked GluN3A inhibition of the mTOR pathway with the specific suppression of a subset of PRPs. First, the induction of Arc and c-Fos proteins, but not of Zif268 protein, was blocked by the specific mTOR inhibitor rapamycin. Second, restoring mTOR activation by expressing a constitutively active form of Rheb was sufficient to normalize Arc and c-Fos induction even in the presence of elevated GluN3A levels (data not shown).

Thus, Partha N. Dey's work provided insight onto the specific restriction by GluN3A of two major signaling pathways involved in long-lasting structural synaptic remodeling and memory consolidation: phosphorylation of the postsynaptic kinase CamKII and activation of the mTOR protein synthesis pathway (Dey, 2017).

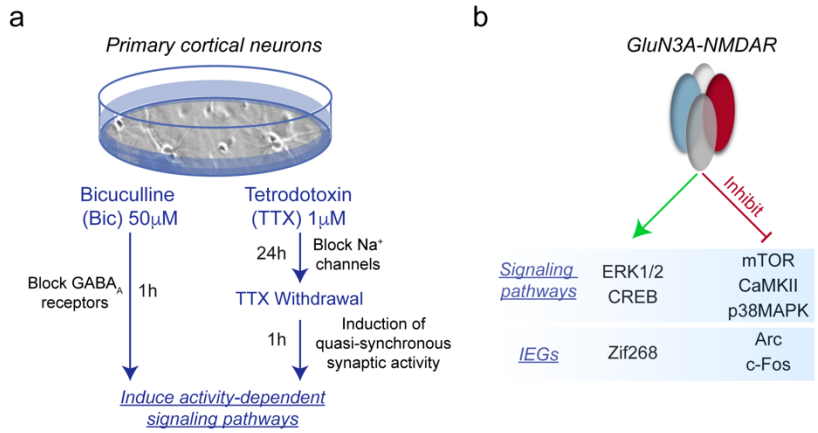

Figure 9. GluN3A-NMDARs selectively inhibit a specific subset of signaling pathways and IEGs.

(a) Scheme of protocols used for the induction of synaptic activity in primary cortical cultures to induce activity-regulated signaling pathways (Dey, 2017). *(b)* Up, GluN3A-NMDARs inhibit a specific subset of signaling pathways involved in structural plasticity and memory consolidation without affecting others. Namely, GluN3A inhibits the activation of mTOR, CaMKII and p38MAPK signaling pathways while it allows ERK1/2 and CREB signaling pathways activation. Down, GluN3A also selectively inhibits the IEGs Arc and c-Fos at the protein level without affecting Zif268.

1.3.6. GluN3A dysregulation is linked to CNS disorders

Growing evidence links even subtle deficits in the balance between synapse maturation and pruning to severe brain disorders, ranging from autism, schizophrenia or bipolar disorder to neurodegenerative conditions that debut in adult life. Notably, adult reactivation of GluN3A expression or function has been shown to reinstate a juvenile state of synapse plasticity and spine turnover which also underlies synaptic and cognitive deficits in major brain disorders. Here, the focus will be placed in human studies (as summarized in a recent review from our group (Crawley et al., 2021)).

Addiction

Substance addictions are chronic and relapsing brain disorders that are extremely dangerous to personal and public health. Recent findings from next-generation sequencing (NGS) or genome-wide association studies (GWAS) have placed GluN3A centre stage in the etiology of addiction (Chen et al., 2018a). *GRIN3A* mRNA levels are increased in the hippocampus and orbitofrontal cortex of

individuals with alcoholism (Jin et al., 2014). Risk of nicotine dependence has also been linked with a number of rare non-synonymous variants in *GRIN3A* gene, as shown in a series of studies performed in European and African-American (Ma et al., 2010; Yang et al., 2015), and Chinese Han populations (Chen et al., 2019a). Moreover, addiction and abstinence to several illicit drugs are also associated to *GRIN3A* gene variants as well as changes in *GRIN3A* mRNA levels of expression. For instance: heroin (Xie et al., 2016), cocaine (Yuan et al., 2013), methamphetamine (Huang et al., 2017) and opioids (Roozafzoon et al., 2010; Wang et al., 2018) addiction.

Behavioral addictions are disorders analogous to substance addiction, with a behavioral core based on repeated performances. Behavioral addictions include from sexual addiction to pathological gambling, being computer game addiction a twenty-first century addiction still barely studied. Interestingly, the mRNA analysis of different NMDAR subunits in human blood lymphocytes revealed a reduction in *GRIN3A* mRNA levels in game addicts (Sadat-Shirazi et al., 2018).

Neuropsychiatric Disorders

GluN3A dysfunction has been linked to psychiatric disorders such as schizophrenia and bipolar disorder. Schizophrenia is believed to originate from a combination of genetic risk and environmental factors, especially *in utero* and in the early postnatal period. Post-mortem studies of individuals with schizophrenia led to controversial results regarding the levels of GluN3A expression in the dorsolateral prefrontal cortex, a relevant region for the pathology that displays reduced spine density in affected individuals (Glantz and Lewis, 2000). Mueller and Meador-Woodruff reported increased GluN3A expression in the dorsolateral prefrontal cortex (Mueller and Meador-Woodruff, 2004), but a second group found no differences of expression in this particular region (Henson et al., 2008). GWAS have identified genetic variants within the protein-coding region of *GRIN3A* in individuals with schizophrenia (Shen et al., 2009; Takata et al., 2013; Yu et al., 2018), with potential functional relevance. Genetic variations or low *GRIN3A* expression levels correlate with improved cognitive performance in traits impaired in schizophrenia, such as working memory (Sadat-Shirazi et al., 2019), associative memory (Papenberg et al., 2014) and prefrontal activation during auditory

processing (Gallinat et al., 2007). Additional links between *GRIN3A* genetic variations and cognitive endophenotypes in schizophrenia are emerging (Greenwood et al., 2011, 2016; Ohi et al., 2015) and a deep analysis will be required.

Bipolar disorder (BD) is a chronic, recurrent and incapacitating mood disorder characterized by episodes of mania/ hypomania and depression interspaced with euthymia. Post-mortem studies of affected individuals revealed a decrease in GluN3A mRNA (Mueller and Meador-Woodruff, 2004) and protein (Rao et al., 2010) levels. On the other hand, a recent publication proposes that drugs employed to treat BD decrease *GRIN3A* mRNA levels by increasing the expression of its negative microRNAs regulators, miR-128 and miR-378 (Kidnapillai et al., 2020).

Finally, (Kazmierski et al., 2014) linked *GRIN3A* genetic variations with post-operative delirium, a neuropsychiatric disorder of unknown pathogenesis.

Neurodegenerative Disorders

Alzheimer's Disease (AD) is a progressive neurodegenerative disorder that results in dementia. One of the few treatments used to mitigate the cognition deficits is the NMDAR antagonist memantine, indicating that a disturbance in glutamatergic transmission might be involved. Surprisingly, studies continuing this line of thinking demonstrate that genetic variations within the coding region of *GRIN3A* are a risk factor for AD in the Taiwanese population (Liu et al., 2009).

Huntington's Disease (HD) is a dominantly inherited neurodegenerative disorder with severe motor, cognitive and psychiatric disturbances that is caused by expansion of a polyglutamine repeat within the N-terminal region of the huntingtin protein. Elevated GluN3A protein levels have been found in the striatum of patients with HD, a region where neurodegeneration is most prominent (Marco et al., 2013). Remarkably, silencing GluN3A expression in a HD mouse model has been proven a potential therapeutic approach, as it improves motor and cognitive symptoms and delays neurodegeneration even at late disease stages (Marco et al., 2018).

2. THE mTOR PATHWAY

In 1994, a Canadian expedition was sent to the Easter Island (natively named Rapa Nui) in search for new compounds. From the soil collected, they isolated a strain of *Streptomyces hygroscopicus* that produced an unknown compound which inhibited yeast growth. They named it rapamycin in deference to its place of origin (Vézina et al., 1975). Further studies boosted the interest in rapamycin, showing that its antiproliferative properties extended beyond fungi and conferred antitumoral and immunosuppressive activities (Eng et al., 1984; Houchens et al., 1983; Martel et al., 1977). However, its mechanism of action remained uncharted for more than 20 years until a series of breakthroughs in the early 90s cracked open both the mystery of rapamycin and one of the most important signaling networks in biology (Liu and Sabatini, 2020; Sabatini, 2017).

First, rapamycin was found to induce immunosuppressant activity by arresting cell cycle at the G1 phase in both mammalian T cells (Bierer et al., 1990; Dumont et al., 1990) and yeasts (Heitman et al., 1991). Second, genetic screening studies using the rapamycin resistant *Saccharomyces cerevisiae* revealed that rapamycin interferes with three genes: FRP1, TOR1 and TOR2. FRP1 encodes the prolyl-isomerase FK-binding protein 12 (FKBP12), an enzyme that assembles with rapamycin in a complex that inhibits cell growth and proliferation (Chung et al., 1992; Heitman et al., 1991). TOR1 and TOR2 (from Target of Rapamycin) encode two protein homologues of a large 289-KDa serine-threonine kinase that were also observed to be essential for yeast cell cycle progression at the G1 phase (Kunz et al., 1993). Nonetheless, the full mechanism of action of rapamycin was only revealed in 1994, when three different groups discovered an eukaryotic TOR orthologue by biochemical affinity purification of the FKBP12 - rapamycin complex: the mechanistic (originally “mammalian”) Target of Rapamycin (mTOR) (Brown et al., 1994; Sabatini et al., 1994; Sabers et al., 1995).

mTOR is an evolutionally conserved serine-threonine kinase that is part of the phosphatidylinositol 3-kinase (PI3K)-related kinase family. Since its discovery, mTOR stood out as a core regulator of signal transduction that integrates extracellular stimuli into intracellular metabolic resources to maintain cellular homeostasis and control cell growth, survival and proliferation (Sabatini, 2017). mTOR is involved in a vast majority of cellular processes: energy metabolism,

lysosome biogenesis, autophagy, cytoskeletal reorganization and lipid, nucleotide and protein synthesis (Liu and Sabatini, 2020). To carry out these functions, mTOR forms two functionally and structurally distinct multiprotein complexes: mTOR complex 1 (mTORC1) and mTOR complex 2 (mTORC2).

2.1. THE MTOR COMPLEXES

mTORC1 and mTORC2 are distinguished by their component proteins, differential sensitivity to rapamycin and distinctive substrates and functions (Figure 10). Besides mTOR, both complexes contain common components: the DEP-domain-containing mTOR-interacting protein (DEPTOR), the mammalian lethal with SEC13 protein 8 (mLST8, also known as GβL) and the scaffold proteins Tti and Tel2 (Costa-Mattioli and Monteggia, 2013; Liu and Sabatini, 2020).

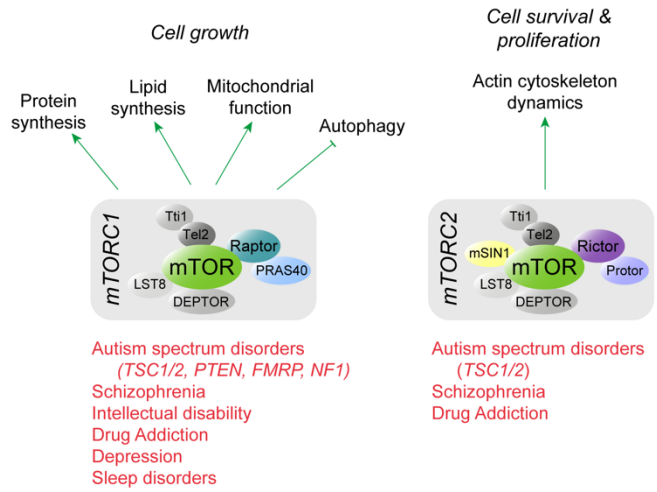

Figure 10. mTORC1 and mTORC2.

mTOR forms two functionally distinct complexes: mTORC1 and mTORC2. mTORC1 integrates information about nutritional abundance and environmental status to tune the balance of anabolism and catabolism in the cell, and thus controlling cell growth. On the other hand, mTORC2 governs cytoskeletal rearrangements and modulates cell survival and proliferation signaling pathways. Unlike mTORC1, which is acutely inhibited by low doses of rapamycin, mTORC2 responds only to chronic rapamycin treatment. Dysregulation of both complexes has been implicated in a variety of neurodevelopmental and neuropsychiatric disorders (further detailed in Dysregulated mTOR and Neurodevelopmental and Neuropsychiatric Disorders).

mTORC1 is characterized by the presence of the regulatory associated protein of mTOR (Raptor) and the proline rich Akt substrate 40 kDa (PRAS40).

Raptor is responsible for the subcellular localization of mTORC1 and mediates substrate recruitment by the recognition of TOR signaling (TOS) motifs (Hara et al., 2002; Kim et al., 2002). Conversely, PRAS40 is an inhibitor of mTORC1 that suppresses substrate recruitment and competes with other mTORC1 targets of phosphorylation (Vander Haar et al., 2007; Sancak et al., 2007). Recent structural studies have shed light on the assembly and activity of mTORC1. mTOR dimerizes with RAPTOR creating a relatively inactive complex that acquires catalytic activity upon binding an essential activator, the small GTPase Rheb (Long et al., 2005; Yang et al., 2017). Crystallography studies show that FKBP12-rapamycin and PRAS40 inhibit mTORC1 by occluding the access of substrates into the kinase active site (Yang et al., 2013, 2017).

mTORC2 contains as defining components the rapamycin-insensitive companion of mTOR (Rictor), mammalian stress-activated MAPK-interacting protein 1 (mSIN1) and the protein observed with Rictor 1 or 2 (Protor 1/ 2). Rictor is a scaffold protein that controls the complex assembly and regulates its substrate specificity (Sarbassov et al., 2004). mSIN1 is involved in the recruitment of substrates into mTORC2 and in its trafficking to de cytoplasmic membrane (Frias et al., 2006; Jacinto et al., 2006; Yang et al., 2006). And Protor 1/ 2 are two Protor isoforms whose regulatory functions are still scarcely known (Pearce et al., 2007; Woo et al., 2007). Unlike mTORC1, only chronic treatment with rapamycin can inhibit the formation and activity of mTORC2, while acute treatment has no effect (Jacinto et al., 2004). Crystallography structural studies revealed that Rictor blocks the FKBP12-rapamycin complex binding site on mTOR and renders mTORC2 insensitive to acute rapamycin treatments (Chen et al., 2018b). Nevertheless, prolonged rapamycin administration can inhibit mTORC2 signaling by sequestering the cellular pool of mTOR into rapamycin-bound complexes that cannot nucleate new mTORC2 (Sarbassov et al., 2006).

2.2. UPSTREAM ACTIVATORS OF MTOR

In neurons, mTORC1 integrates a wide variety of synaptic inputs, including glutamate, changes in cyclic AMP levels and neurotrophins. The latter agglutinates the brain-derived neurotrophic factor (BDNF), insulin and insulin-like growth factor 1 (IGF1) among others. These signals activate NMDAR and/ or tyrosine kinase receptor B (TrkB) and activate the PI3K signaling pathway, probably the best

characterized upstream regulator of mTORC1 (Figure 11) (Costa-Mattioli and Monteggia, 2013; Lipton and Sahin, 2014).

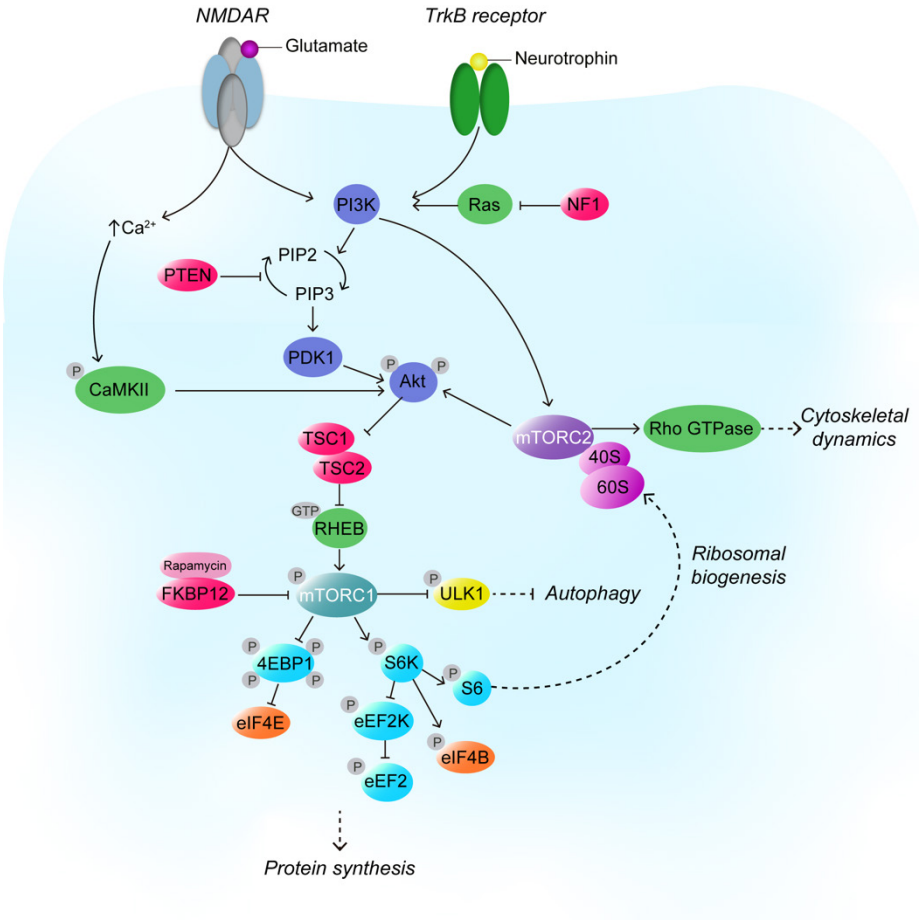

Figure 11. The mTOR signaling pathway in neurons.

Schematic representation of the main upstream and downstream effectors of mTORC1 and mTORC2 as well as their cellular responses.

PI3K activation promotes the conversion of phosphatidylinositol (3,4)-bis-phosphate (PIP2) into phosphatidylinositol (3,4,5)-trisphosphate (PIP3), a process negatively regulated by the phosphatase and tensin homolog (PTEN). Afterwards, PIP3 anchors Akt to the plasma membrane, where it can be phosphorylated and activated by 3-phosphoinositide-dependent protein kinase 1 (PDK1). Akt subsequently phosphorylates and inactivates two proteins in the cascade: PRAS40 and TSC protein 2 (TSC2). PRAS40 inactivation leads to its disassembly from RAPTOR, allowing phosphorylation of mTORC1 targets. TSC2 forms with

TSC1 the TSC1-TSC2 complex, a GAP for the GTPase Rheb. When TSC1-TSC2 is inhibited, Rheb shifts from a GDP-bound inactive conformation into the active GTP-bound one, and activates mTORC1 (Costa-Mattioli and Monteggia, 2013; Lipton and Sahin, 2014).

Little is known about upstream regulation of mTORC2 in the brain. Neurotrophins, glutamate, NMDA and stimuli known to induce long-lasting changes in synapses such as L-LTP have been reported to activate mTORC2 through the PI3K-signaling pathway (Huang et al., 2013). PI3K signaling stimulates mTORC2 binding to the ribosome, which is required for its activation (Zinzalla et al., 2011). Because mTORC1 stimulates ribosome assembly, mTORC1 and mTORC2 are, in some way, both upstream and downstream regulators of each other, which makes the dissection of their tangled signaling properties even more complicated.

2.3. DOWNSTREAM REGULATION OF MTOR

mTOR is a core regulator of neuronal signaling during brain development, and has been implicated in axonal growth and guidance, dendritic development and spine morphogenesis as well as long-term synaptic plasticity. mTOR regulates two main processes necessary for long-term changes that could underlie these roles: *de novo* protein synthesis and structural changes effected by the actin cytoskeleton (Licausi and Hartman, 2018; Lipton and Sahin, 2014).

2.3.1. mTORC1 and protein synthesis

Protein synthesis is the most energy and resource demanding process in growing cells (Buttgereit and Brand, 1995), and it is thus tightly regulated. It follows three main steps: initiation, elongation and termination, with the majority of translational control mechanisms acting at the initiation and elongation steps. At the initiation step, we will focus on mechanisms that regulate the recruitment of the ribosome to the 5'-end of the mRNA, with emphasis on the translation initiation factors eIF2 and the mTORC1-dependent 4E-BPs.

A crucial regulatory step in the initiation of protein synthesis is the assembly of the active eukaryotic initiation factor 2 (eIF2)–GTP and the initiator

methionyl transfer RNA ($tRNA_i^{Met}$) into a ternary complex that binds the 40S ribosome. The initiation factor eIF2 switches from an inactive GDP-bound form to an active GTP-bound one thanks to its GEF, eIF2B. The phosphorylation of eIF2α at Ser^{51} prevents the activity of eIF2B, inhibiting general new protein synthesis and is a strictly regulated molecular event that acts as a master effector of the integrated stress response. Despite this general inhibition, GDP-bound eiF2 permits the translation of a subset of mRNAs that contain upstream open reading frames in their 5'-UTRs, such as the transcription factor ATF4 (Buffington et al., 2014). In recent publications, Sonnenberg, Klann and colleagues proposed eIF2 as the main regulator of *de novo* protein synthesis during LTM consolidation (Sharma et al., 2020; Shrestha et al., 2020a, 2020b). Nonetheless, they also pointed out mTORC1 as a more specific regulator of protein synthesis upon a differential cued threat conditioning paradigm (Shrestha et al., 2020a).

mTORC1 regulates mRNA translation via phosphorylation of two main downstream effectors: the eukaryotic initiation factor 4E (eIF4E)-binding proteins (4E-BPs) and P70S6 kinases (P70S6K/ S6K1 and S6K2) (Figure 11). Most regulated eukaryotic mRNAs bear a methylated guanosine repeat at their 5´-UTRs referred to as ‘‘the cap’’. This structure is regulated by binding of the cap binding protein, eIF4E, which is part of cap-dependent translation complex eIF4F. eIF4E is regulated by binding of 4E-BPs, that inhibit its association with the mRNA cap and suppress translation initiation. mTOR activation promotes 4E-BPs phosphorylation, releases eIF4E from the mRNA cap structure and allows initiation of cap-dependent protein synthesis (Costa-Mattioli et al., 2009). Of note, three different 4E-BP isoforms have been described (4E-BP1/ 2/ 3); 4E-BP2 is the most abundant in the mammalian brain (Banko et al., 2005).

The second mechanism by which mTORC1 regulates translation is phosphorylation of S6K at Thr^{389}, which is a reliable read-out of mTORC1 activity (Ma et al., 2008). S6K promotes protein synthesis by phosphorylating three targets: the 40S ribosomal protein S6, the eukaryotic elongation factor 2 kinase (eEF2K), and the eukaryotic initiation factor 4B (eIF4B). S6 phosphorylation is essential for ribosomal biogenesis and protein synthesis initiation. eEF2K phosphorylation supresses its ability to phosphorylate the eukaryotic elongation factor 2 (eEF2), and dephosphorylated eEF2 stimulates the elongation of nascent peptide chains. Lastly, eIF4B phosphorylation promotes the activity of the RNA

helicase eIF4A and permits the translation of mRNAs with longer 5'-UTRs (Lipton and Sahin, 2014). It has been keenly discussed whether and how mTORC1 signaling regulates specific classes of mRNA transcripts. Global ribosome footprinting analyses have revealed that, although acute mTOR inhibition moderately suppresses general mRNA translation, it predominantly affects mRNAs containing at their 5'-UTR an extensive secondary structure or a 5' terminal oligopyrimidine (TOP) or ''TOP-like'' motifs. TOP mRNAs mainly encode components of the translational machinery, including ribosomal proteins and elongation factors, being translation repressed by this TOP sequences until mTORC1 activation (Costa-Mattioli et al., 2009; Saxton and Sabatini, 2017; Thoreen et al., 2012).

2.3.2. *mTORC1 and autophagy*

Autophagy is a catabolic process that plays a pivotal role in synaptic remodeling and memory formation by maintaining homeostatic protein turnover (Nixon, 2013; Yan et al., 2018). Upon activation, mTOR inhibits autophagy through phosphorylation of Unc-51–like autophagy-activating kinase 1 (ULK1) at Ser^{757}, a target residue of mTORC1 that is a documented as an anti-autophagy site. This, in turn, sequesters ULK-1 away from AMPK, a key activator of autophagy, and prevents the autophagosome formation (Jung et al., 2009; Kim et al., 2011).

2.3.3. *mTORC2 and actin dynamics*

mTORC2 primary functions are the control of cell survival, migration and proliferation. mTORC2 activation is known to regulate actin polymerization by phosphorylating members of the AGC (PKA/ PKG/ PKC) family of protein kinases (Jacinto et al., 2004; Sarbassov et al., 2004) or by directly modulating the Rac1/ PAK signaling pathway (Huang et al., 2013). PKB (also known as Akt) promotes cell survival and growth through the phosphorylation and inhibition of TSC2, that permits mTORC1 activation, or several transcription factors and metabolic regulators (Saxton and Sabatini, 2017).

2.4. mTOR Regulates Brain Physiology and Function

The mTOR pathway is involved in a wide range of neuronal functions, with core roles in early neural development, circuit formation and synaptic plasticity, learning and memory (Figure 12) (Lipton and Sahin, 2014; Liu and Sabatini, 2020).

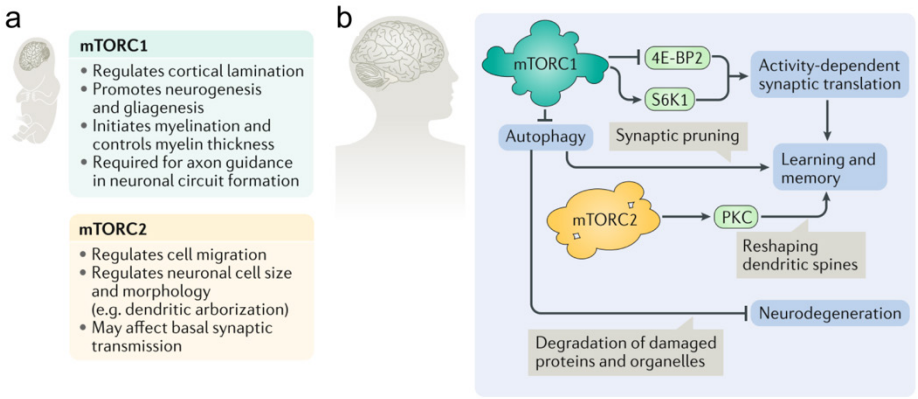

Figure 12. mTOR regulates brain physiology and function.

Figure adapted from (Liu and Sabatini, 2020). *(a)* Roles of mTORC1 and mTORC2 during neuronal development. *(b)* Roles of mTORC1 and mTORC2 in postnatal maintenance of synaptic plasticity. mTORC1 modulates learning and memory through the control of activity-dependent synaptic translation to strengthen or weaken specific neuronal circuits, or via autophagy, to prune obsolete synapses. Autophagy may also play a neuroprotective role by degrading misfolded proteins and damaged organelles. On the other hand, mTORC2 also modulates learning and memory by remodeling the actin cytoskeleton to reshape dendritic spines in response to neuronal signaling.

The first hint demonstrating the relevance of mTOR in brain development came from a mouse mutant ‘‘flat-top’’ that carries a mutation in the mTOR gene. This loss of function mutant exhibited a defect in telencephalon formation and died in mid-gestation (Hentges et al., 2001). A later study using a full mTOR knockout (KO) mouse showed that mTOR controls both cell size and proliferation in early mouse embryos and embryonic stem cells, provoking the early lethality of mTOR KO embryos (Murakami et al., 2004). Complete ablation of the mTOR components Raptor and Rictor also caused embryonic lethality (Guertin et al., 2006; Shiota et al., 2006). Conversely, activation of mTOR at different stages of development led to diverse outcomes. Aiba and colleagues generated transgenic (Tg) mice with gain-of-function mTOR mutations that allow selective activation in the forebrain over defined developmental windows. Early embryonic mTOR activation during

corticogenesis caused the apoptosis of cortical neuronal progenitors without affecting their proliferation, ultimately resulting in cortical atrophy. However, activating mTOR in postmitotic neurons in both juvenile and adult mice caused cortical hypertrophy, increased neuronal cell size and severe epileptic seizures that recapitulates to some extent human TSC (Kassai et al., 2014). Further studies aimed to dissect the roles of mTORC1 and mTORC2 using Raptor and Rictor conditional KOs. mTORC1 was shown to regulate cortical lamination, cell size, neurogenesis and gliogenesis as well as the initiation and thickness of myelination (Bercury et al., 2014; Cloëtta et al., 2013; Wahl et al., 2014). mTORC2 is involved in cell migration and controls neuronal size and dendritic extension (Thomanetz et al., 2013).

mTOR also plays important roles in neural circuit formation and plasticity during development and adulthood (see mTOR and synaptic plasticity, learning and memory; from activity to local protein synthesis). For instance, *Tsc2*$^{+/-}$ mice with disrupted mTOR signaling early in development display aberrant retinotopic mapping due to a defective axonal guidance (Nie et al., 2010), while adolescent (P30) *Tsc2*$^{+/-}$ mice exhibit increased spine density due to defective pruning (Tang et al., 2014).

2.4.1. mTOR localizes at synapses

Localization matters. As previously mentioned mTORC1 controls a wide variety of cellular processes in response to diverse sets of inputs, which requires the proper targeting of mTOR machinery to specific compartments. For instance, mTORC1 response to amino acids rely on its translocation to the lysosome thanks to a concerted action between Rags, Ragulator and v-ATPase that allow its activation by the small GTPase Rheb (Sancak et al., 2008, 2010).

The polarization and extended morphology of neurons makes mTORC1 subcellular localization even more critical for its proper function. Twenty years ago, a pioneer study by Schuman and colleagues demonstrated that mTOR localizes at synapses and is necessary for long-term synaptic plasticity (Tang et al., 2002). Immunostaining experiments in rodent hippocampal neurons found a co-localization of mTOR and its downstream effectors eIF-4E, 4E-BP1, and 4E-BP2 with the postsynaptic protein PSD-95 (Figure 13a). They also found mTOR

expression in the soma, but further experiments in hippocampal slices using the mTOR inhibitor rapamycin pointed towards a local mode of action for mTOR. Rapamycin treatment decreased L-LTP (Figure 13b) and prevented BDNF-induced synaptic potentiation in hippocampal slices (Tang et al., 2002). Later work also supported a L-LTP decrease upon rapamycin treatment in hippocampal slices but only when the drug was applied during induction, being ineffective once L-LTP was established (Cammalleri et al., 2003). This group also found a dendrite-wide activation of S6K in primary hippocampal neurons and slices upon depolarization with KCl or glutamate (Figure 13c). This result suggests a link between the L-LTP induction and the NMDA- and mTOR-dependent activation of S6K in dendrites but not in somas. Consistent with the latter, the sites of dendritic activation of S6K appeared restricted to a subset of spines and discrete compartments along the dendritic shaft, emulating hotspots for fast dendritic translation (Cammalleri et al., 2003).

In parallel, Suzuki and colleagues described mTOR localization at synapses using extensive biochemical characterization of the translational machinery in synaptic fractions (Asaki et al., 2003). Many components of the mTOR pathway –PI3K, Akt, mTOR, 4E-BPs, eIF4E, S6K, S6, eEF2K and eEF2– where present in PSDs, dendritic lipid rafts, and synaptic plasma membrane fractions. Of them, mTOR, 4EBPs, S6 and eEF2K were enriched in the PSD and dendritic fractions (Asaki et al., 2003). The enrichment of S6 in the PSD fraction correlates with the reported presence of ribosomes close to PSDs (Pierce et al., 2000; Steward and Levy, 1982). These findings were corroborated and expanded by Greenberg and colleagues. First, they supported again the presence of the mTOR machinery at the synapse, showing that acute treatment with BDNF caused a rapid activation of S6K and eIF4E in treated dendrites. Second, they proved a functional role of mTOR at the synapse by demonstrating that BDNF induces the local translation of a subset of mRNAs in a rapamycin-dependent manner (Schratt et al., 2004).

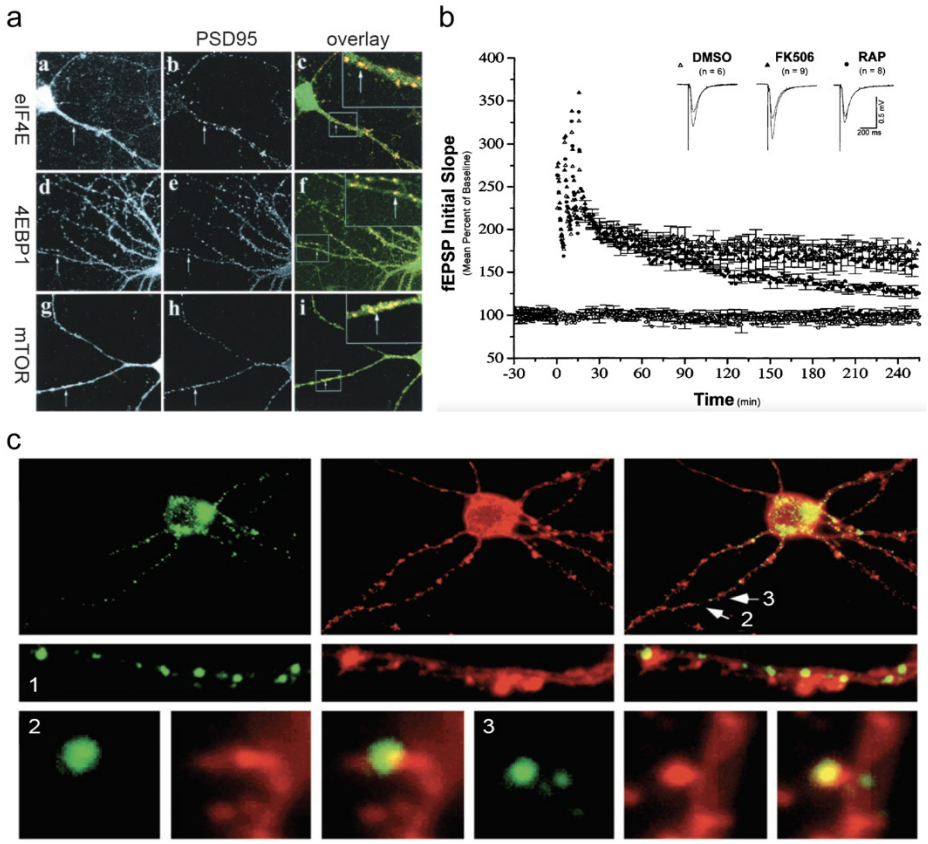

Figure 13. mTOR machinery localizes at postsynaptic compartments.

(a) Modified from (Tang et al., 2002). Synaptic localization of eIF4E ('a'), 4EBP1 ('d') and mTOR ('g') together with PSD-95 ('b', 'e', 'h') in DIV14 primary hippocampal neurons. Insets in the overlays 'c', 'f', and 'I' are higher magnification images from the caged dendritic regions marked by boxes (arrows indicate the synaptic regions that are double-stained). *(b)* From (Tang et al., 2002). Rapamycin decreases the magnitude of late-phase LTP in hippocampal slices. Ensemble averages for DMSO, rapamycin and FK506, a drug that can also bind to FKBP12 but does not inhibit mTOR activity, are presented. *(c)* Modified from (Cammalleri et al., 2003). Dendritic induction of pS6K at Thr^{389} after KCl depolarization in DIV21 primary hippocampal neurons. pS6K staining is shown in green, counterstaining for actin with phycoerythrin-conjugated phalloidin in red and the overlay in yellow. A representative higher magnification of a dendrite is shown in '1'. Higher magnification images showing dendritic spines positive for pS6K immunostaining are shown in '2' and '3'.

Besides its postsynaptic localization, mTOR signaling has also been observed in axons. He and colleagues first demonstrated mTOR to be required for axonal regeneration and survival in the CNS (Park et al., 2008). Using the mTOR downstream effector pS6 as a marker, the authors reported that mTOR is activated after axonal injury in the optic nerve and promotes axonal growth. They also

described a development decline of pS6 expression in retinal ganglion cells (RGCs), suggesting that only a small subset of adult RGCs retain mTOR activity and regeneration capacity. Elimination of mTOR upstream inhibitors such as PTEN and TSC1 also increased axonal growth capacity (Park et al., 2008). This correlated with a second study in which mTOR activity was proven to increase axonal growth in the Peripheral Nervous System (PNS) (Abe et al., 2010). Deletion of the mTOR inhibitor TSC2 in dorsal root ganglial neurons (DRGs) was sufficient to induce axonal growth *in vitro* and *in vivo,* although defects in target innervation were also observed (Abe et al., 2010).

In a later study, mTOR activity was found elevated in axons 3 hours post-injury of the sciatic nerve (SN) (Terenzio et al., 2018). Other components of mTOR signaling (Akt, S6K, S6 and eiF4B) were also activated shortly after injury, together with a decrease in the activity of the upstream inhibitor PTEN. Of note, the authors described that mTOR itself is locally translated after SN injury so it can later regulate axonal local translation. All the effects reported were impaired by the mTOR inhibitor torin-1, suggesting that mTOR regulated its own synthesis in injured axons (Terenzio et al., 2018). Finally, in an elegant study Macklis and colleagues identified the local transcriptomes and proteomes from labelled growth cones (GCs) of single projections *in vivo* (Poulopoulos et al., 2019). They set out to investigate the molecules that form specific connections in GCs and identified mTORC1 foci, but not mTORC2, together with mRNAs that contain mTOR-dependent motifs. They corroborated the results on axonal growth from previous groups, finding that deletion of mTOR resulted in failure of callosal axon growth (Figure 14) (Poulopoulos et al., 2019).

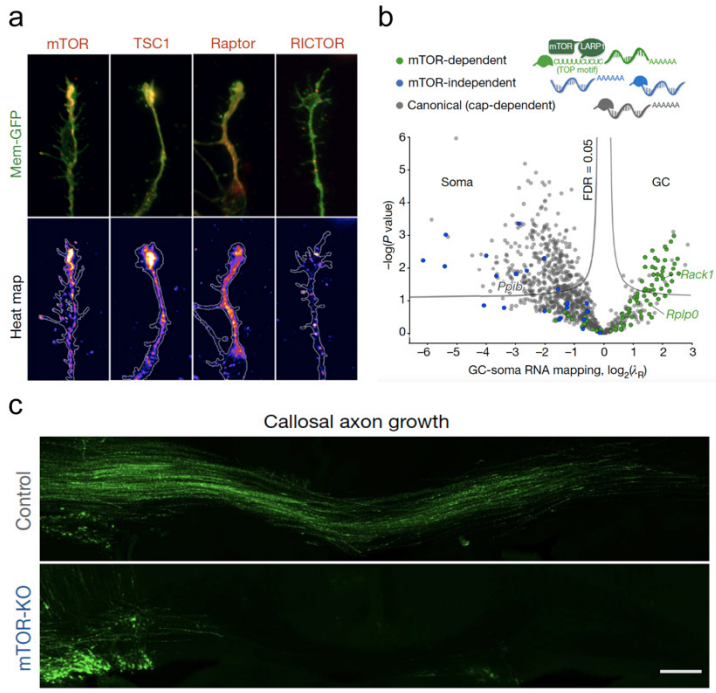

Figure 14. mTOR machinery localizes at presynaptic compartments.

Modified from (Poulopoulos et al., 2019). *(a)* In cultured callosal projection neurons, endogenous mTOR, TSC1 and Raptor appear in dense local foci within GCs from while RICTOR expression is spread in fine granules (red in overlays, heat-mapped in underlying panels) *(b)* Volcano plot of GC–soma RNA mapping, colored according to mTOR-dependent, mTOR-independent or canonical transcript classes. λ_R values plotted for each transcript versus P value (on logarithmic scales). Significance thresholds set to a 0.05 permutation-based false discovery rate (FDR). *(c)* mTOR is required for callosal axon growth. Brains electroporated with GFP (control) or Cre in mice with homozygous floxed-mTOR alleles for conditional KO (mTOR-KO) were examined at P3. Scale bars, 100μm.

2.4.2. mTOR and synaptic plasticity, learning and memory; from activity to local protein synthesis

"…it is possible that synthesis of specific proteins is the essential physical phenomenon paralleling memory, fantasy, and intuition. This hypothesis is supported by the fact that protein synthesis occurs in strongly stimulated neurons and that cells are able to 'learn' to synthesize new specific proteins…."

(Monné A, 1948)

Memories can be divided into short-term memories, lasting from seconds to minutes, and long-term memories, lasting for hours, months, years or even a lifetime (Kandel, 2001). LTP, LTD and associated structural modifications are thought to underlie the long-lasting synaptic changes necessary for the establishment of long-term memories in the brain. More than 70 years ago, it was proposed that the physical root for these processes could be new protein synthesis. It was generally assumed that proteins were synthesized in the soma and later travelled to their final subcellular localization. However, a number of discoveries brought a major shift.

In 1965, Bodian published the first description of ribosome particles in proximal dendrites in monkey spinal cord motoneurons by electron microscopy (Bodian, 1965). In 1982, Steward and Levy revealed polyribosomes at synapses from distal dendrites of dentate granule neurons by electron microscopy as well, indicating that protein synthesis could occur locally at specific synapses (Figure 15a) (Steward and Levy, 1982). In the 90s, Rao and Steward confirmed that isolated synaptoneurosomes could incorporate radiolabeled amino acids into nascent proteins (Rao and Steward, 1991), and Kang and Schuman reported that BDNF-induced LTP requires dendritic protein synthesis, suggesting a functional role in synaptic plasticity (Kang and Schuman, 1996). It was later found that mRNAs are transported to synapses in translationally repressed RNA granules (Martin and Ephrussi, 2009), allowing the selective de-repression of translation (Wang et al., 2010) of activity-induced enriched mRNAs at the base of active dendritic spines (Donlin-Asp et al., 2021). Indeed, many dendritic mRNAs that are translated in response to synaptic stimulation have been found near postsynaptic sites: *Camk2a, Arc, Bdnf, Gria1, Psd95* and many others (Figure 15b,c) (Burgin et al., 1990; Lyford et al., 1995; Muddashetty et al., 2007; Tongiorgi et al., 1997). Moreover dendritic protein synthesis has been dynamically visualized in cultured hippocampal neurons using a combination of puromycin or non-canonical amino acids together with a proximity ligation assay (PLA) to fluorescently tag newly synthesized proteins (Figure 15d) (Dieterich et al., 2010; tom Dieck et al., 2015).

De novo local protein synthesis is a suitable mechanism for a tight spatial and temporal control of gene expression in response to synaptic activity, and the data summarized in mTOR localizes at synapses point towards mTOR as a key regulator (Graber et al., 2013; Jaworski and Sheng, 2006). Beyond the studies

described above (Cammalleri et al., 2003; Schratt et al., 2004; Tang et al., 2002), other publications support such role. Nawa and colleagues demonstrated that BDNF stimulates protein synthesis initiation by activating mTOR signaling (Takei et al., 2001). Using pharmacological inhibition of mTOR by rapamycin or mTOR knockdown (Takei et al., 2004), they showed that local protein synthesis was mTOR-dependent. And, with live cell imaging of primary hippocampal neurons, Sutton and colleagues determined that glycine induced an mTORC1 and protein synthesis dependent structural change in spines (Henry et al., 2017).

Genetic studies shed further light on mTOR-dependent synaptic plasticity. For instance, Costa-Mattioli and colleagues carried out a pharmacogenetic inhibition study using mTOR heterozygous mice ($mTOR^{+/-}$) in combination with a low dose rapamycin treatment (10nM) to inhibit mTORC1 signaling without affecting mTORC2. They concluded that only mTORC1 is required for hippocampal L-LTP (Figure 15e), LTM consolidation and reconsolidation of contextual fear conditioning memory (Stoica et al., 2011). They later used a mTORC2-deficient mouse in which Rictor was conditionally deleted in the murine forebrain postnatally (*Rictor* fb-KO mice). Despite their previous assumptions, they described that both L-LTP and LTM were impaired in hippocampal slices from mTORC2-deficient mice due to defective actin polymerization dynamics (Huang et al., 2013). They also proposed mTORC2 as the main regulator of metabotropic glutamate receptor-mediated long-term depression (mGluR-LTD) (Zhu et al., 2018), a process that is also dependent on new protein synthesis (Huber et al., 2000). Hippocampal DHPG-induced mGluR-LTD was impaired in mTORC2-deficient mice but not in mTORC1-deficient ones (*Raptor* fb-KO mice). They then studied mGluR-LTD contribution to hippocampal learning and memory in these mice using a spatial recognition task and found that only mTORC2-deficient mice displayed impaired novel object recognition (Zhu et al., 2018).

Recently, particular emphasis has been placed on modulation of mTOR-dependent learning by exercise (Chen et al., 2019b) or enriched environment (Hullinger et al., 2015) paradigms. mTOR activation was compared in the motor cortex of runner (subjected to a chronic treadmill exercise training) and nonrunner mice. Enhanced mTOR activity, dendritic spine and PSD formation as well as axonal myelination and increased mTOR-dependent synaptic transmission and motor learning were reported (Chen et al., 2019b). Enriched environment

promoted an enhanced hippocampal LTP that depends on ERK and mTOR activation (Hullinger et al., 2015). By contrast, sleep deprivation reduced mTORC1 activation and the consequent 4EBP2 phosphorylation in the hippocampus, impairing hippocampal protein synthesis *in vivo* (Tudor et al., 2016).

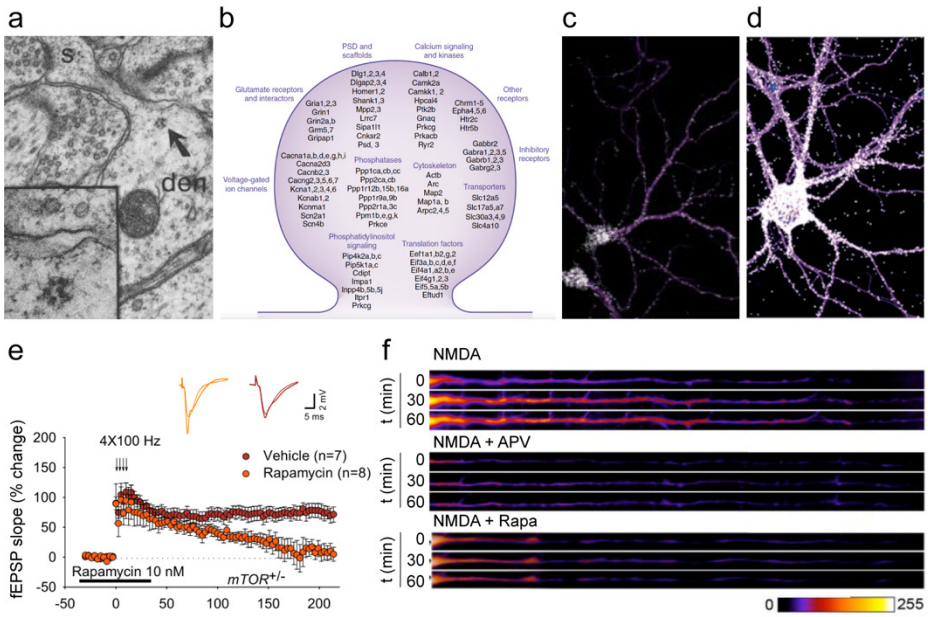

Figure 15. mTOR is a key regulator of synaptic plasticity: from NMDARs to local protein synthesis.

(a) Modified from (Steward and Levy, 1982). Distribution of polyribosomes in dentate granule cells. An arrow indicated the polyribosome; '*s'* indicates a spine head and '*den'* the dendritic shaft. *(b)* From (Cajigas et al., 2012; Holt et al., 2019). Schematic of a subset of mRNAs that encode for synaptically relevant proteins in the postsynaptic compartment. mRNAs were identified by RNA-seq from hippocampal synaptic neuropil. *(c)* Modified from (Holt et al., 2019; Tushev et al., 2018). CamKIIα mRNA (white) detected by FISH in cultured rat hippocampal neurons. Dendrites were immunostained with anti-MAP2 (purple). Scale *(d)* From (Holt et al., 2019). Visualization of newly synthesized CamKIIα protein (white) in neuronal dendrites from hippocampal cultures using the Puro-PLA assay described in (tom Dieck et al., 2015) Dendrites were immunostained with anti-MAP2 (purple) *(e)* From (Stoica et al., 2011). Pharmacogenetic inhibition of mTORC1 impairs L-LTP. Hippocampal slices from mTOR $^{+/-}$ mice treated with a low concentration of rapamycin (10nM) *(f)* Modified from (Gong et al., 2006). mTOR signaling is necessary for NMDAR-dependent dendritic protein synthesis. Dendritic GFP synthesis was induced by NMDA (50μM) and block by the NMDAR antagonist APV (50μM) and the mTOR inhibitor rapamycin (200nm).

2.4.3. mTOR signaling and local protein synthesis are regulated by NMDARs

Neuronal activity regulates the mTOR pathway and NMDARs have been implicated, but the evidence linking NMDAR and mTOR activity is sparse and controversial. In 2005, Lenz and Avruch reported that glutamatergic activation of mTOR in primary cortical neurons is mediated by calcium entry via postsynaptic voltage-dependent Ca^{2+} channels, but insensitive to pharmacological block by APV (Lenz and Avruch, 2005). Snyder and colleagues reported that NMDAR activity decreases mTOR signaling by limiting the uptake of the amino acid L-arginine. Pharmacological block with APV or MK-801 augmented L-arginine transport and increased phosphorylation of S6 and 4E-BP, promoting an increase of GCs and mature mushroom-shaped dendritic spines formation (Huang et al., 2007).

In contrast to the above findings, several publications support a role of NMDAR on activating mTOR. Marin and colleagues reported NMDA-induced phosphorylation of Akt at Ser^{473}, downstream of mTORC2 (Lafon-Cazal et al., 2002). Hardingham and colleagues also demonstrated NMDAR-dependent phosphorylation of Akt at Ser^{473} in response to bicuculline that was blocked with MK-801, and linked synaptic NMDAR and mTOR activity to neuronal survival (Papadia et al., 2005). And as mentioned above, Sanna and colleagues shown NMDAR-dependent increased dendritic phosphorylation of the mTOR downstream effector S6K upon depolarization with KCl or glutamate in both primary hippocampal neurons and slices (Cammalleri et al., 2003).

Specifically, mTORC1-dependent protein synthesis has also been linked to NMDAR activity. In developing synapses, NMDAR-mediated Ca^{2+} influx activates eEF2K, leading to eEF2 phosphorylation and reducing peptide chain elongation. Despite an overall decrease in protein synthesis, CaMKIIα protein levels were significantly increased (Scheetz et al., 2000). The same effect was described by Watson and colleagues (Chotiner et al., 2003). They demonstrated that chemical LTP in hippocampal CA1 lasts for at least 3 hours and requires mRNA and protein synthesis. However, after the first hour of induction there was an unexpected reduction of *de novo* total protein synthesis that was associated to NMDAR-dependent phosphorylation of eEF2 and induction of Arc and c-Fos

proteins (Chotiner et al., 2003). Later studies tried to elucidate if this protein synthesis occurred locally at synaptic places. Tang and colleagues expressed GFP under the control of the 5' and the 3' untranslated regions (UTRs) of CaMKIIα to study its activity regulation. NMDA stimulated dendritic GFP synthesis in a NMDAR and mTOR-dependent manner (Figure 15f) even in the presence of cytoskeleton inhibitors, suggesting again that the synthesis was occurring locally (Gong et al., 2006). Intriguingly, Jan and colleagues found that basal mTOR activity decreased the synthesis of the K_v1.1 voltage-gated potassium channel protein in hippocampal neuronal dendrites, while mTOR block by rapamycin or NMDAR inhibition increased its synthesis (Raab-Graham et al., 2006). Albeit controversial, this finding may imply that mTOR locally increases excitability by decreasing synaptic potassium currents.

Deciphering the contribution of the different NMDAR subunits to mTOR activity could shed light on the conflicting information. For instance, low doses of ketamine induced a rapid activation of mTOR in prefrontal cortex (PFC) synaptoneurosomes and increased PSD-95, Arc, GluR1 and Synapsin I translation and dendritic spine density in a rapamycin-dependent manner (Li et al., 2010, 2011). The GluN2B selective antagonist Ro 25-6981 yielded similar effects to those of ketamine, indicating that GluN2B subunits are main regulators of NMDAR-mediated mTOR signaling (Li et al., 2010). Later work by the authors investigated that both ketamine and Ro 25-6981 reversed depressant-like behaviors upon chronic unpredictable stress (CUS). Blockade of the mTOR pathway obliterates ketamine effects (Li et al., 2011).

Hall and colleagues applied a genetic approach to study the effects of GluN2B subunits on mTOR signaling (Wang et al., 2011). To avoid the perinatal death described in GluN2B full KO, they developed a mouse line where GluN2B subunits were replaced by GluN2A (2B→2A) and a GluN2B conditional KO mice that restricted GluN2B ablation to neocortical and hippocampal glutamatergic neurons (2BΔCtx). Loss of GluN2B in the 2B→2A mouse caused an increase in phosphorylated S6K that was abolished by rapamycin. The result could be interpreted in two ways: GluN2B having an inhibitory role on mTOR or GluN2A having an activatory one. The authors hypothesized that GluN2B exerts a tonic inhibitory effect on mTOR signaling that is needed for homeostatic synaptic plasticity at developing cortical synapses (Wang et al., 2011). Suppression of

mTOR-dependent protein synthesis by GluN2B was further supported by increased dendritic protein synthesis in GluN2B full KO, 2B→2A and 2BΔCtx primary cortical neurons respect to WT neurons that was rescued by rapamycin. The Hall group explored the relevance of these findings to depressive-like behaviors and ketamine-induced protein synthesis (Miller et al., 2014). Cortical neurons and synaptoneurosomal preparations from WT mice injected with ketamine showed a rapid mTOR activation and an increase of dendritic protein synthesis; both effects were occluded in 2BΔCtx mice. The results suggested common mechanisms and linked GluN2B signaling to ketamine's antidepressant actions (Miller et al., 2014). Further evidence came by Fang and colleagues (Yao et al., 2020), which found that the GluN2B antagonist ifenprodil enhances mTOR activity and ameliorates depressive-like behaviors in rats subjected to chronic unpredictable mild stress (CUMS). Ifenprodil treatment also reduced phosphorylation of eEF2 and induced BDNF and GluR1 expression in CUMS rats (Yao et al., 2020). From a mechanistic point of view, Monteggia and colleagues revealed that ketamine block of spontaneous/ tonic NMDARs activity inactivates eEF2K, leading to eEF2 dephosphorylation and enhanced BDNF protein synthesis. Thus, spontaneous NMDAR-mediated activation would modulate the elongation step of protein synthesis rather than the initiation one (Autry et al., 2011; Monteggia et al., 2013).

Independent evidence using a GFP-reporter of dendritic protein synthesis linked GluN2A-containing NMDARs to mTOR-dependent protein synthesis. The GluN2A antagonist NVP-AAM077 but not GluN2B antagonists ifenprodil or Ro 25-6981 blocked the NMDA-induced synthesis of GFP in dendrites of cultured neurons (Tran et al., 2007). Later, Adell and colleagues also proposed GluN2A as the NMDAR subunit controlling mTOR synaptic activity (Gordillo-Salas et al., 2018; Jiménez-Sánchez et al., 2014). The authors reported that the GluN2A specific antagonist NVP-AAM077 elicited rapid antidepressant-like effects, inducing an increased phosphorylation of mTOR that was prevented by the mTOR inhibitor temsirolimus (Gordillo-Salas et al., 2018). Further work is needed to resolve these discrepancies.

References	Model	NMDAR effect on mTOR & protein synthesis	Global NMDAR effect
(Scheetz et al., 2000)	Rat Superior Colliculus synaptoneurosomes treated with NMDA	Increased eEF2 phosphorylation; overall decrease in protein synthesis but increased synthesis of CaMKIIα	Inhibitory
(Lafon-Cazal et al., 2002)	Cultured cerebellar granule neurons treated with NMDA	Increased Akt Ser^{473} phosphorylation	Activatory
(Cammalleri et al., 2003)	Cultured hippocampal neurons and slices treated with NMDA, KCl or glutamate	Increased dendritic S6K phosphorylation	Activatory
(Chotiner et al., 2003)	Hippocampal slices under chemical LTP	Increased eEF2 phosphorylation; overall decrease in protein synthesis but increased Arc and c-Fos	Inhibitory
(Lenz and Avruch, 2005)	Cultured cortical neurons treated with GNA (glutamate + NMDA + APV), BAP (Bicuculline + 4-AP), KCl or BDNF ± APV	mTOR activation is independent on NMDAR activity	None
(Papadia et al., 2005)	Cultured hippocampal neurons treated with BAP ± APV or MK801	Induced Akt Ser^{473} phosphorylation is blocked by NMDAR antagonists	Activatory
(Gong et al., 2006)	Cultured hippocampal neurons treated with NMDA ± APV or rapamycin	NMDAR- and mTOR-dependent dendritic synthesis of a GFP reporter under CaMKIIα UTRs	Activatory
(Raab-Graham et al., 2006)	Cultured hippocampal neurons treated with APV or rapamycin	Increased Kv1.1 synthesis upon NMDAR and mTOR inhibition	Inhibitory
(Huang et al., 2007)	Cultured cortical neurons treated with NMDA ± MK-801	Increased S6 and 4E-BP phosphorylation upon NMDAR blockade; and increased GCs and maturation of dendritic spines upon NMDAR blockade	Inhibitory
(Tran et al., 2007)	Cultured hippocampal neurons treated with NMDA ± NVP-AAM077, ifenprodil or Ro-25-6981	Dendritic synthesis of a GFP reporter under CaMKIIα UTRs is blocked by antagonizing GluN2A	Activatory

(Li et al., 2010, 2011)	Rat PFC synaptoneurosomes treated with ketamine or Ro-25-6981 ± rapamycin	Ketamine and GluN2B antagonists increase mTOR, S6K and 4E-BP1 phosphorylation; increase Arc, Synapsin I, PSD-95 and GluR1 protein levels; and increase dendritic spine density and maturation	Inhibitory
(Autry et al., 2011)	Anterior hippocampal slices from mice receiving ketamine ± MK-801 intraperitoneally (i.p.) and cultured hippocampal neurons treated with ketamine ± APV or TTX	NMDAR blockade by ketamine or APV decreased eEF2 phosphorylation and increased BDNF protein synthesis	Inhibitory
(Wang et al., 2011)	Cultured cortical neurons from WT and 2B→2A mice treated with rapamycin	Increased S6K phosphorylation in 2B→2A neurons in a mTOR-dependent manner	Activatory
(Miller et al., 2014)	Cultured cortical neurons from WT, 2B→2A, 2BΔCtx and 2B full KO mice treated with rapamycin and cortical synaptoneurosomes from WT and 2BΔCtx mice receiving ketamine i.p.	Absence of GluN2B increased basal dendritic protein synthesis in a mTOR-dependent manner occluding further ketamine induction	Activatory
(Gordillo-Salas et al., 2018)	Medial PFC (mPFC) from rat receiving NVP-AAM077 ± temsirolimus i.p.	Increased mTOR phosphorylation upon GluN2A blockade is prevented by temsirolimus; contradictory effect on S6K and 4E-BP1	Inhibitory
(Yang et al., 2019)	NMDA-induced infant spam rat model hippocampus	Increased mTOR and PI3K phosphorylation but not S6K nor Akt	Activatory
(Yao et al., 2020)	Hippocampi and mPFC from rats subjected to CUMS and receiving ifenprodil i.p.	Decreased eEF2 phosphorylation by antagonizing GluN2B; increased BDNF and GluR1 protein levels	Inhibitory

Table 1. NMDAR effects on mTOR signaling and protein synthesis.

Summary of relevant pharmacological and genetic approximations undergone to shed light on the link between NMDAR function and mTOR signaling and its control on protein synthesis.

2.5. DYSREGULATED MTOR AND NEURODEVELOPMENTAL AND NEUROPSYCHIATRIC DISORDERS

mTORpathies are caused by loss-of-function mutations in negative regulators of mTORC1 that result in constitutive or unchecked hyperactivation of mTOR signaling (Liu and Sabatini, 2020) (Figure 10).

Autism Spectrum Disorders (ASDs) stands out as the most studied neurodevelopmental disorders linked to mTOR dysregulation (Costa-Mattioli and Monteggia, 2013; Huber et al., 2015; Lipton and Sahin, 2014). ASDs agglutinates a heterogeneous group of disorders with common symptoms such as impaired social interactions, repetitive behaviors or intellectual disability (DiCicco-Bloom et al., 2006). At the cellular level, ASD patients display increased dendritic spine densities in cortical regions and reduced synaptic pruning during postnatal critical periods (Hutsler and Zhang, 2010; Irwin et al., 2000; Penzes et al., 2011). These disorders are believed to be polygenic, although monogenic syndromes such as TSC, Rett syndrome, Fragile X syndrome (FXS) or Neurofibromatosis type I, have a strong ASD comorbidity (Costa-Mattioli and Monteggia, 2013; Lipton and Sahin, 2014). For instance, mutations in mTOR itself and negative regulators of mTORC1, such as TSC1 or TSC2 (Crino et al., 2006), PTEN (Busch et al., 2019; Zhou and Parada, 2012) and NF1 (Diggs-Andrews and Gutmann, 2013) are associated with upregulation of mTOR signaling and ASD symptoms (Yeung et al., 2017). It is noteworthy that ASD patients holding mutations in *TSC1* or *TSC2* show a loss of cerebellar Purkinje cells and that conditional deletion of *Tsc1* in Purkinje cells of mice recapitulates much of the ASD-like behavior, with both the pathological and behavioral deficits rescued by rapamycin (Bauman and Kemper, 2005; Tsai et al., 2012b).

Recent studies have also linked alterations in mTOR signaling with neuropsychiatric disorders such as depression, schizophrenia or drug addiction. As described in mTOR signaling and local protein synthesis are regulated by NMDAR, many publications link mTOR and depression (Autry et al., 2011; Li et al., 2010, 2011; Miller et al., 2014; Yao et al., 2020). In schizophrenia, knockdown of the disrupted-in-schizophrenia-1 (*Disc1*) gene in newborn neurons in the dentate gyrus induces the activation of both mTORC1-dependent S6 phosphorylation and

mTORC2-dependent Akt Ser^{473} phosphorylation (Kim et al., 2009, 2012). *Disc1* knockdown in adult-born neurons also induces an increased S6 phosphorylation, hyperexcitability and neuronal structure deficits that could be rescued with rapamycin treatment (Zhou et al., 2013).

mTOR has also been linked to drug addiction. Single systemic administration of drugs like cocaine (Wu et al., 2011), tetrahydrocannabinol (THC) (Puighermanal et al., 2009, 2013) or alcohol (Neasta et al., 2010) promote an induction of the mTOR pathway that can be abolished by pre-treatment with rapamycin or temsirolimus. Notably, reconsolidation of alcohol-related memories activates mTORC1 in the amygdala, the mPFC and the orbitofrontal cortex (OFC), and drives the production of plasticity proteins such as Arc, GluN1, GluR1 and PSD-95. Rapamycin-mediated inhibition of mTORC1 in the central amygdala disrupted protein synthesis–dependent alcohol-associated memories, leading to a long-lasting suppression of relapse (Barak et al., 2013).

Finally, mTORC1-dependent autophagy dysregulation is also associated to neurodegenerative disorders (Liu and Sabatini, 2020; Nixon, 2013). Malfunction of autophagic clearance has arisen as a key hallmark of neurotoxic cell death that indorses a progressive but lasting destruction of neurons and the consequent cognition and motor failures. Alzheimer's Disease (Caccamo et al., 2011), Parkinson's Disease (Bové et al., 2011) or Huntington's Disease (Ravikumar et al., 2004) are some representative examples of neurodegenerative disorders that have been related to a mTORC1-dependent autophagy dysfunction.

Objectives

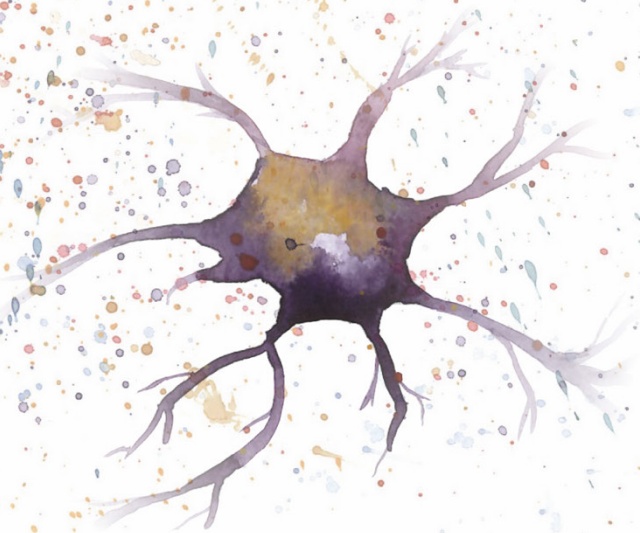

This thesis seeked to untangle signaling and cell biological mechanisms that underlie the effects of juvenile GluN3A-NMDARs in persistent synapse remodeling and memory consolidation. To do so, we set out with the following aims:

I. ***To study the downstream consequences of mTOR inhibition by GluN3A-NMDARs. Specifically, we:***

   i. *Evaluated GluN3A effects on the induction by activity of plasticity-related proteins at the transcriptional and translational level.*

   ii. *Evaluated GluN3A effects on mTOR-dependent protein synthesis.*

II. ***To investigate the mechanisms by which GluN3A expression inhibits synaptic mTOR signaling. With this purpose, the following studies were carried out:***

   i. *Characterization of the role of ionotropic properties and GluN3A C-Terminal Domain interactions on mTOR activation and mTOR-dependent protein synthesis.*

   ii. *Characterization of synaptic GIT1-mTORC1 complexes.*

   iii. *Modulation of GIT1-mTORC1 complexes by GluN3A during development.*

III. ***To evaluate whether and how GluN3A disruption of mTOR signaling modulates cognition.***

Materials & Methods

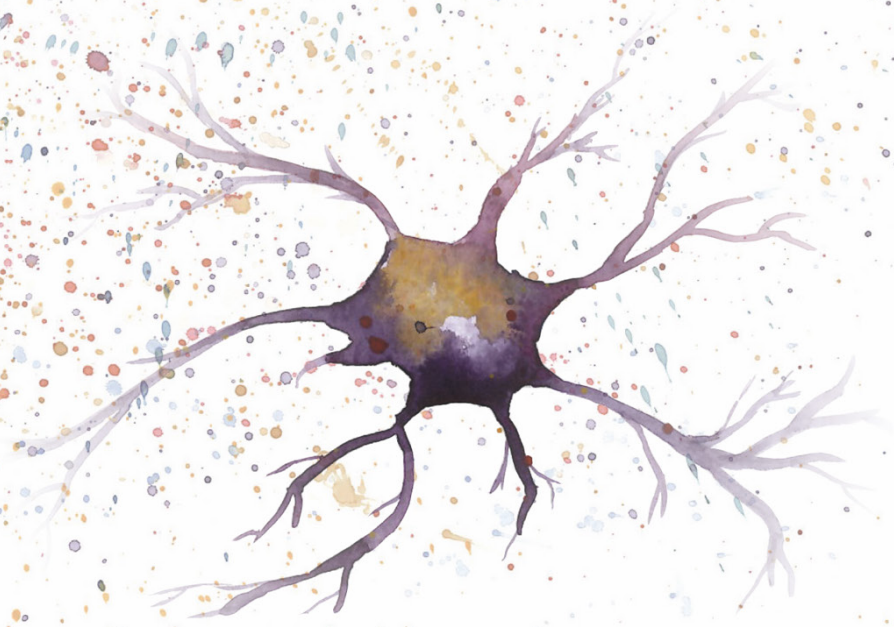

1. ANIMALS

All experimental procedures were carried out according to the Spanish Royal Decree (RD) 53/2013 and Law 6/2013 that transcribes the European Directive 2010/63/UE regarding the "Protection of Vertebrate Animals used for Experimentation and other Scientific Purposes". Procedures involving Genetically Modified Organism satisfied the text in the European Directive 2009/41/CE as well as Spanish Law 9/2003 and RD 178/2004. Procedures were approved by our Animal Experimentation Ethical Committee according to biosafety and bioethical guidelines and authorized by the Spanish Government.

During the first half of the project, mice were maintained at the animal facility of the Centre for Medical Applied Research (CIMA, Pamplona), which is classified as a high standard type II Specific Pathogen – Free (SPF) facility according to the Institute Laboratory Animal Research (ILAR). Later, when our lab moved to the Institute of Neurosciences (IN CSIC-UMH, Alicante), mouse lines were rederived at its animal facility and maintained under standard ILAR type III conditions. In all cases, special attention was given to the implementation of the 3 R's housing and environmental conditions and analgesia to improve the animals' welfare. Mice were regularly screened for pathogens following the Federation for Laboratory Animal Science Associations (FELASA, UK) recommendations for the "Health Monitoring of Mouse Colonies in Breeding and Experimental Units" and maintained in an environment with HEPA (high-efficiency particulate) – filtered air with a rate of 16-20 changes per hour, food and water *ad libitum*, 12 hours light/ dark cycle, regulated temperature of 22 ± 2°C and relative humidity of 55 ± 10%.

1.1. MOUSE LINES

C57Bl/6J JAX™ mice were used as wild-type (WT) controls in the majority of the experiments. Colony founders were obtained from Charles River Europe and raised at CIMA and IN animal facilities. *Grin3a* KO mice (referred as *Grin3a -/-*) were kindly provided by Nobuki Nakanishi and Stuart Lipton (Das et al., 1998) and bred in homozygosis in C57Bl/6J background. Double-transgenic GFP-GluN3A (dtGluN3A) mice backcrossed for 10-12 generations into a C57Bl6/J background were used. dtGluN3A were generated using the tetracycline-controlled transactivator (tTA) system. Briefly, mice expressing the GluN3A coding region

tagged with enhanced green fluorescent protein (GFP-GluN3A) under the control of the tetO promoter, were crossed with mice expressing tTA under the CaMKIIα promoter. The resulting double-transgenic mice expressed GFP-GluN3A in the absence of doxycycline and in a temporal/ spatial pattern dependent on the CaMKIIα promoter (Roberts et al., 2009). Single transgenic mice were used as controls for dtGluN3A mice.

1.2. BRAIN REGION DISSECTION

Dissection of specific brain regions was performed for RNA and protein isolation from WT and *Grin3a* -/- mice at different stages of development. All the procedure was performed using ice-cold reagents and sterilized dissection tools. Mice were sacrificed by decapitation, the skin and the cranium were removed and regions of interest were dissected out using a brain cutting block as a guide and the Allen Brain Atlas as reference. Depending on the experiment, whole cortex, somatosensory cortex or hippocampus were dissected. The resulting fragments of tissue were immediately processed for RNA isolation or snap frozen in liquid nitrogen and stored at -80ºC for protein isolation.

2. CELL CULTURE

2.1. CELL LINES

HEK293T cells (HEK293T/17; ATCC® CRL-11268) were purchased from the American Type Culture Collection (ATCC) due to their high transfectability and capability to produce high titers of infectious viruses. Cells were grown on 75cm^2 flasks (Corning® 430641U) with Dulbecco's Modified Eagle's Medium (D-MEM; Gibco® 10313-021) supplemented with 10% Fetal Bovine Serum (FBS; Gibco® 16140-071), 2% L-glutamine (Gibco® Glutamax™ 35050-061) and 1% Penicillin-Streptomycin (Gibco® 15140-122). Cells were subcultured every 3 days, coinciding with a confluence of 70-80%, in a 1:10 ratio using Trypsin-EDTA (Gibco® 25300-054).

For lentiviral production, cells were cultured with Iscove's Modified Dulbecco's Medium (IMDM + Glutamax™; Gibco® 31980-030) supplemented with

10% FBS, 1% Penicillin-Streptomycin and 1% Sodium Pyruvate (Gibco® 13360-070). This modified media allows the rapid proliferation of high density cell cultures. Culture conditions were 37ºC and 5% CO_2.

2.2. PRIMARY CULTURED NEURONS

Primary cortical and hippocampal neurons were cultured from E19 rat pups as described in (Pérez-Otaño et al., 2006) (Kaech and Banker, 2006) with some modifications. Embryos were obtained from pregnant Sprague-Dawley rats (supplied by Charles River). Mouse cultured neurons were prepared from E17.5 pups from WT and *Grin3a* -/- mice.

For both rat and mouse embryonic primary cortical and hippocampal cultures the protocol followed was the same and is summarized in Figure 16. Briefly, pups were quickly decapitated and the craniums were removed to immerse the brains in cold Hank's Buffer (Sigma-Aldrich® H2387) supplemented with 5μg/ml gentamicin (Gibco® 15710-049) and 10mM HEPES pH 7 (Gibco® 15630-080). Using a dissecting scope, the cerebellum and brainstem were cut out allowing the separation of both hemispheres. The meninges were peeled off and cortical and hippocampal tissues were dissected out. Tissues were digested for 30min at 37ºC with papain (Worthington Biochemical Corporation® LS003126) in the supplemented Hank's buffer detailed above; DNaseI (Sigma-Aldrich® AMPD1-1KT) (50μg/ml) was added for the last 15min. Finally, tissues were washed three times with plating media [Neurobasal medium (Gibco® 21103-049), 5% FBS (Hyclone® SH3007103), 2% B27 supplement (Gibco® 11530-536), 1% Glutamax and 1μg/ml gentamycin] and dissociated into single-cell suspension by a gentle three-steps passage through a 5ml serological pipette.

For biochemistry, cortical neurons were plated on 100mm dishes, 60mm dishes or 6-well plates at a density of $1 \cdot 10^6$, $8 \cdot 10^5$ or $5 \cdot 10^5$ cells/ well respectively. Plates were coated with poly-D-lysine (Sigma-Aldrich® P0899) (100μg/ml) and laminin (Corning® 354232) (1μg/ml) 24h before plating. At day in vitro 3 (DIV3) cells were treated with 10μM of an anti-mitotic mix of 5-fluoro-2'-deoxyuridine (Sigma-Aldrich® F0503) and uridine (Sigma-Aldrich® U3003) (FUDR) to prevent glial overgrowth. Moreover, plating media was sequentially replaced every three

days with serum-free media [Neurobasal medium, 2% B27 supplement, 1% Glutamax and 1μg/ml gentamicin] to achieve cultures serum-deprived.

For immunostaining, hippocampal neurons were plated on 15mm glass coverslips in 12-well plates at a density of $5 \cdot 10^4$ cells/ well. Coverslips were previously washed in absolute ethanol and coated with poly-DL-ornithine (Sigma-Aldrich® P0421) (100μg/ml) and laminin (1μg/ml) 24h before plating. Cells were treated with 10μM of FUDR at DIV5 and fresh feeding media was added every three days.

Our cultures displayed a consistent proportion of GABA-expressing neurons (15-20%) (Dey, 2017).

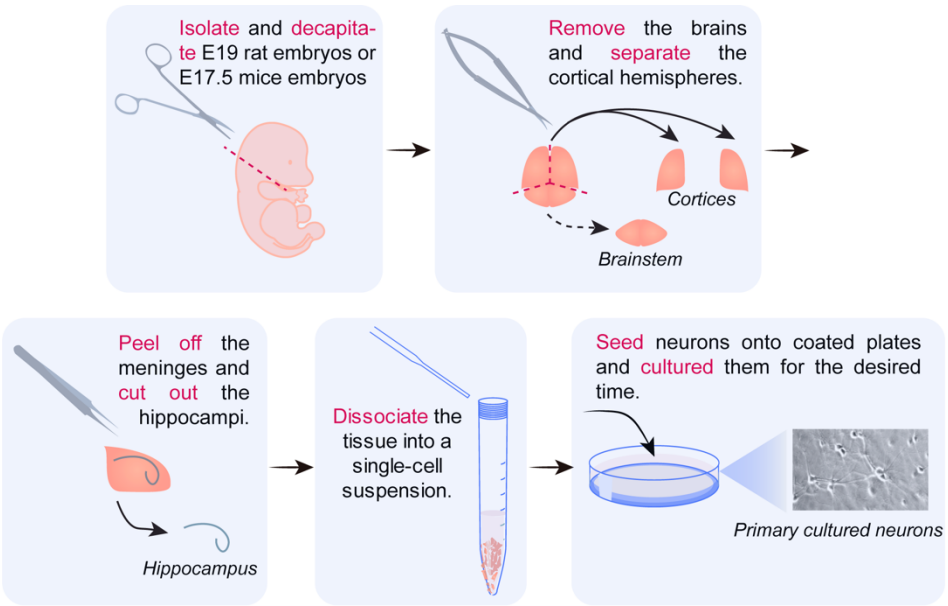

Figure 16. Primary cortical culture.

Schematic diagram of the main steps of the procedure.

3. LENTIVIRAL PRODUCTION

For silencing or prolonging GluN3A expression, and knocking-down its interactor GIT1 in primary cortical cultured neurons, we used lentiviral vectors. Lentiviruses are retroviral vectors consistent on enveloped particles containing a genome based on homodimers of single-stranded RNA (Naldini et al., 1996). They are

characterized for being stably integrated into the host cell genome allowing long-term and constitutive expression of a transgene in both dividing and non-dividing cells (Wollebo et al., 2013). For the reasons given above and their high transduction efficiency, lentiviruses have become a powerful tool for gene transfer in post-mitotic neurons (Gascón et al., 2008).

3.1. RECOMBINANT LENTIVIRAL SYSTEM

A three-plasmid expression system was used to generate infectious but non-replicative lentiviral particles by transient transfection of HEK297T cells.

3.1.1. Transducing vector

Encodes the transgene of interest.

- **hSYNp-WPRE-hSYNp-GFP:** dual-promoter lentiviral vector under the control of the human Synapsin 1 promoter (hSYNp) allow neuron-specific and simultaneous expression of the transgene of interest and GFP, as positive control of the infection (Gascón et al., 2008). This vector was used to prolong GluN3A expression in neurons.
- **pLentiLox3.7-GFP**: lentiviral vector that allows expression of a short hairpin RNA (shRNA) under the U6 promoter and GFP under the cytomegalovirus promoter (CMVp). This vector was used to knockdown GluN3A and GIT1 expression with high specificity.

3.1.2. Packaging vector (pCMVΔR8.91)

Carries the genes necessary for expressing the structural and enzymatic components of the virion (*gag* and *pol*) and for transcriptional and post-transcriptional regulatory functions (*tat* and *rev*).

3.1.3. Envelope vector (pVSVg)

Encodes the G glycoprotein of vesicular stomatitis virus (VSV), which promotes non-specific membrane fusion to broaden the cellular tropism of the vector.

3.2. LENTIVIRAL CONSTRUCTS

The lentiviral constructs used are summarized in Table 2 and Figure 17. Full-length wild-type GluN3A and a set of mutants were cloned into hSYNp-WPRE-hSYNp-GFP: GluN3A1082Δ-GFP lacking the distal 33aa of the CTD (1082-1115) that correspond to the binding site to GIT1 (Fiuza et al., 2013), and GluN3ACt2A-GFP where the CTD of GluN3A was replaced by the corresponding GluN2A's region. For silencing experiments, we used a pLentiLox vector expressing a shRNA against both mouse and rat GluN3A that consist in a 19 base pairs (bp) oligonucleotide directed to the target sequence 'CTACAGCTGAGTTTAGAAA' (shGluN3A1185-GFP; (Yuan et al., 2013)). To silence the scaffolding protein GIT1, we cloned an shRNA against GIT1 directed to the target sequence 'TGATCACAAGAATGGGCATTA' (shGIT1_7730-GFP; (Smithson and Gutmann, 2016)) in a pLentiLox vector.

Name	Transducing vector	Insert	References/ Source
GFP	hSYNp-WPRE-hSYNp-GFP	-	(Gascón et al., 2008)
GFP	pLentiLox3.7-GFP	-	Addgene 11795
GluN3A-GFP	hSYNp-WPRE-hSYNp-GFP	Rat GluN3A (full-length)	(Kehoe et al., 2014)
GluN3A1082Δ-GFP	hSYNp-WPRE-hSYNp-GFP	Rat GluN3A (GluN3A distal CTD mutant lacking the 1082-1115aa)	(Dey, 2017; Fiuza et al., 2013)
GluN3ACt2A-GFP	hSYNp-WPRE-hSYNp-GFP	Rat GluN3A (GluN3A-CTD swapped by GluN2A-CTD)	(Dey, 2017)
shGluN3A1185-GFP	pLentiLox3.7-GFP	shRNA against mouse/ rat GluN3A. Target sequence: CTACAGCTGAGTTTAGAAA	(Yuan et al., 2013)
shGIT1_7730-GFP	pLentiLox3.7-GFP	shRNA against mouse/ rat GIT1. Target sequence: TGATCACAAGAATGGGCATTA	(Smithson and Gutmann, 2016)

Table 2. Lentiviral constructs.

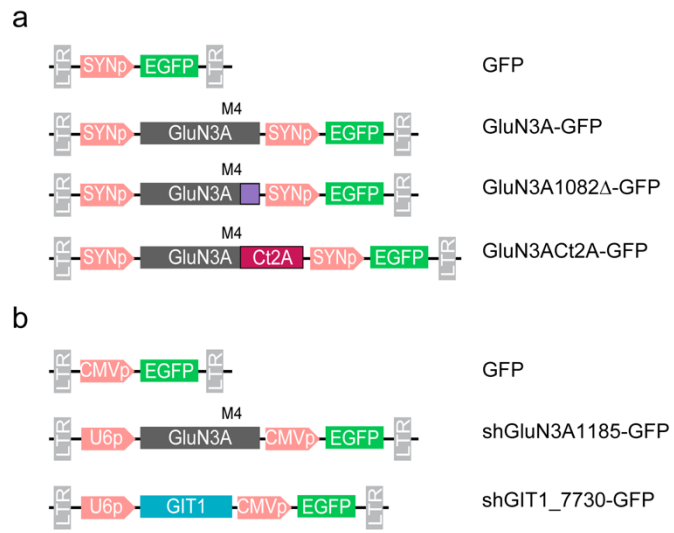

Figure 17. Schematic representation of GluN3A's lentiviral constructs.

Dual promoter lentiviral constructs to prolong *(a)* or silence *(b)* GluN3A expression.

For amplification, the above plasmids were transformed into competent *Escherichia coli* cells (One Shot™ Stbl3™ Chemically Competent E. coli; Invitrogen C7373-03) and grown in selective media. This strain of *E. coli* was chosen because of its reduced rate of homologous recombination of the Long Terminal Repeats (LTRs) present in our lentiviral expression vectors. Plasmid DNA was purified from bacterial cultures using the Nucleobond® Xtra Maxi kit (Macherey-Nagel 740414.50). Briefly, bacteria were lysed and loaded onto the Nucleobond® Xtra column and filter. The lysate was cleared by the filter and the plasmid DNA bound to the column. Finally, the plasmid DNA was washed, eluted, precipitated and dissolved in Milli-Q® water. DNA concentration and purity were assessed with Thermo Scientific™ NanoDrop™ One^{C} Microvolume UV-Vis Spectrophotometer. Furthermore, plasmid DNA integrity was verified by restriction digestion and sequencing.

3.3. LENTIVIRAL PRODUCTION

3.3.1. Transfection of HEK293T/17 – calcium phosphate method

Since its development in the early 1970s, calcium phosphate has been a widely used transfection method due to its low cost and toxicity (Graham and Van der EB,

1973). The principle of the method involves the formation of fine calcium phosphate – DNA precipitates that cells can incorporate by endocytosis thanks to calcium phosphate – mediated binding of the DNA to the cell surface.

The first step was to replace the media of 70-80% confluent HEK293T/17 cells with pre-warmed serum-free Minimum Essential Media (MEM; Gibco® 12492-013) 1h before transfection. In the meantime, the transfection mix was prepared: *i)* we diluted the plasmid DNA in sterile Milli-Q® water in a ratio 2 : 1.5 : 1 (transducing vector : packaging vector : envelope vector); *ii)* we added 312.5mM $CaCl_2$ by the wall and incubated the mix for 5min at room temperature (RT); *iii)* we added the mix dropwise while vortexing to an equal volume of HEPES-buffered saline (HBS) pH 6.97 – 7.03 (2XHBS; 280mM NaCl, 20mM KCl, 0.75mM Na_2HPO_4, 15mM D-glucose, 50mM HEPES); *iv)* the mix was bubbled by pipetting up and down 8-10 times to ensure that the precipitate formed is as fine as possible and incubated in dark for 20min. Then, the transfection mix was added dropwise to each plate and incubated for 6h at 37ºC/ 5% CO_2. After the incubation, the precipitate was dissolved by replacing the media with fresh pre-warmed MEM media and incubating for 16min at 37ºC/ 10% CO_2; this step was repeated twice. Finally, the media was replaced with IMDM supplemented media and incubated for 40h at 37ºC/ 5% CO_2.

3.3.2. Harvest and lentiviral purification

HEK293T/17 cells supernatants were collected 40h after transfection and centrifuged at 1200rpm for 5min to remove cell debris and detached cells. Then, the supernatant was filtered through Millex-HV 0.45μM polyvinylidene difluoride filters (PVDF; Millipore® SLHV033RS) and centrifuged at 28000rpm for 2h at 4ºC using a Beckman Coulter SW28Ti swinging bucket rotor to concentrate the virus particles. The supernatant was carefully removed and the pellets dried out. Later, 180μl of ice cold Phosphate Buffered Saline (PBS) was added to the pellet and left overnight (o/n) at 4ºC. The following day, the pellets were resuspended by pipetting up and down and the viral productions were aliquoted and stored at -80ºC.

3.4. LENTIVIRAL TITRATION IN NEURONAL CULTURES

The transduction efficiency of each viral batch was estimated by immunoblot and immunofluorescence of infected cultured neurons. Immunoblot further allowed us to estimate the degree of silencing or overexpression relative to the endogenous protein levels. In GluN3A overexpression experiments, we only considered apt a 2-to-3-fold overexpression to avoid artefacts. In the following sections, the lentiviral manipulation of GluN3A is taken as example for the titration protocols.

3.4.1. GFP and GluN3A immunoblot

Cortical neurons were infected and lysed at the times indicated in the Results section "Lentiviral Manipulations of GluN3A Expression in Primary Neuronal Cultures". The lentiviral aliquots were thawed slowly in ice and the desired volume was added to each well dropwise. Then, plates were gently swirled to spread the viral particles and were incubated at 37ºC/ 5%CO_2. 24 hours after infection, media was replaced with fresh one to limit toxicity. Four days later, infected neurons were lysed and immunoblotted with antibodies against GluN3A and GluN1, as control.

3.4.2. GFP immunofluorescence

Cortical neurons plated on coated glass coverslips were infected and five days later we performed immunofluorescence staining. The efficiency of neuronal infection was determined by quantifying the co-localization of the neuronal marker NeuN with lentiviral GFP. A minimum of 10 fields per condition were captured using a 10X objective on a Zeiss Axiovert 200M microscope and the percentage of infected *vs* non-infected neurons was calculated. After optimization, we obtained lentiviral batches with a transduction efficiency over 80% that were considered suitable for biochemical experiments (Figure 18).

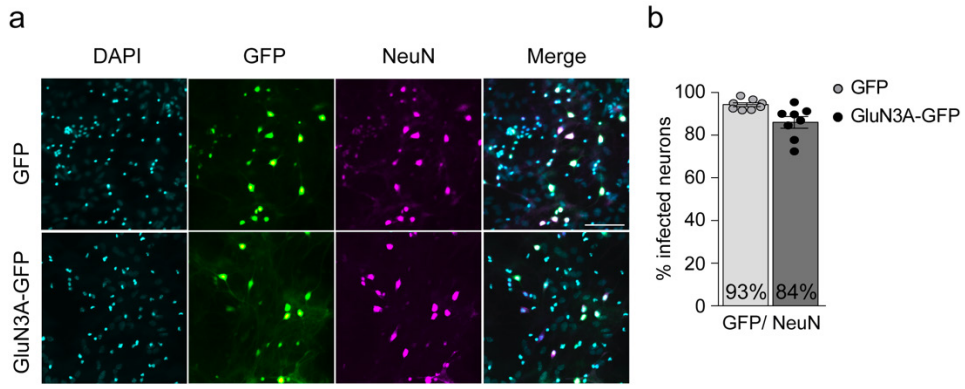

Figure 18. Characterization of transduction efficiency of lentiviral GluN3A.

(a) Representative immunofluorescence images of primary cortical neurons infected with lentiviruses expressing GFP and GluN3A-GFP and immunostained for NeuN (scale bar, 250μM). *(b)* Lentiviral transduction rates calculated as percentage of NeuN positive neurons expressing GFP. Graph corresponds to one batch production (n=8 10X optical fields with a mean of 25 neurons per field from 2 different cultures). Histograms in this and subsequent figures represent mean ± s.e.m. unless otherwise stated.

3.4.3. Biotinylation of Surface Proteins

Cultured neurons plated in 90mm plates at a density of $1 \cdot 10^6$ cells/ well were sequentially washed with DPBS with Ca^{2+} and Mg^{2+} at decreasing temperatures: RT, 10ºC and 4ºC. Next, cells were incubated with 1mg/ml solution of EZ-Link™ Sulfo-NHS-SS-Biotin (ThermoFisher® Scientific™ 211331) for 15min at 4ºC. Excess of biotin was quenched with 50mM glycine (rinsed followed by nutation for 10min 4ºC). and later the glycine solution was removed and cells were harvested with a cell scraper in cold DPBS supplemented with protease and phosphatase inhibitors. Collected cells were centrifuged at 3000rpm for 10min and the pellets were resuspended in Triton X-100 lysis buffer [10mM $NaPO_4$, 150mM NaCl, 5mM EDTA, 0.1% SDS, 1% Triton X-100] also supplemented with proteases and phosphatases inhibitors. Homogenate was sonicated (10 pulses, duty cycle 20, output 3) and kept nutating for 30min at 4ºC. Lysates were then centrifuged at 16000xg for 30min at 4ºC to remove insoluble material. At this point we collected 10% of supernatant and stored it at -80ºC as Total Lysate. The remaining supernatant was incubated with 1:10 dilution of Pierce™ NeutrAvidin™ Plus UltraLink™ Resin (ThermoFisher® Scientific™ 53151) for 2h nutating at 4ºC to obtain the Surface Fractions. Beads were washed 4 times with 500μl of a modified

version of Triton X-100 lysis buffer without SDS by centrifuging at 5000rpm for 5min and bound proteins were eluted in SDS sample buffer for 10min at 65ºC. Surface Fractions and Total Lysates from each sample were analyzed by quantitative Western Blotting.

Surface biotinylation assays were performed to quantify the fraction of exogenously expressed GluN3A that reaches the cell surface in cultured neurons. Comparison of surface-to-total GluN3A levels were in GFP *vs* GluN3A-GFP infected neurons demonstrated that a similar fraction of endogenous and lentiviral GluN3A reached the cell surface; same result was achieved for the AMPAR subunit GluR1, used as positive control of the assay. Therefore, this confirms that regulation of GluN3A surface expression is preserved in our experimental system (Figure 19).

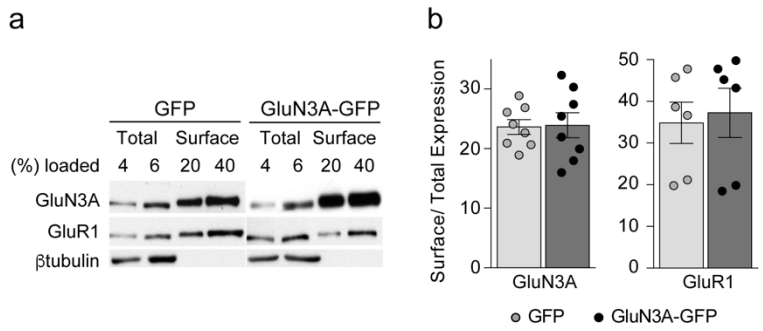

Figure 19. Characterization of surface expression of lentiviral GluN3A.

(a) Surface and total GluN3A and GluR1 protein levels in cultured primary cortical neurons infected with lentiviruses expressing GFP and GluN3A-GFP. Absence of tubulin in the surface fraction validates the effectiveness of the protocol. *(b)* Quantification of surface GluN3A and GluR1 levels normalized to total. n=6-8 from 3-4 independent cultures. ´ns´ paired Student's *t*-test.

4. NEURONAL CULTURE TREATMENTS

Stock solutions of each drug were prepared according to manufacturer's protocols and added to the cultured neurons at the doses and incubation times indicated in (Table 3).

Name and Biological Effect	Dose	Incubation time	Supplier	References
(L,D) APV sodium salt NMDAR antagonist	100μM	15min	TOCRIS® 3693	(Davies et al., 1981; Rao et al., 2006)
Anisomycin Protein synthesis inhibitor	0.8μM	30min	Sigma-Aldrich® A5862	(Aakalu et al., 2001; Grollman, 1967)
BDNF TrkB and p75 receptor stimulator	100ng/ ml	1h	Peprotech® 450-02	(Klein et al., 1991; Takei et al., 2004)
Bicuculline methiodide $GABA_A$ receptor inhibitor	50μM	1h	Abcam® Ab120108	(Curtis DR, Duggan AW, Felix D, 1970; Rao et al., 2006)
CGP-78608 GluN1 competitive antagonist	500nM	Systemic application	TOCRIS® 1493	(Auberson et al., 1999; Grand et al., 2018)
Cycloheximide Protein synthesis inhibitor	25μM	15min	Sigma-Aldrich® C7698	(Baliga et al., 1969; Briz et al., 2017)
Glycine	100μM	6s	TOCRIS® 0219	(Cummings and Popescu, 2015; Grand et al., 2018)
MG-132 Proteasome inhibitor	30μM	1h	TOCRIS® 1748	(Briz et al., 2017; Rao et al., 2006)
Puromycin Label C-terminal of nascent polypeptide chains	10ng/ ml	30min	Sigma-Aldrich® P8833	(Nathans, 1964; Schmidt et al., 2009)
Rapamycin mTOR inhibitor	100nM	1h	Alfa Aesar® J62473	(Heitman et al., 1991; Takei et al., 2004)
U0126 MKK inhibitor	5μM	20min	Abcam® Ab120241	(Barnes et al., 2015; Favata et al., 1998)

Table 3. Drug treatments for cultured neurons.

4.1. BDNF PROTOCOL OPTIMIZATION

We set up a new protocol to induce synaptic activity and mTOR signaling using BDNF. To choose an optimal time-window for mTOR activation, DIV14 serum-deprived primary cortical neurons were incubated with 100ng/ml BDNF for lengths of time ranging from 30min to 4h and induction of the IEG Arc and the mTOR effector p-S6 were evaluated (Figure 20a-c). BDNF treatment for 1h yielded an acute induction of mTOR comparable to the achieved with bicuculline (Figure 20d,e) albeit with higher levels of Arc induction (Figure 20d,f). Taking this into account, we chose 1h of treatment for further experiments.

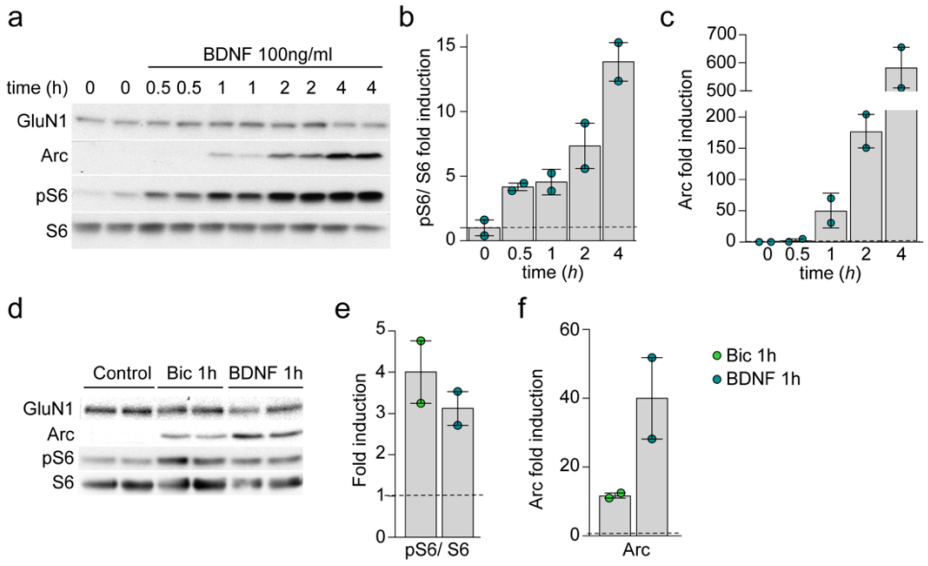

Figure 20. BDNF stimulus as a new protocol for synaptic-activity induction.

(a) Representative western blots of DIV14 serum-deprived cortical neurons treated with BDNF 100ng/ml for increasing periods of time. *(b, c)* Quantification of the induction of phosphorylation of the mTOR downstream effector S6 *(b)* and the IEG Arc *(c)* respect to untreated control neurons. *(d)* Representative western blots of DIV14 serum-deprived cortical neurons treated with bicuculline 50μM and BDNF 100ng/ml for 1h. *(e, f)* Quantification of the induction of phosphorylation of the mTOR downstream effector S6 *(b)* and the IEG Arc *(c)* respect to untreated control neurons. n=2 replicates from 1 preparation of cells.

5. RNA PROFILING

To study the modulation by GluN3A of activity-dependent gene expression programs, we carried out RNA sequencing (RNAseq) and quantitative polymerase chain reactions (qPCR) experiments.

5.1. RNA ISOLATION

5.1.1. *RNA isolation from cell culture*

Cortical cultured neurons plated in 6-well plates at a density of $5 \cdot 10^5$ cells/ well were collected for RNA isolation at DIV14. First, cultures were washed with DPBS with Ca^{2+} and Mg^{2+} (Gibco® 14040-091) and RNA was extracted with the Nucleospin® RNA kit (Macherey-Nagel 740955.50) following the manufacturer's instructions. Briefly, cells were lysed using a buffer that inactivates RNases and favors the adsorption of RNA to the silica membrane of the columns provided. Then, contaminating DNA, salts, and macromolecular cell components were removed with sequential washing steps, and final pure RNA was eluted in 40µl of RNase-free water.

RNA concentration and purity were assessed with NanoDrop™. RNA quality was determined by the RNA Integrity Number (RIN) algorithm using the Agilent® 2100 Bionalyzer Instrument. This equipment performs capillary gel electrophoresis of the RNA samples and generates their electropherogram. Based on the later, RIN algorithm will assign to each sample a score from 1 to 10, being 10 the least degraded; only samples with RIN>9 will match our standards.

5.1.2. *RNA isolation from tissue*

Tissues (see Brain Region Dissection) were weighed upon dissection, homogenized in Qiazol using a tissue disruptor, and RNA isolated using the RNeasy® mini kit (QIAGEN® 74104) following manufacturer's protocol. As above, RNA concentration and integrity were estimated.

5.2. RNASEQ

Whole-genome transcriptional profilingmRNA – strand specific (mRNAseq) were performed in: *1)* cortical cultured neurons, and *2)* tissue samples from the somatosensory cortex and the hippocampus of P11 and P18 WT and *Grin3a* -/- mice. In this thesis, only results from cortical cultured neurons will be discussed.

DIV14 cortical cultured neurons infected at DIV9 with GFP or GluN3A-GFP lentiviruses were treated with bicuculline (50μM, 1h) or BDNF (100ng/ml, 1h) and processed as detailed above. A total of 2-4 samples per condition were collected from 2 different cultures. We performed bulk mRNA sequencing single-end with a length of 50bp using the RNAseq Illumina Hiseq2500. The preparation of the polyA sequencing library, library's quality control and quantification, sequencing run and base calling data were carried out by the Genomics Core Facility of the Centre for Genomic Regulation (CRG, Barcelona). Later, the transcriptomic analysis was performed in collaboration with Prof. Ángel Barco and Sergio Niñerola (IN CSIC-UMH, Alicante). Adapters were trimmed using trim_galore v0.6.4_dev and reads with longer length than 40 bp were selected. Trimmed reads were aligned using star c2.6.1b to the mouse genome (mm10). Reads with mapq >30 were selected using Samtools v1.9. Mapped reads were quantified using R scripts (R version 4.0.3, 2020), Rsubread v2.4.3 and the Mus_musculus.GRCm38.99.gtf annotation data. Differential expression analysis was performed using DESeq2 1.31.1 and limma 3.46.0; genes were annotated using biomaRt v2.46.3 and Volcano plots were performed with EnhancedVolcano 1.6.0. The tracks from the samples were performed with DeepTools v3.5.0, normalized with RPKM and visualization was done in IGV v2.6.3.

5.3. CDNA SYNTHESIS (REVERSE-TRANSCRIPTION)

First strand cDNA was synthesized using the Invitrogen™ SuperScript™ IV First-Strand cDNA Synthesis System (ThermoFisher® Scientific™ 15327696). First, a mix of 1μg of total RNA, 2.5μM Oligo dT primer, 0.5mM dNTP mix and DEPC water was prepared in a final volume of 13μl and incubated for 5min at 65ºC to anneal the primer to template RNA. The reaction was stopped in ice for 1min and later the annealed RNA was combined up to 20μl with the Reverse-Transcription reaction

mix consisting of: 1X SSIV buffer, 5mM DTT, 2U/μl RNaseOUT™ Recombinant RNase Inhibitor and 10U/μl SuperScript® IV Reverse Transcriptase. We briefly centrifuged the mix and incubated it in the PCR Thermocycler at the following conditions: 10min at 50ºC and 10min at 80ºC. Finally, to remove the RNA 1μl of *E. coli* RNase H was added and the mix was incubated for another 20min at 37ºC. The resulting cDNA was stored at -20ºC until use.

5.4. qPCR

qPCR was performed using the Applied Biosystems™ QuantStudio™ 3 Real-Time PCR system and analyzed with the QuantStudio™ 3 Design and Analysis software v1.5.1 from ThermoFisher® Scientific™. First, a 20μl mix was prepared with the ready-to-use PyroTaq EvaGreen qPCR Mix Plus ROX (cmb™ 87H24-001), 5pmol of forward (fwd) and reverse (rv) primers (Table 4) and cDNA. Five-fold serial dilutions of cDNA sample were used to build the standard curve cDNA, being optimal a 1:4 dilution for the target genes and 1:8 for the reference gene GAPDH.

Primer	Host	Sequence (5' – 3')	Fragment size (bp)
Arc_fwd	Mo	GAGCCTACAGAGCCAGGAGA	340bp
Arc_rv	Mo	TGCCTTGAAAGTGTCTTGGA	
Arc_fwd	Rat	GCCACCTGGAAGAGTACCTG	237bp
Arc_rv	Rat	AACTGGTCAAGTGGCTCACC	
BDNF ex. IV_fwd	Mo/ Rat	CGCCATGCAATTTCCACTATCAATAATT TA	273bp
BDNF ex. IV_rv	Mo/ Rat	GCCTTCATGCAACCGAAGTATG	
c-Fos_fwd	Mo/ Rat	CTGCTCTACTTTGCCCCTTCT	215bp
c-Fos_rv	Mo/ Rat	TTTATCCCCACGGTGACAGC	
Egr1_fwd (Zif268)	Mo/ Rat	AGAAGCCTTTTGCCTGTGACA	54bp
Egr1_rv (Zif268)	Mo/ Rat	CGTTCATCACTCCTGGCAAAC	
GAPDH_fwd	Mo/ Rat	CATGGCCTTCCGTGTTCCT	85bp
GAPDH_rv	Mo/ Rat	TGATGTCATCATACTTGGCAGGTT	
Grin1_fwd	Mo/ Rat	TCCACCAAGAGCCCTTCGTG	106bp
Grin1_rv	Mo/ Rat	CCCGTACAGATCACCTTC	
Grin3a_fwd	Mo/ Rat	GCTTCCCAGAGATGCATGAG	176bp
Grin3a_rv	Mo/ Rat	ATGGCTTTCCTACGGTCAGA	

Homer1a_fwd	Mo/ Rat	CAAACACTGTTTATGGACTG	300bp
Homer1a_rv	Mo/ Rat	TGCTGAATTGAATGTGTACC	
Npas4_fwd	Mo/ Rat	CTGGCCCAAGCTTCTTCTCA	419bp
Npas4_rv	Mo/ Rat	TCCATGCTTGGCTTGAAGTCT	

Table 4. List of primers used in qPCR analyses.

Next, qPCR was run in triplicates in the conditions referred in Figure 21. Mean cycle threshold (Ct) values for each reaction were recorded and the relative RNA expression levels were calculated referring to GAPDH: $\Delta Ct = Ct_{GAPDH} - Ct_{target\ gene}$. Then, the gene expression fold change normalized to GAPDH and relative to control sample was calculated as $2^{\Delta Ct}$.

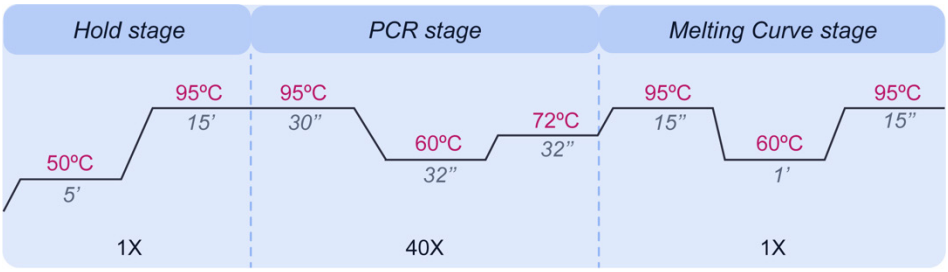

Figure 21. Cycle parameters used for amplification by qPCR.

6. PROTEIN SAMPLE PREPARATION

6.1. CELL CULTURE LYSATES

Cortical neurons were washed with DPBS with Ca^{2+} and Mg^{2+}, and collected with a cell scraper in prewarmed lysis buffer [50mM Tris-HCl pH 6.8, 10% glycerol (Sigma-Aldrich® G5516), 2% SDS (Sigma-Aldrich® L4509), 0.1M fresh (D,L)-Dithiothreitol (DTT; Sigma-Aldrich® D0632), 0.04% bromophenol blue] supplemented with protease (cOmplete™ Protease Inhibitor Cocktail; Sigma-Aldrich® 4693116001) and phosphatase inhibitors (PhosSTOP™; Sigma-Aldrich® 4906845001). Samples were boiled for 10min at 65ºC, centrifuged 1min at maximum speed and stored at -80ºC until processing by Western Blotting. To this effect, equal volume of samples was loaded and Ponceau S staining and GluN1 or β-tubulin were used as loading controls.

6.2. TISSUE LYSATES

The dissected regions of interest (see Brain Region Dissection) were thawed in ice and homogenized using a motor-driven teflon – glass douncer (Heidolph RZR-1, 600-800rpm, 12 strokes) in 15 volumes (w/v) of cold RIPA lysis buffer [50mM Tris-HCl pH 7.5, 150mM NaCl, 1% NP-40 (IGEPAL® CA-630; Sigma-Aldrich® I8896), 0.05% deoxycholate, 0.01% SDS] supplemented with protease and phosphatase inhibitors. Homogenates were sonicated with a Branson tip – sonicator (20 pulses, duty cycle 20, output 3), nutated for 15min at 4ºC, sonicated again using the same parameters and centrifuged for 20min at 16200xg and 4ºC. The resulting supernatant was recovered and stored at -80ºC.

Protein concentration was estimated comparing to a BSA protein standard curve using the Pierce™ BCA Assay kit (ThermoFisher® Scientific™ 23227) and measuring the absorbance at 562nm with a microplate reader (Biochrom EZ Read 400).

6.3. SUBCELLULAR FRACTIONATION

The biochemical fractionation method used was previously described in (Franchini et al., 2019) and is summarized in Figure 22. Briefly, cortical cultured neurons plated in 60mm dishes were washed with DPBS with Ca^{2+} and Mg^{2+} and homogenized using a glass-glass homogenizer at 4ºC in a mild homogenization buffer [320mM sucrose,1mM HEPES, 1mM $NaHCO_3$, 1mM $MgCl_2$, 0.1mM PMSF, 1mM NaF] supplemented with proteases and phosphatases inhibitors. To purify Crude Membrane Fractions (P2) and post-synaptic Triton Insoluble Fractions (TIF), total homogenates (H) were firstly centrifuged at 1000g for 5min at 4ºC to remove nuclei and achieved a Postnuclear Supernatant (PNS or P1). The resulting supernatant was later centrifuged at 13000g for 15min at 4°C. An aliquot of the pellet was taken for the P2 fraction and dissolved in 20mM HEPES buffer. The rest was dissolved in a buffer containing 1% Triton X-100 (Sigma-Aldrich® T8787) and 150mM KCl, incubated on ice for 15min and centrifuged at 100000g for 1h at 4°C. The resulting pellet (TIF) was homogenized using a glass-glass homogenizer in 20mM HEPES buffer.

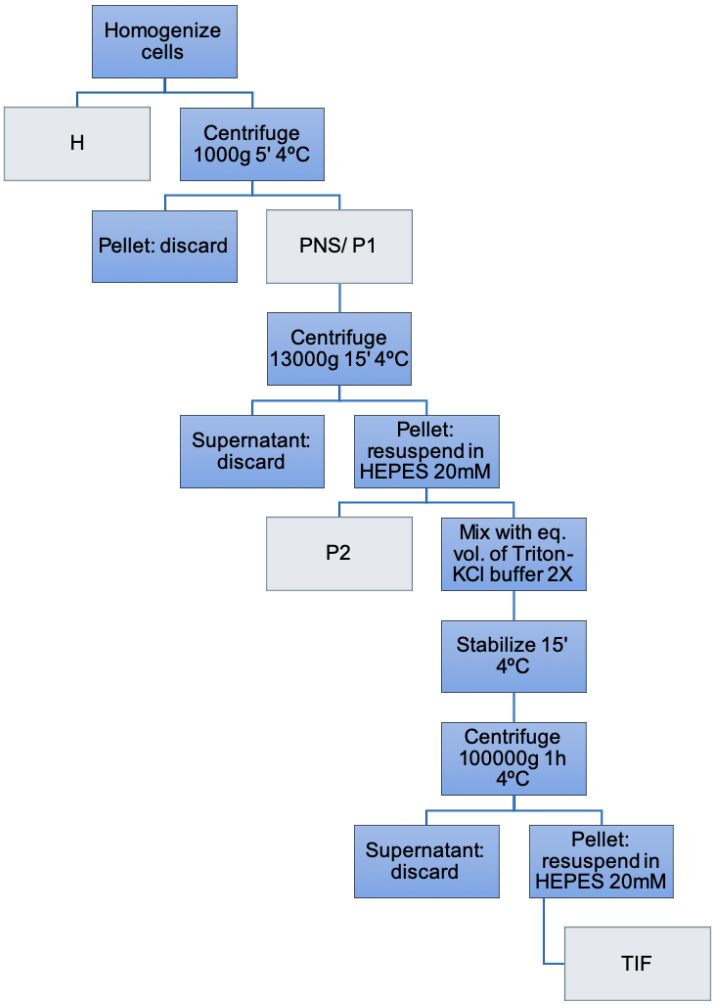

Figure 22. Schematic of the subcellular fractionation protocol.

7. CO-IMMUNOPRECIPITATION

PNS from mouse hippocampus or cortex or total homogenate/ P2/ TIF from cultured cortical neurons were solubilized at 4°C for 30min. For most conditions, 0.1% Triton X-100 + 0.1% SDS lysis buffer [150mM NaCl, 10mM EDTA, 50mM HEPES, 0.1% Triton X-100, 0.1% SDS] supplemented with protease/ phosphatase inhibitors was used. However, Triton X-100 disrupts the interaction between mTOR and Raptor (Kim et al., 2002). Thus, to study this particular interaction, we used a 0.3% CHAPS lysis buffer [150mM NaCl, 1mM EDTA, 40mM HEPES, 0.3% CHAPS (Sigma-Aldrich® C3023)] supplemented with protease/ phosphatase inhibitors.

Insoluble material was removed by centrifugation at 16.250g for 15min and the resulting supernatants were incubated overnight at 4°C with primary antibody (Table 5). As control, samples were incubated in the same experimental conditions without antibody (IgG- control). Later, samples were incubated with a 1:1 mix of protein A and protein G magnetic beads (BioRad® Surebeads™ 1614013 – 1614023) for additional 2h at 4ºC on a wheel. Beads were precipitated using a magnetic rack, washed thrice in lysis buffer, and immunoprecipitated proteins were eluted with SDS sample buffer to resolve them by Western Blotting. For the input lane, 10% of the sample used for the co-immunoprecipitation (co-IP) experiment was loaded onto the gels.

Antibody	Supplier	Catalog number	Host	Working dilution
GIT-1	Cell Signaling Technology® (CST)	2919S	Rabbit	1:200
mTOR	CST	2972S	Rabbit	1:100

Table 5. Primary antibodies used for co-IP.

8. WESTERN BLOTTING

8.1. SDS-PAGE ELECTROPHORESIS

Proteins were resolved in a discontinuous denaturing buffer system using sodium dodecyl sulfate – polyacrylamide gel electrophoresis (SDS-PAGE). The Criterion™ System (BioRad® 1656025) was selected to run midi-format vertical electrophoresis with capacity up to 26 samples per gel.

Hand-casted gels were prepared in commercial cassettes (BioRad® 345990-1/2/3) and consisted of a large-pore stacking section on top of a small-pore resolving one. Different concentrations of polyacrylamide (6-14%) were used in the resolving gel to separate proteins from a wide range of molecular weights. The resolving gel [Acrylamide/ Bis-Acrylamide 37.1:1 (BioRad® 161-0148), 375mM Tris-HCl pH 8.8, 0.1% SDS, 0.05% APS (Sigma-Aldrich® A3678), 0.05% TEMED (Sigma-Aldrich® T9281), distilled water] was mixed in a falcon and poured smoothly in the cassette. The solution was overlaid with 2-propanol to achieve an aligned upper border and left to polymerize for 30min. Once solidified, 2-propanol

was removed and the gel surface was rinsed with distilled water. The stacking gel (Acrylamide/ Bis-Acrylamide, 125mM Tris-HCl pH 6.8, 0.025% SDS, 0.05% APS, 0.1% TEMED, distilled water) was then poured on top of the resolving gel and the comb, with a variable number of wells depending on the experiment, was inserted in the cassette and left to polymerize for another 30min.

The polymerized gels were placed in the electrophoresis chamber and filled with Electrophoresis Running Buffer (25mM Tris-HCl, 192mM glycine, 0.1% SDS). The combs were removed and denatured samples were loaded into the wells along with a prestained protein weight marker (Nippon Genetics® MWP04). Electrophoresis was performed at 100V till the samples piled up onto the resolving section and then at 120V to allow the protein migration until the dye front reached the bottom of the gel. When the electrophoresis was over, the cassettes containing the gels were carefully broken to take out the gels.

8.2. IMMUNOBLOTTING

Proteins were transferred from the gel to 0.45μM PVDF membranes (GE Healthcare® 10600023). First, gels were equilibrated for 10min in Transfer Buffer (10mM Tris-HCl, 100mM glycine, 5% methanol) to wash out the excess of SDS and the PVDF membranes were pre-activated in methanol. Next, using the Criterion Blotter set the transfer cassettes sandwiches were prepared by sequentially adding one fiber pad, three Whatman® filter papers, the gel, the PVDF membrane, three Whatman® filter papers and another fiber pad. Finally, the transfer cassettes were closed avoiding bubbles formation and placed within the chamber with the gel facing the cathode end so proteins can migrate from the negative to the positive pole. The chamber was filled with cold Transfer Buffer and blotting was carried out at constant 300mA for 2h at 4ºC.

Blotting efficiency was verified with a Ponceau S staining [0.1% (w/v) Ponceau S (Sigma-Aldrich® P3504) in 5% (v/v) acetic acid]. For that purpose, membranes were taken from the transfer sandwich, rinsed with distilled water and incubated in Ponceau S for 10min.

Unoccupied protein-binding sites on the membranes were saturated to prevent nonspecific binding of antibodies by blocking with 5% Bovine Serum

Albumin (BSA; Sigma-Aldrich® A9647) in Tris Buffer Saline 0.05% Tween 20 (TBS-T) for 1h at RT.

8.3. IMMUNODETECTION

The blots were probed for the proteins of interest with specific primary antibodies (Table 6) diluted in TBS-T + 2% BSA o/n at 4ºC.

Antibody	Supplier	Catalog number	Host	Working dilution
Arc (clone C-7)	Santa Cruz Biotechnology® (SCB)	Sc-17839	Mo	1:100
β-PIX, SH3 domain	Millipore®	07-1450	Rb	1:1000
c-Fos (clone 4)	SCB	Sc-52	Rb	1:500
eEF2	CST	2232S	Rb	1:1000
Egr-1 (also named Zif268) (clone 588)	SCB	Sc-110	Rb	1:500
GFP (clone JL-8)	Clontech®	632381	Mo	1:2000
GIT-1	CST	2919	Rb	1:1000
GluN1 (clone R1JHL)	Millipore®	MAB1586	Mo	1:1000
GluN2A (clone A12W)	Millipore®	05-901R	Rb	1:1000
GluN2B (clone BWJHL)	Millipore®	05-920	Mo	1:1000
GluN2A/B	Millipore®	AB1548	Rb	1:1000
GluN3A	Millipore®	07-356	Rb	1:1000
GluN3A	Neuromab®-University of California (produced by Jim Trimmer)		Mo	1:100
GluR1	Millipore®	AB1504	Rb	1:1000
mTOR	CST	2972S	Rb	1:1000
Meox2	ThermoFisher® Scientific™	PAS-51005	Rb	1:1000
P44/42 MAPK (Erk 1/2)	CST	9102S	Rb	1:1000
P70 S6 kinase	CST	9202S	Rb	1:1000
Phospho-4EBP1 (Thr37/46)	CST	2855S	Rb	1:500
Phospho-eEF2 (Thr56)	CST	2331S	Rb	1:1000
Phospho-mTOR (Ser2448)	CST	2971S	Rb	1:1000

Phospho-p44/42 MAPK (Erk1/2) (Thr202/ Tyr204)	CST	9101S	Rb	1:1000
Phospho-p70 S6 kinase (Thr389) (clone 108D2)	CST	9234S	Rb	1:1000
Phospho-p70 S6 kinase (Thr421/ Ser424)	CST	9204S	Rb	1:1000
Phospho-S6 ribosomal protein (Ser240/244)	CST	2215S	Rb	1:1000
Puromycin (clone 12D10)	SIGMA-Aldrich®	MABE343	Mo	1:2000
Raptor (clone 53A2)	CST	2114	Rb	1:500
Rictor (clone 24C12)	CST	2280	Rb	1:1000
Rheb (clone E1G1R)	CST	13879S	Rb	1:1000
S6 ribosomal protein (clone 5G10)	CST	2217S	Rb	1:1000
Synaptophysin (clone SY38)	Millipore®	MAB5258	Mo	1:2000
β-Actin	SIGMA-Aldrich®	A5441	Mo	1:15000
β-Tubulin class III	SIGMA-Aldrich®	T8660	Mo	1:20000

Table 6. Primary antibodies used for immunoblotting.

The membranes were washed with TBS-T for 30min and incubated with horseradish peroxidase (HRP)-conjugated secondary antibodies (Table 7) diluted in TBS-T + 2% BSA for 1h at RT. They were then washed with TBS-T for another 20min and with TBS for 10min.

Antibody	Supplier	Catalog number	Host	Working dilution
HRP-mouse IgG	GE-Healthcare®	NA931V	Sheep	1:10000
HRP-rabbit IgG	GE-Healthcare®	NA934V	Donkey	1:10000

Table 7. Secondary antibodies used for immunoblotting.

Proteins were visualized using an Enhanced Chemiluminescence (ECL) Western Blotting Detection Reagent (GE Healtcare® RPN2209 & ThermoFisher® Scientific™ 32132) an exposed onto photographic films (GE Healtcare® 28-9068-37). The films were scanned with an imaging densitometer (GS800 Bio-Rad®) and the individual bands were quantified using the ImageQuant 5.2 software.

9. SURFACE SENSING OF TRANSLATION (SUNSET)

Basal protein translation was measured using the SUnSET assay as described in (Schmidt et al., 2009) with minor modifications. Briefly, primary cortical cultures were treated with 10ng/ ml of puromycin for 30min, and then lysed as in Cell Culture Lysates. Untreated neurons and neurons treated with 25μM of the protein synthesis inhibitor cycloheximide 15min before puromycin were used as negative controls; 0.8μM of the protein synthesis inhibitor anisomycin led to equal inhibition rates than cycloheximide (data not shown). Proteins were resolved as described in Western Blotting and analyzed using an anti-puromycin antibody (see Table 6 for further information). Ponceau S staining was used as protein loading control.

10. IMMUNOFLUORESCENCE STAINING OF TOTAL PROTEINS

Immunofluorescence for total and surface proteins was performed on neurons grown in glass coverslips as indicated (see Primary Cultured Neurons). First, culture media was removed and coverslips were washed with DPBS with Ca^{2+} and Mg^{2+}. Neurons were then fixed with 4% paraformaldehyde (PFA) + 4% sucrose in PBS pH 7.4 for 10min at 4ºC. After 3-5min's washes with PBS, neurons were permeabilized with 0.2% Triton X-100 for 15min at RT, blocked with 5% BSA for 30min and incubated o/n at 4ºC with primary antibody (Table 8).

Antibody	Supplier	Catalog number	Host	Working dilution
NeuN	Millipore®	MAB377	Mo	1:1000
GFP	Millipore®	AB16901	Chk	1:300
GFP	Synaptic Systems	132002	Rb	1:1000

Table 8. Primary antibodies used for immunostaining.

The following day, neurons were rinsed in PBS 3 times for 5min and blocked with 2% BSA + 4% normal serum for 30min at RT. Next, neurons were incubated with the corresponding fluorescent secondary antibody (Table 9) in dark for 1h at RT. The secondary antibody was washed out with 3-5min's washes of PBS and neurons were incubated with DAPI (Sigma-Aldrich® D9542) for 2min at RT. Finally, coverslips were mounted using Dako Fluorescent Mounting Medium

(Dako S3023). Images were acquired with an epifluorescent Zeiss Axiovert 200M microscope using 10X and 25X objectives and a CoolSnap HQ camera (Roper Scientific) and analyzed with Metamorph software (Universal Imaging).

Antibody	Supplier	Catalog number	Fluorescing dye	Working dilution
Alexa Fluor 488 Goat anti-Chicken IgG	Invitrogen	A11039	Green	1:1000
Alexa Fluor 488 Goat anti-Rabbit IgG	ThermoFisher® Scientific™	A11008	Green	1:1000
Cy™3-AffiniPure Goat Anti-Rabbit IgG	Jackson Immunoresearch	111-165-003	Red	1:1000
Cy™3-AffiniPure Goat Anti-Mouse IgG	Jackson Immunoresearch	115-165-003	Red	1:1000
Cy™5 AffiniPure Goat Anti-Mouse IgG	Jackson Immunoresearch	115-175-166	Far-red	1:500

Table 9. Secondary antibodies used for immunostaining.

11. PROXIMITY LIGATION ASSAY

Proximity Ligation Assay (PLA) allows the detection, visualization and easily quantification of protein-protein interactions in very close proximity (<40 nm). PLA was performed as described in (Dinamarca et al., 2016) using the Duolink™ In Situ Red Starter Kit Mouse/ Rabbit (Sigma-Aldrich® DUO92101). Cultured neurons transfected with GFP were fixed at DIV17 with 4% PFA + 4% sucrose in PBS (RT, 10min), permeabilized with 0.2% Triton X-100 (RT, 15min) and incubated with blocking solution. Cells were then incubated with a mix of rabbit/ mouse primary antibodies (Table 10) overnight at 4°C, washed thrice with Wash Buffer A and incubated for 1h with the PLA secondary probes (anti-mouse Plus and anti-rabbit Minus, 1:5) at 37°C. Cells were washed thrice with Wash Buffer A and incubated with the ligase (1:40) in ligase buffer for 30 min at 37°C. After three additional washes with Wash Buffer A, cells were incubated with DNA polymerase (1:80) in the amplification buffer for 100 min at 37°C in darkness. Cells were later washed thrice with Wash Buffer B and GFP signal was enhanced following the immunofluorescence protocol detailed above. Finally, coverslips were mounted using Fluoroshield™ mounting medium (Sigma-Aldrich® F6182). Fluorescence images were acquired by using Nikon A1 Ti2 system with a sequential acquisition

setting at 1024 x 1024 pixels resolution. Cells were randomly selected from different coverslips and analyzed with Fiji software.

Antibody	Supplier	Catalog number	Host	Working dilution
GIT-1	SCB	Sc-365084	Mouse	1:150
mTOR	CST	2972S	Rabbit	1:150

Table 10. Primary antibodies used for PLA.

12. ELECTROPHYSIOLOGY

Electrophysiology experiments were performed thanks to collaborations with Dr. Steven J. Tavalin, from the University of Tennessee and Dr. Pierre Paoletti from L´Institut de Biologie de l'Ecole Normale Supérieure (IBENS).

HEK293 cells were cultured, transfected and recorded as previously described in (Chowdhury et al., 2013). Cells were transfected with pcDNA1 vectors expressing GluN1-1A and GluN2A, and either a pCI-neo vector expressing GFP-GluN3A or GFP-GluN3A1082Δ in a 1 : 1 : 3 ratio and maintained in medium with APV (250μM). GFP was used as a transfection marker in cells where GluN3A constructs were omitted. Whole-cell recordings were made with on GFP-positive cells using a Multiclamp 700A amplifier (Molecular Devices) 24h following transfection. Patch pipettes (2-to-4MΩ) contained: 140mM Cs methanesulfonate, 10mM HEPES, 5mM adenosine triphosphate (sodium salt), 5mM $MgCl_2$, 200μM $CaCl_2$, and 10mM BAPTA (pH 7.4). The extracellular solution contained: 150mM NaCl, 5mM KCl, 2 or 10mM $CaCl_2$, 10mM HEPES, 10mM glucose (pH 7.4) and was adjusted to 330mOsm with sucrose. Currents were digitized at 2kHz and filtered at 1kHz. Series resistance (90 to 95%) and whole-cell capacitance compensation were employed. Experiments were performed at a holding potential of -80mV with ramps (300ms to +50mV) elicited following a 3s application of glutamate (1mM) and glycine (100μM) at 20°C. The ΔErev, was calculated by subtracting the Erev obtained in 2mM Ca^{2+} from the Erev measured in 10mM Ca^{2+} and corrected for the junction potential between solutions. Initial peak currents were obtained from 1s agonist applications in 2mM Ca^{2+} and used to calculate the current density.

Experiments on glycine-gated di-heteromeric GluN1/ 3A receptors expressed in HEK293 cells were performed as previously described in (Grand et al., 2018) using GluN1-1A and GFP-GluN3A or GFP-GluN3A1082Δ subcloned in pCI-neo and transfected in a 1 : 3 ratio. 500nM CGP-78608 was systematically applied before 100μM of glycine perfusion.

13. BEHAVIOR

13.1. CONDITIONED TASTE AVERSION TEST (CTA)

CTA test was adapted from (Adaikkan and Rosenblum, 2015). Briefly, mice were trained to drink from two bottles of water for 6 days. On conditioning day, water was changed for 0.2% (regular CTA) or 0.1% (weak CTA) saccharin for 40 minutes (regular) or 5 hours (weak) after the exposure, mice were injected LiCl i.p. at 0.15M (regular) or 0.025M (weak). Saccharin preference was evaluated 24 hours after injection.

For unconditioned taste preference, mice were presented two drinking bottles for 48 hours: one contained water and the other one of the following solutions: Sucrose 5% (sweet), NaCl 75 mM (salty), Quinine 300 μM (bitter) and HCl 0.03 M (sour). Bottle sides were switched after 24 hours to avoid potential side bias. Solution preference was evaluated at 48 hours.

For assessing sensitivity to LiCl toxicity, “lying on belly” (LOB) behavior was registered after injection of LiCl (0.15M) or saline. This behavior consists in a totally general suppression of activity, and localization of the mouse in the cage’s corner. The activity was measured for 20 minutes.

14. STATISTICAL ANALYSIS

Statistical analyses were conducted with GraphPad Prism software version 7.00 for Windows. Sample size ‘n’ refers to the number of plates or mice analyzed, being the number of independent experiments specified in each figure. Comparison of quantitative variables between two groups were performed using parametric two-tailed unpaired or paired Student’s *t*-test. One-way or two-way

analysis of variance (ANOVA) followed by a post-hoc Tukey's multiple comparison tests were used when more than two groups were compared. Results were presented as mean ± standard error of the mean (SEM) from the indicated number of independent experiments and expressed as fold of the indicated control. P values > 0.05 were regarded as not significant (ns), whereas significant values were indicated with '*' ($p < 0.05$), '**' ($p < 0.01$) and '***' ($p < 0.001$).

Results

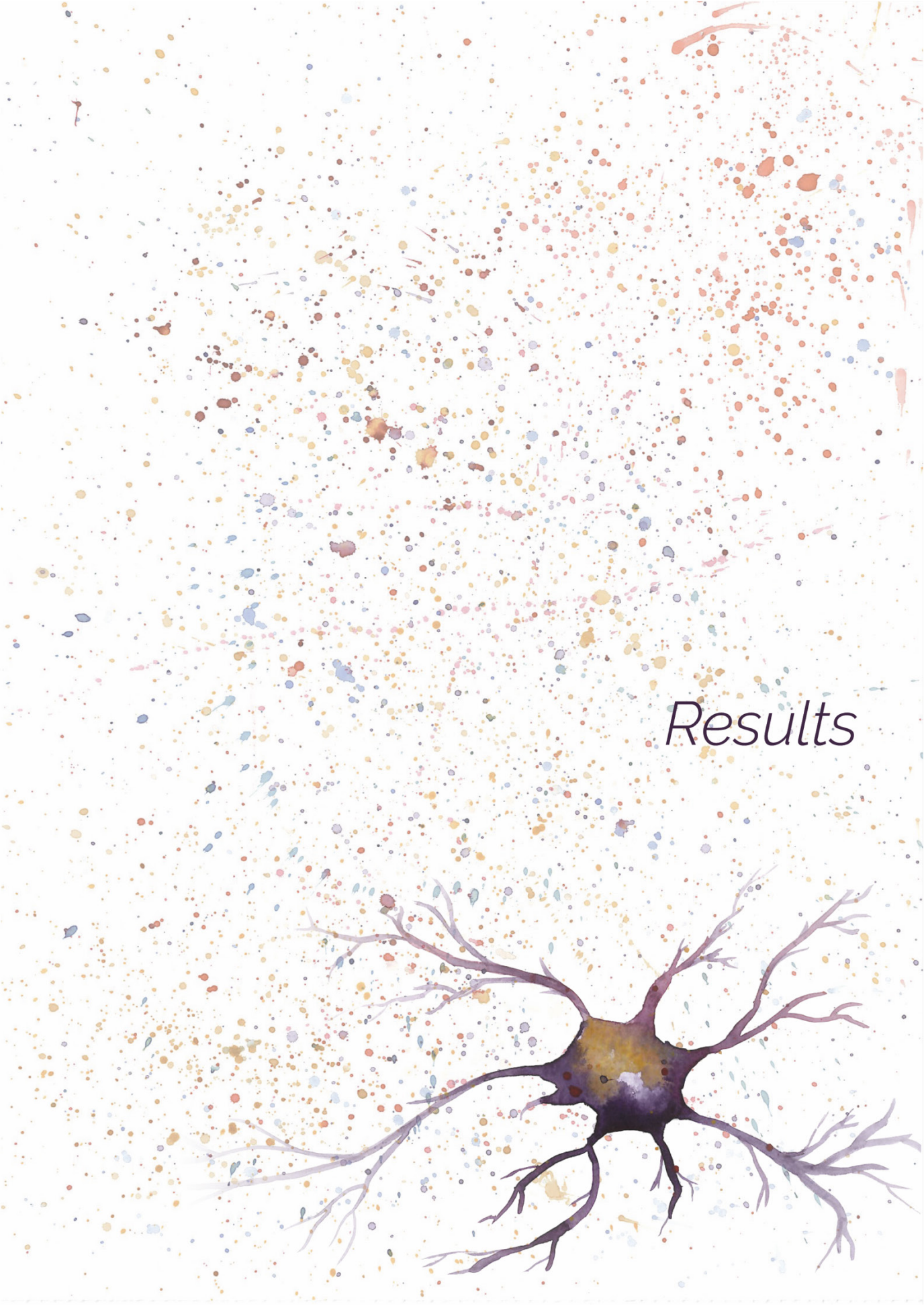

1. MODEL SYSTEM AND OTHER TOOLS

As mentioned, previous work in our laboratory discovered a selective modulation by GluN3A subunits of a subset of activity-dependent signaling pathways, and pointed towards a remarkable inhibition of mTOR (see Signaling pathways mediating the effects of GluN3A-NMDARs**;** (Dey, 2017)). Yet many questions remained. Answering them has been the goal of my Thesis work, with an emphasis on identifying the underlying mechanisms and the physiological roles of GluN3A-mediated inhibition of mTOR signaling.

Below I describe key aspects of the model systems used. A main difference from the initial work was the use of primary mouse cultures rather than rat cultures (see Primary Cultured Neurons), which allowed us to take advantage of *Grin3a -/-* mice for rescue and mechanistic experiments.

1.1. LENTIVIRAL MANIPULATIONS OF GLUN3A EXPRESSION IN PRIMARY NEURONAL CULTURES

To investigate GluN3A effects on activity-dependent signaling, we chose primary neurons in culture as they: 1) recapitulate the formation and refinement of neuronal networks and share a commonality of mechanisms; 2) recapitulate the peak and down-regulation of GluN3A expression seen *in vivo*; and 3) are amenable to genetic manipulation with a well-defined time-course. I used a collection of lentiviruses to enhance or silence GluN3A expression, and to replace GluN3A with mutant versions harboring modified CTDs (see Figure 17). Within NMDAR subunits, the CTD is critical for interaction with signaling proteins and has been shown to control synapse stabilization and maturation (Barria and Malinow, 2005; Wang et al., 2011). Selective neuronal expression was achieved by using the human Synapsin 1 promoter (Gascón et al., 2008).

As outlined in the INTRODUCTION, GluN3A-NMDARs are typically expressed before and during postnatal critical periods and largely reduced afterwards in most brain regions. In the rodent brain, highest expression is observed over the first two postnatal weeks *in vivo* with a peak around P5-P8 (Pérez-Otaño et al., 2016). *In vitro* models including organotypic hippocampal slice cultures (Kehoe et al., 2014) or our dissociated cortical culture model (Dey, 2017)

recapitulated the GluN3A peak of expression at DIV8-12 and subsequent down-regulation, that overlapped the period when intense synaptic refinements involving synapse maturation and elimination are taking place in culture (Figure 23a).

For overexpression or rescue experiments, infection was timed to enhance GluN3A expression from the onset of its down-regulation; neurons were infected at DIV9 and analyzed at DIV12-14 (top, Figure 23b). For silencing experiments, neurons were infected at DIV3 and analyzed at DIV7-9 to suppress GluN3A expression at times when levels are highest (bottom, Figure 23b).

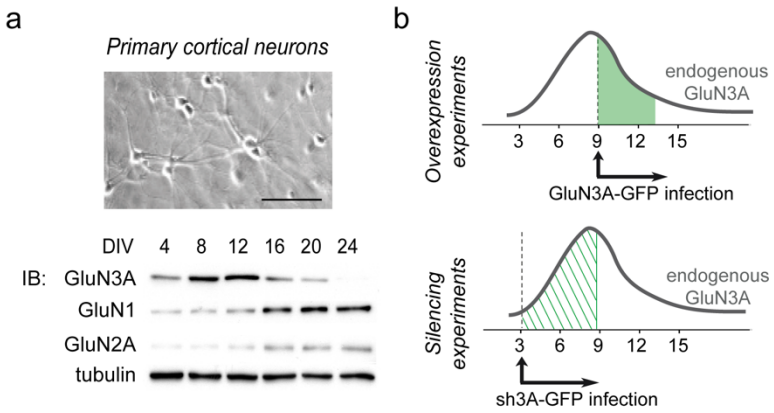

Figure 23. Timings for lentiviral infections.

(a) Light-field image of cultured primary cortical neurons (scale bar, 250μM) and representative immunoblot showing the time course of expression of NMDAR subunits. In this and subsequent western blots, membranes were re-probed for β-tubulin to verify protein loading. *(b)* Schematic of endogenous GluN3A expression (grey) and the windows of lentiviral infection (green square) in primary cortical neurons. *Top,* for overexpressing experiments, cortical neurons were infected with GFP, GluN3A-GFP and its mutant variants at DIV9 and analyzed at DIV12-14, when endogenous GluN3A's expression starts to decrease. *Bottom,* for silencing experiments, cortical neurons were infected at DIV3 with the lentiviruses shGluN3A1185-GFP (hereinafter referred to as sh3A-GFP) or control GFP and analyzed at DIV7-9, within endogenous GluN3A's peak of expression.

The transduction efficiency of lentiviral batches was tested after each production by infecting neuronal cultures with increasing virus doses followed by immunoblotting and immunostaining analysis (see Lentiviral Titration in Neuronal Cultures in the Materials and Methods section for further details). The goal was to control two key parameters: 1) the fraction of infected neurons; 2) the levels of GluN3A overexpression. We titrated exogenous GluN3A expression to ensure that it does not exceed by 2 to 3-fold the endogenous levels and avoid overexpression

artifacts (Figure 24). Same approach was conducted to titrate other overexpressing (data not shown) and silencing (Figure 32) constructs.

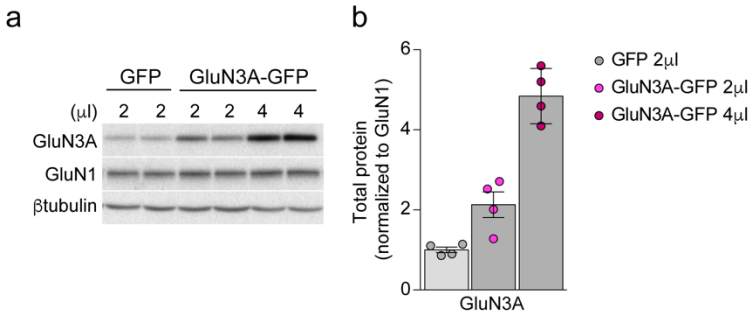

Figure 24. Titration of GluN3A-GFP lentiviruses.

(a) Representative western blots of DIV14 cortical neurons infected at DIV9 with different doses of lentiviruses expressing GFP and GluN3A-GFP. *(b)* Quantification of GluN3A protein levels upon infection with different virus doses without detectable changes in the obligatory subunit GluN1 (n=4 from 2 independent cultures).

1.2. SYNAPTIC STIMULATION PROTOCOLS

We induced synaptic activation with two well-established protocols to examine the modulation by GluN3A of known activity- and NMDAR-dependent signaling pathways. In the first protocol we treated neurons for 1 hour (h) with bicuculline, which inhibits ɣ-aminobutyric acid (GABA) transmission and triggers bursts of action potential firing (Hardingham and Bading, 2002). In the second, we treated neurons with BDNF because it is a potent activator of mTOR signaling and local protein synthesis (Takei et al., 2004; Troca-Marin et al., 2010). BDNF protocol optimization is summarized in the Materials and Methods section "BDNF Protocol Optimization".

2. GLUN3A INHIBITS THE INDUCTION OF PLASTICITY-RELATED PROTEINS AT THE POST-TRANSCRIPTIONAL LEVEL

As mentioned, GluN3A-NMDARs selectively inhibit a subset of activity-dependent signaling pathways that are activated by conventional NMDARs (see Signaling pathways mediating the effects of GluN3A-NMDARs). A crucial end result of conventional NMDAR signaling is *de novo* expression of plasticity proteins that will

drive persistent structural and functional modifications leading to the stabilization of synapses and consolidation of memories (Rao et al., 2006; Saha et al., 2011). *De novo* expression is mediated by both transcriptional and translational regulation. Transcriptional activation generates a neuron-wide pool of mRNAs, while local translational control is thought to fine-tune neuronal function by ensuring that activity-induced gene products are deployed to selected synapses. mTOR inhibition indicated a role of GluN3A-NMDARs on translation but effects on activity-dependent transcription were examined.

To dissect out impacts of GluN3A-NMDARs on transcriptional *vs* translational regulation, DIV9 primary cortical neurons were infected with GFP or GluN3A-GFP lentiviruses, treated at DIV14 with bicuculline or BDNF, and sister wells collected for protein (Western Blot) and mRNA (RNAseq) analysis. As previously shown, bicuculline potently induced the production of IEGs Arc, c-Fos and Zif268 (Rao et al., 2006). Remarkably, the induction of Arc and c-Fos proteins was significantly reduced upon GluN3A expression while Zif268 induction was unaffected suggesting independent regulatory mechanisms (Figure 25). Analysis at the mRNA level showed that GluN3A does not affect the production of these IEGs by limiting activity-dependent transcription. We conducted global gene expression analysis using mRNA-strand specific RNAseq to identify genes differentially induced in primary cortical cultures infected with GFP or GluN3A-GFP. In basal conditions, the only gene differentially expressed was *Grin3a* due to its exogenous overexpression (Figure 26a). Later, we compared the bicuculline-induced genes in GFP and GluN3A-GFP infected neurons. The data were represented in Volcano plots to compare the statistical significance (p value) *vs* the magnitude of change between control and bicuculline induction conditions (fold change), and no change was observed (Figure 26b). We further validated the RNAseq data of selected IEGs with roles in synaptic plasticity by qPCR. *Arc, c-Fos* and *Zif268* mRNA levels were robustly induced by bicuculline in both GFP- and GluN3A-GFP-infected neurons with similar time-courses of induction (Figure 26c). The transcriptional induction by bicuculline of other IEGs such as *Npas4* was also unaffected by GluN3A (Figure 26c). Similarly, there were no changes in the induction of late-response genes (LRGs) that regulate synapse development and function, such as *Homer1a* or *BDNF* (Figure 26d).

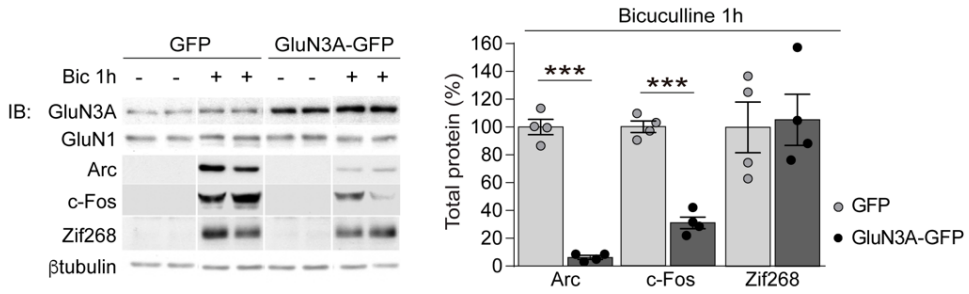

Figure 25. Inhibition of bicuculline-dependent protein production of IEGs by GluN3A.

Cortical neurons infected with GFP or GluN3A-GFP on DIV9 were stimulated with bicuculline (50μM, 1h) and collected at DIV14. Left, representative western blots showing that GluN3A inhibits the synaptic activation of the IEGs *Arc* and *c-Fos* with no changes on *Zif268*. Right, signal intensities of the indicated proteins as percentage of stimulated GFP-infected neurons. n=4 from 2 independent cultures, ***p<0.001, unpaired t-test.

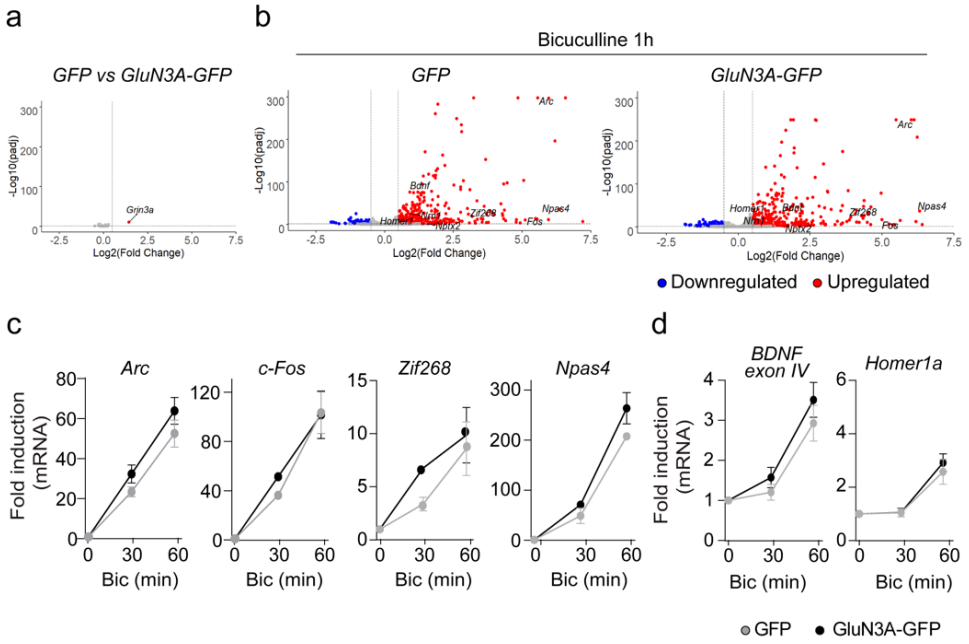

Figure 26. GluN3A does not alter bicuculline-dependent iEGs' mRNA production.

Cortical neurons infected with GFP or GluN3A-GFP on DIV9 were stimulated with bicuculline (50μM, 1h) and collected at DIV14. *(a)* Volcano plot comparing GFP and GluN3A-GFP differentially expressed genes in basal conditions (padj < 0.05 and log 2(Fold Change) > 1). The x-axis represents the log 2(Fold Change), while y-axis represents statistical significance for each gene. Grey dots symbolize no change of expression. *(b)* Volcano plot comparing the differential fold-change expression of hundreds of genes upon bicuculline induction. GFP and GluN3A-GFP infected neurons were plotted separately and representative genes are noted. *(c)* qPCR analysis of the induction time-course upon bicuculline treatment of the IEGs *Arc*, *c-Fos, Zif268* and *Npas4*, and *(d)* the LRGs *BDNF (exon IV)* and *Homer 1a*.

Plotted values are shown as fold induction relative to non-stimulated neurons. n=2-4 from 2 independent cultures.

An analogous dissociation between inhibited protein expression (Figure 27) and preserved transcriptional induction (Figure 28) was observed upon stimulation of GluN3A-infected neurons with the mTOR activator BDNF. These results suggest that GluN3A-NMDARs regulate the translation of specific mRNAs into protein without affecting cell-wide transcriptional programs, consistent with their lack of effect on the induction of CREB and ERK1/2 that are the two major pathways for activity-dependent transcription (Flavell and Greenberg, 2008; Hardingham et al., 2001) (Figure 29).

It is worth noting that the selective inhibition of activity-dependent signaling by GluN3A largely differed from the effects of the general NMDAR antagonist APV that blocked all signaling pathways tested as well as the induction of IEGs at both mRNA (Figure 30) and protein levels (Dey, 2017). This result argued against a general dominant-negative effect of GluN3A subunits on NMDAR signaling.

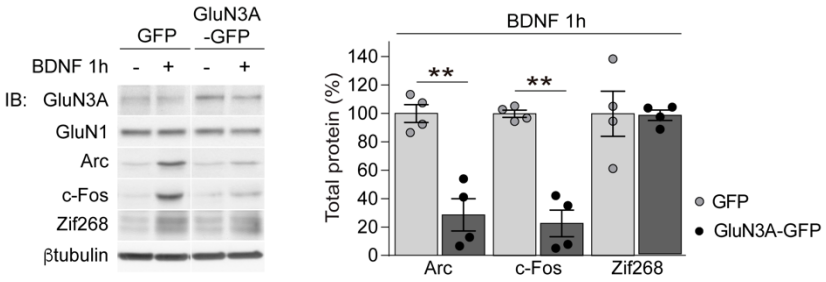

Figure 27. Inhibition of BDNF-dependent protein production of IEGs by GluN3A.

Cortical neurons infected with GFP or GluN3A-GFP on DIV9 were stimulated with BDNF (100ng/ml, 1h) and collected at DIV14. Left, representative western blots showing that GluN3A inhibits the synaptic activation of the IEGs *Arc* and *c-Fos* with no changes on *Zif268*. Right, signal intensities of the indicated proteins as percentage of stimulated GFP-infected neurons. n=4 from 2 independent cultures, **p<0.01, unpaired t-test.

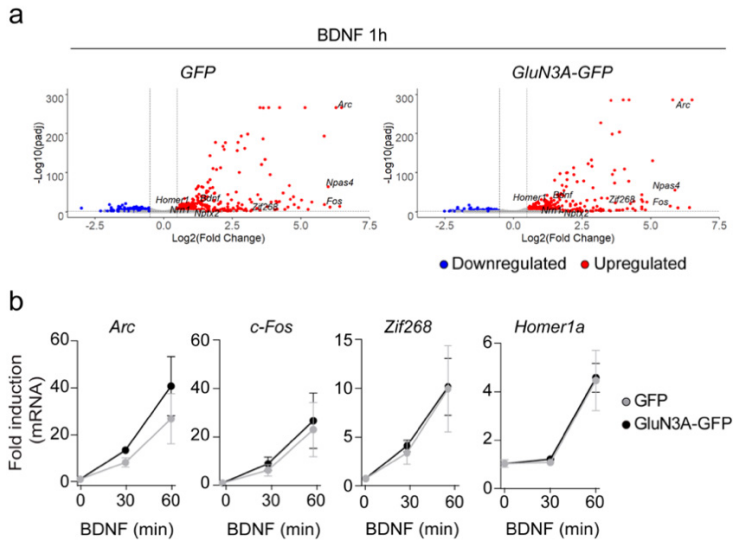

Figure 28. GluN3A does not alter BDNF-dependent iEGs' mRNA production.

Cortical neurons infected with GFP or GluN3A-GFP on DIV9 were stimulated with BDNF (100ng/ml, 1h) and collected at DIV14. *(a)* Volcano plot comparing the differential fold-change expression of hundreds of genes upon BDNF induction (padj < 0.05 and log 2(Fold Change) > 1). GFP and GluN3A-GFP infected neurons were plotted separately and representative genes are noted. *(b)* qPCR analysis of the induction time-course upon BDNF treatment of the IEGs *Arc*, *c-Fos* and *Zif268*, and the LRG *Homer 1a*. Plotted values are shown as fold induction relative to non-stimulated neurons. n=2-4 from 2 independent cultures.

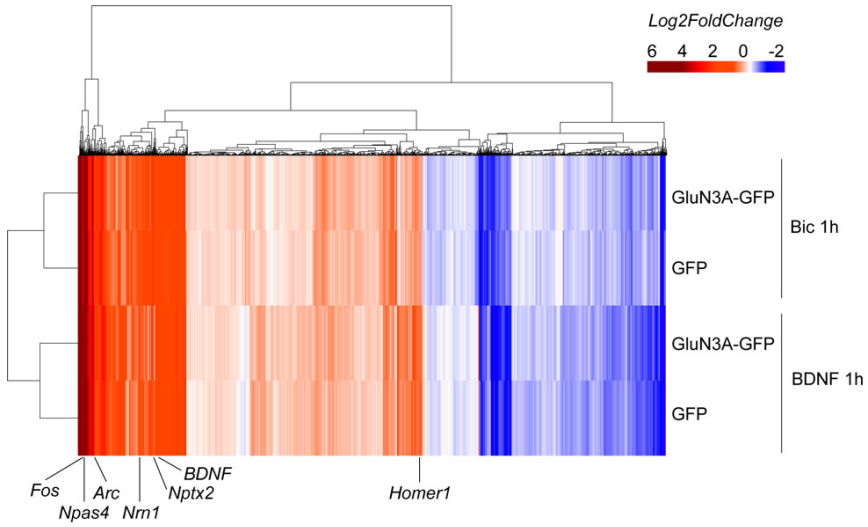

Figure 29. Transcriptomic profile of GFP and GluN3A-GFP neurons upon bicuculline and BDNF stimuli.

Heatmap showing relative mRNA expression of all genes upon 1h bicuculline or BDNF treatment.

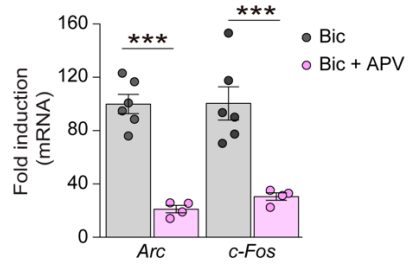

Figure 30. General blockade by APV of IEGs mRNA induction.

Quantitative analysis of the IEGs *Arc* and *c-Fos* mRNA induction from DIV14 cultured cortical neurons pretreated with APV (50μM, 30min) before stimulation with bicuculline (50μM, 1h). n=4-6 from 2-3 independent cultures, ***p<0.001 one-way ANOVA followed by Bonferroni´s test.

Finally, we ruled out alternative mechanisms such as enhanced IEGs degradation by GluN3A-NMDARs. IEGs are mostly degraded in the proteasome, so we took advantage of the proteasome inhibitor MG-132 to promote IEGs accumulation (Rao et al., 2006). DIV14 cortical neurons were treated with MG-132 or vehicle for 1h prior 1h BDNF stimulation. Selectively inhibited induction of IEGs by GluN3A was not rescued by pre-treatment with MG-132 (Figure 31). Altogether, these results point towards a selective role of GluN3A-NMDARs in repressing the translation of specific activity-regulated mRNAs.

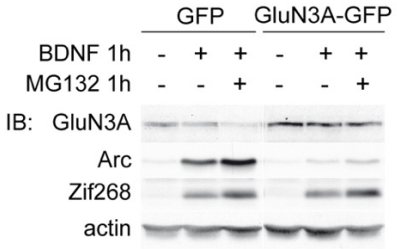

Figure 31. Proteasome blockade did not rescue GluN3A inhibition of IEGs protein production.

DIV14 neurons were treated with MG132 (30μM, 1h before and during BDNF treatment). Representative western blot probed with the indicated antibodies is shown.

3. POTENTIATED MTOR SIGNALING AND IEG PRODUCTION IN THE ABSENCE OF GLUN3A

We expanded the initial characterization of GluN3A modulation of mTOR pathway, by assessing the effects of GluN3A deletion. First, we tested the effects of silencing

GluN3A using a validated sh3A construct (sh3A-GFP) that efficiently and selectively silences GluN3A expression (Figure 32; (Kehoe et al., 2014)). Primary cortical neurons were infected at DIV3 with GFP or sh3A-GFP lentiviruses and analyzed at DIV7-9 in basal and stimulated conditions. Lentiviral knockdown of GluN3A enhanced basal mTOR activation, as shown by enhanced phosphorylation of its downstream effectors S6K and S6 (Figure 33). Moreover, the induction of the IEGs Arc and c-Fos in response to both bicuculline (Figure 34a) and BDNF (Figure 34b) was enhanced by GluN3A removal.

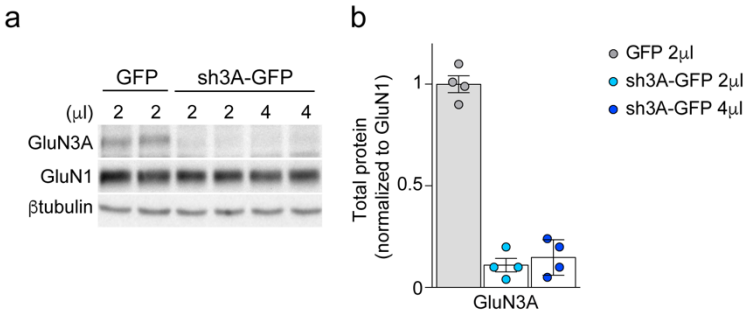

Figure 32. Titration of sh3A-GFP lentiviruses.

(a) Representative western blots of DIV7 cortical neurons infected at DIV3 with different doses of GFP and sh3A-GFP lentiviruses. *(b)* Quantification of downregulation of endogenous GluN3A protein levels upon infection with different virus doses. n=4 from 2 independent cultures.

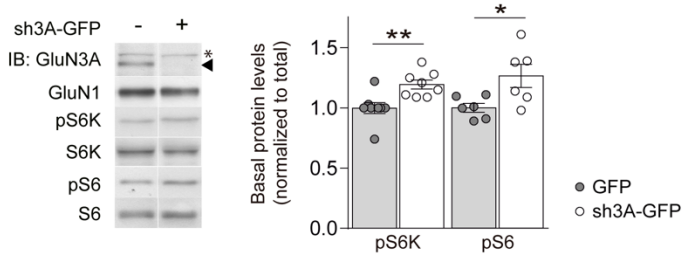

Figure 33. GluN3A knockdown potentiates basal mTOR activation in young neurons.

Neurons were infected on DIV3 with lentiviruses expressing either GFP or sh3A-GFP and collected at DIV7-9. *Left,* representative western blots and, *right,* quantification of phosphorylated mTOR effectors S6K and S6 normalized to total protein (n=6-8 from 3-4 independent cultures). GluN3A specific band is indicated with a black arrow while a star indicates an unspecific one. *p< 0.05, **p< 0.01, two-tailed paired t-test.

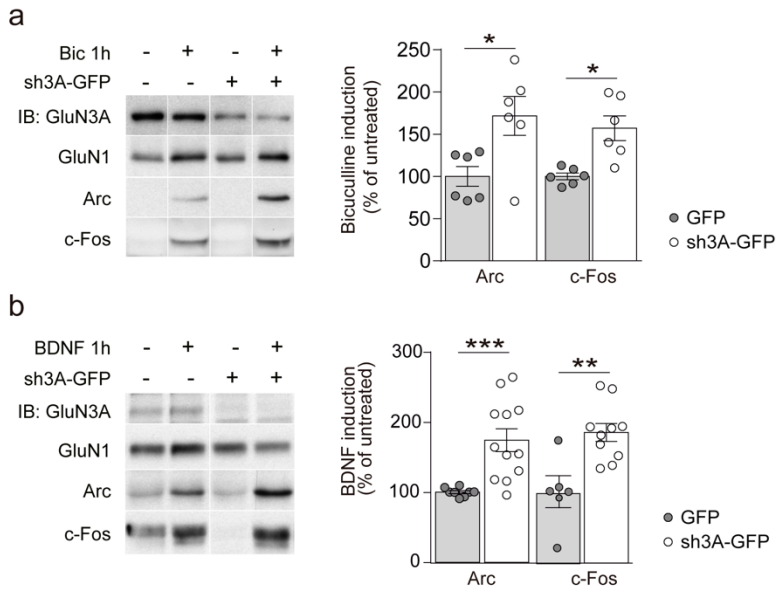

Figure 34. GluN3A knockdown potentiates IEG induction in young neurons.

Neurons were infected on DIV3 with lentiviruses expressing either GFP or sh3A-GFP and collected at DIV7-9. *(a,b)* Representative western blots and quantification of IEG induction upon stimulation with bicuculline (*a*; 50µM, 1h) and BDNF (*b*; 100ng/ml, 1h) in GFP and sh3A-GFP expressing neurons (n=6-12 from 3 independent cultures). *p< 0.05, **p< 0.01, ***p< 0.001, two-tailed paired t-test.

To determine whether enhanced IEG induction was linked to the enhanced mTOR activity, we blocked mTORC1 with the pharmacological inhibitor rapamycin. In order to selectively block mTORC1, we acutely administered a low dose (100nM) of rapamycin to which mTORC2 is insensitive (Sarbassov et al., 2006; Stoica et al., 2011). Cortical cultures infected at DIV3 with GFP or sh3A-GFP lentiviruses were treated at DIV7-9 with rapamycin or vehicle for 1h prior to 1h of BDNF stimulation (Figure 35). Enhanced mTOR activation upon BDNF stimulation in sh3A-GFP expressing neurons was completely abolished in the presence of rapamycin (Figure 35a,b) while there was no inhibitory effect on the ERK pathway (Figure 35a). Regarding the IEG Arc induction, rapamycin treatment in sh3A-GFP expressing neurons rescued the induction levels to those achieved in control GFP-expressing neurons (Figure 35c). Rapamycin had no significant effects on control GFP neurons (Figure 35c). Thus, we could conclude that lack of GluN3A promotes the emergence of a mTOR-dependent component in the induction of the IEG Arc.

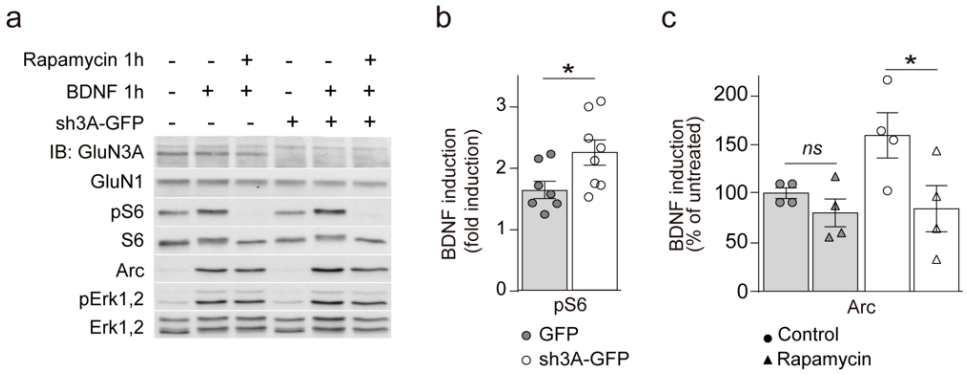

Figure 35. mTOR and Arc potentiation in GluN3A knockdown neurons is rapamycin dependent.

Neurons were infected on DIV3 with lentiviruses expressing either GFP or sh3A-GFP and collected at DIV7-9. *(a)* Representative western blots of phosphorylated mTOR effector S6, the IEG Arc, and unchanged ERK. *(b)* Quantification of phosphorylated S6 upon stimulation with BDNF (100ng/ml, 1h). Plotted values are shown as fold induction relative to non-stimulated neurons (n=7-8 from 4 independent cultures). *(c)* Quantification of Arc induction upon stimulation with BDNF (100ng/ml, 1h) with or without a rapamycin pre-treatment (100nM; 1h) in GFP and sh3A-GFP expressing neurons (n=4 from 2 independent cultures). *p< 0.05, two-tailed paired t-test.

Similarly enhanced basal mTOR activation was found in primary cortical cultures from *Grin3a* -/- mice (relative to control) at DIV4, as shown by enhanced phosphorylation of mTOR, S6K, S6 and 4EBP1 (Figure 36a). Here, an early stage of GluN3A expression was chosen to identify first consequences and rule out compensatory effects. Likewise, hyperactivation of mTOR was detected in hippocampal lysates of *Grin3a* -/- mice over postnatal refinement stages (P8 and P16; Figure 36b,c), as revealed by the increased phosphorylation of the mTOR downstream effectors S6K and S6.

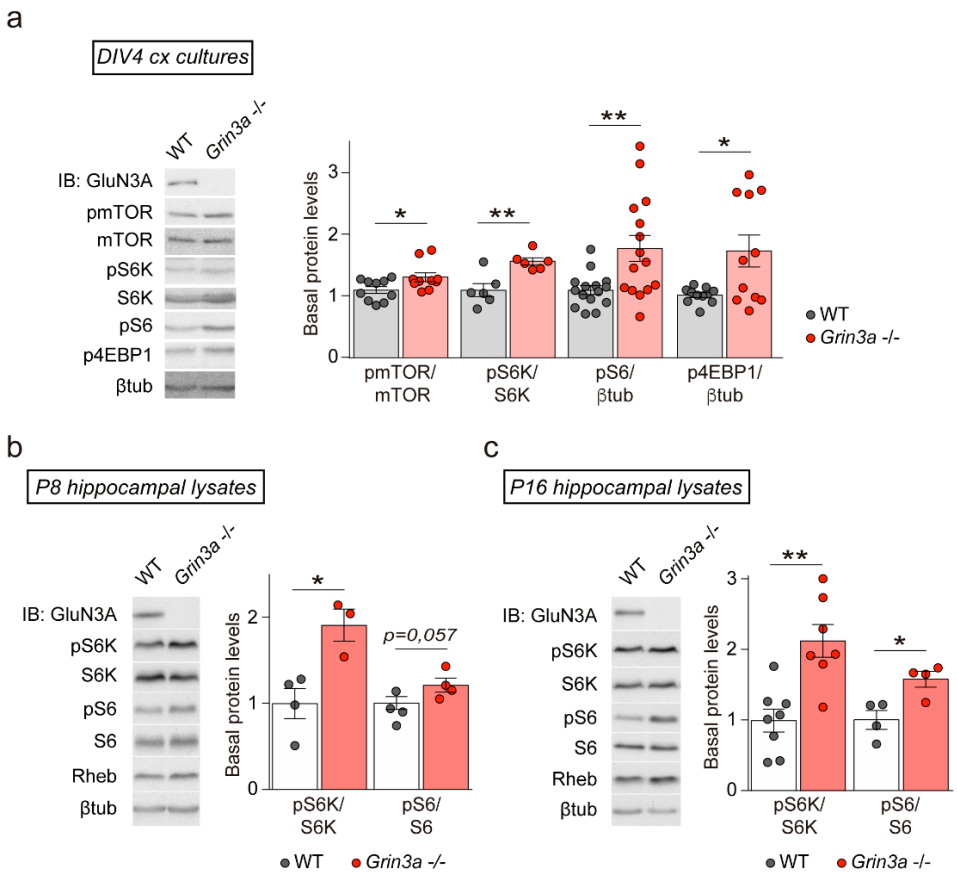

Figure 36. Potentiation of mTOR signaling in *Grin3a -/-*.

(a) Paired DIV4 WT and *Grin3a -/-* primary cortical cultures showing an increased basal activation of the mTOR pathway in *Grin3a -/-* respect to WT (n=6-15 from 3-7 independent cultures). *(b-c)* Status of S6K and S6 phosphorylation in lysates prepared from wild-type (WT) and *Grin3a -/-* hippocampi at P8 *(b)* and P16 *(c)*. Left, representative western blots, and right, quantification (n=4-8 mice). *p< 0.05, **p< 0.01, two-tailed unpaired t-test.

4. GLUN3A PREVENTS THE DEPHOSPHORYLATION OF EEF2, KEY REGULATOR OF THE ELONGATION STEP OF PROTEIN SYNTHESIS

A branch of the mTOR pathway that had not been explored regulates the phosphorylation of eEF2 (see mTORC1 and protein synthesis). eEF2 is required for the elongation step of protein synthesis and blocks general translation when it is phosphorylated (Dever and Green, 2012).

In a first set of experiments, we prolonged or downregulated GluN3A expression in WT primary neuronal cultures and measured basal levels of peEF2 (Figure 37). Higher levels of peEF2 were observed in cortical neurons infected with GluN3A-GFP (Figure 37a,b). Conversely, GluN3A knockdown neurons showed lower levels of peEF2 than control neurons (Figure 37c,d). Collectively, these results demonstrate that GluN3A modulates the phosphorylation status of eEF2.

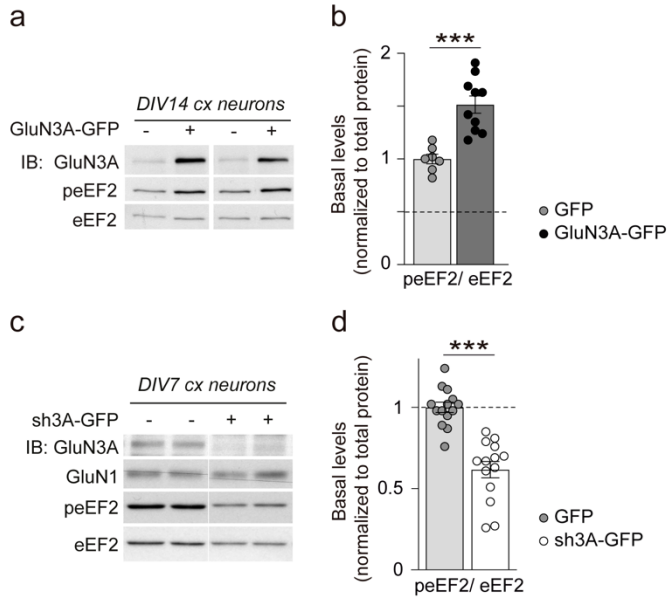

Figure 37. GluN3A modulates eEF2 phosphorylation status.

(a,b) WT cortical neurons were infected on DIV9 with lentiviruses expressing either GFP or GluN3A-GFP and collected at DIV14. *(a)* Representative western blots of the phosphorylation status of eEF2. *(b)* Quantification of basal phosphorylated eEF2 (n = 7-10 from 4 independent cultures). *(c-d)* WT cortical neurons were infected on DIV3 with lentiviruses expressing either GFP or sh3A-GFP and collected at DIV7. *(c)* Representative western blots of the phosphorylation status of eEF2. *(d)* Quantification of basal phosphorylated eEF2 (n = 14 from 5 independent cultures). ***p<0.001, two-tailed unpaired t-test.

We then conducted rescue experiments in primary neuronal cultures from *Grin3a* -/- embryos. We infected the neurons at DIV7 with GFP or GluN3A-GFP lentiviruses and pretreated them at DIV12 with rapamycin or vehicle prior to stimulation (Figure 38). Both bicuculline (Figure 38a,b, white bars) and BDNF (Figure 38c,d, white bars) increased the level of the active unphosphorylated form of eEF2 in *Grin3a* -/- neurons. eEF2 dephosphorylation was mTOR-dependent as judged by inhibition with rapamycin as previously described in (Inamura et al.,

2005; Kenney et al., 2015). However, eEF2 dephosphorylation and its rapamycin inhibition was occluded in *Grin3a* -/- neurons infected with GluN3A-GFP (Figure 38, grey bars). Together, these results demonstrate that GluN3A modulates mTORC1-dependent eEF2 dephosphorylation.

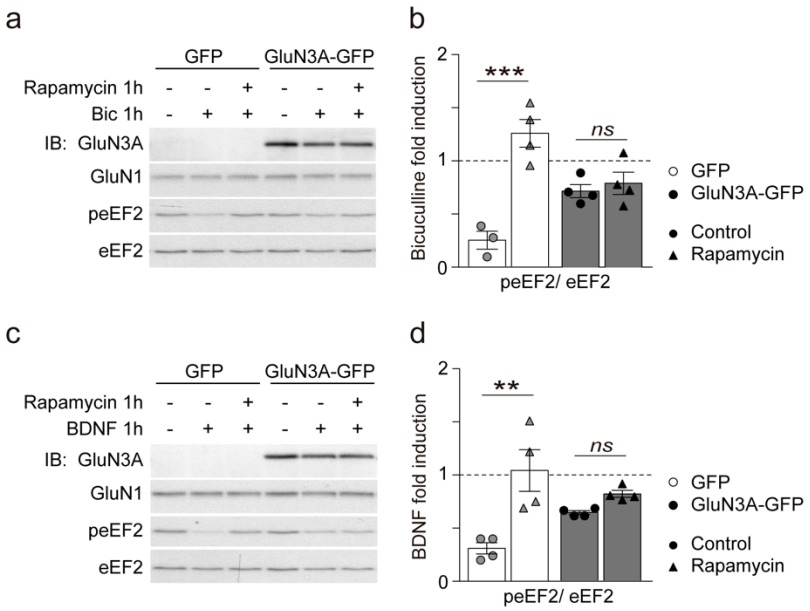

Figure 38. GluN3A prevents the mTOR-dependent dephosphorylation of eEF2.

Grin3a -/- cortical neurons were infected on DIV7 with lentiviruses expressing either GFP or GluN3A-GFP and collected at DIV12. *(a)* Representative western blots of the phosphorylation status of eEF2 upon bicuculline (50μM, 1h) and rapamycin (100nM, 1h prior bicuculline) treatment showing that GluN3A abolish the activity-mediated dephosphorylation and occludes its rapamycin inhibition. *(b)* Quantification of phosphorylated eEF2 upon stimulation with bicuculline. Plotted values are shown as fold induction relative to non-stimulated neurons. *(c-d)* Analogous experiments upon stimulation with BDNF (100ng/ml, 1h). n=4 from 2 independent cultures. **p<0.01, ***p<0.001, two-tailed paired t-test.

5. GluN3A Controls the Postnatal Emergence of mTORC1-Dependent Protein Synthesis

Our results thus expanded the previous work and demonstrated that GluN3A bidirectionally modulates mTOR activation *in vivo* and *in vitro*. We then asked whether GluN3A-modulation of mTOR signaling affects protein synthesis. For this, we measured translational rates in cortical neurons in the presence or absence of rapamycin using a non-radioactive puromycin-labeling assay: Surface Sensing of

Translation (SUnSET). Puromycin, an aminonucleoside antibiotic produced by *Streptomyces alboniger*, is a structural analog of aminoacyl tRNAs that enters ribosomes actively engaged in translation and becomes covalently attached to the carboxy terminus of nascent polypeptide chains preventing elongation (Figure 39) (Nathans, 1964). When used in low amounts, puromycin incorporation into newly synthesized proteins reflects the rate of mRNA translation *in vitro*, allowing its monitorization and quantification (Schmidt et al., 2009).

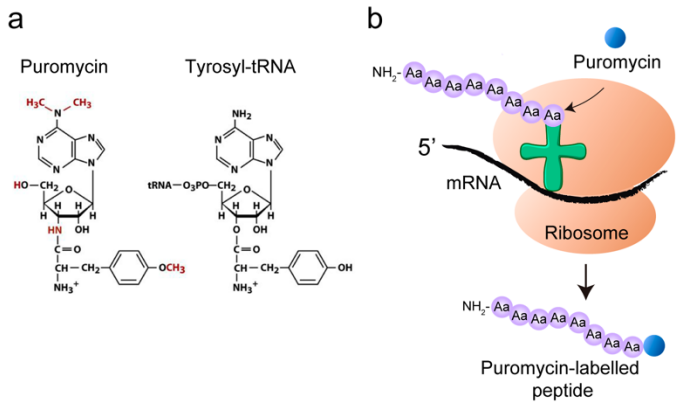

Figure 39. SUnSET assay.

(a) Comparison of the molecular structure of puromycin and tyrosyl-tRNA. *(b)* Puromycin's mode of action involves its incorporation into growing peptide chains via the formation of a peptide bound. Then, the puromycin-labelled peptide is unable to undergo further elongation and is released from the ribosome.

Due to its mode of action, puromycin can be toxic for the cells at high doses. We thus first established the optimal dose of puromycin that allowed us to measure the translational rates avoiding cell death but also yielding signal saturation in the later western blotting. To that end, we performed a dose-dependent curve considering the already described working doses (Briz et al., 2017; Fortin et al., 2012; Di Prisco et al., 2014), and chose a 10ng/ml dose for 30 minutes.

5.1. LACK OF GLUN3A ACCELERATES THE EMERGENCE OF MTOR-DEPENDENT TRANSLATION

In a first approach, we measured protein synthesis rates in cortical neurons at different developmental stages, DIV7 and DIV14, and analyzed its mTORC1-

dependence by pre-treating the neurons with rapamycin 100nM (Figure 40). We found that protein synthesis in young cortical neurons (DIV7) is not dependent on mTORC1 activation, while strong rapamycin sensitivity emerges at later stages (DIV14) (Figure 40a,c). Moreover, basal protein synthesis increased throughout development (Figure 40b).

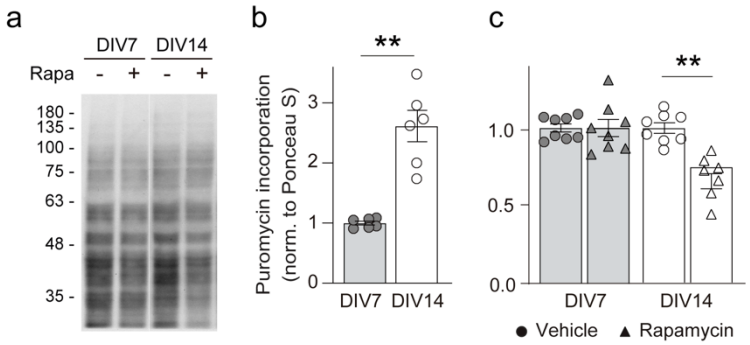

Figure 40. Age-dependence of mTORC1-dependent protein synthesis.

(a) Representative blots and *(b,c)* quantification of puromycin incorporation (10ng/ml, 30min incubation) and sensitivity to rapamycin (rapa, 100nM, 1h incubation) in WT DIV7 and DIV14 cortical neurons. Neurons non-incubated with puromycin were used as negative control. Puromycin levels were normalized to Ponceau S staining. n=6-8 samples from 3-4 independent cultures; **p<0.01, *(b)* two-tailed unpaired t-test and *(c)* two-way ANOVA followed by Tukey's test.

To assess the effect of GluN3A expression, we first knocked-down GluN3A from WT cortical neurons using GFP or sh3A-GFP lentiviruses, and basal protein synthesis was analyzed at DIV7-9. Knockdown of GluN3A caused a large increase in protein synthesis in young neurons (DIV7-9), which exhibited a strong rapamycin-dependence compared to controls (Figure 41), and closer to the typical of later developmental stages (Figure 40). Thus, GluN3A places inhibitory constraints on the emergence of mTOR-dependent protein synthesis which are relieved upon removal.

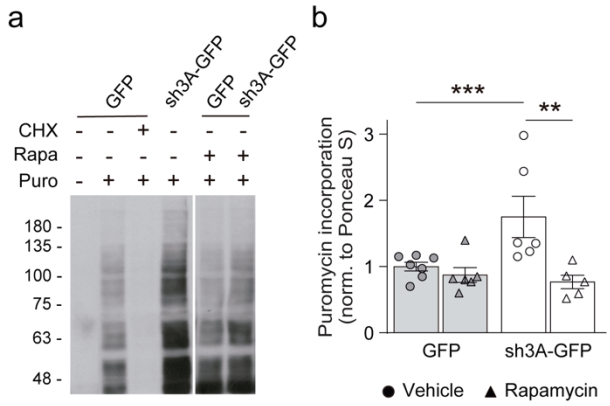

Figure 41. GluN3A knockdown boosts mTORC1-dependent protein synthesis.

WT cortical neurons were infected on DIV3 with lentiviruses expressing GFP or sh3A-GFP and protein synthesis was analyzed at DIV7-9. *(a)* Representative western blot showing puromycin incorporation (puro, 10ng/ml, 30min incubation) in GFP and sh3A-GFP expressing neurons treated with rapamycin (rapa, 100nM, 1h incubation), the protein synthesis inhibitor cycloheximide (CHX, 25μM, 15min incubation) or vehicle. Neurons non-incubated with puromycin were used as negative control. *(b)* Quantification of puromycin levels normalized to Ponceau S staining. n=5-7 from 4 independent cultures; **p<0.01, ***p<0.001, two-way ANOVA followed by Tukey's test.

5.2. GluN3A Rescues Increased mTOR-Dependent Translation in *Grin3a -/-* Cortical Neurons

Robust mTOR-dependent protein synthesis was also observed in cortical neurons from *Grin3a-/- mice* in line with the knockdown result (Figure 42). The GluN3A role was tested in rescue experiments where neurons were infected at DIV6 with GFP or GluN3A-GFP lentiviruses and SUnSET was performed at DIV12. Re-expression of GluN3A was sufficient to decrease basal protein synthesis rates to physiological levels (Figure 42a,b). Neurons were also subjected to treatments with the mTOR inhibitor rapamycin (Figure 42c) and the MEK/ ERK inhibitor U0126 (Figure 42d). U0126 promoted a global inhibition in both GFP- and GluN3A-infected neurons at further greater levels than rapamycin. On the other hand, GluN3A expression obliterated rapamycin sensitivity as was described above, turning neurons into a juvenile state in which protein synthesis is no longer mTORC1-dependent.

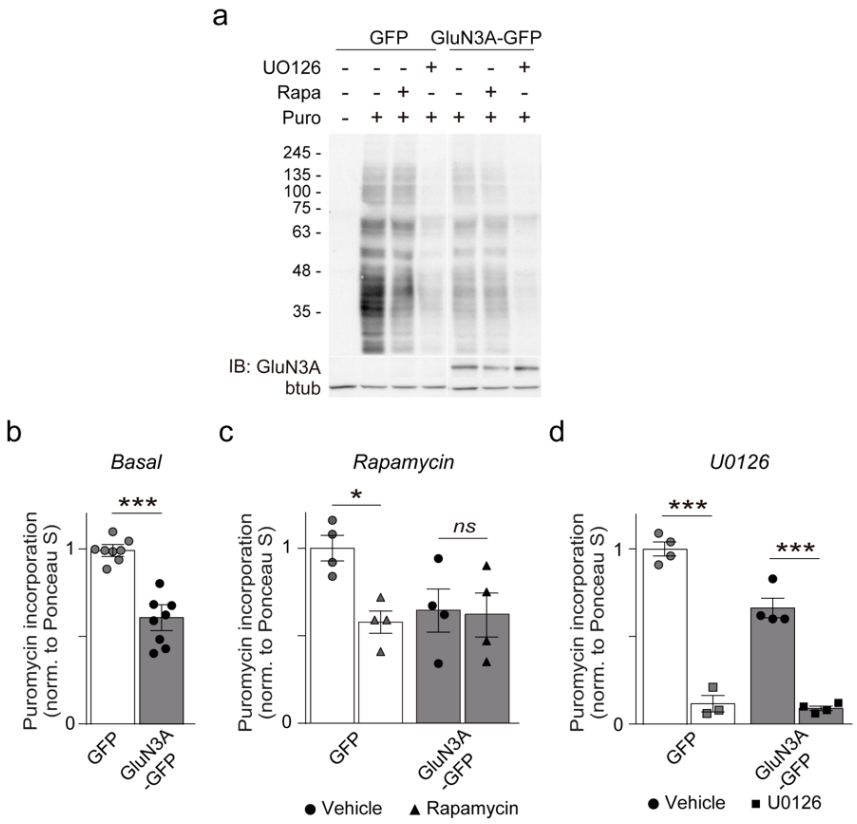

Figure 42. GluN3A rescues exacerbated mTOR-dependent protein synthesis.

Grin3a-/- cortical neurons were infected at DIV6 with lentiviruses expressing GFP or GluN3A-GFP and protein synthesis was analyzed at DIV12. *(a)* Representative western blot and *(b-d)* quantification of puromycin incorporation (puro, 10ng/ml, 30min incubation) in infected neurons in basal conditions, *(b)* or upon rapamycin (rapa, 100nM, 1h incubation) *(c)* and U0126 (5μM, 20min incubation) treatment. Puromycin levels were normalized to Ponceau S staining. GluN3A expression levels are shown (IB). n=4-8 from 4 independent cultures; *p<0.05, ***p<0.001, two-way ANOVA followed by Tukey's test.

6. mTOR Inhibition Requires GluN3A C-Terminal Domain Interactions

Two broad mechanisms could in principle be involved in these differences in signaling: 1) inhibition of NMDAR-mediated calcium influx and voltage-dependent magnesium block by GluN3A ("*ionotropic function*"); 2) recruitment by GluN3A, through interactions of its intracellular CTD ("*metabotropic function*"). GluN3A-CTD binds scaffolding and signaling proteins that anchor the receptor to the actin cytoskeleton and regulate functions such as synaptic plasticity, spine stabilization

and morphogenesis (see GluN3A-CTD interacts with a unique set of intracellular proteins).

To evaluate whether GluN3A modulates the mTOR pathway via metabotropic interactions of its CTD, we generated a GluN3A mutant lacking the whole CTD. However, the truncated version did not go to the cell surface, precluding further experiments (data not shown) (Dey, 2017). As an alternative, we used a previously characterized GluN3A mutant lacking the distal 33aa of the GluN3A-CTD (GluN3A1082Δ-GFP; Figure 17). This mutant displays similar distribution and targeting to the cell surface than full-length GluN3A (Fiuza et al., 2013).

Primary cortical neurons from *Grin3a* -/- embryos were then infected at DIV6 with lentiviruses expressing GFP, full-length GluN3A (GluN3A-GFP) or GluN3A1082Δ-GFP and treated at DIV12 with bicuculline or BDNF for 1h (Figure 43). While full-length GluN3A fully reversed enhanced mTOR activation (Figure 43b,e, white *vs*. grey bars) and hyper-induction of Arc and c-Fos (Figure 43c,f, white *vs*. grey bars) by either bicuculline or BDNF, the GluN3A1082Δ mutant failed to do so (Figure 43b,c,e,f, white *vs*. pale blue bars). Furthermore, GluN3A1082Δ did not affect other activity-dependent signaling pathways like MAPK-ERK pathway or induction of Zif268 (Figure 43d), as was already described for full-length GluN3A (Dey, 2017).

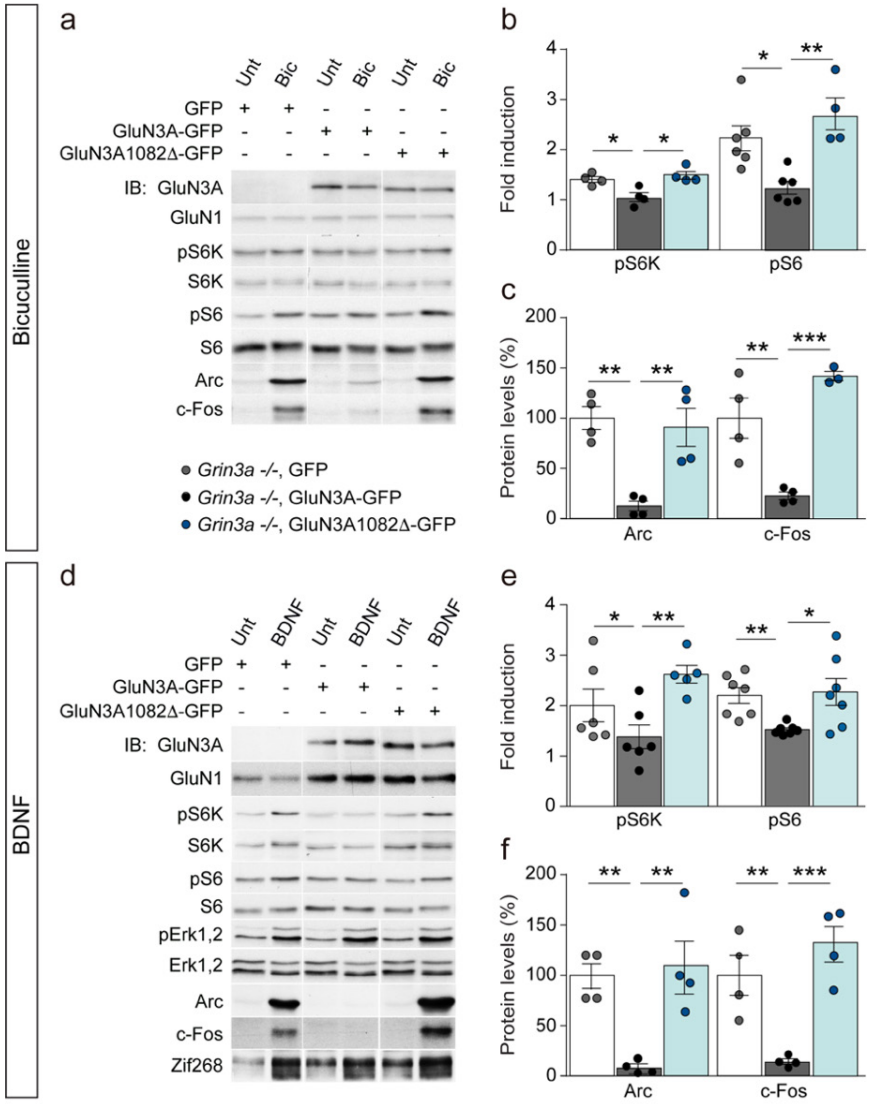

Figure 43. Inhibition of mTOR requires GluN3A-CTD interactions.

(a) Experimental design for re-expression of full-length or mutant GluN3A in *Grin3a -/-* cortical neurons. Neurons were infected with lentiviruses expressing GFP, GluN3A-GFP or GluN3A1082Δ-GFP, and stimulated with bicuculline *(b, c)* or BDNF *(e, f)* for 1h. *(a)* Representative western blots of lysates from bicuculline-treated neurons probed for the indicated antibodies. *(b)* Fold-induction of phosphorylated S6K and S6 (normalized to total levels), Arc and c-Fos in response to bicuculline (n=3-6 from 2-3 independent cultures, *p<0.05, **p<0.01, ***p<0.001 one-way ANOVA followed by Tukey's test). *(d-f)* Analogous experiments to those represented in *(a-c)* upon BDNF stimulation (n=4-7 from 2-4 independent cultures, *p<0.05, **p<0.01, ***p<0.001 one-way ANOVA followed by Tukey's test).

To evaluate potential differences in ionotropic function, we studied the Ca^{2+} permeability and response to glycine of receptors containing full-length

GluN3A or GluN3A1082Δ in collaboration with Dr. Stephen J. Tavalin (University of Tennessee) and Dr. Pierre Paoletti (L´Institut de Biologie de l'Ecole Normale Supérieure -IBENS-, Paris). GFP-GluN3A and GFP-GluN3A1082Δ constructs were co-transfected with GluN1-1A and GluN2A in HEK293 cells to analyze the electrophysiological responses to acutely applied glutamate. GluN3A and GluN3A1082Δ yielded similarly reduced shifts in reversal potential (ΔErev) compared to conventional GluN1-1A/GluN2A NMDARs (Chowdhury et al., 2013; Pérez-Otaño et al., 2006), measured during steady-state I-V relations obtained via a voltage-ramp protocol in 2 and 10mM extracellular Ca^{2+}, indicating that differences could not be attributed to Ca^{2+} permeability (Figure 44a,b). Additionally, both GluN3A versions harbored similarly reduced current densities compared to conventional NMDARs, suggesting that the truncation does not affect the extent to which these subunits incorporate into functional triheteromeric receptors (Figure 44c).

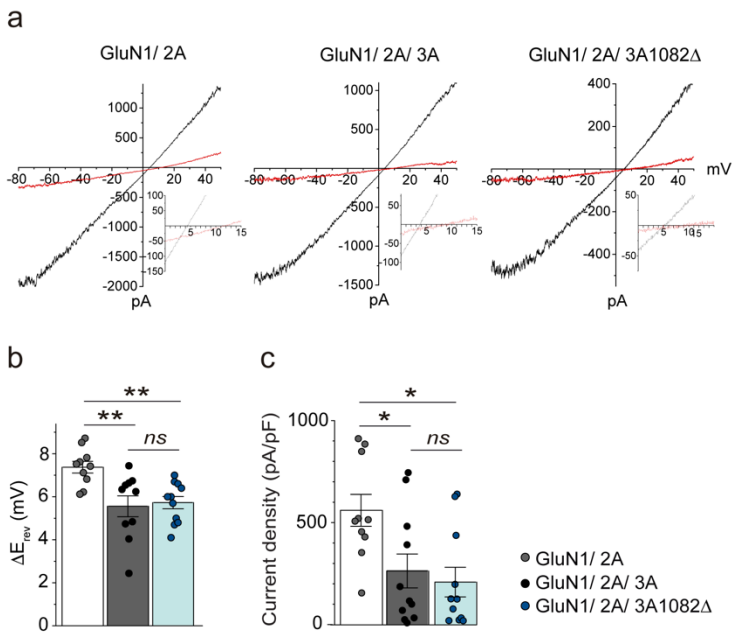

Figure 44. GluN3A and GluN3A1082Δ have no ionotropic differences.

(a) Representative steady-state glutamate-evoked ramp currents obtained with 2mM (black) and 10mM (red) extracellular Ca^{2+} for HEK293 cells expressing GluN1A/ 2A alone, or with either GFP-GluN3A or GFP-GluN3A1082Δ. Insets show currents on expanded scale to highlight the E_{rev}. *(b)* Summary graph of the ΔErev obtained from multiple experiments. *(c)* Summary graph depicting current density from HEK293 cells expressing GluN1-1A/GluN2A alone, or with either GFP-GluN3A or GFP-GluN3A1082Δ. n = 10–11, *p< 0.05, **p< 0.01 one-way ANOVA followed by Bonferroni post-hoc test.

We additionally ruled out the possibility that the deletion modified responses to glycine of diheteromeric GluN1/ 3 receptors. We took advantage of the GluN1 antagonist CGP-78608, which prevents glycine binding to GluN1 (Auberson et al., 1999; Yao and Mayer, 2006). It therefore bypasses desensitization and unmask large glycine-activated currents mediated by GluN1/ 3A receptors (Grand et al., 2018). No differences in evoked glycine currents were observed between GluN1/ 3A and GluN1/ 3A1082Δ (Figure 45).

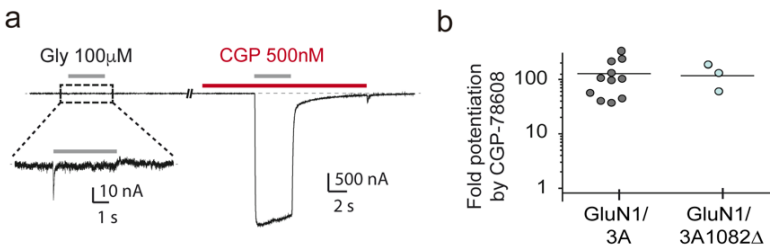

Figure 45. GluN1/ 3A and GluN1/ 3A1082Δ receptors generate equally evoked glycine currents.

(a) Responses to glycine of HEK293 cells expressing GluN1/ 3A receptors in absence or presence of CGP-78608 (500 nM). *(b)* Quantification of fold potentiation by CGP-78608 for GluN1/ 3A and GluN1/ 3A1082Δ receptors (n = 3-11).

Collectively, the absence of any evident ionotropic differences and the involvement of distal 33aa of the GluN3A-CTD supports the idea that inhibition of mTOR involves metabotropic interactions of GluN3A-containing NMDARs with synaptic adaptors or scaffolds.

6.1. GLUN3A-CTD IS NECESSARY TO DECREASE ENHANCED PROTEIN SYNTHESIS RATES IN *GRIN3A -/-* CORTICAL NEURONS

Given the role of GluN3A-CTD in the control of mTORC1 activity and mTORC1-dependent IEG induction, we directly analyzed its role on mTORC1-dependent protein synthesis. *Grin3a -/-* neurons were infected at DIV6 with lentiviruses expressing GFP, full-length GluN3A (GluN3A-GFP) or the mutant GluN3A1082Δ-GFP and treated at DIV12 with rapamycin or vehicle for 1h (Figure 46). As shown above, GluN3A expression obliterated rapamycin sensitivity, turning neurons into a juvenile mode of protein synthesis which is no longer mTORC1-dependent (Figure 46b white *vs*. grey bars). By contrast, the CTD mutant GluN3A1082Δ did not reduced basal protein synthesis rates and mTORC1-dependence was

preserved as demonstrated by rapamycin sensitivity (Figure 46b white *vs*. pale blue bars). This finding further confirmed that the distal 33aa region of GluN3A-CTD is critical for the control of mTORC1-dependent protein synthesis.

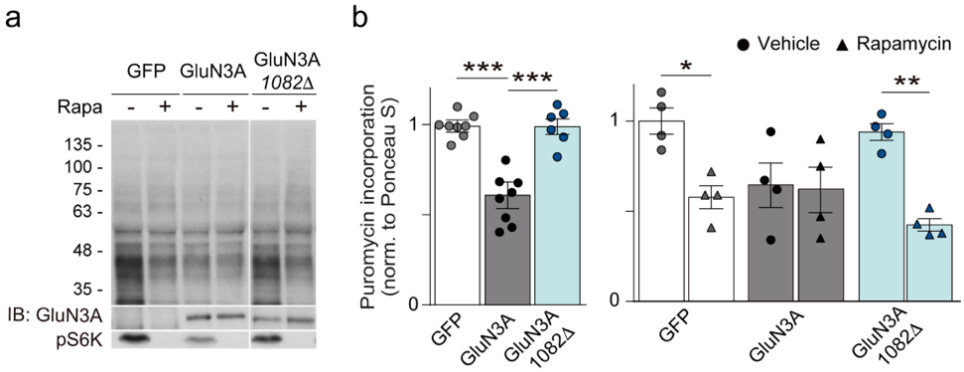

Figure 46. GluN3A rescues the increased mTOR-dependent protein synthesis in *Grin3a -/-* neurons.

Grin3a-/- cortical neurons were infected at DIV6 with lentiviruses expressing GFP, GluN3A-GFP or GluN3A1082Δ-GFP and protein synthesis was analyzed at DIV12. *(a)* Representative western blot and *(b)* quantification of puromycin incorporation (10ng/ml, 30min incubation) in infected neurons in the presence or absence of rapamycin (rapa, 100nM, 1h) normalized to Ponceau S staining. GluN3A expression levels and status of mTOR activation were monitored with the indicated antibodies (IB). GFP and GluN3A data points are the same than in Figure 42. n=4-8 from 4 independent cultures; *p<0.05, **p<0.01, ***p<0.001, two-way ANOVA followed by Tukey's test.

We conducted an independent experiment to address the role of the GluN3A-CTD in protein synthesis using a mutant where the GluN3A-CTD was replaced by the GluN2A-CTD (GluN3ACt2A-GFP; see Figure 17). Because the longer GluN2A-CTD couples NMDARs to different signaling molecules than GluN3A-CTD (Hardingham, 2019; Pérez-Otaño et al., 2016; Sun et al., 2018), we would expect the GluN3A-Ct2A to abolish GluN3A-mediated metabotropic signaling. Additionally, GluN2A has been reported to activate mTOR thus having an opposite role to the GluN3A-driven repression of mTOR that we observe here (Gordillo-Salas et al., 2018; Tran et al., 2007). In this experiment, *Grin3a -/-* cortical neurons were infected at DIV6 with GFP, GluN3A-GFP and GluN3ACt2A-GFP, and protein synthesis analyzed at DIV12. As GluN3A1082Δ-GFP (Figure 46), GluN3ACt2A-GFP mutant did not rescue enhanced protein synthesis in contrast to the full-length GluN3A (Figure 47a,b, grey *vs* pink column). Remarkably, GluN3ACt2A-GFP boosted protein synthesis above the already high basal rates

of *Grin3a -/-* neurons (Figure 47b, white *vs* pink column). The effect is in-line with the previously reported activation of mTOR and demonstrates that NMDAR subunit composition determines the modes and magnitude of protein synthesis.

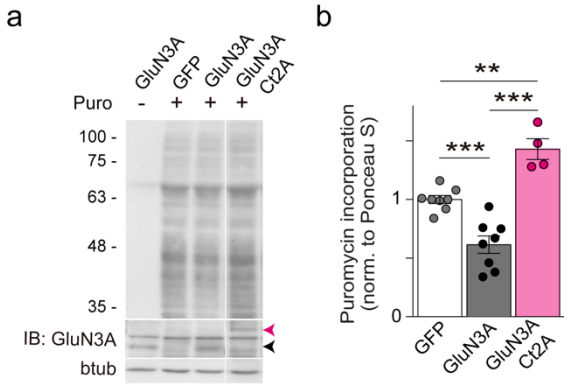

Figure 47. GluN3ACt2A mutant boosts protein synthesis.

Grin3a-/- cortical neurons were infected at DIV6 with lentiviruses expressing GFP, GluN3A-GFP or GluN3ACt2A-GFP and protein synthesis was analyzed at DIV12. *(a)* Representative western blot and *(b)* quantification of puromycin incorporation in infected neurons normalized to Ponceau S staining. GluN3ACt2A has a higher molecular weight (pink arrow) than full-length GluN3A (black arrow) as shown in the IB. GFP and GluN3A data points are the same than in Figure 42. n=4-8 from 2-4 independent cultures; **p<0.01, ***p<0.001, two-way ANOVA followed by Tukey's test.

7. GluN3A-CTD Interactions Control the Assembly of Synaptic GIT1-mTORC1 Complexes

We then searched for GluN3A partners that bind the CTD and could mediate its ability to inhibit mTOR-dependent translation. A prominent candidate is the postsynaptic scaffold GIT1. Binding to GluN3A sequesters GIT1 away from synaptic locations and impairs its ability to nucleate actin regulators such as the Rac1-GEF β-PIX in dendritic spines (see GIT1; Intriguingly, proteomic work detected GIT1 in mTOR immunoprecipitates from mouse astrocytes but neither the complex composition nor a function for the interaction could be established (Smithson and Gutmann, 2016). GIT1 binds GluN3A through the distal 33aa of its CTD. As shown above, those 33aa are required for mTOR inhibition. We reasoned that, analogous to β-PIX, GluN3A sequestration of GIT1 might impair mTOR

function by: 1) displacing mTOR from synapses, and/ or 2) inhibiting the formation of mTOR complexes.

7.1. GIT1-mTORC1 COMPLEXES ARE SYNAPTIC AND FUNCTIONAL

We first conducted a series of biochemical experiments to examine whether mTOR and GIT1 form a complex in neurons and to identify other putative components of the complex. Using reciprocal co-immunoprecipitation (co-IP) assays with GIT1 or mTOR antibodies, we identified mTOR-GIT1 complexes in P16 WT mice hippocampal (Figure 48a) and cortical (Figure 48b) PNS fractions. Using a standard co-IP buffer (0.1% TX-100 + 0.1% SDS) we were able to coprecipitate the mTOR–GIT1–β-PIX complex previously described by (Smithson and Gutmann, 2016) (Figure 48). However, the adaptor proteins Raptor or Rictor, constitutive part of mTORC1 and mTORC2 respectively, were not pulled down by the mTOR antibody. To preserve the physiological interactions, we modified lysis conditions and used a buffer containing the detergent 0.3% CHAPS (Kim et al., 2002). Under this condition, the mTOR antibody pulled down both Raptor and Rictor (Figure 49a; mTOR IP lane). However, only Raptor was identified in GIT1 immunoprecipitates (Figure 49a; GIT1 IP lane), indicating that GIT1-mTOR interaction was exclusive for mTORC1 (Figure 49c). Moreover, we detected phosphorylated mTOR at Ser^{2448} in GIT1 immunoprecipitates, demonstrating GIT1-mTORC1 complex functionality (Figure 49b).

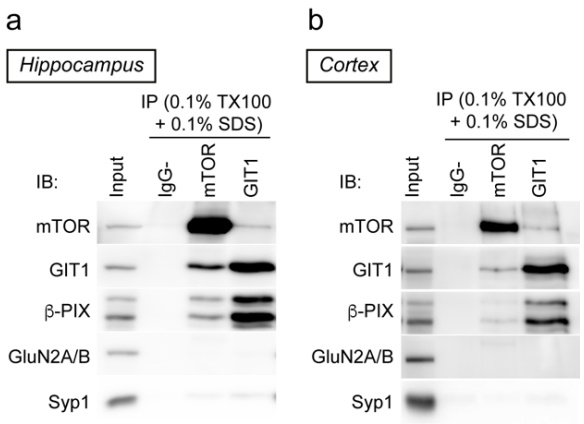

Figure 48. mTOR and GIT1 interaction in mouse brain.

Representative IB of a co-IP experiment on PNS of *(a)* hippocampal and *(b)* cortical tissue from P16 WT mice using a buffer containing 0.1% TX-100 + 0.1% SDS. mTOR and GIT1 were

immunoprecipitated and mTOR, GIT1, β-PIX, GluN2A/B and Synaptophysin1 (Syp1) revealed by western blotting in the immunoprecipitated material. For the input lane, 10% of the PNS used for the co-IP experiment was loaded onto the gels. IgG- refers to a negative control in which the sample was incubated without antibody.

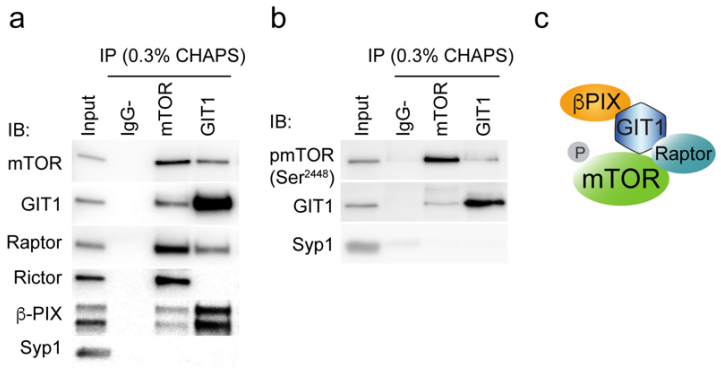

Figure 49. Functional GIT1-mTORC1 complexes.

(a) Representative IB of a co-IP experiment on PNS of hippocampal tissue from P16 WT mice using a buffer containing 0.3% CHAPS. mTOR and GIT1 were immunoprecipitated and mTOR, GIT1, Raptor, Rictor, β-PIX and Syp1 revealed by western blotting in the immunoprecipitated material. *(b)* Analogous experiment to *(a)* in which pmTOR (Ser^{2448}), GIT1 and Syp1 were revealed by western blotting in the immunoprecipitated material. For the input lane, 10% of the PNS used for the co-IP experiment was loaded onto the gels. IgG- refers to a negative control in which the sample was incubated without antibody. *(c)* Schematic of the GIT1-mTOR partners detected in our experiments.

We then asked if GIT1-mTORC1 complexes are found in synaptic compartments. To answer this question, we first carried out a subcellular fractionation as in (Franchini et al., 2019) (Figure 50). Starting from total homogenates (H) of DIV14 rodent primary hippocampal neurons, we purified P2 and TIF fractions (the detailed protocol is in the Materials and Methods section Subcellular Fractionation). GIT1 was enriched in postsynaptic compartments, as previously described in (Fiuza et al., 2013). Other components of the mTOR machinery were also found in the TIF fraction (Figure 50a). Remarkably, mTOR machinery (mTOR, Raptor and the effector S6) was also present in the P2 and TIF fractions. We further discovered that GIT1 coprecipitated with mTOR and Raptor in both P2 and synaptic (TIF) fractions from DIV14 primary hippocampal neurons (Figure 50b).

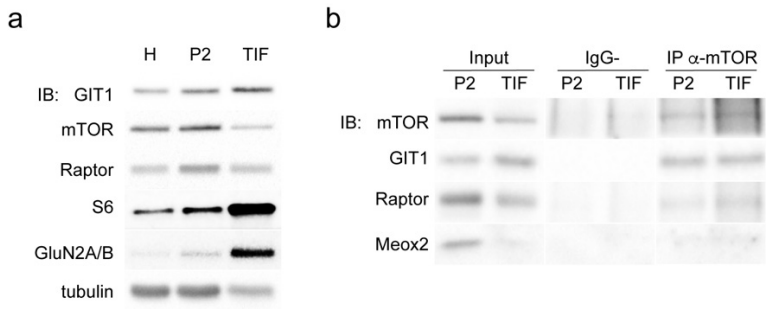

Figure 50. GIT1 co-immunoprecipitates with mTOR in synaptic TIF fractions.

(a) Characterization of the protein enrichment of GIT1, mTOR, Raptor, S6 and GluN2A/B, positive control, by western blotting after a subcellular fractionation of DIV14 primary hippocampal neurons (H, homogenate; P2; Crude Membrane Fraction; TIF, Triton Insoluble Fraction). *(b)* Representative IB of a co-IP experiment on DIV14 primary hippocampal neurons P2 and TIF. mTOR was immunoprecipitated and mTOR, GIT1, Raptor and Meox2 revealed by western blotting in the immunoprecipitated material. For the input lane, 40% of the P2 or TIF used for the co-IP experiment was loaded onto the gels. IgG- refers to a negative control without antibody.

To further examine the subcellular localization of GIT1-mTORC1 complexes in cultured neurons, we conducted an *in situ* Proximity Ligation Assay (PLA) with antibodies against GIT1 and mTOR. DIV17 hippocampal neurons transfected at DIV9 with GFP were processed as described in the methods section "Proximity Ligation Assay". PLA puncta were present along the dendritic shaft and often localized within or at the base of dendritic spines (Figure 51), suggesting that GIT1 provides a mode to position ready-to-use pools of mTORC1 translational machinery near synaptic sites to support fast dendritic protein synthesis in response to synaptic signals.

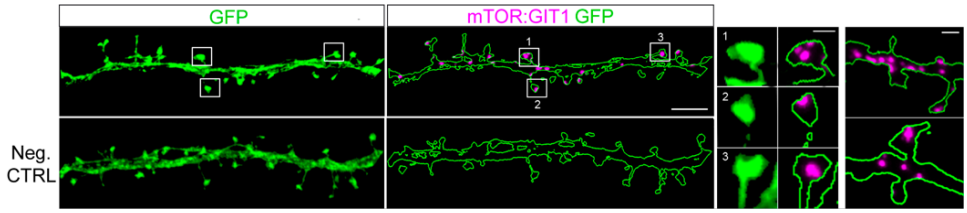

Figure 51. mTOR and GIT1 directly interact in synaptic compartments.

Representative images of PLA for mTOR-GIT1 (magenta) in DIV17 hippocampal neurons transfected with GFP to visualize dendritic morphology (scale bar, 5μm). High magnification examples of spines (scale bar, 0.5μm) and dendrites (scale bar, 1μm) containing mTOR-GIT1 complexes are shown in the right. As negative control, only mTOR primary antibody was used.

To study if GIT1-mTORC1 complexes respond to activity, we stimulated DIV14 cortical neurons with BDNF or bicuculline and quantified mTOR phosphorylation in the GIT1 immunoprecipitates. Both bicuculline and BDNF induced large increases in the phosphorylation of GIT1-bound mTOR on Ser^{2448} (Figure 52a,b). The phosphorylation of mTOR in GIT1-mTORC1 complexes was much higher than phosphorylation of the total cellular mTOR pool (Figure 52c) (BDNF: 1.98 ± 0.38 fold-increase in total lysates *vs* 4.2 ± 1.15 in GIT1-immunoprecipates; bicuculline: 1.42 ± 0.15 *vs* 4.63 ± 1.24). Altogether, these experiments demonstrate the existence of neuronal mTORC1 complexes composed of GIT1, mTOR and Raptor that mediate mTORC1 activation by synaptic stimuli.

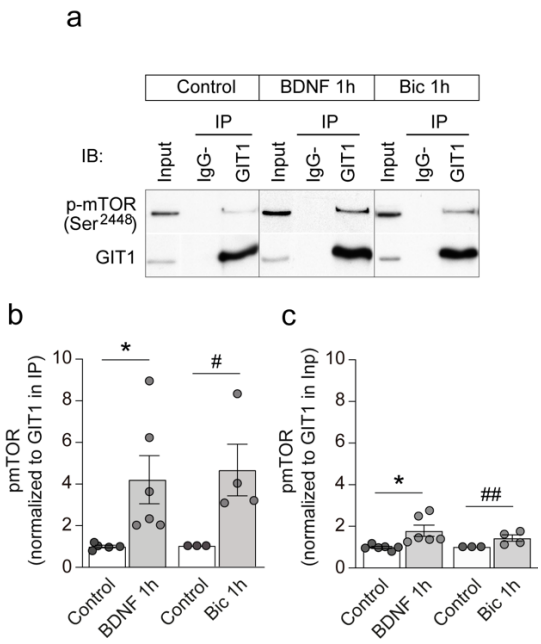

Figure 52. GIT1-mTORC1 complexes respond to activity.

Cortical neurons stimulated with BDNF (100 ng/ml, 1h) or bicuculline (50μM, 1h) were solubilized with 0.3% CHAPS and incubated with GIT1 antibody (IP). *(a)* Representative immunoblots. *(b,c)* Quantification of mTOR phosphorylation in *(b)* GIT1 immunoprecipitates and *(c)* total lysates. n = 3-6 from 3 independent cultures; *p<0.05, # = 0.06, ## = 0.07, two-tailed unpaired t-test.

7.2. GLUN3A REGULATES THE ASSEMBLY OF GIT1-MTORC1 COMPLEXES

Given the unique expression profile of GluN3A subunits, we studied the abundance of GIT1-mTORC1 complexes over postnatal brain development. Hippocampal (Figure 53a) and cortical (Figure 53b) extracts from P7, P10 and P16 WT mice were lysed with 0.1% TX100 + 0.1% SDS buffer and immunoprecipitated with GIT1 antibody. GIT1-mTORC1 complexes were absent at P7 and P10, and were not observed until P16 (Figure 53a,b; red asterisk), matching the timing of synaptic GluN3A down-regulation and suggesting a negative regulatory role of GluN3A expression on complex assembly (see GluN3A-NMDARs display a unique expression pattern; (Henson et al., 2012)). To test this idea, we compared the formation of GIT1-mTORC1 complexes in P10 WT *vs Grin3a -/-* hippocampal extracts (Figure 54). This postnatal age overlaps GluN3A's peak of expression and did not reveal GIT1-mTORC1 complex in WT mice (Figure 53). However, genetic deletion of GluN3A was sufficient to unleash the formation of GIT1-mTORC1 complexes, as shown by enhanced GIT1-mTOR and GIT1-Raptor binding (Figure 54a,b).

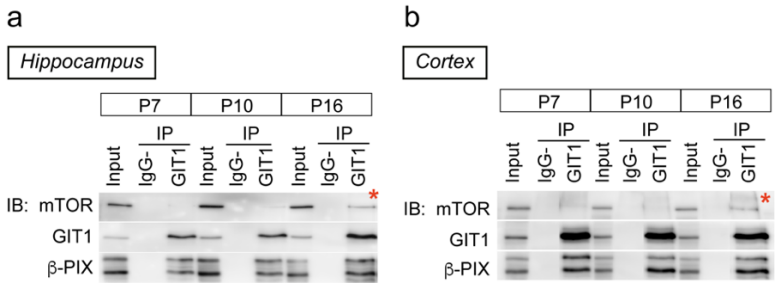

Figure 53. GIT1-mTORC1 complexes are regulated through postnatal development.

(a) Hippocampal and *(b)* cortical PNS extracts from P7, P10 and P16 WT mice were lysed with 0.1% TX100 + 0.1% SDS buffer, immunoprecipitated with GIT1 antibody, and immunoprecipitates probed for the indicated antibodies (IB). Input is 10% of the lysate used for immunoprecipitation. IgG- refers to a negative control without antibody. Red asterisks indicate mTOR-bound GIT1.

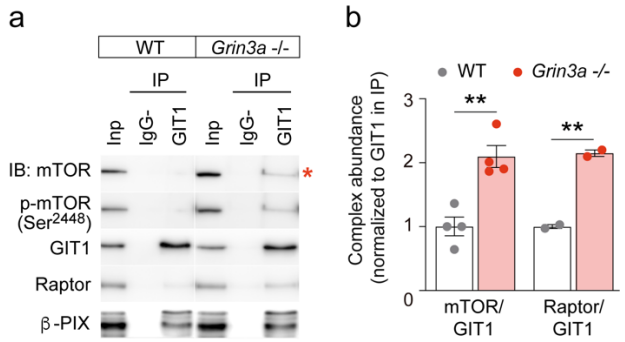

Figure 54. GIT1-mTORC1 complex formation is enhanced in P10 *Grin3a-/-* hippocampus.

(a) Representative IB and *(b)* quantifications of a co-IP experiment on PNS of hippocampal tissue from P10 WT and *Grin3a -/-* mice using a buffer containing 0.3% CHAPS. GIT1 was immunoprecipitated and mTOR, pmTOR (Ser^{2448}), GIT1, Raptor and β-PIX revealed by western blotting in the immunoprecipitated material. n=2-4 mice; **p<0.01 two-tailed unpaired t-test. Bound mTOR and Raptor were normalized to GIT1 levels in the immunoprecipitate. For the input lane, 10% of the PNS used for the co-IP experiment was loaded onto the gels. IgG- refers to a negative control in which the sample was incubated without antibody.

7.3. GluN3A-CTD interactions are required for the modulation of GIT1-mTORC1 complex assembly

We finally assessed if GluN3A control over GIT1-mTORC1 interaction was mediated by the GluN3A-GIT1 interaction through the distal CTD 33aa. For that purpose, we carried out *in vitro* rescue experiments using DIV13 primary cortical neurons from *Grin3a-/-* mice infected with lentiviruses expressing full-length GluN3A-GFP, the GluN3A1082Δ-GFP mutant and control GFP. We discovered that only full-length GluN3A but not GluN3A1082Δ was capable to reduce the amount of mTOR bound to GIT1 (Figure 55). Together, these results demonstrate that modulation of GluN3A expression could offer a key local regulatory mechanism to set modes of translational control poised for synapse and perhaps memory selection.

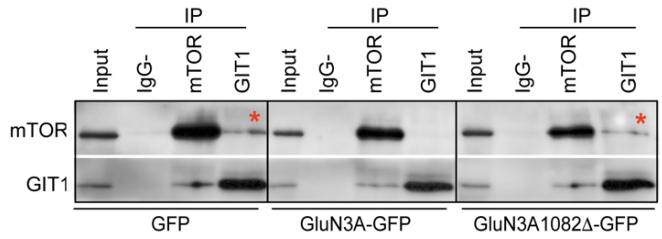

Figure 55. GluN3A but not GluN3A1082Δ disrupt GIT1-mTORC1 interactions.

DIV13 cortical neurons derived from *Grin3a-/-* mice were infected at DIV7 with GFP, GluN3A-GFP and GluN3A1082Δ-GFP and solubilized with 0.1% TX100 + 0.1% SDS buffer. Lysates were incubated with GIT1 or mTOR antibodies and immunoprecipitated materials were blotted with the indicated antibodies (IB). Input is 10% of the lysate used for immunoprecipitation. IgG- refers to a negative control without antibody. Red asterisks indicate mTOR-bound GIT1.

8. THE SYNAPTIC SCAFFOLDING PROTEIN GIT1 IS NECESSARY FOR MTORC1-DEPENDENT PROTEIN SYNTHESIS

To test whether GIT1 is required for nucleating synaptic mTORC1 signaling, we knocked-down expression using a validated shGIT1 that silenced GIT1 expression levels in an effective and selective manner (Figure 56; (Smithson and Gutmann, 2016)). Primary cortical neurons were infected at DIV10 with GFP or shGIT1-GFP lentiviruses and analyzed at DIV14 upon BDNF stimulation in the presence or absence of rapamycin (Figure 57). Lentiviral knockdown of GIT1 reduced mTORC1 responses to BDNF, as shown by reduced phosphorylation of S6 and S6K (Figure 57a,b). Moreover, GIT1 knockdown decreased the rapamycin-sensitive translation of Arc (Figure 57a,c).

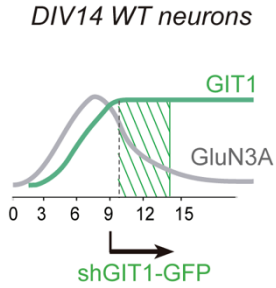

Figure 56. Experimental timing for GIT1 knockdown.

Schematic of endogenous GIT1 (green) and GluN3A (grey) expression and the windows of lentiviral infection (green square) in primary cortical neurons. For silencing experiments, cortical neurons were

infected at DIV10 with the lentiviruses shGIT1_7730-GFP (hereinafter referred to as shGIT1-GFP) or control GFP and analyzed at DIV14, when endogenous GIT1 expression is maximum.

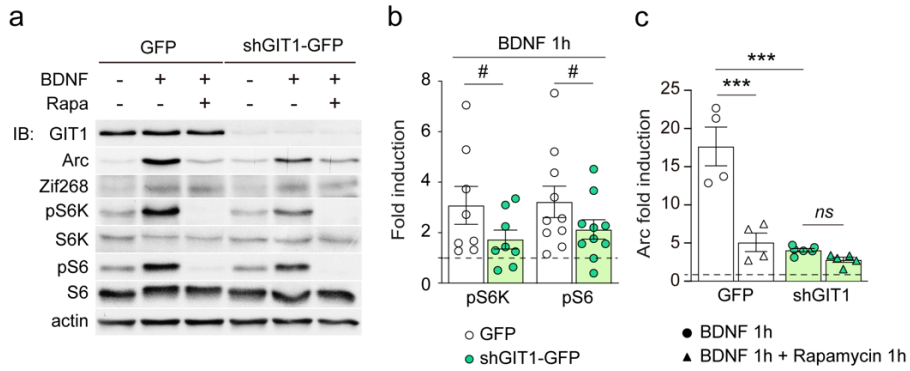

Figure 57. GIT1 knockdown reduces mTORC1 activation by BDNF and rapamycin-sensitive Arc translation.

Cortical neurons infected at DIV10 with shGIT1-GFP were stimulated at DIV14 with BDNF (100ng/ml, 1h) with or without pre-incubation with rapamycin (100nM, 1h). *(a)* Representative western blot probed with the indicated antibodies (IB). *(b)* BDNF induction of phosphorylated S6K and S6 normalized to total protein levels (n = 8-10 samples from 4-5 independent cultures; # pS6K: p=0.13, # pS6: p=0.05, two-tailed paired t-test). *(c)* BDNF induction of Arc protein production (n = 4-6 samples from 2 independent cultures; ***p<0.001, two-way ANOVA followed by Tukey's test).

Further evidence was provided by SUnSET measures of protein synthesis rates upon GIT1 silencing. Primary cortical neurons were infected with GFP or shGIT1 lentiviruses at DIV10 and SUnSET was performed at DIV14. GIT1 knockdown reduced protein synthesis in a dose-dependent manner, with higher inhibition in lower GIT1 expression levels (Figure 58a,b). Then, we studied if GIT1 inhibition was mTORC1-dependent (Figure 59). As previously shown in conditions of GlluN3A overexpression, knocking-down GIT1 was sufficient to prevent the onset of mTORC1-dependent protein synthesis in mature neurons, as evident by lack of rapamycin-dependence in DIV14 cortical neurons (Figure 59a,c). Together, these results further indicate that GIT1 is necessary for the emergence of mature, mTORC1-dependent protein synthesis.

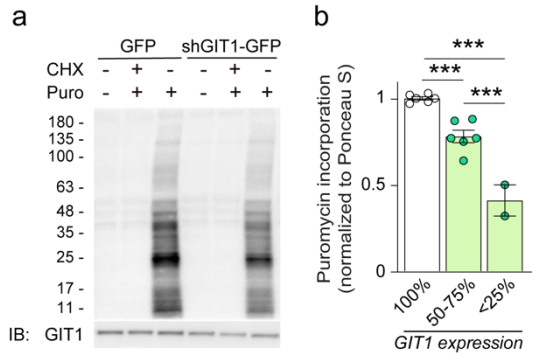

Figure 58. GIT1 knockdown reduces protein synthesis in a dose-dependent manner.

Cortical neurons were infected at DIV10 with lentiviruses expressing GFP or shGIT1-GFP and treated with vehicle or CHX (25μM, 15min) prior puromycin incubation (puro, 10ng/ml, 30min) *(a)* Representative IB of puromycin incorporation and GIT1 levels. *(b)* Quantification of puromycin incorporation related to the achieved GIT1 silencing. In all cases, puromycin levels were normalized to Ponceau S staining. n = 2-6 from 3 independent cultures; ***p<0.001, one-way ANOVA followed by Tukey's test.

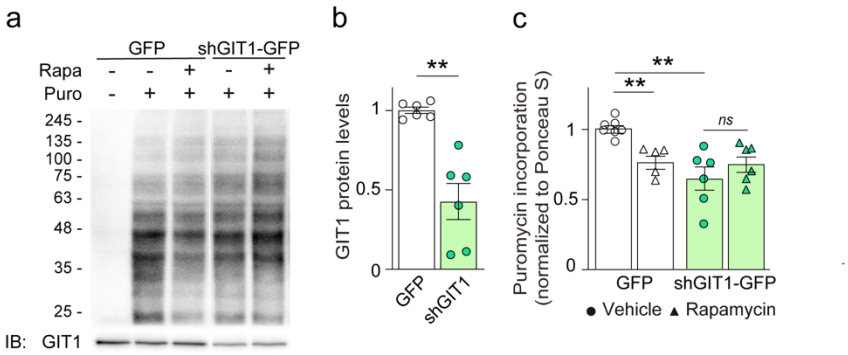

Figure 59. GIT1 knockdown reduces mTORC1-dependent protein synthesis.

Cortical neurons were infected at DIV10 with lentiviruses expressing GFP or shGIT1-GFP and responses to rapamycin (rapa, 100nM, 1h) were analyzed at DIV14 after puromycin (puro, 10ng/ml, 30min) incubation. *(a)* Representative IB and quantification of *(b)* GIT1 silencing and *(c)* puromycin incorporation in GFP and shGIT1-GFP expressing neurons in the presence or absence of rapamycin are shown. In all cases, puromycin levels were normalized to Ponceau S staining. n = 5-7 from 4 independent cultures; *p<0.05, **p<0.01, ***p<0.001, two-way ANOVA followed by Tukey's test.

9. GLUN3A CONSTRAINTS ON MTOR ACTIVATION FAVORS THE FORMATION OF ASSOCIATIVE MEMORIES

To test whether the modulation of protein synthesis by GluN3A affects memory formation, we assessed the ability of genetically modified GluN3A mice to store associative memories in collaboration with a postdoc in the lab, Dr. Luis García-Rabaneda. For this purpose, we took advantage of a well-established learning and memory paradigm: Conditioned Taste Aversion (CTA). CTA is a classical conditioning test in which mice learn to associate a novel taste (conditioned stimulus -CS-, saccharin) with an aversive unconditioned stimulus that induces nausea (US, LiCl) (Welzl et al., 2001). Associative memory formation in this task requires protein synthesis and can be achieved with a single pairing of CS-US allowing stable LTM formation (Adaikkan and Rosenblum, 2015; Rosenblum et al., 1993).

In a first set of experiments, double transgenic mice expressing high GluN3A levels into adulthood (dtGluN3A) and control mice (single transgenic mice) were habituated for 6 days to drink water from 2 different bottles placed on their cages. At day 7, the water was replaced with saccharin 0.2% (CS) and 40 minutes later mice were injected i.p. with saline or LiCl 0.15M (US). Mice were subjected to a two-bottle preference test 24 hours later, in which the animal is given the opportunity to choose between the familiar (water) and novel (saccharin) fluid (Figure 60a). Under these conditions, dtGluN3A displayed deficits in the CTA paradigm, exhibiting similar preference for saccharin after treatment with saline or LiCl (Figure 60b, green bars). A series of control experiments ruled out the possibility that the deficit was due to insensitivity to LiCl or to defects in distinguishing flavors (sweet, bitter, etc.) (Figure 60d-e). Conversely, *Grin3a -/-* mice did not display differences in CTA memory (Figure 60c).

Differences emerged when using more demanding versions of the task. The Rosenblum's group demonstrated that the LiCl dose and temporal contiguity between CS-US can be regulated to evaluate standard memory, as above, or "enhanced" memory by using a weaker paradigm (Adaikkan and Rosenblum, 2015). In a second set of experiments, we used a weak CTA paradigm where the strength of the US was reduced (LiCl 0.025 M) and the US and CS were separated by 5 hours (Figure 61a). Under this new set-up, only *Grin3a -/-* mice were able to

assciate the CS-US, as shown by their significantly reduced preference for saccharin after LiCl injection but intact preference in WT controls (Figure 61b). To determine whether this memory was mTOR-dependent, we treated mice with rapamycin using a subthreshold dosing regime (20 mg/kg for 5 days) that does not affect standard CTA memory in wild-type or *Grin3a-/-* mice (Figure 61d). Rapamycin completely erased the weak CTA memory in *Grin3a-/-* mice (Figure 61c). Thus, relief of GluN3A limitations on mTOR activation increases the ability of mice to form associative memories.

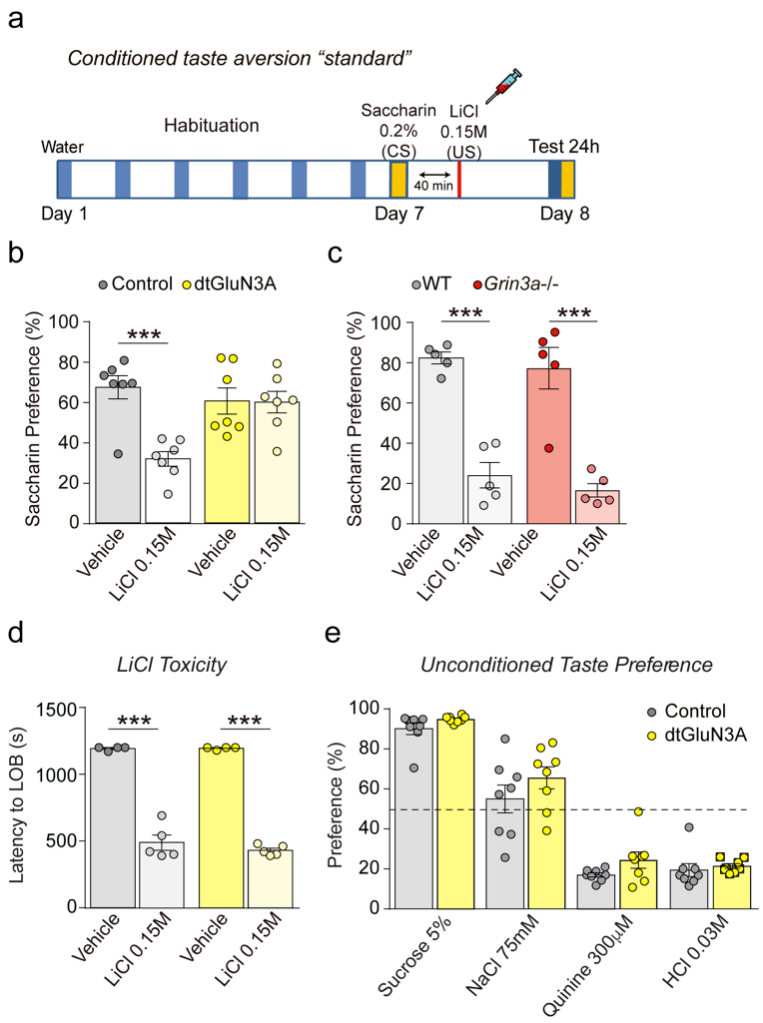

Figure 60. dtGluN3A mice, but not *Grin3a-/-* mice, exhibited aberrant regular associative memories.

(a) Standard CTA paradigm. *(b)* Saccharin preference of control and dtGluN3A mice, and *(c)* WT and *Grin3a-/-* mice after vehicle or LiCl (0.15M i.p.) injection (n=5-7 mice per group; ***p<0.001, two-way

ANOVA followed by Bonferroni post-hoc test). *(d)* dtGluN3A and control mice showed similar "lying on belly" (LOB) latencies after a 0.15M LiCl injection (n=4-5 mice per group; ***p<0.001, unpaired two-tailed t-test). *(e)* dtGluN3A and control mice showed similar taste preferences (n=8 mice per group).

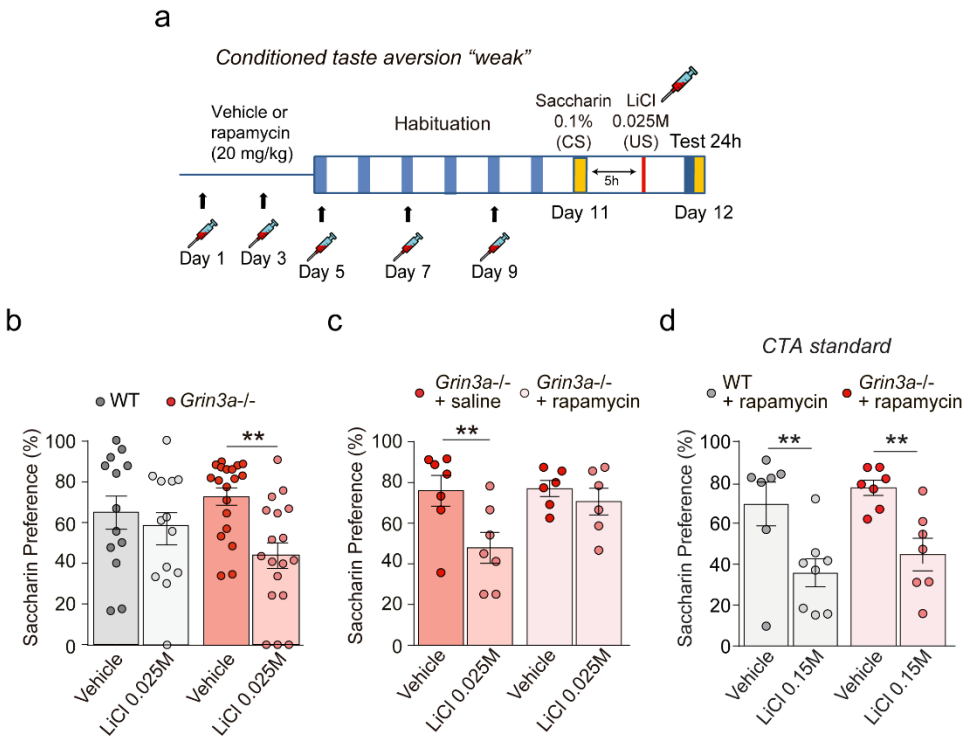

Figure 61. Rapamycin reverses enhanced associative memory in *Grin3a-/-* mice.

(a) Schematic of the weak CTA paradigm and rapamycin treatment regime. *(b-c)* Quantification of the saccharin preference after the weak CTA showing that *Grin3a-/-* mice exhibited a decreased preference *(b)* reversed by rapamycin 20mg/kg *(c)* (n=13-19 mice per group; **p<0.01, two-way ANOVA followed by Bonferroni post-hoc test). *(d)* Rapamycin treatment does not affect standard CTA memory in WT nor *Grin3a-/-* mice (n=6-8 mice per group; **p<0.01, two-way ANOVA with Bonferroni post-hoc test).

Discussion

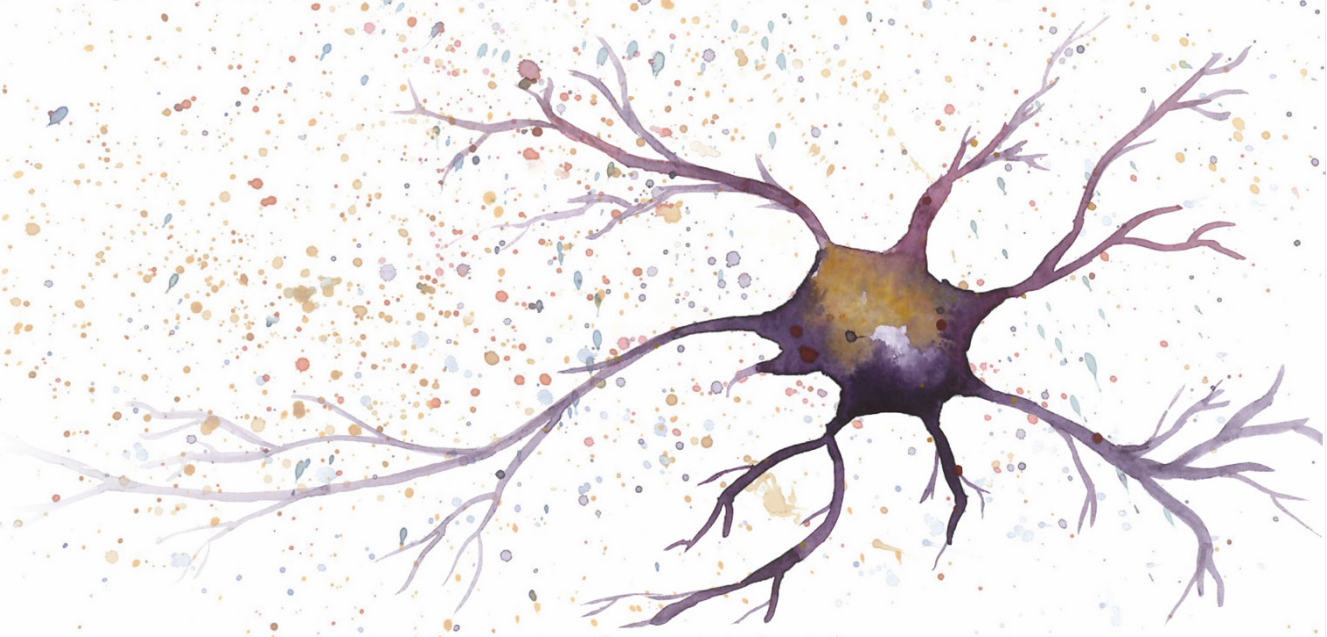

The aim of this thesis was to untangle cell biological mechanisms including receptor activated intracellular signaling that underlie the effects of juvenile GluN3A-NMDARs in long-term synapse remodeling and memory consolidation during postnatal development critical periods. In doing so, we have identified a novel mechanism that affords spatiotemporal control of synaptic mTORC1 activation and translation of a subset of activity-regulated mRNAs without affecting neuron-wide transcriptional responses. Specifically, we found that GluN3A-NMDARs prevent the assembly of GIT1-mTORC1 signaling complexes and limit local activation of mTORC1 through direct physical interaction with the postsynaptic scaffold GIT1. On the contrary, developmental or genetic removal of GluN3A enables the formation of GIT1-mTORC1 complexes and potentiates mTORC1 signaling both *in vitro* and *in vivo*. Among the physiological impacts, we show that GluN3A regulates the onset of mature, mTORC1-dependent protein synthesis in developing brains, and that this modulation endures until adulthood to place boundaries on LTM consolidation that determine which types of memories will be stored.

I. GluN3A regulates the assembly of GIT1-mTORC1 complexes

Several lines of evidence point towards juvenile GluN3A-NMDARs as key regulators of postnatal circuit refinements: *i)* GluN3A has a peak of expression in the postnatal brain that precedes and overlaps critical periods of experience-dependent synaptic refinement (Figure 6); *ii)* GluN3A prevents premature synapse maturation/ stabilization; *iii)* GluN3A later targets non-used synapses for pruning (Pérez-Otaño et al., 2016); and *iv)* activity-dependent endocytic removal from specific synapses promotes their maturation and long-lasting stabilization (Kehoe et al., 2014).

In an effort to decipher the molecular mechanisms, previous work from our lab demonstrated that GluN3A constrains the maturation and growth of inactive synapses by sequestering GIT1 away from synaptic locations (Fiuza et al., 2013). GluN3A physically interacts with GIT1 through the distal 33aa of its CTD (Figure 5), decreases its ability to nucleate β-PIX and in turn disrupts the activation of the Rac1/ PAK actin-remodelling pathway in dendritic spines.

Subsequent work from our group further screened the effects of GluN3A on activity-dependent signaling, finding that GluN3A selectively restricts the induction of a subset of NMDAR-dependent pathways including the phosphorylation of CaMKII, p38MAPK and mTOR (Figure 9b) (Dey, 2017). The serine/ threonine kinase mTOR stands out due to its major role in long-lasting structural synaptic and memory consolidation. Specifically, mTORC1 is a central cellular hub that promotes protein synthesis and cell growth in response to a diverse set of signals including nutrients availability, energy levels, insulin, growth factors and synaptic inputs. A number of previous studies associated stimulation of NMDARs to mTORC1 activation (summarized in mTOR signaling and local protein synthesis are regulated by NMDAR), but tonic repression of mTORC1-dependent protein synthesis by GluN2B-containing NMDARs has also been described (Miller et al., 2014; Wang et al., 2011). Our work expands the concept that activation or repression of mTOR is determined by subunit composition, with GluN2A-NMDARs activating but GluN3A or GluN2B repressing mTOR signaling likely under different physiological conditions (Gordillo-Salas et al., 2018; Miller et al., 2014; Tran et al., 2007; Wang et al., 2011). However, until now, the molecular determinants of stimulation or repression of protein synthesis had not been addressed and whether GluN3A and GluN2B share common mechanisms remains to be deciphered.

One major advance in the mTOR field was the discovery that mTOR has to be localized at specific subcellular compartments to sense couple the many diverse signals that trigger its activation (Liu and Sabatini, 2020). For instance, mTORC1 responses to amino acids require its recruitment to lysosomal membranes by the Ragulator-Rag complex (Sancak et al., 2008, 2010). A number of publications have previously reported that mTOR is localized in postsynaptic (Cammalleri et al., 2003; Schratt et al., 2004; Tang et al., 2002) and presynaptic (Poulopoulos et al., 2019; Terenzio et al., 2018) compartments, but the targeting mechanisms or complexes that coupled mTOR to synaptic signals remained undefined (further reviewed in mTOR localizes at synapses). Our work here suggest that GIT1 plays a scaffolding role targeting mTORC1 to dendritic synapses and, possibly presynaptic compartments as well. At the synapse, mTOR could sense synaptic signals and ensure their long-term structural stabilization, while GluN3A would negatively regulate mTORC1-translation at specific developmental

times or at immature or inactive synapses in an analogous manner to the translational repression by FMRP-CYFIP1 complexes (DeRubeis et al., 2013).

In this thesis we identified for the first time GIT1-mTORC1 complexes in neurons and characterized their composition and localization. Neuronal GIT1-mTORC1 complexes contain Raptor but not Rictor (Figure 48 & Figure 49) and are at dendritic and synaptic locations where they might provide the postulated "hot-spots" for dendritic translation (Figure 50 & Figure 51). We show that GIT1-mTORC1 complexes are functional and respond to synaptic stimuli, as shown by phosphorylation of mTOR on Ser^{2448} preferentially within the complex (Figure 52). Likewise, knockdown of GIT1 is sufficient to reduce synaptic mTORC1 signaling and mTORC1-dependent protein synthesis of specific activity-regulated genes (Figure 57 & Figure 59).

The abundance of GIT1-mTORC1 is upregulated during development and is bidirectionally modulated by GluN3A expression (Figure 53 & Figure 54). Rescue experiments demonstrated that a mutant lacking the GIT1-binding site does not prevent GIT1-mTOR assembly (Figure 55) or synaptic mTORC1 activation (Figure 43). Given that GluN3A and mTOR bind overlapping regions within GIT1 (Figure 62) (Fiuza et al., 2013; Smithson and Gutmann, 2016), we hypothesize that GluN3A competes for mTOR access to its binding site. Of note, the results presented in this work indicate that GluN3A exerts a more potent regulation over GIT1-mTORC1 than GIT1–β-PIX complexes (Figure 54), suggesting that modulation of mTOR signaling is the leading event.

It is worth noting that GIT1 KO mice display similar deficits to those with elevated adult GluN3A expression (dtGluN3A), including: reduced spine size, impaired stabilization of spines and learning and memory deficits in LTM (Martyn et al., 2018). However, deficits related to STM have also been described in GIT1 KO but appear intact in the dtGluN3A mice (Martyn et al., 2018; Roberts et al., 2009). Additional phenotypes reported in mice and flies upon GIT1 deletion bears close resemblance to that of mTOR KO, such as microcephaly, reduced neuronal size or hyperactivity (Badea et al., 2021; Hong and Mah, 2015; Won et al., 2011). And, similarly to GluN3A (see GluN3A dysregulation is linked to CNS disorders) and mTOR (see Dysregulated mTOR and Neurodevelopmental and Neuropsychiatric Disorders), GIT1 signaling is likewise related to substance

addictions (Shao et al., 2020) and neuropsychiatric disorders like schizophrenia. Rare coding variants in GIT1 have been also identified in schizophrenic patients (Kim et al., 2017), and brain-specific deletion of GIT1 expression in the brain impairs cognition and the activation of synaptic proteins involved in this disease, such as CamKIIα or Shank1 (Fass et al., 2018). However, constitutive GIT1 KO have high lethality rates in the first postnatal weeks and further work on conditional mice should address specific roles on neuronal mTOR functions.

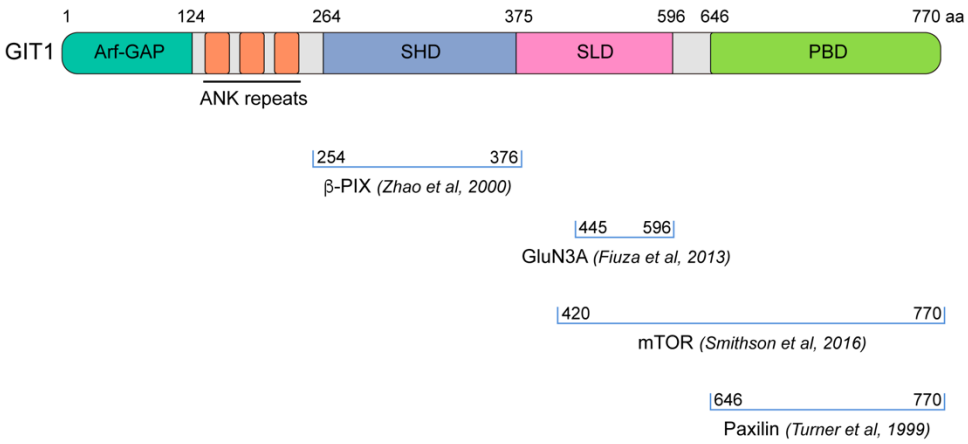

Figure 62. GIT1 binding domains.

GIT1 is a multimodular protein that contains a N-terminal ADP ribosylation factor-GAP domain (Arf-GAP) and three ankyrin (ANK) repeats involved in receptor endocitosis, a Spa2 homology domain (SHD), a central synaptic localization domain (SLD), and a C-terminal paxillin-binding domain (PBD). Regions of interaction with β-PIX, GluN3A, mTOR and paxillin (Turner et al., 1999) are indicated.

Our biochemical and transcriptomic analyses indicate that GluN3A acts strictly at the level of translation (Figure 25-Figure 29), while conventional NMDARs operate at both transcriptional and translational levels (Figure 30). This selectivity of GluN3A would preserve the supply of activity-induced plasticity mRNAs but restrict their active translation to specific synapses. However, GluN3A knockdown in cultured neurons was recently reported to enhance the transcription of a subset of mRNAs (Chen et al., 2020). The effect was detected upon prolonged synaptic activation (6-8 hours TTX withdrawal *vs* 1h TTX withdrawal in a previous work from the lab (Dey, 2017) or 1h bicuculline/ BDNF in the present study) and included genes involved in repression of synaptic firing, suggesting later/ chronic modulation by GluN3A of compensatory or homeostatic responses.

II. RESTRICTING TRANSLATION FOR PRECISE CIRCUIT REFINEMENTS AND LTM STORAGE

The consolidation of synapses and memories requires protein synthesis (Monné A, 1948). Thousands of mRNAs are found in axons and dendrites, and it is assumed that regulating their transport and distribution to sites of localized signaling machinery is crucial for controlling where and when proteins are to be synthesized. LTP and LTD orchestrate long-lasting synaptic changes necessary for the establishment of LTMs in the brain, translating synaptic activity-derived signals into structural changes in spine morphology that ultimately rely on *de novo* local protein synthesis for persistence. For instance, injections of the protein synthesis inhibitor puromycin into rodent brains during specific time windows after training blocked LTM formation (Flexner et al., 1963). Importantly, several models propose that the limitation of protein synthesis to specific sites of active translation underlies phenomena such as the competition between spines for lasting LTP or the clustered dendritic plasticity (Fonseca et al., 2004; Govindarajan et al., 2011). In a recent work, induction of chemical LTP or mGluR-LTD *in vitro* resulted in decreased mRNA motility and specific enrichment of mRNAs at the base of dendritic spines. mRNA accumulation in close proximity to localized signaling pathways was proposed to control which specific sets of transcripts are translated and when, resulting in a tailored remodeling of the proteome at individual synapses (Donlin-Asp et al., 2021).

GluN3A-NMDARs act as molecular switches for persistent synaptic structural plasticity, and control whether a synapse will be maintained or eliminated. In this work, we provide mechanistic insight by revealing bidirectional regulation by GluN3A of synaptic mTORC1 signaling: removing GluN3A expression potentiates and accelerates, while prolonging GluN3A inhibits the onset of mTORC1-dependent protein synthesis (Figure 41 & Figure 42). Translational repression is consistent with gain and loss-of-function studies demonstrating that GluN3A expression selectively affects long-term synaptic modifications and memory encoding. For example, analyses of spine dynamics upon GluN3A overexpression showed that chemical LTP-induced plasticity prompts an enlargement of synapses although later stabilization is impaired (Kehoe et al., 2014). At the behavioral level, transgenic mice with elevated GluN3A expression exhibit defects in memory consolidation (Roberts et al., 2009) while

GluN3A deletion enhances LTM (Mohamad et al., 2013), but STM is preserved in both mouse lines.

We propose a model whereby the lack or presence of GluN3A at synaptic locations contributes to synapse-specific translation by setting a GO or NO-GO biochemical environment for mTORC1 signaling. This function will be influenced by: *i)* the age, as demonstrated by the GluN3A-dependent switch from mTORC1-independent to mTORC1-dependent protein synthesis (Figure 40); and *ii)* the activity history of each synapse, that is key for its strengthening (Redondo and Morris, 2011). At early postnatal stages, immature synapses express GluN3A-NMDARs, which bind GIT1 via their CTD preventing the nucleation of GIT1-mTORC1 complexes (Figure 63). At juvenile/ adult stages, the arrival of sensory experience triggers GluN3A-NMDARs endocytosis and disrupts GluN3A binding to GIT1 (Chowdhury et al., 2013; Larsen et al., 2011; Pérez-Otaño et al., 2006). Activity-dependent removal of GluN3A-NMDARs would thus drive the assembly of GIT1-mTORC1 complexes. Such removal would prime active synapses for mTORC1-dependent protein synthesis of plasticity mRNAs involved in synapse and memory consolidation upon further stimulation, offering an advantage for consolidation *vs* less-active neighbors. In our model, synapse selection would occur via competition for the signaling machinery required for mTORC1-dependent protein synthesis (Fonseca et al., 2004). Competition would provide a way for selective synapse stabilization and storage of relevant events, while defects in this process would allow the consolidation of otherwise lost synaptic changes. Hallmarks of this competition-based model are: *i)* the restricted localization of GluN3A to small, immature synapses in adult brains seen by electron microscopy (Roberts et al., 2009); *ii)* the enhanced availability of GIT1-mTORC1 complexes upon GluN3A deletion (Figure 54); and, *iii)* the lower thresholds for consolidation of associative memories when deleting GluN3A, which are revealed with weak training protocols normally insufficient for attaining stable memories in wild-type mice and that can be reversed by rapamycin (Figure 61). This model might broaden the arsenal for new ways of testing how these phenomena determine memory capacity and efficiency and for amending cognitive dysfunction.

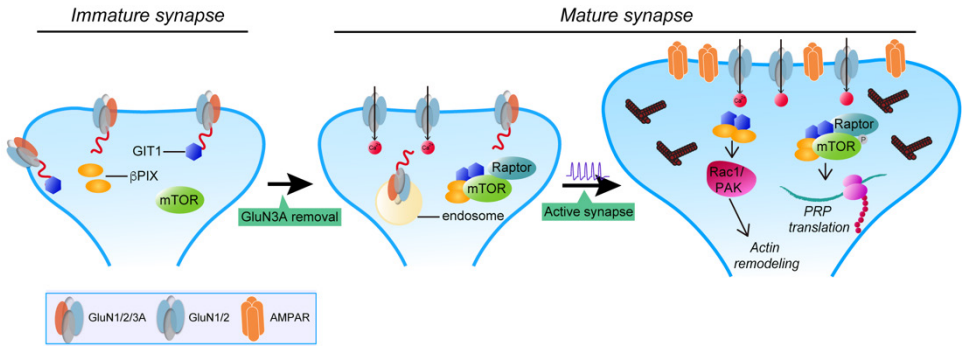

Figure 63. Model for GIT1/ GluN3A control of mTORC1-dependent protein synthesis.

Left, immature synapses express GluN3A-NMDARs, which bind the postsynaptic scaffold GIT1 via their CTD preventing the nucleation of GIT1-mTORC1 complexes. *Middle,* later global and synapse-specific down-regulation of GluN3A enables the formation of GIT1-mTOR-Raptor complexes. *Right*, upon synaptic stimulation, primed synapses are ready to undergo mTORC1-dependent protein synthesis of mRNAs involved in synapse and memory consolidation.

The behavioral analysis reported here demonstrates that GluN3A expression continues to play a role in gating cognitive processing in the adult brain beyond its better recognized functions in postnatal neural circuit refinements. For instance, temporal contiguity of events is required for many forms of associative learning: within the scale of seconds to minutes for classical conditioning paradigms and minutes to hours in other types of memory. Specifically, in the CTA the CS and US can be hours apart, with temporal boundaries set by the strength of the US (Adaikkan and Rosenblum, 2015). The results presented in this thesis show that GluN3A deletion extends this temporal limit and facilitates the learning of demanding tasks. The effects can be prevented by inhibiting mTOR signaling with rapamycin, suggesting that enhanced readiness of the translational machinery in mice lacking GluN3A increases the range for consolidation of memory traces (Figure 61). Yet significant adult GluN3A levels are retained in defined areas of the mouse and human brain which have in common strong plasticity or functional integration needs (Fulcher et al., 2019; Murillo et al., 2021), and genetic variations in *GRIN3A* have been shown to modulate prefrontal cortex activity and episodic memory (Crawley et al., 2021; Gallinat et al., 2007; Papenberg et al., 2014). Future studies using mouse lines where GluN3A can be controlled in a temporal and cell-specific manner should determine whether other domains of memory and cognition are compromised by GluN3A deletion or whether the action of GluN3A is restricted to specific cell-types.

III. GLUN3A AND SYNAPTIC LOCAL PROTEIN SYNTHESIS AS SELECTIVE THERAPEUTIC TARGETS

The effects in cognition of enhancing mTOR signaling or protein synthesis fall at both sides of the spectrum (see Dysregulated mTOR and Neurodevelopmental and Neuropsychiatric Disorders). Loss of constraints on protein synthesis due to mutations in negative regulators of translation (*FMR1*, *MECP2*, or mTORC1 suppressors including *NF1*, *TSC1/2* or the phosphatase *PTEN*) are associated with cognitive impairment and high incidence of autism spectrum disorders and intellectual disability (Kelleher and Bear, 2008). Yet a fraction of autistic individuals exhibit enhanced cognitive skills within specific domains (Heaton and Wallace, 2004). Lowered memory thresholds had been reported after inhibiting the phosphorylation of eIF2α, which increases globally protein synthesis (Costa-Mattioli et al., 2005, 2007; Stern et al., 2013), or by enhancing mTORC1 activity through removal of FKBP12 (Hoeffer et al., 2008). However, cognitive enhancement came at the cost of reduced memory fidelity and cognitive flexibility even when cell-type specific modulation was attempted (Santini et al., 2013; Shrestha et al., 2020a, 2020b; Trinh et al., 2012), which we did not observe here. Key differences could be that other negative regulators of mTOR such as FMRP, PTEN or Tsc1/2 lack neuronal/ synapse specificity, as demonstrated by mutation linkage to altered cell growth and appearance of tumors (Lipton and Sahin, 2014). Moreover, in some of the above situations, protein synthesis is constitutively activated and responses to incoming signals might be occluded. By contrast, lack of GluN3A does not obliterate mTORC1 activation but rather seems to prime mTOR activation by synaptic stimuli.

At present, the enhancement of learning and memory produced by loss of GluN3A suggests that targeting GluN3A expression or signaling functions might be of therapeutic benefit. For instance, small molecules that perturb the GluN3A-GIT1 association might work in subtler ways by specifically modulating synaptic mTORC1 signaling.

Conclusions/ Conclusiones

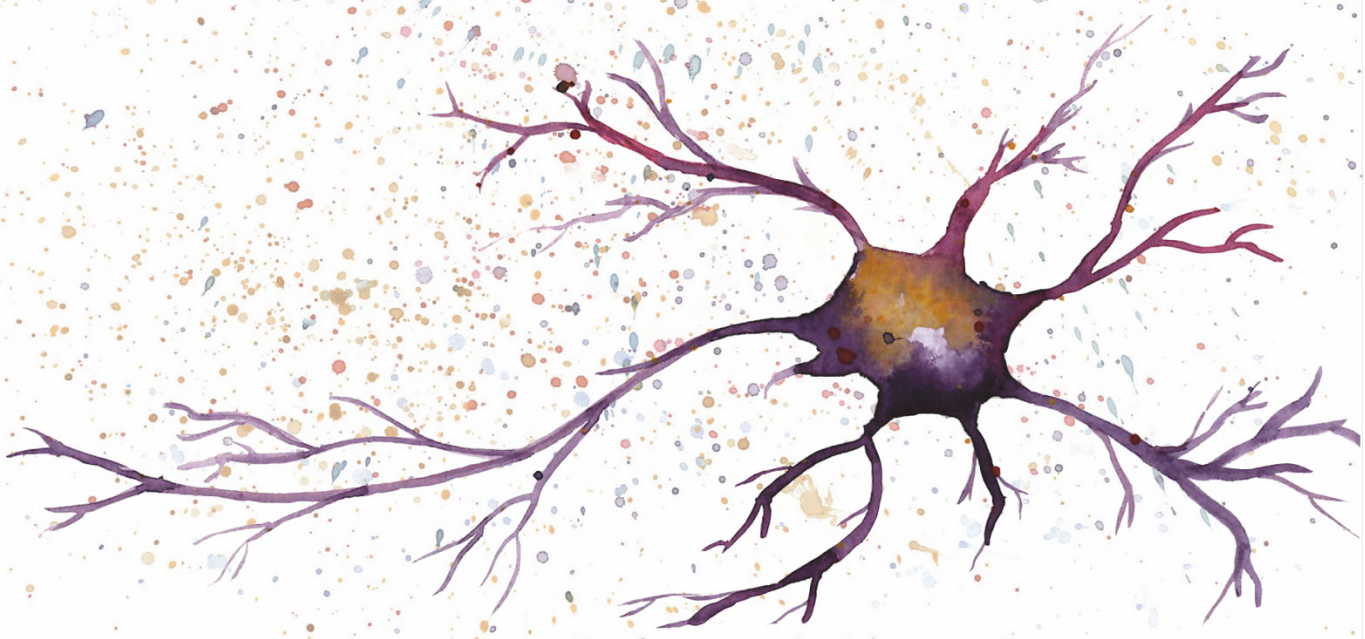

The present study investigated the molecular mechanisms that underlie the effects of GluN3A-NMDARs in long-term synapse remodeling and memory consolidation, yielding the following novel findings and conclusions:

I. *GluN3A modulates synaptic mTORC1 activation and mTORC1-mediated protein synthesis of specific activity-regulated mRNAs, without altering neuron-wide transcriptional programs of gene expression.*

II. *Neuronal signaling complexes composed of mTOR, Raptor and GIT1 localize in synaptic compartments and nucleate the activation of mTOR by synaptic signals, providing a to-date lacking mechanism for controlling translation at the synapse level.*

III. *Inhibitory constraints on mTORC1 signaling are mediated by a distal region within the GluN3A C-terminal distal domain that directly associates with the postsynaptic adaptor GIT1, impeding the assembly of synaptic GIT1-mTORC1 signaling complexes and limiting the local activation of mTOR by synaptic signals.*

IV. *The selective modulation of translation by GluN3A is a suitable mechanism for selective synapse and memory stabilization, and determines the postnatal emergence of mTORC1-dependent protein synthesis in developing brains and the types of memories that will be persistently stored in adult brains.*

El presente estudio investigó los mecanismos moleculares que subyacen a los efectos de GluN3A-NMDARs en la remodelación de la sinapsis y la consolidación de la memoria a largo plazo, arrojando los siguientes hallazgos y conclusiones novedosos:

I. *GluN3A modula la activación sináptica de mTORC1 y la síntesis de proteínas mediada por mTORC1 de ARNm específicos regulados por actividad, sin alterar los programas transcripcionales de expresión génica neuronal.*

II. *Los complejos de señalización neuronal compuestos por mTOR, Raptor y GIT1 se localizan en compartimentos sinápticos y nuclean la activación de mTOR por señales sinápticas, proporcionando un mecanismo para el control de la traducción a nivel de sinapsis carente hasta la fecha.*

III. *Las restricciones inhibitorias sobre la señalización de mTORC1 están mediadas por una región distal del dominio C-terminal de GluN3A que interacciona directamente con el adaptador postsináptico GIT1, impidiendo el ensamblaje de los complejos de señalización sinápticos GIT1-mTORC1 y limitando la activación local de mTOR por señales sinápticas.*

IV. *La modulación selectiva de la traducción por GluN3A es un mecanismo adecuado para la estabilización selectiva de sinapsis y memoria, y determina la emergencia postnatal de la síntesis de proteínas dependiente de mTORC1 en los cerebros en desarrollo y los tipos de memorias que se almacenarán de forma persistente en los cerebros adultos.*

References

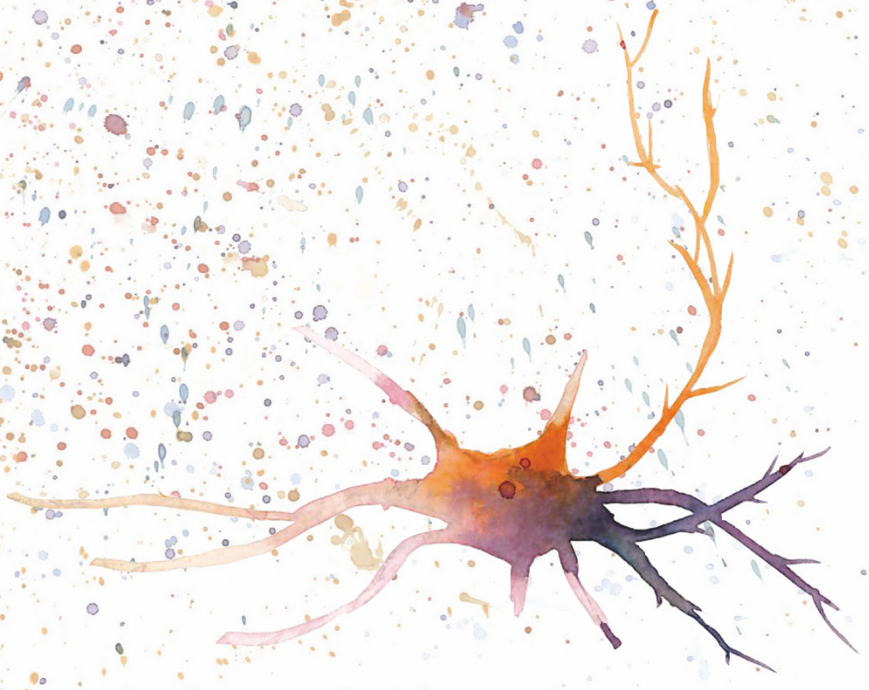

Aakalu, G., Smith, W.B., Nguyen, N., Jiang, C., and Schuman, E.M. (2001). Dynamic Visualization of Local Protein Synthesis in Hippocampal Neurons. Neuron *30*, 489–502.

Abe, N., Borson, S.H., Gambello, M.J., Wang, F., and Cavalli, V. (2010). Mammalian Target of Rapamycin (mTOR) activation increases axonal growth capacity of injured peripheral nerves. J. Biol. Chem. *285*, 28034–28043.

Adaikkan, C., and Rosenblum, K. (2015). A molecular mechanism underlying gustatory memory trace for an association in the insular cortex. Elife *4*, 1–15.

Andersson, O., Stenqvist, A., Attersand, A., and Von Euler, G. (2001). Nucleotide sequence, genomic organization, and chromosomal localization of genes encoding the human NMDA receptor subunits NR3A and NR3B. Genomics *78*, 178–184.

Asaki, C., Usuda, N., Nakazawa, A., Kametani, K., and Suzuki, T. (2003). Localization of translational components at the ultramicroscopic level at postsynaptic sites of the rat brain. Brain Res. *972*, 168–176.

Atkins, C.M., Selcher, J.C., Petraitis, J.J., Trzaskos, J.M., and Sweatt, J.D. (1998). The MAPK cascade is required for mammalian associative learning. Nat. Neurosci. *1*, 602–609.

Auberson, Y.P., Acklin, P., Bischoff, S., Moretti, R., Ofner, S., Schmutz, M., and Veenstra, S.J. (1999). N-phosphonoalkyl-5-aminomethylquinoxaline-2,3-diones: In vivo active AMPA and NMDA(glycine) antagonists. Bioorganic Med. Chem. Lett. *9*, 249–254.

Autry, A.E., Adachi, M., Nosyreva, E., Na, E.S., Los, M.F., Cheng, P.F., Kavalali, E.T., and Monteggia, L.M. (2011). NMDA receptor blockade at rest triggers rapid behavioural antidepressant responses. Nature *475*, 91–96.

Badea, A., Schmalzigaug, R., Kim, W., Bonner, P., Ahmed, U., Johnson, G.A., Cofer, G., Foster, M., Anderson, R.J., Badea, C., et al. (2021). Microcephaly with altered cortical layering in GIT1 deficiency revealed by quantitative neuroimaging. Magn. Reson. Imaging *76*, 26–38.

Baliga, B.S., Pronczvuk, A.W., and Munro, H.N. (1969). Mechanism in a Cell-free of Cycloheximide System Prepared Inhibition from Rat of Protein Liver. J. Biol. Chem. *244*, 4480–4489.

Banko, J.L., Poulin, F., Hou, L., DeMaria, C.T., Sonenberg, N., and Klann, E. (2005). The translation repressor 4E-BP2 is critical for eIF4F complex formation, synaptic plasticity, and memory in the hippocampus. J. Neurosci. *25*, 9581–9590.

Barak, S., Liu, F., Ben Hamida, S., Yowell, Q. V, Neasta, J., Kharazia, V., Janak, P.H., and Ron, D. (2013). Disruption of alcohol-related memories by mTORC1 inhibition prevents relapse. Nat. Neurosci. *16*, 1111–1117.

Bard, L., Sainlos, M., Bouchet, D., Cousins, S., Mikasova, L., Breillat, C., Stephenson, F.A.,

Imperiali, B., Choquet, D., and Groc, L. (2010). Dynamic and specific interaction between synaptic NR2-NMDA receptor and PDZ proteins. Proc. Natl. Acad. Sci. U. S. A. *107*, 19561–19566.

Barnes, S.A., Wijetunge, L.S., Jackson, A.D., Katsanevaki, D., Osterweil, E.K., Komiyama, N.H., Grant, S.G.N., Bear, M.F., Nagerl, U. V., Kind, P.C., et al. (2015). Convergence of Hippocampal Pathophysiology in Syngap+/- and Fmr1-/y Mice. J. Neurosci. *35*, 15073–15081.

Barria, A., and Malinow, R. (2002). Subunit-specific NMDA receptor trafficking to synapses. Neuron *35*, 345–353.

Barria, A., and Malinow, R. (2005). NMDA receptor subunit composition controls synaptic plasticity by regulating binding to CaMKII. Neuron *48*, 289–301.

Bauman, M.L., and Kemper, T.L. (2005). Neuroanatomic observations of the brain in autism: a review and future directions. Int. J. Dev. Neurosci. Off. J. Int. Soc. Dev. Neurosci. *23*, 183–187.

Bellone, C., and Nicoll, R.A. (2007). Rapid Bidirectional Switching of Synaptic NMDA Receptors. Neuron *55*, 779–785.

Bercury, K.K., Dai, J., Sachs, H.H., Ahrendsen, J.T., Wood, T.L., and Macklin, W.B. (2014). Conditional ablation of raptor or rictor has differential impact on oligodendrocyte differentiation and CNS myelination. J. Neurosci. *34*, 4466–4480.

Bierer, B.E., Mattila, P.S., Standaert, R.F., Herzenberg, L.A., Burakoff, S.J., Crabtree, G., and Schreiber, S.L. (1990). Two distinct signal transmission pathways in T lymphocytes are inhibited by complexes formed between an immunophilin and either FK506 or rapamycin. Proc. Natl. Acad. Sci. U. S. A. *87*, 9231–9235.

Bodian, D. (1965). A SUGGESTIVE RELATIONSHIP OF NERVE CELL RNA WITH SPECIFIC SYNAPTIC SITES. Proc. Natl. Acad. Sci. *53*, 418 LP – 425.

Boksa, P. (2012). Abnormal synaptic pruning in schizophrenia: Urban myth or reality? J. Psychiatry Neurosci. *37*, 75–77.

Bové, J., Martínez-Vicente, M., and Vila, M. (2011). Fighting neurodegeneration with rapamycin: mechanistic insights. Nat. Rev. Neurosci. *12*, 437–452.

Briz, V., Restivo, L., Pasciuto, E., Juczewski, K., Mercaldo, V., Lo, A.C., Baatsen, P., Gounko, N. V., Borreca, A., Girardi, T., et al. (2017). The non-coding RNA BC1 regulates experience-dependent structural plasticity and learning. Nat. Commun. *8*, 1–16.

Brody, S.A., Nakanishi, N., Tu, S., Lipton, S.A., and Geyer, M.A. (2005). A developmental influence of the N-methyl-D-aspartate receptor NR3A subunit on prepulse inhibition of startle. Biol. Psychiatry *57*, 1147–1152.

Brown, E.J., Albers, M.W., Shin, T.B., Ichikawa, K., Keith, C.T., Lane, W.S., and Schreiber,

S.L. (1994). A mammalian protein targeted by G1-arresting rapamycin-receptor complex. Nature *369*, 756–758.

Buffington, S. a, Huang, W., and Costa-Mattioli, M. (2014). Translational Control in Synaptic Plasticity and Cognitive Dysfunction. Annu. Rev. Neurosci. *37*, 17–38.

Burgin, K.E., Waxham, M.N., Rickling, S., Westgate, S.A., Mobley, W.C., and Kelly, P.T. (1990). In situ hybridization histochemistry of Ca2+/calmodulin-dependent protein kinase in developing rat brain. J. Neurosci. *10*, 1788–1798.

Burzomato, V., Frugier, G., Pérez-Otaño, I., Kittler, J.T., and Attwell, D. (2010). The receptor subunits generating NMDA receptor mediated currents in oligodendrocytes. J. Physiol. *588*, 3403–3414.

Busch, R.M., Srivastava, S., Hogue, O., Frazier, T.W., Klaas, P., Hardan, A., Martinez-Agosto, J.A., Sahin, M., and Eng, C. (2019). Neurobehavioral phenotype of autism spectrum disorder associated with germline heterozygous mutations in PTEN. Transl. Psychiatry *9*, 253.

Buttgereit, F., and Brand, M.D. (1995). A hierarchy of ATP-consuming processes in mammalian cells. Biochem. J. *312 (Pt 1*, 163–167.

Caccamo, A., Maldonado, M.A., Majumder, S., Medina, D.X., Holbein, W., Magrí, A., and Oddo, S. (2011). Naturally secreted amyloid-beta increases mammalian target of rapamycin (mTOR) activity via a PRAS40-mediated mechanism. J. Biol. Chem. *286*, 8924–8932.

Cajigas, I.J., Tushev, G., Will, T.J., tom Dieck, S., Fuerst, N., and Schuman, E.M. (2012). The local transcriptome in the synaptic neuropil revealed by deep sequencing and high-resolution imaging. Neuron *74*, 453–466.

Cammalleri, M., Lütjens, R., Berton, F., King, A.R., Simpson, C., Francesconi, W., and Sanna, P.P. (2003). Time-restricted role for dendritic activation of the mTOR-p70 S6K pathway in the induction of late-phase long-term potentiation in the CA1. Proc. Natl. Acad. Sci. U. S. A. *100*, 14368–14373.

Cavara, N.A., and Hollmann, M. (2008). Shuffling the deck anew: How NR3 tweaks NMDA receptor function. Mol. Neurobiol. *38*, 16–26.

Chan, S.F., and Sucher, N.J. (2001). An NMDA receptor signaling complex with protein phosphatase 2A. J. Neurosci. *21*, 7985–7992.

Chatterton, J.E., Awobuluyi, M., Premkumar, L.S., Takahashi, H., Talantova, M., Shin, Y., Cui, J., Tu, S., Sevarinok, K.A., Nakanishi, N., et al. (2002). Excitatory glycine receptors containing the NR3 family of NMDA receptor subunits. *415*, 793–798.

Chen, J., Ma, Y., Fan, R., Yang, Z., and Li, M.D. (2018a). Implication of Genes for the N-

Methyl-d-Aspartate (NMDA) Receptor in Substance Addictions. Mol. Neurobiol. *55*, 7567–7578.

Chen, J., Liu, Q., Fan, R., Han, H., Yang, Z., Cui, W., Song, G., and Li, M.D. (2019a). Demonstration of critical role of GRIN3A in nicotine dependence through both genetic association and molecular functional studies. Addict. Biol. 1–11.

Chen, K., Zheng, Y., Wei, J. an, Ouyang, H., Huang, X., Zhang, F., Wan Lai, C.S., Ren, C., So, K.F., and Zhang, L. (2019b). Exercise training improves motor skill learning via selective activation of mTOR. Sci. Adv. *5*, 1–12.

Chen, L.-F., Lyons, M.R., Liu, F., Green, M. V., Hedrick, N.G., Williams, A.B., Narayanan, A., Yasuda, R., and West, A.E. (2020). The NMDA receptor subunit GluN3A regulates synaptic activity-induced and myocyte enhancer factor 2C (MEF2C)-dependent transcription. J. Biol. Chem. jbc.RA119.010266.

Chen, X., Liu, M., Tian, Y., Li, J., Qi, Y., Zhao, D., Wu, Z., Huang, M., Wong, C.C.L., Wang, H.-W., et al. (2018b). Cryo-EM structure of human mTOR complex 2. Cell Res. *28*, 518–528.

Chotiner, J.K., Khorasani, H., Nairn, A.C., O'Dell, T.J., and Watson, J.B. (2003). Adenylyl cyclase-dependent form of chemical long-term potentiation triggers translational regulation at the elongation step. Neuroscience *116*, 743–752.

Chowdhury, D., Marco, S., Brooks, I.M., Zandueta, A., Rao, Y., Haucke, V., Wesseling, J.F., Tavalin, S.J., and Pérez-Otaño, I. (2013). Tyrosine phosphorylation regulates the endocytosis and surface expression of GluN3A-containing NMDA receptors. J. Neurosci. *33*, 4151–4164.

Chung, J., Kuo, C.J., Crabtree, G.R., and Blenis, J. (1992). Rapamycin-FKBP specifically blocks growth-dependent activation of and signaling by the 70 kd S6 protein kinases. Cell *69*, 1227–1236.

Ciabarra, A.M., Sullivan, J.M., Gahn, L.G., Pecht, G., Heinemann, S., and Sevarino, K.A. (1995). Cloning and characterization of χ-1: A developmentally regulated member of a novel class of the ionotropic glutamate receptor family. J. Neurosci. *15*, 6498–6508.

Cloëtta, D., Thomanetz, V., Baranek, C., Lustenberger, R.M., Lin, S., Oliveri, F., Atanasoski, S., and Rüegg, M.A. (2013). Inactivation of mTORC1 in the developing brain causes microcephaly and affects gliogenesis. J. Neurosci. *33*, 7799–7810.

Costa-Mattioli, M., and Monteggia, L.M. (2013). mTOR complexes in neurodevelopmental and neuropsychiatric disorders. Nat Neurosci *16*, 1537–1543.

Costa-Mattioli, M., Gobert, D., Harding, H., Herdy, B., Azzi, M., Bruno, M., Bidinosti, M., Ben Mamou, C., Marcinkiewicz, E., Yoshida, M., et al. (2005). Translational control of hippocampal synaptic plasticity and memory by the eIF2alpha kinase GCN2. Nature *436*, 1166–1173.

Costa-Mattioli, M., Gobert, D., Stern, E., Gamache, K., Colina, R., Cuello, C., Sossin, W., Kaufman, R., Pelletier, J., Rosenblum, K., et al. (2007). eIF2alpha Phosphorylation Bidirectionally Regulates the Switch from Short- to Long-Term Synaptic Plasticity and Memory. Cell *129*, 195–206.

Costa-Mattioli, M., Sossin, W.S., Klann, E., and Sonenberg, N. (2009). Translational Control of Long-Lasting Synaptic Plasticity and Memory. Neuron *61*, 10–26.

Crair, M.C., and Malenka, R.C. (1995). A critical period for long-term potentiation at thalamocortical synapses. Nature *375*, 325–328.

Crawley, O., Conde-Dusman, M.J., and Pérez-Otaño, I. (2021). GluN3A NMDA receptor subunits: more enigmatic than ever? J. Physiol. *0*, 1–16.

Crino, P.B., Nathanson, K.L., and Henske, E.P. (2006). The tuberous sclerosis complex. N. Engl. J. Med. *355*, 1345–1356.

Cummings, K.A., and Popescu, G.K. (2015). Glycine-dependent activation of NMDA receptors. J. Gen. Physiol. *145*, 513–527.

Curtis DR, Duggan AW, Felix D, J.G. (1970). GABA, Bicuculline and Central Inhibition. Nature *226*, 1222–1224.

Das, S., Sasaki, Y.F., Rothe, T., Premkumar, L.S., Takasu, M., Crandall, J.E., Dikkes, P., Conner, D.A., Rayudu, P. V, Cheung, W., et al. (1998). Increased NMDA current and spine density in mice lacking the NMDA receptor subunit NR3A. Nature *393*, 377–381.

Davies, J., Francis, A.A., Jones, A.W., and Watkins, J.C. (1981). 2-Amino-5-phosphonovalerate (2APV), a potent and selective antagonist of amino acid-induced and synaptic excitation. Neurosci. Lett. *21*, 77–81.

DeRubeis, S., Pasciuto, E., Li, K.W., Fernández, E., DiMarino, D., Buzzi, A., Ostroff, L.E., Klann, E., Zwartkruis, F.J.T., Komiyama, N.H., et al. (2013). CYFIP1 coordinates mRNA translation and cytoskeleton remodeling to ensure proper dendritic Spine formation. Neuron *79*, 1169–1182.

Dever, T.E., and Green, R. (2012). The Elongation , Termination , and Recycling Phases of Translation in Eukaryotes. Cold Spring Harb. Lab. Press.

Dey, P.N. (2017). Signaling via non-conventional NMDA receptors containing GluN3A subunits. University of Navarra.

DiCicco-Bloom, E., Lord, C., Zwaigenbaum, L., Courchesne, E., Dager, S.R., Schmitz, C., Schultz, R.T., Crawley, J., and Young, L.J. (2006). The developmental neurobiology of autism spectrum disorder. J. Neurosci. *26*, 6897–6906.

Dieterich, D.C., Hodas, J.J.L., Gouzer, G., Shadrin, I.Y., Ngo, J.T., Triller, A., Tirrell, D. a, and Schuman, E.M. (2010). In situ visualization and dynamics of newly synthesized proteins in rat

hippocampal neurons. Nat. Neurosci. *13*, 897–905.

Diggs-Andrews, K.A., and Gutmann, D.H. (2013). Modeling cognitive dysfunction in neurofibromatosis-1. Trends Neurosci. *36*, 237–247.

Dinamarca, M.C., Guzzetti, F., Karpova, A., Lim, D., Mitro, N., Musardo, S., Mellone, M., Marcello, E., Stanic, J., Samaddar, T., et al. (2016). Ring finger protein 10 is a novel synaptonuclear messenger encoding activation of NMDA receptors in hippocampus. Elife *5*, e12430.

Donlin-Asp, P.G., Polisseni, C., Klimek, R., Heckel, A., and Schuman, E.M. (2021). Differential regulation of local mRNA dynamics and translation following long-term potentiation and depression. PNAS *118*.

Dumont, F.J., Staruch, M.J., Koprak, S.L., Melino, M.R., and Sigal, N.H. (1990). Distinct mechanisms of suppression of murine T cell activation by the related macrolides FK-506 and rapamycin. J. Immunol. *144*, 251–258.

Emamian, E.S., Karayiorgou, M., and Gogos, J.A. (2004). Decreased phosphorylation of NMDA receptor type 1 at serine 897 in brains of patients with Schizophrenia. J. Neurosci. *24*, 1561–1564.

Eng, C.P., Sehgal, S.N., and Vézina, C. (1984). Activity of rapamycin (AY-22,989) against transplanted tumors. J. Antibiot. (Tokyo). *37*, 1231–1237.

Eriksson, M., Samuelsson, H., Samuelsson, E.B., Liu, L., McKeehan, W.L., Benedikz, E., and Sundström, E. (2007a). The NMDAR subunit NR3A interacts with microtubule-associated protein 1S in the brain. Biochem. Biophys. Res. Commun. *361*, 127–132.

Eriksson, M., Nilsson, A., Samuelsson, H., Samuelsson, E.B., Mo, L., Åkesson, E., Benedikz, E., and Sundström, E. (2007b). On the role of NR3A in human NMDA receptors. Physiol. Behav. *92*, 54–59.

Eriksson, M., Samuelsson, H., Björklund, S., Tortosa, E., Avila, J., Samuelsson, E.B., Benedikz, E., and Sundström, E. (2010). MAP1B binds to the NMDA receptor subunit NR3A and affects NR3A protein concentrations. Neurosci. Lett. *475*, 33–37.

Fass, D., Lewis, M., Ahmad, R., Szucs, M., Zhang, Q., Fleishman, M., Wang, D., Kim, M., Biag, J., Carr, S., et al. (2018). Brain-Specific Deletion of GIT1 Impairs Cognition and Alters Phosphorylation of Synaptic Protein Networks Implicated in Schizophrenia Susceptibility. BioRxiv.

Favata, M.F., Horiuchi, K.Y., Manos, E.J., Daulerio, A.J., Stradley, D.A., Feeser, W.S., Van Dyk, D.E., Pitts, W.J., Earl, R.A., Hobbs, F., et al. (1998). Identification of a novel inhibitor of mitogen-activated protein kinase kinase. J. Biol. Chem. *273*, 18623–18632.

Fiuza, M., González-González, I., and Pérez-Otaño, I. (2013). GluN3A expression restricts

spine maturation via inhibition of GIT1/Rac1 signaling. Proc. Natl. Acad. Sci. U. S. A. *110*, 20807–20812.

Flavell, S.W., and Greenberg, M.E. (2008). Signaling mechanisms linking neuronal activity to gene expression and plasticity of the nervous system. Annu. Rev. Neurosci. *31*, 563–590.

Flexner, J.B., Flexner, L.B., and Stellar, E. (1963). Memory in Mice as Affected by Intracerebral Puromycin. Science (80-.). *141*, 57 LP – 59.

Fonseca, R., Nägerl, U.V., Morris, R.G.M., and Bonhoeffer, T. (2004). Competing for memory: hippocampal LTP under regimes of reduced protein synthesis. Neuron *44*, 1011–1020.

Fortin, D.A., Srivastava, T., Dwarakanath, D., Pierre, P., Nygaard, S., Derkach, V.A., and Soderling, T.R. (2012). Brain-Derived Neurotrophic Factor Activation of CaM-Kinase Kinase via Transient Receptor Potential Canonical Channels Induces the Translation and Synaptic Incorporation of GluA1-Containing Calcium-Permeable AMPA Receptors. J. Neurosci. *32*, 8127–8137.

Franchini, L., Stanic, J., Ponzoni, L., Mellone, M., Carrano, N., Musardo, S., Zianni, E., Olivero, G., Marcello, E., Pittaluga, A., et al. (2019). Linking NMDA Receptor Synaptic Retention to Synaptic Plasticity and Cognition. IScience *19*, 927–939.

Frias, M.A., Thoreen, C.C., Jaffe, J.D., Schroder, W., Sculley, T., Carr, S.A., and Sabatini, D.M. (2006). mSin1 is necessary for Akt/PKB phosphorylation, and its isoforms define three distinct mTORC2s. Curr. Biol. *16*, 1865–1870.

Fulcher, B.D., Murray, J.D., Zerbi, V., and Wang, X.J. (2019). Multimodal gradients across mouse cortex. Proc. Natl. Acad. Sci. U. S. A.

Gallinat, J., Götz, T., Kalus, P., Bajbouj, M., Sander, T., and Winterer, G. (2007). Genetic variations of the NR3A subunit of the NMDA receptor modulate prefrontal cerebral activity in humans. J. Cogn. Neurosci. *19*, 59–68.

Gambrill, A.C., and Barria, A. (2011). NMDA receptor subunit composition controls synaptogenesis and synapse stabilization. Proc. Natl. Acad. Sci. U. S. A. *108*, 5855–5860.

Gascón, S., Paez-Gomez, J.A., Díaz-Guerra, M., Scheiffele, P., and Scholl, F.G. (2008). Dual-promoter lentiviral vectors for constitutive and regulated gene expression in neurons. J. Neurosci. Methods *168*, 104–112.

Gladding, C.M., and Raymond, L.A. (2011). Mechanisms underlying NMDA receptor synaptic/extrasynaptic distribution and function. Mol. Cell. Neurosci. *48*, 308–320.

Glantz, L.A., and Lewis, D.A. (2000). Decreased dendritic spine density on prefrontal cortical pyramidal neurons in schizophrenia. Arch. Gen. Psychiatry *57*, 65–73.

Gong, R., Chang, S.P., Abbassi, N.R., and Tang, S.J. (2006). Roles of glutamate receptors

and the mammalian target of rapamycin (mTOR) signaling pathway in activity-dependent dendritic protein synthesis in hippocampal neurons. J. Biol. Chem. *281*, 18802–18815.

Gordillo-Salas, M., Pilar-Cuéllar, F., Auberson, Y.P., and Adell, A. (2018). Signaling pathways responsible for the rapid antidepressant-like effects of a GluN2A-preferring NMDA receptor antagonist. Transl. Psychiatry *8*.

Govindarajan, A., Israely, I., Huang, S.-Y., and Tonegawa, S. (2011). The dendritic branch is the preferred integrative unit for protein synthesis-dependent LTP. Neuron *69*, 132–146.

Graber, T.E., McCamphill, P.K., and Sossin, W.S. (2013). A recollection of mTOR signaling in learning and memory. Learn. Mem. *20*, 518–530.

Graham, F.L., and Van der EB, A.. (1973). A new technique for the Assay of Infectivity of Human Adenovirus 5 DNA. Virology *467*, 456–467.

Grand, T., Abi Gerges, S., David, M., Diana, M.A., and Paoletti, P. (2018). Unmasking GluN1/GluN3A excitatory glycine NMDA receptors. Nat. Commun. *9*.

Greenwood, T.A., Lazzeroni, L.C., Murray, S.S., Cadenhead, K.S., Calkins, M.E., Dobie, D.J., Green, M.F., Gur, R.E., Gur, R.C., Hardiman, G., et al. (2011). Analysis of 94 Candidate Genes and 12 endophenotypes for Schizophrenia from the Consortium on the Genetics of Schizophrenia. Am J Psychiatry *168*, 930–946.

Greenwood, T.A., Lazzeroni, L.C., Calkins, M.E., Freedman, R., Green, M.F., Gur, R.E., Gur, R.C., Light, G.A., Nuechterlein, K.H., Olincy, A., et al. (2016). Genetic assessment of additional endophenotypes from the Consortium on the Genetics of Schizophrenia Family Study. Schizophr. Res. *170*, 30–40.

Grollman, A.P. (1967). Inhibitors of Protein Synthesis II. Mode of Action of Anisomycin. J. Biol. Chem. *242*, 3226–3233.

Guertin, D.A., Stevens, D.M., Thoreen, C.C., Burds, A.A., Kalaany, N.Y., Moffat, J., Brown, M., Fitzgerald, K.J., and Sabatini, D.M. (2006). Ablation in mice of the mTORC components raptor, rictor, or mLST8 reveals that mTORC2 is required for signaling to Akt-FOXO and PKCalpha, but not S6K1. Dev. Cell *11*, 859–871.

Guzowski, J.F., Setlow, B., Wagner, E.K., and McGaugh, J.L. (2001). Experience-dependent gene expression in the rat hippocampus after spatial learning: A comparison of the immediate-early genes Arc, c-fos, and zif268. J. Neurosci. *21*, 5089–5098.

Vander Haar, E., Lee, S.-I., Bandhakavi, S., Griffin, T.J., and Kim, D.-H. (2007). Insulin signalling to mTOR mediated by the Akt/PKB substrate PRAS40. Nat. Cell Biol. *9*, 316–323.

Hall, B.J., Ripley, B., and Ghosh, A. (2007). NR2B Signaling Regulates the Development of

Synaptic AMPA Receptor Current. J. Neurosci. *27*, 13446–13456.

Hansen, K.B., Yi, F., Perszyk, R.E., Menniti, F.S., and Traynelis, S.F. (2017). NMDA Receptors in the Central Nervous System. Methods Mol. Biol. *1677*, 1–80.

Hansen, K.B., Yi, F., Perszyk, R.E., Furukawa, H., Wollmuth, L.P., Gibb, A.J., and Traynelis, S.F. (2018). Structure, function, and allosteric modulation of NMDA receptors. J. Gen. Physiol. *150*, 1081–1105.

Hara, K., Maruki, Y., Long, X., Yoshino, K., Oshiro, N., Hidayat, S., Tokunaga, C., Avruch, J., and Yonezawa, K. (2002). Raptor, a binding partner of target of rapamycin (TOR), mediates TOR action. Cell *110*, 177–189.

Hardingham, G.E. (2019). NMDA receptor C-terminal signaling in development, plasticity, and disease [version 1; peer review: 2 approved]. F1000Research *8*, 1547.

Hardingham, G.E., and Bading, H. (2002). Coupling of extrasynaptic NMDA receptors to a CREB shut-off pathway is developmentally regulated. Biochim. Biophys. Acta - Proteins Proteomics *1600*, 148–153.

Hardingham, G.E., and Bading, H. (2010). Synaptic versus extrasynaptic NMDA receptor signalling: Implications for neurodegenerative disorders. Nat. Rev. Neurosci. *11*, 682–696.

Hardingham, G.E., Arnold, F.J., and Bading, H. (2001). A calcium microdomain near NMDA receptors: on switch for ERK-dependent synapse-to-nucleus communication. Nat. Neurosci. *4*, 565–566.

Hatton, C.J., and Paoletti, P. (2005). Modulation of triheteromeric NMDA receptors by N-terminal domain ligands. Neuron *46*, 261–274.

Heaton, P., and Wallace, G.L. (2004). Annotation: the savant syndrome. J. Child Psychol. Psychiatry. *45*, 899–911.

Heitman, J., Movva, N.R., and Hall, M.N. (1991). Targets for cell cycle arrest by the immunosuppressant rapamycin in yeast. Science *253*, 905–909.

Henry, F.E., Hockeimer, W., Chen, A., Mysore, S.P., and Sutton, M.A. (2017). Mechanistic target of rapamycin is necessary for changes in dendritic spine morphology associated with long-term potentiation. Mol. Brain *10*, 1–17.

Henson, M.A., Roberts, A.C., Salimi, K., Vadlamudi, S., Hamer, R.M., Gilmore, J.H., Jarskog, L.F., and Philpot, B.D. (2008). Developmental regulation of the NMDA receptor subunits, NR3A and NR1, in human prefrontal cortex. Cereb. Cortex *18*, 2560–2573.

Henson, M.A., Roberts, A.C., Pérez-Otaño, I., and Philpot, B.D. (2010). Influence of the NR3A subunit on NMDA receptor functions. Prog. Neurobiol. *91*, 23–37.

Henson, M.A., Larsen, R.S., Lawson, S.N., Pérez-Otaño, I., Nakanishi, N., Lipton, S.A., and Philpot, B.D. (2012). Genetic deletion of NR3A accelerates Glutamatergic synapse maturation. PLoS One *7*.

Hentges, K.E., Sirry, B., Gingeras, A.C., Sarbassov, D., Sonenberg, N., Sabatini, D., and Peterson, A.S. (2001). FRAP/mTOR is required for proliferation and patterning during embryonic development in the mouse. Proc. Natl. Acad. Sci. U. S. A. *98*, 13796–13801.

Hestrin, S. (1992). Developmental regulation of NMDA receptor-mediated synaptic currents at a central synapse. Nature *357*, 686–689.

Hoeffer, C.A., Tang, W., Wong, H., Santillan, A., Patterson, R.J., Martinez, L.A., Tejada-Simon, M. V, Paylor, R., Hamilton, S.L., and Klann, E. (2008). Removal of FKBP12 enhances mTOR-Raptor interactions, LTP, memory, and perseverative/repetitive behavior. Neuron *60*, 832–845.

Holt, C.E., Martin, K.C., and Schuman, E.M. (2019). Local translation in neurons: visualization and function. Nat. Struct. Mol. Biol. *26*, 557–566.

Holtmaat, A.J.G.D., Trachtenberg, J.T., Wilbrecht, L., Shepherd, G.M., Zhang, X., Knott, G.W., and Svoboda, K. (2005). Transient and persistent dendritic spines in the neocortex in vivo. Neuron *45*, 279–291.

Hong, S.-T., and Mah, W. (2015). A Critical Role of GIT1 in Vertebrate and Invertebrate Brain Development. Exp. Neurobiol. *24*, 8–16.

Houchens, D.P., Ovejera, A.A., Riblet, S.M., and Slagel, D.E. (1983). Human brain tumor xenografts in nude mice as a chemotherapy model. Eur. J. Cancer Clin. Oncol. *19*, 799–805.

Huang, Y.Y., and Kandel, E.R. (1994). Recruitment of long-lasting and protein kinase A-dependent long-term potentiation in the CA1 region of hippocampus requires repeated tetanization. Learn. Mem. *1*, 74–82.

Huang, W., Zhu, P.J., Zhang, S., Zhou, H., Stoica, L., Galiano, M., Krnjević, K., Roman, G., and Costa-Mattioli, M. (2013). MTORC2 controls actin polymerization required for consolidation of long-term memory. Nat. Neurosci. *16*, 441–448.

Huang, X., Chen, Y.-Y., Shen, Y., Cao, X., Li, A., Liu, Q., Li, Z., Zhang, L.-B., Dai, W., Tan, T., et al. (2017). Methamphetamine abuse impairs motor cortical plasticity and function. Mol. Psychiatry *22*, 1274–1281.

Huang, Y., Kang, B.N., Tian, J., Liu, Y., Luo, H.R., Hester, L., and Snyder, S.H. (2007). The cationic amino acid transporters CAT1 and CAT3 mediate NMDA receptor activation-dependent changes in elaboration of neuronal processes via the mammalian target of rapamycin mTOR pathway. J. Neurosci. *27*, 449–458.

Huber, K.M., Kayser, M.S., and Bear, M.F. (2000). Role for rapid dendritic protein synthesis in hippocampal mGluR-dependent long-term depression. Science *288*, 1254–1257.

Huber, K.M., Klann, E., Costa-Mattioli, M., and Zukin, R.S. (2015). Dysregulation of Mammalian Target of Rapamycin Signaling in Mouse Models of Autism. J. Neurosci. *35*, 13836–13842.

Hullinger, R., O'Riordan, K., and Burger, C. (2015). Environmental enrichment improves learning and memory and long-term potentiation in young adult rats through a mechanism requiring mGluR5 signaling and sustained activation of p70s6k. Neurobiol. Learn. Mem. *125*, 126–134.

Hutsler, J.J., and Zhang, H. (2010). Increased dendritic spine densities on cortical projection neurons in autism spectrum disorders. Brain Res. *1309*, 83–94.

Inamura, N., Nawa, H., and Takei, N. (2005). Enhancement of translation elongation in neurons by brain-derived neurotrophic factor: Implications for mammalian target of rapamycin signaling. J. Neurochem. *95*, 1438–1445.

Irwin, S.A., Galvez, R., and Greenough, W.T. (2000). Dendritic spine structural anomalies in fragile-X mental retardation syndrome. Cereb. Cortex *10*, 1038–1044.

Ishii, T., Moriyoshi, K., Sugihara, H., Sakurada, K., Kadotani, H., Yokoi, M., Akazawa, C., Shigemoto, R., Mizuno, N., and Masu, M. (1993). Molecular characterization of the family of the N-methyl-D-aspartate receptor subunits. J. Biol. Chem. *268*, 2836–2843.

Jacinto, E., Loewith, R., Schmidt, A., Lin, S., Rüegg, M.A., Hall, A., and Hall, M.N. (2004). Mammalian TOR complex 2 controls the actin cytoskeleton and is rapamycin insensitive. Nat. Cell Biol. *6*, 1122–1128.

Jacinto, E., Facchinetti, V., Liu, D., Soto, N., Wei, S., Jung, S.Y., Huang, Q., Qin, J., and Su, B. (2006). SIN1/MIP1 maintains rictor-mTOR complex integrity and regulates Akt phosphorylation and substrate specificity. Cell *127*, 125–137.

Jaworski, J., and Sheng, M. (2006). The growing role of mTOR in neuronal development and plasticity. Mol. Neurobiol. *34*, 205–219.

Jiménez-Sánchez, L., Campa, L., Auberson, Y.P., and Adell, A. (2014). The role of GluN2A and GluN2B subunits on the effects of NMDA receptor antagonists in modeling schizophrenia and treating refractory depression. Neuropsychopharmacol. Off. Publ. Am. Coll. Neuropsychopharmacol. *39*, 2673–2680.

Jin, Z., Bhandage, A.K., Bazov, I., Kononenko, O., Bakalkin, G., Korpi, E.R., and Birnir, B. (2014). Selective increases of AMPA, NMDA, and kainate receptor subunit mRNAs in the hippocampus and orbitofrontal cortex but not in prefrontal cortex of human alcoholics. Front. Cell. Neurosci. *8*, 1–10.

Jung, C.H., Jun, C.B., Ro, S.-H., Kim, Y.-M., Otto, N.M., Cao, J., Kundu, M., and Kim, D.-H.

(2009). ULK-Atg13-FIP200 complexes mediate mTOR signaling to the autophagy machinery. Mol. Biol. Cell *20*, 1992–2003.

Kaech, S., and Banker, G. (2006). Culturing hippocampal neurons. Nat. Protoc. *1*, 2406–2415.

Kandel, E.R. (2001). The molecular biology of memory storage: a dialogue between genes and synapses. Science *294*, 1030–1038.

Kang, H., and Schuman, E.M. (1996). A requirement for local protein synthesis in neurotrophin-induced hippocampal synaptic plasticity. Science (80-.). *273*, 1402–1406.

Káradóttir, R., Cavelier, P., Bergersen, L.H., and Attwell, D. (2005). NMDA receptors are expressed in oligodendrocytes and activated in ischaemia. Nature *438*, 1162–1166.

Karakas, E., Simorowski, N., and Furukawa, H. (2011). Subunit arrangement and phenylethanolamine binding in GluN1/GluN2B NMDA receptors. Nature *475*, 249–253.

Kasai, H., Ziv, N.E., Okazaki, H., Yagishita, S., and Toyoizumi, T. (2021). Spine dynamics in the brain, mental disorders and artificial neural networks. Nat. Rev. Neurosci. *22*, 407–422.

Kassai, H., Sugaya, Y., Noda, S., Nakao, K., Maeda, T., Kano, M., and Aiba, A. (2014). Selective activation of mTORC1 signaling recapitulates microcephaly, tuberous sclerosis, and neurodegenerative diseases. Cell Rep. *7*, 1626–1639.

Katz, L.C., and Shatz, C.J. (1996). Synaptic Activity and the Construction of Cortical Circuits. *274*, 1133–1138.

Kazmierski, J., Sieruta, M., Banys, A., Jaszewski, R., Sobow, T., Liberski, P., and Kloszewska, I. (2014). The assessment of the T102C polymorphism of the 5HT2a receptor gene, 3723G/A polymorphism of the NMDA receptor 3A subunit gene (GRIN3A) and 421C/A polymorphism of the NMDA receptor 2B subunit gene (GRIN2B) among cardiac surgery patients with and without d. Gen. Hosp. Psychiatry *36*, 753–756.

Kehoe, L.A., Bellone, C., De Roo, M., Zandueta, A., Dey, P.N., Perez-Otano, I., and Muller, D. (2014). GluN3A Promotes Dendritic Spine Pruning and Destabilization during Postnatal Development. J. Neurosci. *34*, 9213–9221.

Kelleher, R.J. 3rd, and Bear, M.F. (2008). The autistic neuron: troubled translation? Cell *135*, 401–406.

Kenney, J.W., Sorokina, O., Genheden, M., Sorokin, A., Armstrong, J.D., and Proud, C.G. (2015). Dynamics of Elongation Factor 2 Kinase Regulation in Cortical Neurons in Response to Synaptic Activity. *35*, 3034–3047.

Kidnapillai, S., Wade, B., Bortolasci, C.C., Panizzutti, B., Spolding, B., Connor, T., Crowley,

T., Jamain, S., Gray, L., Leboyer, M., et al. (2020). Drugs used to treat bipolar disorder act via microRNAs to regulate expression of genes involved in neurite outgrowth. J. Psychopharmacol. *34*, 370–379.

Kim, D.H., Sarbassov, D.D., Ali, S.M., King, J.E., Latek, R.R., Erdjument-Bromage, H., Tempst, P., and Sabatini, D.M. (2002). mTOR interacts with raptor to form a nutrient-sensitive complex that signals to the cell growth machinery. Cell *110*, 163–175.

Kim, J., Kundu, M., Viollet, B., and Guan, K.-L. (2011). AMPK and mTOR regulate autophagy through direct phosphorylation of Ulk1. Nat. Cell Biol. *13*, 132–141.

Kim, J.Y., Duan, X., Liu, C.Y., Jang, M.-H., Guo, J.U., Pow-anpongkul, N., Kang, E., Song, H., and Ming, G. (2009). DISC1 regulates new neuron development in the adult brain via modulation of AKT-mTOR signaling through KIAA1212. Neuron *63*, 761–773.

Kim, J.Y., Liu, C.Y., Zhang, F., Duan, X., Wen, Z., Song, J., Feighery, E., Lu, B., Rujescu, D., St Clair, D., et al. (2012). Interplay between DISC1 and GABA signaling regulates neurogenesis in mice and risk for schizophrenia. Cell *148*, 1051–1064.

Kim, M.J., Biag, J., Fass, D.M., Lewis, M.C., Zhang, Q., Fleishman, M., Gangwar, S.P., Machius, M., Fromer, M., Purcell, S.M., et al. (2017). Functional analysis of rare variants found in schizophrenia implicates a critical role for GIT1-PAK3 signaling in neuroplasticity. Mol. Psychiatry *22*, 417–429.

Klein, R., Nanduri, V., Jing, S., Lamballe, F., Tapley, P., Bryant, S., Cordon-Cardo, C., Reichardt, L.F., and Barbacid, M. (1991). The trkB Tyrosine Protein Kinase Is a Receptor for Brain-Derived Neurotrophic Factor and Neurotrophin-3. Cell *66*, 395–403.

Kunz, J., Henriquez, R., Schneider, U., Deuter-Reinhard, M., Movva, N.R., and Hall, M.N. (1993). Target of rapamycin in yeast, TOR2, is an essential phosphatidylinositol kinase homolog required for G1 progression. Cell *73*, 585–596.

Lafon-Cazal, M., Perez, V., Bockaert, J., and Marin, P. (2002). Akt mediates the anti-apoptotic effect of NMDA but not that induced by potassium depolarization in cultured cerebellar granule cells. Eur. J. Neurosci. *16*, 575–583.

Larsen, R.S., Corlew, R.J., Henson, M.A., Roberts, A.C., Mishina, M., Watanabe, M., Lipton, S.A., Nakanishi, N., Pérez-Otaño, I., Weinberg, R.J., et al. (2011). NR3A-containing NMDARs promote neurotransmitter release and spike timing-dependent plasticity. Nat. Neurosci. *14*, 338–344.

Larsen, R.S., Smith, I.T., Miriyala, J., Han, J.E., Corlew, R.J., Smith, S.L., and Philpot, B.D. (2014). Synapse-Specific Control of Experience-Dependent Plasticity by Presynaptic NMDA Receptors. Neuron *83*, 879–893.

Lee, J.H., Wei, L., Deveau, T.C., Gu, X., and Yu, S.P. (2016). Expression of the NMDA

receptor subunit GluN3A (NR3A) in the olfactory system and its regulatory role on olfaction in the adult mouse. Brain Struct. Funct. *221*, 3259–3273.

Lee, J.H., Zhang, J.Y., Wei, Z.Z., and Yu, S.P. (2018). Impaired social behaviors and minimized oxytocin signaling of the adult mice deficient in the N-methyl-D-aspartate receptor GluN3A subunit. Exp. Neurol. *305*, 1–12.

Lee, M.-C., Ting, K.K., Adams, S., Brew, B.J., Chung, R., and Guillemin, G.J. (2010a). Characterisation of the expression of NMDA receptors in human astrocytes. PLoS One *5*, e14123.

Lee, M.C., Yasuda, R., and Ehlers, M.D. (2010b). Metaplasticity at Single Glutamatergic Synapses. Neuron *66*, 859–870.

Lenz, G., and Avruch, J. (2005). Glutamatergic regulation of the p70S6 kinase in primary mouse neurons. J. Biol. Chem. *280*, 38121–38124.

Li, N., Lee, B., Liu, R.-J., Banasr, M., Dwyer, J.M., Iwata, M., Li, X.-Y., Aghajanian, G., and Duman, R.S. (2010). mTOR-dependent synapse formation underlies the rapid antidepressant effects of NMDA antagonists. Science *329*, 959–964.

Li, N., Liu, R.J., Dwyer, J.M., Banasr, M., Lee, B., Son, H., Li, X.Y., Aghajanian, G., and Duman, R.S. (2011). Glutamate N-methyl-D-aspartate receptor antagonists rapidly reverse behavioral and synaptic deficits caused by chronic stress exposure. Biol. Psychiatry *69*, 754–761.

Licausi, F., and Hartman, N.W. (2018). Role of mTOR complexes in neurogenesis. Int. J. Mol. Sci. *19*.

Lipton, J.O., and Sahin, M. (2014). The Neurology of mTOR. Neuron *84*, 275–291.

Liu, G.Y., and Sabatini, D.M. (2020). mTOR at the nexus of nutrition, growth, ageing and disease. Nat. Rev. Mol. Cell Biol. *21*, 183–203.

Liu, E., Knutzen, C.A., Krauss, S., Schweiger, S., and Chiang, G.G. (2011). Control of mTORC1 signaling by the Opitz syndrome protein MID1. Proc. Natl. Acad. Sci. U. S. A. *108*, 8680–8685.

Liu, H.P., Lin, W.Y., Liu, S.H., Wang, W.F., Tsai, C.H., Wu, B.T., Wang, C.K., and Tsai, F.J. (2009). Genetic variation in N-methyl-D-aspartate receptor subunit NR3A but not NR3B influences susceptibility to Alzheimer's disease. Dement. Geriatr. Cogn. Disord. *28*, 521–527.

Long, X., Lin, Y., Ortiz-Vega, S., Yonezawa, K., and Avruch, J. (2005). Rheb binds and regulates the mTOR kinase. Curr. Biol. *15*, 702–713.

Lüscher, C., and Malenka, R.C. (2012). NMDA Receptor-Dependent Long-Term Potentiation and Long-Term Depression (LTP / LTD). Cold Spring Harb. Perspect. Biol. *4*, 1–16.

Lyford, G.L., Yamagata, K., Kaufmann, W.E., Barnes, C.A., Sanders, L.K., Copeland, N.G., Gilbert, D.J., Jenkins, N.A., Lanahan, A.A., and Worley, P.F. (1995). Arc, a growth factor and activity-regulated gene, encodes a novel cytoskeleton-associated protein that is enriched in neuronal dendrites. Neuron *14*, 433–445.

Ma, O.K., and Sucher, N.J. (2004). Molecular interaction of NMDA receptor subunit NR3A with protein phosphatase 2A. Neuroreport *15*, 1447–1450.

Ma, J.Z., Payne, T.J., and Li, M.D. (2010). Significant association of glutamate receptor, ionotropic N-methyl-d-aspartate 3A (GRIN3A), with nicotine dependence in European- and African-American smokers. Hum. Genet. *127*, 503–512.

Ma, X.M., Yoon, S.-O., Richardson, C.J., Jülich, K., and Blenis, J. (2008). SKAR links pre-mRNA splicing to mTOR/S6K1-mediated enhanced translation efficiency of spliced mRNAs. Cell *133*, 303–313.

Madry, C., Mesic, I., Bartholomäus, I., Nicke, A., Betz, H., and Laube, B. (2007). Principal role of NR3 subunits in NR1/NR3 excitatory glycine receptor function. Biochem. Biophys. Res. Commun. *354*, 102–108.

Marco, S., Giralt, A., Petrovic, M.M., Pouladi, M. a, Martínez-Turrillas, R., Martínez-Hernández, J., Kaltenbach, L.S., Torres-Peraza, J., Graham, R.K., Watanabe, M., et al. (2013). Suppressing aberrant GluN3A expression rescues synaptic and behavioral impairments in Huntington's disease models. Nat. Med.

Marco, S., Murillo, A., and Pérez-Otaño, I. (2018). RNAi-Based GluN3A Silencing Prevents and Reverses Disease Phenotypes Induced by Mutant huntingtin. Mol. Ther. *26*, 1965–1972.

Martel, R.R., Klicius, J., and Galet, S. (1977). Inhibition of the immune response by rapamycin, a new antifungal antibiotic. Can. J. Physiol. Pharmacol. *55*, 48–51.

Martin, K.C., and Ephrussi, A. (2009). mRNA localization: gene expression in the spatial dimension. Cell *136*, 719–730.

Martínez-Turrillas, R., Puerta, E., Chowdhury, D., Marco, S., Watanabe, M., Aguirre, N., and Pérez-Otaño, I. (2012). The NMDA receptor subunit GluN3A protects against 3-nitroproprionic-induced striatal lesions via inhibition of calpain activation. Neurobiol. Dis. *48*, 290–298.

Martyn, A.C., Toth, K., Schmalzigaug, R., Hedrick, N.G., Rodriguiz, R.M., Yasuda, R., Wetsel, W.C., and Premont, R.T. (2018). GIT1 regulates synaptic structural plasticity underlying learning. PLoS One *13*, e0194350.

Matsuda, K., Fletcher, M., Kamiya, Y., and Yuzaki, M. (2003). Specific Assembly with the NMDA Receptor 3B Subunit Controls Surface Expression and Calcium Permeability of NMDA Receptors. J. Neurosci. *23*, 10064–10073.

Matsuzaki, M., Honkura, N., Ellis-Davies, G.C.R., and Kasai, H. (2004). Structural basis of long-term potentiation in single dendritic spines. Nature *429*, 761–766.

McClymont, D.W., Harris, J., and Mellor, I.R. (2012). Open-channel blockade is less effective on GluN3B than GluN3A subunit-containing NMDA receptors. Eur. J. Pharmacol. *686*, 22–31.

Mehra, A., Guérit, S., Macrez, R., Gosselet, F., Sevin, E., Lebas, H., Maubert, E., De Vries, H.E., Bardou, I., Vivien, D., et al. (2020). Nonionotropic Action of Endothelial NMDA Receptors on Blood-Brain Barrier Permeability via Rho/ROCK-Mediated Phosphorylation of Myosin. J. Neurosci. *40*, 1778–1787.

Miller, O.H., Yang, L., Wang, C.C., Hargroder, E.A., Zhang, Y., Delpire, E., and Hall, B.J. (2014). GluN2B-containing NMDA receptors regulate depression-like behavior and are critical for the rapid antidepressant actions of ketamine. Elife *2014*, 1–22.

Mohamad, O., Song, M., Wei, L., and Yu, S.P. (2013). Regulatory roles of the NMDA receptor GluN3A subunit in locomotion, Pain perception and cognitive functions in adult mice. J. Physiol. *591*, 149–168.

Monné A, L. (1948). Functioning of the Cytoplasm. In Advances in Enzymology and Related Areas of Molecular Biology, (John Wiley & Sons, Ltd), pp. 1–69.

Monteggia, L.M., Gideons, E., and Kavalali, E.T. (2013). The role of eukaryotic elongation factor 2 kinase in rapid antidepressant action of ketamine. Biol. Psychiatry *73*, 1199–1203.

Monyer, H., Sprengel, R., Schoepfer, R., Herb, A., Higuchi, M., Lomeli, H., Burnashev, N., Sakmann, B., and Seeburg, P.H. (1992). Heteromeric NMDA receptors: molecular and functional distinction of subtypes. Science *256*, 1217–1221.

Morgan, J.I., Cohen, D.R., Hempstead, J.L., and Curran, T. (1987). Mapping patterns of c-fos expression in the central nervous system after seizure. Science *237*, 192–197.

Moriyoshi, K., Masu, M., Ishii, T., Shigemoto, R., Mizuno, N., and Nakanishi, S. (1991). Molecular cloning and characterization of the rat NMDA receptor. Nature *354*, 31–37.

Muddashetty, R.S., Kelić, S., Gross, C., Xu, M., and Bassell, G.J. (2007). Dysregulated metabotropic glutamate receptor-dependent translation of AMPA receptor and postsynaptic density-95 mRNAs at synapses in a mouse model of fragile X syndrome. J. Neurosci. *27*, 5338–5348.

Mueller, H.T., and Meador-Woodruff, J.H. (2004). NR3A NMDA receptor subunit mRNA expression in schizophrenia, depression and bipolar disorder. Schizophr. Res. *71*, 361–370.

Murakami, M., Ichisaka, T., Maeda, M., Oshiro, N., Hara, K., Edenhofer, F., Kiyama, H., Yonezawa, K., and Yamanaka, S. (2004). mTOR Is Essential for Growth and Proliferation in Early Mouse Embryos and Embryonic Stem Cells. Mol. Cell. Biol. *24*, 6710 LP – 6718.

Murillo, A., Navarro, A.I., Puelles, E., Zhang, Y., Petros, T.J., and Pérez-Otaño, I. (2021). Temporal Dynamics and Neuronal Specificity of Grin3a Expression in the Mouse Forebrain. Cereb. Cortex *31*, 1914–1926.

Murugan, M., Sivakumar, V., Lu, J., Ling, E.-A., and Kaur, C. (2011). Expression of N-methyl D-aspartate receptor subunits in amoeboid microglia mediates production of nitric oxide via NF-κB signaling pathway and oligodendrocyte cell death in hypoxic postnatal rats. Glia *59*, 521–539.

Naldini, L., Blomer, U., Gallay, P., Ory, D., Mulligan, R., Gage, F.H., Verma, I.M., and Trono, D. (1996). In Vivo Gene Delivery and Stable Transduction of Nondividing Cells by a Lentiviral Vector. Science (80-.). *272*, 263–267.

Nathans, D. (1964). Puromycin inhibition of protein synthesis: incorporation of puromycin into peptide chains. Proc. Natl. Acad. Sci. U. S. A. *51*, 585–592.

Neasta, J., Ben Hamida, S., Yowell, Q., Carnicella, S., and Ron, D. (2010). Role for mammalian target of rapamycin complex 1 signaling in neuroadaptations underlying alcohol-related disorders. Proc. Natl. Acad. Sci. U. S. A. *107*, 20093–20098.

Nicoll, R.A., and Malenka, R.C. (1999). Expression mechanisms underlying NMDA receptor-dependent long-term potentiation. Ann. N. Y. Acad. Sci. *868*, 515–525.

Nie, D., Di Nardo, A., Han, J.M., Baharanyi, H., Kramvis, I., Huynh, T., Dabora, S., Codeluppi, S., Pandolfi, P.P., Pasquale, E.B., et al. (2010). Tsc2-Rheb signaling regulates EphA-mediated axon guidance. Nat. Neurosci. *13*, 163–172.

Nilsson, A., Eriksson, M., Muly, E.C., Akesson, E., Samuelsson, E.-B., Bogdanovic, N., Benedikz, E., and Sundström, E. (2007). Analysis of NR3A receptor subunits in human native NMDA receptors. Brain Res. *1186*, 102–112.

Nishi, M., Hinds, H., Lu, H.P., Kawata, M., and Hayashi, Y. (2001). Motoneuron-specific expression of NR3B, a novel NMDA-type glutamate receptor subunit that works in a dominant-negative manner. J. Neurosci. *21*, 1–6.

Nixon, R.A. (2013). The role of autophagy in neurodegenerative disease. Nat. Med. *19*, 983–997.

Ohi, K., Hashimoto, R., Ikeda, M., Yamamori, H., Yasuda, Y., Fujimoto, M., Umeda-Yano, S., Fukunaga, M., Fujino, H., Watanabe, Y., et al. (2015). Glutamate Networks Implicate Cognitive Impairments in Schizophrenia: Genome-Wide Association Studies of 52 Cognitive Phenotypes. Schizophr. Bull. *41*, 909–918.

Otsu, Y., Darcq, E., Pietrajtis, K., Mátyás, F., Schwartz, E., Bessaih, T., Abi Gerges, S., Rousseau, C. V., Grand, T., Dieudonné, S., et al. (2019). Control of aversion by glycine-gated GluN1/GluN3A NMDA receptors in the adult medial habenula. Science (80-.). *366*, 250–254.

Pachernegg, S., Strutz-Seebohm, N., and Hollmann, M. (2012). GluN3 subunit-containing NMDA receptors: Not just one-trick ponies. Trends Neurosci. *35*, 240–249.

Palygin, O., Lalo, U., and Pankratov, Y. (2011). Distinct pharmacological and functional properties of NMDA receptors in mouse cortical astrocytes. Br. J. Pharmacol. *163*, 1755–1766.

Paoletti, P., Ascher, P., and Neyton, J. (1997). High-affinity zinc inhibition of NMDA NR1-NR2A receptors. J. Neurosci. *17*, 5711–5725.

Paoletti, P., Bellone, C., and Zhou, Q. (2013). NMDA receptor subunit diversity: impact on receptor properties, synaptic plasticity and disease. Nat. Rev. Neurosci. *14*, 383–400.

Papadia, S., Stevenson, P., Hardingham, N.R., Bading, H., and Hardingham, G.E. (2005). Nuclear Ca2+ and the cAMP Response Element-Binding Protein Family Mediate a Late Phase of Activity-Dependent Neuroprotection. Neuroscience *25*, 4279–4287.

Papenberg, G., Li, S.C., Nagel, I.E., Nietfeld, W., Schjeide, B.M., Schröder, J., Bertram, L., Heekeren, H.R., Lindenberger, U., and Bäckman, L. (2014). Dopamine and glutamate receptor genes interactively influence episodic memory in old age. Neurobiol. Aging *35*, 1213.e3-1213.e8.

Park, A.J., Havekes, R., Fu, X., Hansen, R., Tudor, J.C., Peixoto, L., Li, Z., Wu, Y.C., Poplawski, S.G., Baraban, J.M., et al. (2017). Learning induces the translin/trax RNase complex to express activin receptors for persistent memory. Elife *6*, 1–19.

Park, K.K., Kai Liu, Hu, Y., Smith, P.D., Wang, C., Cai, B., Xu, B., Connolly, L., Kramvis, I., Sahin, M., et al. (2008). Promoting Axon Regeneration in the Adult CNS by Modulation of the PTEN/mTOR Pathway. Science (80-.). *322*, 963–967.

Paul, A., Crow, M., Raudales, R., He, M., Gillis, J., and Huang, Z.J. (2017). Transcriptional Architecture of Synaptic Communication Delineates GABAergic Neuron Identity. Cell *171*, 522-539.e20.

Pearce, L.R., Huang, X., Boudeau, J., Pawłowski, R., Wullschleger, S., Deak, M., Ibrahim, A.F.M., Gourlay, R., Magnuson, M.A., and Alessi, D.R. (2007). Identification of Protor as a novel Rictor-binding component of mTOR complex-2. Biochem. J. *405*, 513–522.

Penzes, P., Cahill, M.E., Jones, K.A., VanLeeuwen, J.-E., and Woolfrey, K.M. (2011). Dendritic spine pathology in neuropsychiatric disorders. Nat. Neurosci. *14*, 285–293.

Perez-Otano, I., Schulteis, C.T., Contractor, A., Lipton, S.A., Trimmer, J.S., Sucher, N.J., and Heinemann, S.F. (2001). Assembly with the NR1 Subunit Is Required for Surface Expression of NR3A-Containing NMDA Receptors. J. Neurosci. *21*, 1228–1237.

Pérez-Otaño, I., and Ehlers, M.D. (2004). Learning from NMDA receptor trafficking: Clues to the development and maturation of glutamatergic synapses. NeuroSignals *13*, 175–189.

Pérez-Otaño, I., Luján, R., Tavalin, S.J., Plomann, M., Modregger, J., Liu, X.B., Jones, E.G., Heinemann, S.F., Lo, D.C., and Ehlers, M.D. (2006). Endocytosis and synaptic removal of NR3A-containing NMDA receptors by PACSIN1/syndapin1. Nat. Neurosci. *9*, 611–621.

Pérez-Otaño, I., Larsen, R.S., and Wesseling, J.F. (2016). Emerging roles of GluN3-containing NMDA receptors in the CNS. Nat. Publ. Gr.

Petralia, R.S., Wang, Y.X., Hua, F., Yi, Z., Zhou, A., Ge, L., Stephenson, F.A., and Wenthold, R.J. (2010). Organization of NMDA receptors at extrasynaptic locations. Neuroscience *167*, 68–87.

Pfeffer, C.K., Xue, M., He, M., Huang, Z.J., and Scanziani, M. (2013). Inhibition of inhibition in visual cortex: The logic of connections between molecularly distinct interneurons. Nat. Neurosci. *16*, 1068–1076.

Philpot, B.D., Sekhar, A.K., Shouval, H.Z., and Bear, M.F. (2001). Visual experience and deprivation bidirectionally modify the composition and function of NMDA receptors in visual cortex. Neuron *29*, 157–169.

Pierce, J.P., Van Leyen, K., and McCarthy, J.B. (2000). Translocation machinery for synthesis of integral membrane and secretory proteins in dendritic spines. Nat. Neurosci. *3*, 311–313.

Piña-Crespo, J.C., Talantova, M., Micu, I., States, B., Chen, H.S.V., Tu, S., Nakanishi, N., Tong, G., Zhang, D., Heinemann, S.F., et al. (2010). Excitatory glycine responses of CNS myelin mediated by NR1/NR3 “NMDA” receptor subunits. J. Neurosci. *30*, 11501–11505.

Poulopoulos, A., Murphy, A.J., Ozkan, A., Davis, P., Hatch, J., Kirchner, R., and Macklis, J.D. (2019). Subcellular transcriptomes and proteomes of developing axon projections in the cerebral cortex. Nature *565*, 356–360.

Di Prisco, G.V., Huang, W., Buffington, S.A., Hsu, C.-C., Bonnen, P.E., Placzek, A.N., Sidrauski, C., Krnjevic, K., Kaufman, R.J., Walter, P., et al. (2014). Translational control of mGluR-dependent long-term depression and object-place learning by eIF2alpha; Nat. Neurosci. *17*, 1–13.

Puighermanal, E., Marsicano, G., Busquets-Garcia, A., Lutz, B., Maldonado, R., and Ozaita, A. (2009). Cannabinoid modulation of hippocampal long-term memory is mediated by mTOR signaling. Nat. Neurosci. *12*, 1152–1158.

Puighermanal, E., Busquets-Garcia, A., Gomis-González, M., Marsicano, G., Maldonado, R., and Ozaita, A. (2013). Dissociation of the pharmacological effects of THC by mTOR blockade. Neuropsychopharmacol. Off. Publ. Am. Coll. Neuropsychopharmacol. *38*, 1334–1343.

Raab-Graham, K.F., Haddick, P.C.G., Jan, Y.N., and Jan, L.Y. (2006). Activity- and mTOR-Dependent Suppression of Kv1.1 Channel mRNA Translation in Dendrites. Science (80-.). 144–148.

Racca, C., Stephenson, F.A., Streit, P., Roberts, J.D., and Somogyi, P. (2000). NMDA

receptor content of synapses in stratum radiatum of the hippocampal CA1 area. J. Neurosci. *20*, 2512–2522.

Rakic, P., Bourgeois, J., Eckenhoff, M.F., Zecevic, N., and Goldman-rakic, P.S. (1986). Concurrent Overproduction of Synapses in Diverse Regions of the Primate Cerebral Cortex. Science (80-.). *232*, 232–235.

Rao, A., and Steward, O. (1991). Evidence that protein constituents of postsynaptic membrane specializations are locally synthesized: analysis of proteins synthesized within synaptoneurosomes. J. Neurosci. Res. *11*, 2881–2895.

Rao, J.S., Harry, G.J., Rapoport, S.I., and Kim, H.W. (2010). Increased excitotoxicity and neuroinflammatory markers in postmortem frontal cortex from bipolar disorder patients. Mol. Psychiatry *15*, 384–392.

Rao, V.R., Pintchovski, S. a, Chin, J., Peebles, C.L., Mitra, S., and Finkbeiner, S. (2006). AMPA receptors regulate transcription of the plasticity-related immediate-early gene Arc. Nat. Neurosci. *9*, 887–895.

Ravikumar, B., Vacher, C., Berger, Z., Davies, J.E., Luo, S., Oroz, L.G., Scaravilli, F., Easton, D.F., Duden, R., O'Kane, C.J., et al. (2004). Inhibition of mTOR induces autophagy and reduces toxicity of polyglutamine expansions in fly and mouse models of Huntington disease. Nat. Genet. *36*, 585–595.

Redondo, R.L., and Morris, R.G.M. (2011). Making memories last: the synaptic tagging and capture hypothesis. Nat. Rev. Neurosci. *12*, 17–30.

Roberts, A.C., Diez-Garcia, J., Rodriguiz, R.M., Lopez, I.P., Lujan, R., Martinez-Turrillas, R., Pico, E., Henson, M.A., Bernardo, D.R., Jarrett, T.M., et al. (2009). Downregulation of NR3A-Containing NMDARs Is Required for Synapse Maturation and Memory Consolidation. Neuron *63*, 342–356.

Rodenas-Ruano, A., Chávez, A.E., Cossio, M.J., Castillo, P.E., and Zukin, R.S. (2012). REST-dependent epigenetic remodeling promotes the developmental switch in synaptic NMDA receptors. Nat. Neurosci. *15*, 1382–1390.

Roozafzoon, R., Goodarzi, A., Vousooghi, N., Sedaghati, M., Yaghmaei, P., and Zarrindast, M.R. (2010). Expression of NMDA receptor subunits in human peripheral blood lymphocytes in opioid addiction. Eur. J. Pharmacol. *638*, 29–32.

Rosenblum, K., Meiri, N., and Dudai, Y. (1993). Taste memory: the role of protein synthesis in gustatory cortex. Behav. Neural Biol. *59*, 49–56.

Rozeboom, A.M., Queenan, B.N., Partridge, J.G., Farnham, C., Wu, J. young, Vicini, S., and Pak, D.T.S. (2015). Evidence for glycinergic GluN1/GluN3 NMDA receptors in hippocampal metaplasticity. Neurobiol. Learn. Mem. *125*, 265–273.

Sabatini, D.M. (2017). Twenty-five years of mTOR: Uncovering the link from nutrients to growth. Proc. Natl. Acad. Sci. U. S. A. *114*, 11818–11825.

Sabatini, D.M., Erdjument-Bromage, H., Lui, M., Tempst, P., and Snyder, S.H. (1994). RAFT1: a mammalian protein that binds to FKBP12 in a rapamycin-dependent fashion and is homologous to yeast TORs. Cell *78*, 35–43.

Sabers, C.J., Martin, M.M., Brunn, G.J., Williams, J.M., Dumont, F.J., Wiederrecht, G., and Abraham, R.T. (1995). Isolation of a protein target of the FKBP12-rapamycin complex in mammalian cells. J. Biol. Chem. *270*, 815–822.

Sadat-Shirazi, M.S., Vousooghi, N., Alizadeh, B., Makki, S.M., Zarei, S.Z., Nazari, S., and Zarrindast, M.R. (2018). Expression of NMDA receptor subunits in human blood lymphocytes: A peripheral biomarker in online computer game addiction. J. Behav. Addict. *7*, 260–268.

Sadat-Shirazi, M.S., Ashabi, G., Hessari, M.B., Khalifeh, S., Neirizi, N.M., Matloub, M., Safarzadeh, M., Vousooghi, N., and Zarrindast, M.R. (2019). NMDA receptors of blood lymphocytes anticipate cognitive performance variations in healthy volunteers. Physiol. Behav. *201*, 53–58.

Saha, R.N., Wissink, E.M., Bailey, E.R., Zhao, M., Fargo, D.C., Hwang, J.-Y., Daigle, K.R., Fenn, J.D., Adelman, K., and Dudek, S.M. (2011). Rapid activity-induced transcription of Arc and other IEGs relies on poised RNA polymerase II. Nat. Neurosci. *14*, 848–856.

Salter, M.G., and Fern, R. (2005). NMDA receptors are expressed in developing oligodendrocyte processes and mediate injury. Nature *438*, 1167–1171.

Sancak, Y., Thoreen, C.C., Peterson, T.R., Lindquist, R.A., Kang, S.A., Spooner, E., Carr, S.A., and Sabatini, D.M. (2007). PRAS40 is an insulin-regulated inhibitor of the mTORC1 protein kinase. Mol. Cell *25*, 903–915.

Sancak, Y., Peterson, T.R., Shaul, Y.D., Lindquist, R.A., Thoreen, C.C., Bar-Peled, L., and Sabatini, D.M. (2008). The Rag GTPases bind raptor and mediate amino acid signaling to mTORC1. Science *320*, 1496–1501.

Sancak, Y., Bar-Peled, L., Zoncu, R., Markhard, A.L., Nada, S., and Sabatini, D.M. (2010). Ragulator-Rag complex targets mTORC1 to the lysosomal surface and is necessary for its activation by amino acids. Cell *141*, 290–303.

Santini, E., Huynh, T.N., MacAskill, A.F., Carter, A.G., Pierre, P., Ruggero, D., Kaphzan, H., and Klann, E. (2013). Exaggerated translation causes synaptic and behavioural aberrations associated with autism. Nature *493*, 411–415.

Sarbassov, D.D., Ali, S.M., Kim, D.-H., Guertin, D.A., Latek, R.R., Erdjument-Bromage, H., Tempst, P., and Sabatini, D.M. (2004). Rictor, a novel binding partner of mTOR, defines a rapamycin-insensitive and raptor-independent pathway that regulates the cytoskeleton. Curr. Biol. *14*, 1296–1302.

Sarbassov, D.D., Ali, S.M., Sengupta, S., Sheen, J.-H., Hsu, P.P., Bagley, A.F., Markhard, A.L., and Sabatini, D.M. (2006). Prolonged rapamycin treatment inhibits mTORC2 assembly and Akt/PKB. Mol. Cell *22*, 159–168.

Sasaki, Y.F., Rothe, T., Premkumar, L.S., Das, S., Cui, J., Talantova, M. V., Wong, H.K., Gong, X., Chan, S.F., Zhang, D., et al. (2002). Characterization and comparison of the NR3A subunit of the NMDA receptor in recombinant systems and primary cortical neurons. J. Neurophysiol. *87*, 2052–2063.

Saxton, R.A., and Sabatini, D.M. (2017). mTOR Signaling in Growth, Metabolism, and Disease. Cell *168*, 960–976.

Scheetz, a J., Nairn, a C., and Constantine-Paton, M. (2000). NMDA receptor-mediated control of protein synthesis at developing synapses. Nat. Neurosci. *3*, 211–216.

Schmidt, E.K., Clavarino, G., Ceppi, M., and Pierre, P. (2009). SUnSET, a nonradioactive method to monitor protein synthesis. Nat. Methods *6*, 275–277.

Schratt, G.M., Nigh, E.A., Chen, W.G., Hu, L., and Greenberg, M.E. (2004). BDNF regulates the translation of a select group of mRNAs by a mammalian target of rapamycin-phosphatidylinositol 3-kinase-dependent pathway during neuronal development. J. Neurosci. *24*, 7366–7377.

Shao, X., Liu, L., Wei, F., Liu, Y., Wang, F., Yi, J., Sun, L., Huang, Y., Song, Z., Yin, W., et al. (2020). Fas and GIT1 signalling in the prefrontal cortex mediate behavioural sensitization to methamphetamine in mice. Brain Res. Bull. *164*, 361–371.

Sharma, V., Sood, R., Khlaifia, A., Eslamizade, M.J., Hung, T.Y., Lou, D., Asgarihafshejani, A., Lalzar, M., Kiniry, S.J., Stokes, M.P., et al. (2020). eIF2α controls memory consolidation via excitatory and somatostatin neurons. Nature *586*, 412–416.

Shen, Y.C., Liao, D.L., Chen, J.Y., Wang, Y.C., Lai, I.C., Liou, Y.J., Chen, Y.J., Luu, S.U., and Chen, C.H. (2009). Exomic sequencing of the glutamate receptor, ionotropic, N-methyl-d-aspartate 3A gene (GRIN3A) reveals no association with schizophrenia. Schizophr. Res. *114*, 25–32.

Sheng, M., Cummings, J., Roldan, L.A., Jan, Y.N., and Jan, L.Y. (1994). Changing subunit composition of heteromeric NMDA receptors during development of rat cortex. Nature *368*, 144–147.

Shiota, C., Woo, J.-T., Lindner, J., Shelton, K.D., and Magnuson, M.A. (2006). Multiallelic disruption of the rictor gene in mice reveals that mTOR complex 2 is essential for fetal growth and viability. Dev. Cell *11*, 583–589.

Shrestha, P., Shan, Z., Mamcarz, M., Ruiz, K.S.A., Zerihoun, A.T., Juan, C.Y., Herrero-Vidal, P.M., Pelletier, J., Heintz, N., and Klann, E. (2020a). Amygdala inhibitory neurons as loci for translation in emotional memories. Nature *586*, 407–411.

Shrestha, P., Ayata, P., Herrero-Vidal, P., Longo, F., Gastone, A., LeDoux, J.E., Heintz, N., and Klann, E. (2020b). Cell-type-specific drug-inducible protein synthesis inhibition demonstrates that memory consolidation requires rapid neuronal translation. Nat. Neurosci. *23*, 281–292.

Smithson, L.J., and Gutmann, D.H. (2016). Proteomic analysis reveals GIT1 as a novel mTOR complex component critical for mediating astrocyte survival. Genes Dev. *30*, 1383–1388.

Stern, E., Chinnakkaruppan, A., David, O., Sonenberg, N., and Rosenblum, K. (2013). Blocking the eIF2α kinase (PKR) enhances positive and negative forms of cortex-dependent taste memory. J. Neurosci. *33*, 2517–2525.

Steward, O., and Levy, W.B. (1982). Preferential localization of polyribosomes under the base of dendritic spines in granule cells of the dentate gyrus. J. Neurosci. *2*, 284–291.

Stocca, G., and Vicini, S. (1998). Increased contribution of NR2A subunit to synaptic NMDA receptors in developing rat cortical neurons. J. Physiol. *507*, 13–24.

Stoica, L., Zhu, P.J., Huang, W., Zhou, H., Kozma, S.C., and Costa-Mattioli, M. (2011). Selective pharmacogenetic inhibition of mammalian target of Rapamycin complex I (mTORC1) blocks long-term synaptic plasticity and memory storage. Proc. Natl. Acad. Sci. U. S. A. *108*, 3791–3796.

Strack, S., Zaucha, J.A., Ebner, F.F., Colbran, R.J., and Wadzinski, B.E. (1998). Brain protein phosphatase 2A: developmental regulation and distinct cellular and subcellular localization by B subunits. J. Comp. Neurol. *392*, 515–527.

Sucher, N.J., Akbarian, S., Chi, C.L., Leclerc, C.L., Awobuluyi, M., Deitcher, D.L., Wu, M.K., Yuan, J.P., Jones, E.G., and Lipton, S.A. (1995). Developmental and regional expression pattern of a novel NMDA receptor- like subunit (NMDAR-L) in the rodent brain. J. Neurosci. *15*, 6509–6520.

Sucher, N.J., Yu, E., Chan, S.F., Miri, M., Lee, B.J., Xiao, B., Worley, P.F., and Jensen, F.E. (2011). Association of the small GTPase Rheb with the NMDA receptor subunit NR3A. NeuroSignals *18*, 203–209.

Sun, L., Margolis, F.L., Shipley, M.T., and Lidow, M.S. (1998). Identification of a long variant of mRNA encoding the NR3 subunit of the NMDA receptor: Its regional distribution and developmental expression in the rat brain. FEBS Lett. *441*, 392–396.

Sun, Y., Xu, Y., Cheng, X., Chen, X., Xie, Y., Zhang, L., Wang, L., Hu, J., and Gao, Z. (2018). The differences between GluN2A and GluN2B signaling in the brain. J. Neurosci. Res. *96*, 1430–1443.

Takata, A., Iwayama, Y., Fukuo, Y., Ikeda, M., Okochi, T., Maekawa, M., Toyota, T., Yamada, K., Hattori, E., Ohnishi, T., et al. (2013). A population-specific uncommon variant in GRIN3A associated with schizophrenia. Biol. Psychiatry *73*, 532–539.

Takei, N., Kawamura, M., Hara, K., Yonezawa, K., and Nawa, H. (2001). Brain-derived

neurotrophic factor enhances neuronal translation by activating multiple initiation processes: Comparison with the effects of insulin. J. Biol. Chem. *276*, 42818–42825.

Takei, N., Inamura, N., Kawamura, M., Namba, H., Hara, K., Yonezawa, K., and Nawa, H. (2004). Brain-Derived Neurotrophic Factor Induces Mammalian Target of Rapamycin-Dependent Local Activation of Translation Machinery and Protein Synthesis in Neuronal Dendrites. J. Neurosci. *24*, 9760–9769.

Tang, G., Gudsnuk, K., Kuo, S.H., Cotrina, M.L., Rosoklija, G., Sosunov, A., Sonders, M.S., Kanter, E., Castagna, C., Yamamoto, A., et al. (2014). Loss of mTOR-Dependent Macroautophagy Causes Autistic-like Synaptic Pruning Deficits. Neuron *83*, 1131–1143.

Tang, S.J., Reis, G., Kang, H., Gingras, A.C., Sonenberg, N., and Schuman, E.M. (2002). A rapamycin-sensitive signaling pathway contributes to long-term synaptic plasticity in the hippocampus. Proc. Natl. Acad. Sci. U. S. A. *99*, 467–472.

Tashiro, A., Minden, A., and Yuste, R. (2000). Regulation of dendritic spine morphology by the rho family of small GTPases: antagonistic roles of Rac and Rho. Cereb. Cortex *10*, 927–938.

Terenzio, M., Koley, S., Samra, N., Rishal, I., Zhao, Q., Sahoo, P.K., Urisman, A., Marvaldi, L., Oses-prieto, J.A., Forester, C., et al. (2018). Locally translated mTOR controls axonal local translation in nerve injury. Science (80-.). *359*, 1416–1421.

Thomanetz, V., Angliker, N., Cloëtta, D., Lustenberger, R.M., Schweighauser, M., Oliveri, F., Suzuki, N., and Rüegg, M.A. (2013). Ablation of the mTORC2 component rictor in brain or Purkinje cells affects size and neuron morphology. J. Cell Biol. *201*, 293–308.

Thoreen, C.C., Chantranupong, L., Keys, H.R., Wang, T., Gray, N.S., and Sabatini, D.M. (2012). A unifying model for mTORC1-mediated regulation of mRNA translation. Nature *485*, 109–113.

tom Dieck, S., Kochen, L., Hanus, C., Heumüller, M., Bartnik, I., Nassim-Assir, B., Merk, K., Mosler, T., Garg, S., Bunse, S., et al. (2015). Direct visualization of newly synthesized target proteins in situ. Nat. Methods *12*, 411–414.

Tong, G., Takahashi, H., Tu, S., Shin, Y., Talantova, M., Zago, W., Xia, P., Nie, Z., Goetz, T., Zhang, D., et al. (2008). Modulation of NMDA receptor properties and synaptic transmission by the NR3A subunit in mouse hippocampal and cerebrocortical neurons. J. Neurophysiol. *99*, 122–132.

Tongiorgi, E., Righi, M., and Cattaneo, A. (1997). Activity-Dependent Dendritic Targeting of BDNF and TrkB mRNAs in Hippocampal Neurons. J. Neurosci. *17*, 9492 LP – 9505.

Tovar, K.R., and Westbrook, G.L. (1999). The incorporation of NMDA receptors with a distinct subunit composition at nascent hippocampal synapses in vitro. J. Neurosci. *19*, 4180–4188.

Tran, D.H., Gong, R., and Tang, S.-J. (2007). Differential roles of NR2A and NR2B subtypes

in NMDA receptor-dependent protein synthesis in dendrites. Neuropharmacology *53*, 252–256.

Traynelis, S.F., Wollmuth, L.P., McBain, C.J., Menniti, F.S., Vance, K.M., Ogden, K.K., Hansen, K.B., Yuan, H., Myers, S.J., and Dingledine, R. (2010). Glutamate receptor ion channels: structure, regulation, and function. Pharmacol. Rev. *62*, 405–496.

Trinh, M.A., Kaphzan, H., Wek, R.C., Pierre, P., Cavener, D.R., and Klann, E. (2012). Brain-specific disruption of the eIF2α kinase PERK decreases ATF4 expression and impairs behavioral flexibility. Cell Rep. *1*, 676–688.

Troca-Marin, J.A., Alves-Sampaio, A., Tejedor, F.J., and Montesinos, M.L. (2010). Local translation of dendritic RhoA revealed by an improved synaptoneurosome preparation. Mol. Cell. Neurosci. *43*, 308–314.

Tsai, N.-P., Wilkerson, J.R., Guo, W., Maksimova, M.A., DeMartino, G.N., Cowan, C.W., and Huber, K.M. (2012a). Multiple autism-linked genes mediate synapse elimination via proteasomal degradation of a synaptic scaffold PSD-95. Cell *151*, 1581–1594.

Tsai, P.T., Hull, C., Chu, Y., Greene-Colozzi, E., Sadowski, A.R., Leech, J.M., Steinberg, J., Crawley, J.N., Regehr, W.G., and Sahin, M. (2012b). Autistic-like behaviour and cerebellar dysfunction in Purkinje cell Tsc1 mutant mice. Nature *488*, 647–651.

Tudor, J.C., Davis, E.J., Peixoto, L., Wimmer, M.E., Tilborg, E. Van, Park, A.J., Poplawski, S.G., Chung, C.W., Havekes, R., Huang, J., et al. (2016). Sleep deprivation impairs memory by attenuating mTORC1-dependent protein synthesis. Sci. Signal. *9*, 1–9.

Turner, C.E., Brown, M.C., Perrotta, J.A., Riedy, M.C., Nikolopoulos, S.N., McDonald, A.R., Bagrodia, S., Thomas, S., and Leventhal, P.S. (1999). Paxillin LD4 motif binds PAK and PIX through a novel 95-kD ankyrin repeat, ARF-GAP protein: A role in cytoskeletal remodeling. J. Cell Biol. *145*, 851–863.

Tushev, G., Glock, C., Heumüller, M., Biever, A., Jovanovic, M., and Schuman, E.M. (2018). Alternative 3' UTRs Modify the Localization, Regulatory Potential, Stability, and Plasticity of mRNAs in Neuronal Compartments. Neuron *98*, 495-511.e6.

Vézina, C., Kudelski, A., and Sehgal, S.N. (1975). Rapamycin (AY-22,989), a new antifungal antibiotic. I. Taxonomy of the producing streptomycete and isolation of the active principle. J. Antibiot. (Tokyo). *28*, 721–726.

Wahl, S.E., McLane, L.E., Bercury, K.K., Macklin, W.B., and Wood, T.L. (2014). Mammalian target of rapamycin promotes oligodendrocyte differentiation, initiation and extent of CNS myelination. J. Neurosci. *34*, 4453–4465.

Wang, C.C., Held, R.G., Chang, S.C., Yang, L.L., Delpire, E., Ghosh, A., and Hall, B.J. (2011). A critical role for GluN2B-containing NMDA receptors in cortical development and function.

Neuron *72*, 789–805.

Wang, D.O., Martin, K.C., and Zukin, R.S. (2010). Spatially restricting gene expression by local translation at synapses. Trends Neurosci. *33*, 173–182.

Wang, R.Y., Chen, H.J., Huang, C.L., Wang, J.Y., Lee, T.E., Lee, H.Y., and Hung, C.C. (2018). Impacts of GRIN3A, GRM6 and TPH2 genetic polymorphisms on quality of life in methadone maintenance therapy population. PLoS One *13*, 1–15.

Watanabe, M., Inoue, Y., Sakimura, K., and Mishina, M. (1992). Developmental changes in distribution of NMDA receptor channel subunit mRNAs. Neuroreport *3*, 1138–1140.

Wee, K.S.L., Tan, F.C.K., Cheong, Y.P., Khanna, S., and Low, C.M. (2016). Ontogenic profile and synaptic distribution of GluN3 proteins in the rat brain and hippocampal neurons. Neurochem. Res. *41*, 290–297.

Welzl, H., D'Adamo, P., and Lipp, H.P. (2001). Conditioned taste aversion as a learning and memory paradigm. Behav. Brain Res. *125*, 205–213.

Wollebo, H.S., Woldemichaele, B., and White, M.K. (2013). Lentiviral transduction of neuronal cells. Methods Mol. Biol. *1078*, 141–146.

Won, H., Mah, W., Kim, E., Kim, J.-W., Hahm, E.-K., Kim, M.-H., Cho, S., Kim, J., Jang, H., Cho, S.-C., et al. (2011). GIT1 is associated with ADHD in humans and ADHD-like behaviors in mice. Nat. Med. *17*, 566–572.

Wong, H.K., Liu, X.B., Matos, M.F., Chan, S.F., Pérez-Otaño, I., Boysen, M., Cui, J., Nakanishi, N., Trimmer, J.S., Jones, E.G., et al. (2002). Temporal and regional expression of NMDA receptor subunit NR3A in the mammalian brain. J. Comp. Neurol. *450*, 303–317.

Woo, S.-Y., Kim, D.-H., Jun, C.-B., Kim, Y.-M., Haar, E. Vander, Lee, S., Hegg, J.W., Bandhakavi, S., Griffin, T.J., and Kim, D.-H. (2007). PRR5, a novel component of mTOR complex 2, regulates platelet-derived growth factor receptor beta expression and signaling. J. Biol. Chem. *282*, 25604–25612.

Wu, G.Y., Deisseroth, K., and Tsien, R.W. (2001). Spaced stimuli stabilize MAPK pathway activation and its effects on dendritic morphology. Nat. Neurosci. *4*, 151–158.

Wu, J., McCallum, S.E., Glick, S.D., and Huang, Y. (2011). Inhibition of the mammalian target of rapamycin pathway by rapamycin blocks cocaine-induced locomotor sensitization. Neuroscience *172*, 104–109.

Xie, X., Liu, H., Zhang, J., Chen, W., Zhuang, D., Duan, S., and Zhou, W. (2016). Association between genetic variations of NMDA receptor NR3 subfamily genes and heroin addiction in male Han Chinese. Neurosci. Lett. *631*, 122–125.

Yamagata, K., Sanders, L.K., Kaufmann, W.E., Yee, W., Barnes, C.A., Nathans, D., and Worley, P.F. (1994). Rheb, a growth factor- and synaptic activity-regulated gene, encodes a novel Ras-related protein. J. Biol. Chem. *269*, 16333–16339.

Yan, J., Porch, M.W., Court-Vazquez, B., Bennett, M.V.L., and Zukin, R.S. (2018). Activation of autophagy rescues synaptic and cognitive deficits in fragile X mice. Proc. Natl. Acad. Sci. U. S. A. *115*, E9707–E9716.

Yang, G., Wang, J., Wan, L., Shi, X.Y., Meng, Y., Ren, W.H., and Zou, L.P. (2019). Regulatory role of hippocampal PI3K and mTOR signaling pathway in NMDA-induced infant spasm rats. Neurol. Res. *41*, 1075–1082.

Yang, H., Rudge, D.G., Koos, J.D., Vaidialingam, B., Yang, H.J., and Pavletich, N.P. (2013). mTOR kinase structure, mechanism and regulation. Nature *497*, 217–223.

Yang, H., Jiang, X., Li, B., Yang, H.J., Miller, M., Yang, A., Dhar, A., and Pavletich, N.P. (2017). Mechanisms of mTORC1 activation by RHEB and inhibition by PRAS40. Nature *552*, 368–373.

Yang, J., Wang, S., Yang, Z., Hodgkinson, C.A., Iarikova, P., Ma, J.Z., Payne, T.J., Goldman, D., and Li, M.D. (2015). The contribution of rare and common variants in 30 genes to risk nicotine dependence. Mol. Psychiatry *20*, 1467–1478.

Yang, Q., Inoki, K., Ikenoue, T., and Guan, K.-L. (2006). Identification of Sin1 as an essential TORC2 component required for complex formation and kinase activity. Genes Dev. *20*, 2820–2832.

Yao, Y., and Mayer, M.L. (2006). Characterization of a soluble ligand binding domain of the NMDA receptor regulatory subunit NR3A. J. Neurosci. *26*, 4559–4566.

Yao, Y., Harrison, C.B., Freddolino, P.L., Schulten, K., and Mayer, M.L. (2008). Molecular mechanism of ligand recognition by NR3 subtype glutamate receptors. EMBO J. *27*, 2158–2170.

Yao, Y., Ju, P., Liu, H., Wu, X., Niu, Z., Zhu, Y., Zhang, C., and Fang, Y. (2020). Ifenprodil rapidly ameliorates depressive-like behaviors, activates mTOR signaling and modulates proinflammatory cytokines in the hippocampus of CUMS rats. Psychopharmacology (Berl). *237*, 1421–1433.

Yeung, K.S., Tso, W.W.Y., Ip, J.J.K., Mak, C.C.Y., Leung, G.K.C., Tsang, M.H.Y., Ying, D., Pei, S.L.C., Lee, S.L., Yang, W., et al. (2017). Identification of mutations in the PI3K-AKT-mTOR signalling pathway in patients with macrocephaly and developmental delay and/or autism. Mol. Autism *8*, 66.

Yu, Y., Lin, Y., Takasaki, Y., Wang, C., Kimura, H., Xing, J., Ishizuka, K., Toyama, M., Kushima, I., Mori, D., et al. (2018). Rare loss of function mutations in N-methyl-d-aspartate glutamate receptors and their contributions to schizophrenia susceptibility. Transl. Psychiatry *8*.

Yuan, T., Mameli, M., O'Connor, E.C., Dey, P., Verpelli, C., Sala, C., Perez-Otano, I., Lüscher, C., and Bellone, C. (2013). Expression of Cocaine-Evoked Synaptic Plasticity by GluN3A-Containing NMDA Receptors. Neuron *80*, 1025–1038.

Zhang, H., Webb, D.J., Asmussen, H., and Horwitz, A.F. (2003). Synapse formation is regulated by the signaling adaptor GIT1. J. Cell Biol. *161*, 131–142.

Zhang, H., Webb, D.J., Asmussen, H., Niu, S., and Horwitz, A.F. (2005). A GIT1/PIX/Rac/PAK signaling module regulates spine morphogenesis and synapse formation through MLC. J. Neurosci. *25*, 3379–3388.

Zhao, Z.S., Manser, E., Loo, T.H., and Lim, L. (2000). Coupling of PAK-interacting exchange factor PIX to GIT1 promotes focal complex disassembly. Mol. Cell. Biol. *20*, 6354–6363.

Zhou, J., and Parada, L.F. (2012). PTEN signaling in autism spectrum disorders. Curr. Opin. Neurobiol. *22*, 873–879.

Zhou, M., Li, W., Huang, S., Song, J., Kim, J.Y., Tian, X., Kang, E., Sano, Y., Liu, C., Balaji, J., et al. (2013). mTOR Inhibition ameliorates cognitive and affective deficits caused by Disc1 knockdown in adult-born dentate granule neurons. Neuron *77*, 647–654.

Zhu, M., Wang, J., Liu, M., Du, D., Xia, C., Shen, L., and Zhu, D. (2012). Upregulation of Protein Phosphatase 2A and NR3A-Pleiotropic Effect of Simvastatin on Ischemic Stroke Rats. PLoS One *7*, 1–11.

Zhu, P.J., Chen, C.J., Mays, J., Stoica, L., and Costa-Mattioli, M. (2018). MTORC2, but not mTORC1, is required for hippocampal mGluR-LTD and associated behaviors. Nat. Neurosci. *21*, 799–802.

Zinzalla, V., Stracka, D., Oppliger, W., and Hall, M.N. (2011). Activation of mTORC2 by association with the ribosome. Cell *144*, 757–768.

Zuo, Y., Lin, A., Chang, P., and Gan, W.B. (2005). Development of long-term dendritic spine stability in diverse regions of cerebral cortex. Neuron *46*, 181–189.

Appendix I: Scientific Publications

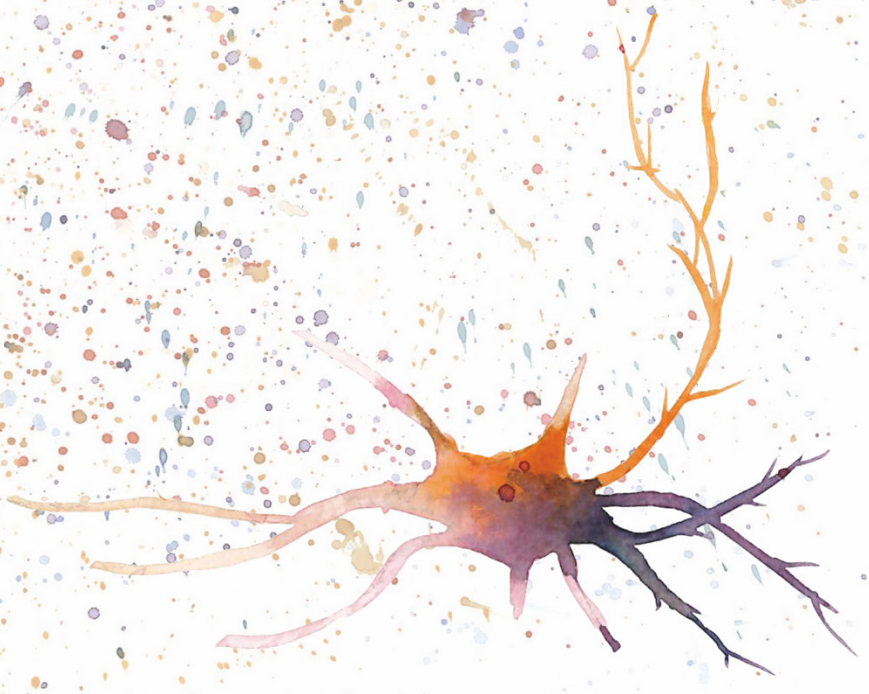

1. GLUN3A NMDA RECEPTOR SUBUNITS: MORE ENIGMATIC THAN EVER?

Crawley, O., Conde-Dusman, M. J.*, & Pérez-Otaño, I. (2021). GluN3A NMDA receptor subunits: more enigmatic than ever?. The Journal of Physiology, 10.1113/JP280879. Advance online publication. https://doi.org/10.1113/JP280879*

GluN3A NMDA receptor subunits: more enigmatic than ever?

Oliver Crawley*, María J. Conde-Dusman*, Isabel Pérez-Otaño

Unidad de Neurobiología Celular y de Sistemas, Instituto de Neurociencias (CSIC-UMH), San Juan de Alicante 03550, Spain.

Correspondence to: I. Pérez-Otaño (otano@umh.es)

* Oliver Crawley and María J. Conde-Dusman contributed equally to this study.

ABSTRACT

Non-conventional N-Methyl-D-Aspartate receptors (NMDARs) containing GluN3A subunits have unique biophysical, signaling and localization properties within the NMDAR family, and are typically thought to counterbalance functions of classical NMDARs made up of GluN1/2 subunits. Beyond their recognized roles in synapse refinement during postnatal development, recent evidence is building a wider perspective for GluN3A functions. Here we draw particular attention to the latest developments for this multifaceted and unusual subunit: from finely-timed expression patterns that correlate with plasticity windows in developing brains or functional hierarchies in the mature brain to new insight onto presynaptic GluN3A-NMDARs, excitatory glycine receptors and behavioural impacts, alongside further connections to a range of brain disorders.

 doi: 10.1113/JP280879.

INTRODUCTION

N-Methyl-D-Aspartate receptors (NMDARs) are a major class of ionotropic glutamate receptors that mediate a slow component of excitatory neurotransmission in the central nervous system (CNS), acting as critical mediators of experience-dependent synaptic plasticity, learning and memory (Paoletti et al., 2013). NMDARs are large tetrameric complexes composed of an obligatory GluN1 subunit and combinations of GluN2 (A-D) and GluN3 (A-B) subunits. Each subunit confers distinct properties to NMDARs, such as ion permeability, subcellular localization and trafficking patterns, or signalling interactions, and displays unique spatiotemporal expression profiles across the nervous system (Lau & Zukin, 2007; Paoletti et al., 2013; Hansen et al., 2018). Complexes composed of GluN1 and GluN2 subunits have been more extensively studied and are referred to as classical or conventional NMDARs whereas non-conventional NMDARs denote incorporation of GluN3 subunits.

One of the most enigmatic of the NMDAR subunits is GluN3A (encoded by the human gene *GRIN3A*, *Grin3a* in rodents); the more widely expressed of the 'non-conventional' GluN3 subfamily. Work to date has established GluN3A as an important regulator of neural circuit refinements by preventing the maturation of synapses until the arrival of sensory experience and later determining which synapses will be maintained or eliminated (Pérez-Otaño et al., 2016). In line with this role, in many brain regions GluN3A shows a characteristic peak of expression during narrow windows of postnatal development that precedes or overlaps with critical periods of experience-dependent plasticity. However, here we highlight how growing evidence is expanding this view and places GluN3A as a broader regulator of brain functions at later ages, in multiple areas and cell types.

This article briefly encompasses some of the established knowledge around GluN3A that has been previously discussed in several thorough reviews (Henson et al., 2010; Low & Wee, 2010; Pachernegg et al., 2012; Pérez-Otaño et al., 2016) but is primarily focused on more recent findings. In doing so, we hope to draw attention to the strides forward that are being made, especially in building a more complete picture of the spatiotemporal distribution of GluN3A throughout the CNS within the context of brain-wide functional implications, and the underappreciated roles of this subunit in excitatory glycine receptors and at presynaptic locations as well as the ever-expanding links between brain disorders and GluN3A.

GLUN3A EXPRESSION PATTERNS IN THE CNS

Temporal and regional patterns: GluN3A expression begins at low levels in the embryonic CNS and rises after birth, peaking at the end of the first postnatal week in rodents (early

years in humans) (Henson et al., 2010; Jantzie et al., 2015; Pérez-Otaño et al., 2016; Wee et al., 2016) (Fig. 1A). During this zenith high GluN3A levels are found in many brain regions including the cortex, hippocampus CA1, thalamus, amygdala, hypothalamus, olfactory nuclei and others (Wong et al., 2002; Henson et al., 2010; Pachernegg et al., 2012; Pérez-Otaño et al., 2016), demonstrating the broad roles of this non-canonical subunit. Expression drops during the second and third postnatal weeks in rodents (childhood and adolescence in humans) (Fig. 1A). Yet the time-courses of GluN3A emergence and down-regulation vary across brain regions, correlating with differences in the timing of circuit maturation, sensory modality, and degrees of functional specialization (Murillo et al., 2021). For instance, a detailed time series across postnatal days revealed that in primary somatosensory cortex GluN3A expression is initially constrained to layer 5 and later extends to layers 2-4 (Murillo et al., 2021) (Fig. 1B). This layer profile sequence evokes the inside-outside patterning model of cortical maturation and was found to be conserved in motor, visual and auditory cortices. However, both GluN3A expression and down-regulation are delayed in primary visual cortex, which matures later following eye-opening (around P12-P14 in rodents) (Murillo et al., 2021); and visual deprivation further delays the developmental loss of GluN3A, demonstrating a remarkable coupling of GluN3A expression with sensory experience (Larsen et al., 2014) (Fig. 1A). Studies where the calcium-regulated transcription factor CaRF promotes GluN3A expression (Lyons et al., 2016) further supported a link between neuronal activity and GluN3A levels and offered mechanistic insight into how regional and temporal patterns might be produced.

This distinctive profile of postnatal expression coinciding with windows of experience-driven synaptic plasticity and refinements is a unique hallmark of GluN3A among glutamate receptor subunits. However, GluN3A levels are retained into adulthood to some extent ((Wong et al., 2002); Allen Brain Atlas) and a recent paper systematically mapped regions where *Grin3a* mRNA expression persists in the adult mouse brain (Murillo et al., 2021), most notably in nuclei of the amygdala, medial habenula (MHb), association cortices and high-order thalamic nuclei. The work elegantly complements a different study which identified *Grin3a* as one of the genes most strongly correlated with hierarchy gradients of functional integration across the neocortex –from primary sensorimotor to higher-order association areas—established using the MRI T1w:T2w ratio (Fig. 1C). Low T1w:T2w ratios and high GluN3A expression were found to be typical of less differentiated association and transmodal cortical areas with strong needs for plasticity and functional integration throughout life such as the claustrum, rhinal, insular or prefrontal cortex (Fulcher et al., 2019; Murillo et al., 2021). By contrast, low adult *Grin3a* expression was observed in primary sensorimotor unimodal cortices with highly consolidated circuitry and lower plasticity requirements. Correlations between functional hierarchy and *Grin3a* expression also apply to organization of the primate and human brain (Burt et al., 2018; Fulcher et al., 2019).

Cell-type specificity: Expression of GluN3A has been documented in excitatory neurons and also within inhibitory GABAergic or cholinergic interneurons (Pérez-Otaño et al., 2016). Using RNAscope hybridization techniques, the Murillo et al. study dissected the proportion of GluN3A-expressing cells belonging to particular neuron types and demonstrated particularly strong *Grin3a* expression in somatostatin (SST) interneurons of the neocortex (Fig. 1D) and hippocampus. This is in-line with single-cell transcriptomic analyses of mouse somatosensory and visual cortex interneurons (Pfeffer et al., 2013; Paul et al., 2017) (Fig. 1E) that identified *Grin3a* as a secondary molecular marker for SST interneurons, most prominently Martinotti cells. Further work found the *Grin3a* locus in SST interneurons to be a site of prominently open chromatin and low DNA methylation (Yao et al., 2020), two marks of actively transcribed genes that promote/maintain cell identity. Of note, SST cell densities, like *Grin3a* expression, are negatively correlated with T1w:T2w ratios (Fulcher et al., 2019). SST interneurons innervate distal dendrites of pyramidal neurons and other interneurons to control the gating of dendritic inputs, consistent with integrative transmodal areas having a preference towards greater input control. Beyond neurons, morphological and RNAseq methods detected GluN3A/ *Grin3a* expression in oligodendrocytes (Káradóttir et al., 2005; Salter & Fern, 2005; Spitzer et al., 2019), microglia (Murugan et al., 2011) and brain endothelial cells (Mehra et al., 2020).

Subcellular localization: A defining characteristic of classical NMDARs is their concentration at postsynaptic densities (PSDs) of excitatory synapses. By contrast, high-resolution electron microscopy (EM) and biochemical fractionation studies have shown that GluN3A, while present at PSDs, predominates at perisynaptic and extrasynaptic locations (Fig. 2A-C). Within the PSD itself, GluN3A particle density increases towards the lateral edge differing from GluN1 that concentrates at the center (Fig. 2C). This localization has been attributed to decreased physical association with PSDs relative to classical GluN1/2 NMDARs due to the absence in GluN3A of PDZ-binding motifs for synaptic scaffolds (Pérez-Otaño et al., 2016), and could reflect a specialized function such as sensing specific patterns of glutamate release or activating signalling pathways in dendrites. Alternatively, it might reflect a higher mobility of GluN3A-NMDARs in and out of the plasma membrane via endo-exocytosis or lateral diffusion that might contribute to keep synapses in a labile state. The latter is supported by the observation that the density of GluN3A particles peaks at the PSD edge, indicating the presence of a rate-limiting step at this level which is in-line with models of the PSD acting as a ´diffusion trap´ (Fig. 2C). Of note, the postsynaptic enrichment of GluN3A is higher at early postnatal stages and declines into adulthood in contrast to the progressive synaptic stabilization of GluN1 or GluN2 subunits (Pérez-Otaño & Ehlers, 2004; Pérez-Otaño et al., 2006; Henson et al., 2012). These observations broadly correlate with proposed roles of GluN3A in postsynaptic signalling and refinement of dendritic spines (see below) (Das et al., 1998; Roberts et al., 2009; Fiuza et al., 2013; Kehoe et al., 2014).

On the other hand, immunogold EM studies have also observed GluN3A at presynaptic locations (Fig. 2B). Presynaptic GluN3A-NMDARs are rarer than their postsynaptic counterparts and exhibit remarkable synapse, temporal and circuit selectivity. To date, they have been identified in layer 4 to layer 2/3 synapses of the juvenile visual cortex (Larsen et al., 2011) and perforant path (PP) synapses in juvenile and adult hippocampus (Savtchouk et al., 2019). Interestingly, presynaptic GluN3A immunolabeling was almost exclusively found in medial perforant path (MPP) axon terminals but not in lateral perforant path (LPP) terminals, away from the synaptic cleft and often facing astrocytic membranes (Fig. 2B). At both synapses, presynaptic labeling decreased with age, but the decline was sharp at visual cortex (between P16-P23) while significant expression (~50%) persisted into adulthood at MPP axons. These topographical data are supported by electrophysiology experiments where presynaptic GluN3A function was isolated by blocking postsynaptic NMDAR activity (Larsen et al., 2011, 2014; Savtchouk et al., 2019).

NON-CONVENTIONAL GLUN3A-NMDARS AND EXCITATORY GLYCINE RECEPTORS

GluN3A can assemble with other NMDAR subunits to form two types of functional complexes: 1) GluN1/2/3A triheteromers that display non-conventional biophysical and signalling properties, and 2) GluN1/3A diheteromers that behave as excitatory glycine receptors (Fig. 3A).

GluN1/2/3A triheteromeric NMDARs (or "non-conventional" GluN3A-NMDARs): Composed of GluN1, GluN2 and GluN3A subunits, GluN3A-NMDARs receptors are activated by glutamate or NMDA and require glycine as co-agonist, as such they are considered bona fide NMDARs (Henson et al., 2010; Low & Wee, 2010; Pachernegg et al., 2012; Pérez-Otaño et al., 2016). Compared to classical GluN1/2 NMDARs, they exhibit atypical biophysical properties such smaller single-channel conductance (Perez-Otano et al., 2001); 10-fold lower Ca2+ permeability (Sasaki et al., 2002); and diminished sensitivity to Mg2+ block at hyperpolarized potentials (Sasaki et al., 2002; Roberts et al., 2009) (Fig. 3A, B). FRET-based assembly studies support a GluN1:GluN2:GluN3 stoichiometry of 2:1:1 (Schüler et al., 2008), but see (Ulbrich & Isacoff, 2008). The identity of the GluN2 subunit varies: using biochemical or electrophysiological approaches GluN3A has been shown to complex with GluN2A or 2B in neurons (Das et al., 1998; Al-Hallaq et al., 2002; Nilsson et al., 2007; Larsen et al., 2011; Martínez-Turrillas et al., 2012; Pilli & Kumar, 2012; Savtchouk et al., 2019) and with GluN2C in oligodendrocytes (Káradóttir et al., 2005; Burzomato et al., 2010).

Because of their non-conventional properties GluN3A subunits have been hypothesized to act as negative regulators of classical NMDAR activity (Pachernegg et al., 2012; Kehoe et al., 2013; Pérez-Otaño et al., 2016). In a traditional view, postsynaptically located NMDARs detect coincident pre- and postsynaptic activity and couple calcium entry to intracellular signalling pathways that trigger long-lasting synaptic structural and functional plasticity (Hardingham, 2019). By contrast, GluN3A-NMDARs inhibit synapse plasticity and stabilization and have been shown to delay synapse maturation until the arrival of sensory experience and later target non-used synapses for pruning (Roberts et al., 2009) as summarized in (Pérez-Otaño et al., 2016). This model is supported by: 1) restriction of GluN3A expression to immature synapses shown by EM; 2) the match of GluN3A expression and down-regulation with the timing of plasticity and refinements across different brain regions; 3) the control of synaptic GluN3A levels by activity and sensory experience. How this works at a mechanistic level is unknown and might involve impaired coincident detection due to the lesser Mg2+ block of GluN3A-NMDARs, inhibition of calcium-activated signalling cascades or coupling to distinct signalling adaptors (see below). Furthermore, a series of recent studies have brought to light other unconventional modes of NMDAR signalling that do not rely on ion flux or postsynaptic localization. As such, NMDARs can be dynamically regulated by synaptic activity even in the absence of Ca2+-dependent functions or via presynaptic localization (summarized in (Dore et al., 2017)).

Presynaptic GluN3A: Despite the canonical view of NMDARs as postsynaptic coincidence detectors, presynaptic NMDARs have been reported in many locations of the nervous system (Bouvier et al., 2015; Banerjee et al., 2016; Wong et al., 2021). The first reports of a presynaptic GluN3A function (Larsen et al., 2011, 2014) demonstrated a role of (likely GluN1/2B/3A) in promoting spontaneous glutamate release and mediating spike-timing-dependent long-term depression (tLTD) at young visual cortex synapses (L4 to L2/3). Loss of presynaptic GluN3A expression was associated to the developmental loss of tLTD, a form of plasticity thought to be involved in the refinement of visual maps (Larsen et al., 2011).

Presynaptic GluN3A-NMDARs have been more recently identified in juvenile mouse hippocampus (P17-22) at PP synapses onto dentate gyrus granule cells (GCs) (Savtchouk et al., 2019). As in visual cortex, presynaptic GluN3A-NMDARs contained GluN2B subunits and increased glutamate release probability in a circuit-specific manner due to their selective localization at MPP (but not LPP) axons. LTP is strongly influenced by presynaptic release probability and was enhanced in *Grin3a*-null mice, which could be explained by the lack of basal ‘prepotentiation’ dependent on pre-NMDARS at GluN3A-null MPP-GC synapses and consequently increased dynamic range for LTP induction. Blocking local astrocyte Ca2+ signalling in wild-type controls reproduced the enhanced LTP at MPP synapses found in *Grin3a* knockouts (Savtchouk et al., 2019), implying astrocyte modulation

in conferring differential release and plasticity properties to LPP-GC and MPP-GC synapses. As in visual L4 to L2/3 synapses, GluN3A expression decays with age but the significant levels retained into adulthood support a life-long role in setting different modes of information processing between LPP and MPP circuits. The presence of GluN3A, which confers low calcium permeability, has been suggested as an explanation for why many studies failed to detect presynaptic NMDAR-mediated calcium signals (Wong et al., 2021). It would also explain why presynaptic NMDARs can be activated tonically in the absence of axon firing or previous depolarization.

GluN1/3A diheteromeric NMDARs: Initial work in recombinant systems showed that GluN3A co-assembles with GluN1 in the absence of GluN2 subunits to form functional excitatory glycine receptors (Chatterton et al., 2002). These complexes are: 1) not activated by NMDA nor glutamate, 2) insensitive to APV, a competitive antagonist at the glutamate binding site in GluN2 subunits, as well as to open-channel NMDAR blockers such as Mg2+, memantine or MK-801, and 3) relatively Ca2+-impermeable (Chatterton et al., 2002; Madry et al., 2010) but see (Otsu et al., 2019) (Fig. 3A). Studies with selective antagonists and site-directed mutagenesis revealed that glycine binding to the GluN3A ligand binding domain (LBD) triggers channel opening and activation whereas binding to the GluN1 LBD causes rapid desensitization (Madry et al., 2007; Awobuluyi et al., 2007).

Demonstrating the existence of GluN1/3A receptors in vivo proved difficult due to the rapid desensitization that derives from the GluN1 glycine binding site, combined with ambient levels of free glycine in brain slice preparations. Intriguingly, native GluN1/3A receptors were first observed in oligodendrocytes (OLs) of mice optic nerves rather than neurons, and specifically within myelin sheaths but not somas of OLs (Piña-Crespo et al., 2010). The exact role of these receptors in myelin remains a mystery but is in line with GluN3A expression in the OL lineage (see GluN3A expression patterns in the CNS). Work on neuronal cultures later proposed a role in metaplasticity of excitatory hippocampal synapses by showing that, upon induction of chemical LTP, putative GluN1/3 receptors are recruited to enlarged synapses to facilitate depotentiation (Rozeboom et al., 2015).

Strong evidence has more recently emerged thanks to the use of CGP-78608, a competitive antagonist with pronounced preference for the glycine-binding site of GluN1 over GluN3A (Yao & Mayer, 2006; Grand et al., 2018). By preventing glycine binding to GluN1, CGP-78608 bypasses desensitization and unmasked large glycine-activated currents mediated by GluN1/3A receptors (Fig. 3C). Recordings of CA1 neurons in young (P8-P12) mouse hippocampal slices in the presence of CGP-78608 revealed a massive potentiation of glycine-induced inward currents in wild-type but not *Grin3a* knockout mice (Grand et al., 2018), clearly implicating GluN1/3A receptor function. Although expression of GluN3A is typically highest in young brains as discussed earlier, regions such as the MHb retain high

levels into adulthood. Building from their initial study, the same group demonstrated the presence of GluN1/3 receptors in this region in adult mice (Otsu et al., 2019). In wild-type (but not GluN3A knockout) MHb neurons, glycine puffs increased firing rates and induced rapidly rising inward currents. GluN3A immunolabeling was detected in dendrites and somata of MHb neurons, often in juxtaposition to glial profiles. Selective expression of DREADDs in glial cells pointed towards astrocytes as the physiological source of glycine (Otsu et al., 2019), resembling the ability of this cell type to modulate specific circuit functions via presynaptic GluN3A-NMDARs (Savtchouk et al., 2019). Aptly, behavioural tests found a specific requirement of MHb GluN1/3 receptors for the ability to acquire conditioned place-aversion, a readout that depends on this region.

Pharmacology: The lack of pharmacological reagents has hampered our understanding of the physiological roles of NMDA or glycine GluN3A-containing receptors, particularly triheteromeric GluN1/2/3 given the difficulty of expressing a pure population in cell lines. Among the limited information available, GluN3A-NMDARs have been shown to be blocked by the general NMDAR antagonist APV ((Sasaki et al., 2002) and (Larsen et al., 2014) for pre-GluN3A-NMDARs), and are less sensitive to open-channel blockers such as memantine or MK-801 in-line with the lesser Mg2+ block (McClymont et al., 2012). More extensive compound screening using glycine-activated GluN1/3A receptors has led to the identification of GluN3A- and GluN3B- competitive (TK80) and non-competitive (TK13 and TK30) antagonists with modest (5-10 fold) preference for GluN1/3A or 3B vs GluN1/2 receptors (Kvist et al., 2013) and a remarkably selective negative allosteric modulator, EU1180-438 (Zhu et al., 2020) (Table 1). EU1180-438 produced robust inhibition of native GluN1/3A glycine-activated currents in hippocampal CA1 pyramidal neurons (Zhu et al., 2020). This work demonstrates that the structural differences between the glycine-binding sites of GluN1 and GluN3 can be exploited to develop GluN3A-selective ligands (Kvist et al., 2013). Information regarding these ligands´ effects on GluN1/2/3A triheteromeric receptors is lacking.

GLUN3A MODULATES PLASTICITY AND COGNITION

Structural plasticity allows stable rewiring of synaptic networks through the formation of new connections and the stabilization of specific contacts with pruning of others. Converging lines of evidence place GluN3A as a critical modulator of functional and structural plasticity. First, regulated GluN3A expression has been shown to control the timing of long-lasting forms of plasticity implicated in the opening and closure of critical periods of postnatal development. At CA3-CA1 hippocampal synapses, ablation of GluN3A accelerates the developmental onset of LTP while prolonging expression beyond the physiological window reduces the magnitude of LTP (Roberts et al., 2009). At L4-L2/3 visual cortex synapses,

developmental down-regulation of GluN3A correlates with reductions in tonic glutamate release and ability to induce presynaptic tLTD, both processes linked to the stabilization of sensory maps (Larsen et al., 2011; Feldman, 2012). Genetic deletion or overexpression of GluN3A was sufficient to accelerate or delay the plasticity loss. Crucially, sensory input was identified as a driving force for down-regulation of GluN3A and the associated shifts in functional properties of visual cortex synapses (Larsen et al., 2014). In both preparations, loss of GluN3A allows a switch to GluN1/2 NMDARs that changes plasticity properties: GluN1/2A (Henson et al., 2012); or GluN1/2B (Larsen et al., 2014). Further work will be required to establish whether this is a general mechanism that operates at other synapses to control different modes of developmental plasticity, as suggested by the conserved profile of GluN3A down-regulation in primary cortices.

Second, studies in vivo and with organotypic slices showed that GluN3A inhibits the long-lasting stabilization of excitatory synapses by plasticity-inducing stimuli and regulates the number of synapses and associated dendritic spines without modifying initial spine formation (Roberts et al., 2009; Kehoe et al., 2014). Inhibition of actin cytoskeleton remodeling by direct binding to the postsynaptic scaffold and actin regulator GIT1 has been implicated (Fiuza et al., 2013). Whether GluN3A also modulates NMDAR-dependent gene expression remains largely unexplored, but a recent study in cortical cultures suggests that GluN3A might interfere with MEF2C-mediated transcription (Chen et al., 2020).

Genetically modified mice have provided some initial insight onto how GluN3A expression impacts behavioural output. Young (3-4 week-old) *Grin3a* knockout mice exhibit increased pre-pulse inhibition (Brody et al., 2005), an indicator of sensorimotor gating related to schizophrenia but the phenotype fades later on. Enhanced object recognition and spatial learning have been reported in adult *Grin3a* knockouts (Mohamad et al., 2013), in-line with human studies that correlate enhanced cognitive performance with low GluN3A levels (Sadat-Shirazi et al., 2019). Whether this is a consequence of altered developmental plasticity or reflects adult roles of GluN3A in cognition is yet to be established, but will be of paramount importance for the development of GluN3A-based therapeutics (see below). The retention of adult GluN3A expression in areas implicated in higher cognitive processing with strong requirements for plasticity and input control supports the latter, as does the observation that elevating GluN3A levels in adult brain is sufficient to impair memory consolidation (Roberts et al., 2009). Also, genetic variations in *GRIN3A* influence prefrontal cortex activation during attention tasks and consolidation of episodic memories (Gallinat et al., 2007; Papenberg et al., 2014). Additional studies report altered odor discrimination (Lee et al., 2016) and social deficits (Lee et al., 2018) in constitutive *Grin3a* knockouts, consistent with high GluN3A levels in olfactory areas and defects in oxytocin signalling in the prefrontal cortex. CRISPR-generated *Grin3a* knockouts are short-sleepers and display lower

transitions from awake to sleep states, possibly reflecting GluN3A expression in brain centers mediating wakefulness (Sunagawa et al., 2016; Murillo et al., 2021). Finally, glycine-gated GluN1/3A receptors in the MHb have been implicated in the control of aversive behaviours (Otsu et al., 2019).

GLUN3A/*GRIN3A* DISEASE LINKS

Genetic and expression data are unveiling connections between brain diseases and GluN3A which implicate this subunit not only in neurodevelopmental processes, but also in disorders where adult reactivation of GluN3A expression reinstates juvenile modes of plasticity thought to underlie many of the synaptic and behavioural alterations (Table 2).

Schizophrenia – One of the most prominently GluN3A-associated disorders is schizophrenia, a psychiatric disease characterized by delusions, hallucinations and impaired cognition and where aberrant synapse pruning is a key neuropathological feature. Elevated *Grin3a* transcripts have been found in schizophrenic brains (Mueller & Meador-Woodruff, 2004) and prepulse inhibition (PPI) (Brody et al., 2005), a behavioural readout strongly related to schizophrenia, is altered in *Grin3a* knockout mice. Human genetic studies have reported altered prevalence of common and rare *GRIN3A* variants in schizophrenia patients (Table 2), as well as a linkage peak on chromosome 9 close to the *GRIN3A* locus in a schizophrenia family study (Greenwood et al., 2016), correlated to specific cognitive traits in patients. *GRIN3A* variants have also been associated with post-operative delirium (Kazmierski et al., 2014), a disorder sharing major features with schizophrenia.

Bipolar disorder – Early studies found reduced mRNA and protein levels for GluN3A in the frontal cortex of Bipolar Disorder (BD) patients (Mueller & Meador-Woodruff, 2004; Rao et al., 2010). Later genetic work identified a *GRIN3A* SNP as the top associated variant with severely (suicide attempters) versus milder affected patients (Table 2). A further connection was suggested by the finding that *Grin3a* was among the top three downregulated genes in neurons treated with widely prescribed BD drugs (Kidnapillai et al., 2020).

Neurodevelopmental disorders - Autism spectrum disorder (ASD) is thought to arise from incorrect configuration of circuits due to altered synapse refinement and resulting excitation/inhibition imbalances (Peça & Feng, 2012). Deficits in social behaviour tasks, a hallmark of ASD (Lee et al., 2018), have been observed in *Grin3a* knockout mice alongside decreases in oxytocin signalling in the prefrontal cortex, correlating with claims that oxytocin treatment improves symptoms in ASD patients (Gordon et al., 2013). Interestingly, a study that also looked at schizophrenia concurrently found some rare missense *GRIN3A* variants in ASD patients (Yu et al., 2018), disorders with overlap in symptoms and genetic risk factors. A recent meta-analysis combining RNA-seq and microarray data from multiple ASD

mouse models with human brain transcriptional datasets identified *Grin3a* as a hub gene within the 'Juvenile-Cortex' and 'Adult-Hippocampus' gene networks (Duan et al., 2020). Single cell transcriptomics in cortex samples from human patients with epilepsy, another primarily neurodevelopmental disorder, showed major upregulation of *GRIN3A* (Pfisterer et al., 2020). Upregulation was particularly evident in certain L5/6 excitatory neurons and two SST interneuron subtypes.

Addiction and hedonistic behaviour - Substance addictions are chronic and relapsing disorders that are extremely dangerous to personal and public health. Next-generation sequencing (NGS) or genome-wide association (GWA) approaches have placed GluN3A centre-stage in the etiology of nicotine and alcohol addiction (Chen et al., 2018). *GRIN3A* mRNA levels are increased in the hippocampus and orbitofrontal cortex of individuals with alcoholism (Jin et al., 2014). Risk of nicotine dependence has been linked with a number of rare non-synonymous variants in *GRIN3A*, as shown in a series of studies in European, African-American and Chinese Han populations (Table 2). Moreover, *GRIN3A* gene variants or changes in GluN3A expression have been associated with addiction to illicit drugs such as heroin and opioids (Table 2) (Roozafzoon et al., 2010; Liu et al., 2020). In mouse studies, a single cocaine injection drives the insertion of GluN3A-NMDARs at synapses in reward-related regions with subsequent recruitment of calcium-permeable AMPARs, a form of adaptive plasticity involved in relapse (Yuan et al., 2013). Chronic methamphetamine also enhances GluN3A expression, reducing cortical plasticity and impairing motor learning (Huang et al., 2017).

Behavioural addictions are disorders analogous to substance addiction, in which there is a behavioural core based on repeated performances. The analysis of mRNA levels of different NMDAR subunits in human blood lymphocytes surprisingly revealed a reduction in *GRIN3A* mRNA levels in computer game addicts (Sadat-Shirazi et al., 2018). Dysregulated *Grin3a* expression has also been observed during transgenerational transmission of hedonistic and addictive behaviours such as increased preference of palatable foods (Sarker et al., 2019).

Neurodegeneration – Reactivation of GluN3A expression in adult medium-spiny neurons of the striatum has been documented in human and mouse models of Huntington´s disease (HD) (Marco et al., 2013; Wesseling & Pérez-Otaño, 2015; Mahfooz et al., 2016). The disease mechanism involves sequestration by mutant huntingtin of the GluN3A-selective adaptor PACSIN1, leading to accumulation of GluN3A-NMDARs at the cell surface of striatal neurons and age-inappropriate synapse pruning (Marco et al., 2013). Suppressing aberrant GluN3A expression by genetic deletion or AAV-mediated RNAi in HD mouse models was able to prevent and even reverse disease phenotypes, including striatal dendritic spine loss and motor performance (Marco et al., 2013, 2018). Also, *GRIN3A*

genetic variants have been associated with increased risk of developing Alzheimer's disease (Table 2)

SUMMARY AND FUTURE DIRECTIONS

Research into GluN3A continues to reveal new and surprising functions for this unusual NMDAR subunit. The expanding knowledge of GluN3A expression is transforming our perception, and paves the way to a better understanding of its roles in neurodevelopment and adult functions. Of note, the remarkable correlation between GluN3A expression in the mature brain and functional hierarchy adds particular weight to argument for the importance of this subunit in the adult beyond its better recognized functions in controlling developmental plasticity. An open question is how such specific spatio-temporal patterns of GluN3A are achieved between areas, cell types and cellular compartments? Also, how do these patterns influence the wider assembly and function of circuits, and how is behavioural output impacted by local or collective expression across the brain?

The continued support for presynaptic GluN3A in long-term plasticity at very particular circuits and synapses (Savtchouk et al., 2019) raises questions on how exactly do presynaptic GluN3A-NMDARs mediate their function. Is it via ionotropic or metabotropic mechanisms? Is there preferential trafficking regulation to axons in certain cell types? Why do astrocytes appear to be important for the function of synapses containing GluN3A-NMDARs presynaptically, as well as postsynaptically in certain situations? (Otsu et al., 2019). The evidence for functional roles of excitatory glycine-gated GluN1/3A receptors in the CNS and impacts on behaviour are especially compelling (Grand et al., 2018; Otsu et al., 2019), but much is still to learn. Do these receptors co-exist with non-conventional GluN1/2/3A receptors in terms of temporal, regional or cell type patterns? What governs their preference at certain cell types or subcellular compartments? What synaptic and circuit properties do they provide to neurons? Are these the same in all locations where they exist?

The increasing breadth of studies documenting the effects of GluN3A on forms of plasticity and multiple readouts including sensory processing, social cognition, sleep and learning place GluN3A as an important regulator of various behaviours and add insight to some of the disease links for this gene. More extensive behavioural profiling in transgenic mice in which GluN3A is removed at specific developmental times should allow us to distinguish defects caused by altered development from GluN3A functions within the adult brain. Finally, the long and diverse list of diseases from psychiatric and addiction disorders to neurodevelopmental and neurodegeneration that continue to show links to GluN3A over recent years demonstrates the remarkable brain-wide impacts of this unusual NMDAR subunit. Future studies in disease models, as well as new tools, are required to elucidate how GluN3A influences the various diseases it is linked to, which could lead to direct

therapies for these disorders, as hinted at for HD (Marco et al., 2018). Such work may additionally provide avenues for improving symptoms in other conditions where affected brain regions and phenotypes overlap with the diverse roles for GluN3A.

BIBLIOGRAPHY

Al-Hallaq RA, Jarabek BR, Fu Z, Vicini S, Wolfe BB & Yasuda RP (2002). Association of NR3A with the N-methyl-D-aspartate receptor NR1 and NR2 subunits. Mol Pharmacol 62, 1119–1127.

Awobuluyi M, Yang J, Ye Y, Chatterton JE, Godzik A, Lipton SA & Zhang D (2007). Subunit-specific roles of glycine-binding domains in activation of NR1/NR3 N-methyl-D-aspartate receptors. Mol Pharmacol 71, 112–122.

Banerjee A, Larsen RS, Philpot BD & Paulsen O (2016). Roles of Presynaptic NMDA Receptors in Neurotransmission and Plasticity. Trends Neurosci 39, 26–39.

Bouvier G, Bidoret C, Casado M & Paoletti P (2015). Presynaptic NMDA receptors: Roles and rules. Neuroscience 311, 322–340.

Brody SA, Nakanishi N, Tu S, Lipton SA & Geyer MA (2005). A developmental influence of the N-methyl-D-aspartate receptor NR3A subunit on prepulse inhibition of startle. Biol Psychiatry 57, 1147–1152.

Burt JB, Demirtaş M, Eckner WJ, Navejar NM, Ji JL, Martin WJ, Bernacchia A, Anticevic A & Murray JD (2018). Hierarchy of transcriptomic specialization across human cortex captured by structural neuroimaging topography. Nat Neurosci 21, 1251–1259.

Burzomato V, Frugier G, Pérez-Otaño I, Kittler JT & Attwell D (2010). The receptor subunits generating NMDA receptor mediated currents in oligodendrocytes. J Physiol 588, 3403–3414.

Cacabelos R, Martínez R, Fernández-Novoa L, Carril JC, Lombardi V, Carrera I, Corzo L, Tellado I, Leszek J, McKay A & Takeda M (2012). Genomics of Dementia: APOE- and CYP2D6-Related Pharmacogenetics. Int J Alzheimers Dis 2012, 518901.

Chatterton JE, Awobuluyi M, Premkumar LS, Takahashi H, Talantova M, Shin Y, Cui J, Tu S, Sevarinok KA, Nakanishi N, Tong G, Lipton SA & Zhang D (2002). Excitatory glycine receptors containing the NR3 family of NMDA receptor subunits. 415, 793–798.

Chen J, Liu Q, Fan R, Han H, Yang Z, Cui W, Song G & Li MD (2019). Demonstration of critical role of GRIN3A in nicotine dependence through both genetic association and molecular functional studies. Addict Biol1–11.

Chen J, Ma Y, Fan R, Yang Z & Li MD (2018). Implication of Genes for the N-Methyl-d-Aspartate (NMDA) Receptor in Substance Addictions. Mol Neurobiol 55, 7567–7578.

Chen L-F, Lyons MR, Liu F, Green M V., Hedrick NG, Williams AB, Narayanan A, Yasuda R & West AE (2020). The NMDA receptor subunit GluN3A regulates synaptic activity-induced and myocyte enhancer factor 2C (MEF2C)-dependent transcription. J Biol Chemjbc.RA119.010266.

Costantine MM, Clark EAS, Lai Y, Rouse DJ, Spong CY, Mercer BM, Sorokin Y, Thorp JM, Ramin SM, Malone FD, Carpenter M, Miodovnik M, O'Sullivan MJ, Peaceman AM & Caritis SN (2012). Association of polymorphisms in

neuroprotection and oxidative stress genes and neurodevelopmental outcomes after preterm birth. Obstet Gynecol 120, 542–550.

Das S, Sasaki YF, Rothe T, Premkumar LS, Takasu M, Crandall JE, Dikkes P, Conner DA, Rayudu P V, Cheung W, Chen HS, Lipton SA & Nakanishi N (1998). Increased NMDA current and spine density in mice lacking the NMDA receptor subunit NR3A. Nature 393, 377–381.

Dore K, Stein IS, Brock JA, Castillo PE, Zito K & Sjöström PJ (2017). Unconventional NMDA receptor signaling. J Neurosci 37, 10800–10807.

Duan W, Wang K, Duan Y, Chu X, Ma R, Hu P & Xiong B (2020). Integrated Transcriptome Analyses Revealed Key Target Genes in Mouse Models of Autism. Autism Res 13, 352–368.

Feldman DE (2012). The spike-timing dependence of plasticity. Neuron 75, 556–571.

Fiuza M, González-González I & Pérez-Otaño I (2013). GluN3A expression restricts spine maturation via inhibition of GIT1/Rac1 signaling. Proc Natl Acad Sci U S A 110, 20807–20812.

Fulcher BD, Murray JD, Zerbi V & Wang XJ (2019). Multimodal gradients across mouse cortex. Proc Natl Acad Sci U S A; DOI: 10.1073/pnas.1814144116.

Gallinat J, Götz T, Kalus P, Bajbouj M, Sander T & Winterer G (2007). Genetic variations of the NR3A subunit of the NMDA receptor modulate prefrontal cerebral activity in humans. J Cogn Neurosci 19, 59–68.

Gaynor SC, Breen ME, Monson ET, de Klerk K, Parsons M, DeLuca AP, Scheetz TE, Zandi PP, Potash JB & Willour VL (2016). A targeted sequencing study of glutamatergic candidate genes in suicide attempters with bipolar disorder. Am J Med Genet Part B Neuropsychiatr Genet 171, 1080–1087.

Gordon I, Vander Wyk BC, Bennett RH, Cordeaux C, Lucas M V, Eilbott JA, Zagoory-Sharon O, Leckman JF, Feldman R & Pelphrey KA (2013). Oxytocin enhances brain function in children with autism. Proc Natl Acad Sci U S A 110, 20953–20958.

Grand T, Abi Gerges S, David M, Diana MA & Paoletti P (2018). Unmasking GluN1/GluN3A excitatory glycine NMDA receptors. Nat Commun; DOI: 10.1038/s41467-018-07236-4.

Greenwood TA et al. (2016). Genetic assessment of additional endophenotypes from the Consortium on the Genetics of Schizophrenia Family Study. Schizophr Res 170, 30–40.

Hansen KB, Yi F, Perszyk RE, Furukawa H, Wollmuth LP, Gibb AJ & Traynelis SF (2018). Structure, function, and allosteric modulation of NMDA receptors. J Gen Physiol 150, 1081–1105.

Hardingham GE (2019). NMDA receptor C-terminal signaling in development, plasticity, and disease [version 1; peer review: 2 approved]. F1000Research 8, 1547.

Henson MA, Larsen RS, Lawson SN, Pérez-Otaño I, Nakanishi N, Lipton SA & Philpot BD (2012). Genetic deletion of NR3A accelerates Glutamatergic synapse maturation. PLoS One; DOI: 10.1371/journal.pone.0042327.

Henson MA, Roberts AC, Pérez-Otaño I & Philpot BD (2010). Influence of the NR3A subunit on NMDA receptor functions. Prog Neurobiol 91, 23–37.

Huang X, Chen Y-Y, Shen Y, Cao X, Li A, Liu Q, Li Z, Zhang L-B, Dai W, Tan T, Arias-Carrion O, Xue Y-X, Su H & Yuan T-F (2017). Methamphetamine abuse impairs motor cortical plasticity and function. Mol Psychiatry 22, 1274–1281.

Jantzie LL, Talos DM, Jackson MC, Park HK, Graham DA, Lechpammer M, Folkerth RD, Volpe JJ & Jensen FE (2015). Developmental expression of N-methyl-d-aspartate (NMDA) receptor subunits in human white and gray matter: Potential mechanism of increased vulnerability in the immature brain. Cereb Cortex 25, 482–495.

Jin Z, Bhandage AK, Bazov I, Kononenko O, Bakalkin G, Korpi ER & Birnir B (2014). Selective increases of AMPA, NMDA, and kainate receptor subunit mRNAs in the hippocampus and orbitofrontal cortex but not in prefrontal cortex of human alcoholics. Front Cell Neurosci 8, 1–10.

Káradóttir R, Cavelier P, Bergersen LH & Attwell D (2005). NMDA receptors are expressed in oligodendrocytes and activated in ischaemia. Nature 438, 1162–1166.

Kazmierski J, Sieruta M, Banys A, Jaszewski R, Sobow T, Liberski P & Kloszewska I (2014). The assessment of the T102C polymorphism of the 5HT2a receptor gene, 3723G/A polymorphism of the NMDA receptor 3A subunit gene (GRIN3A) and 421C/A polymorphism of the NMDA receptor 2B subunit gene (GRIN2B) among cardiac surgery patients with and without d. Gen Hosp Psychiatry 36, 753–756.

Kehoe LA, Bellone C, De Roo M, Zandueta A, Dey PN, Perez-Otano I & Muller D (2014). GluN3A Promotes Dendritic Spine Pruning and Destabilization during Postnatal Development. J Neurosci 34, 9213–9221.

Kehoe LA, Bernardinelli Y & Muller D (2013). GluN3A: An NMDA receptor subunit with exquisite properties and functions. Neural Plast; DOI: 10.1155/2013/145387.

Kidnapillai S, Wade B, Bortolasci CC, Panizzutti B, Spolding B, Connor T, Crowley T, Jamain S, Gray L, Leboyer M, Berk M & Walder K (2020). Drugs used to treat bipolar disorder act via microRNAs to regulate expression of genes involved in neurite outgrowth. J Psychopharmacol 34, 370–379.

Kvist T, Greenwood JR, Hansen KB, Traynelis SF & Bräuner-Osborne H (2013). Structure-based discovery of antagonists for GluN3-containing N-methyl-d-aspartate receptors. Neuropharmacology 75, 324–336.

Larsen RS, Corlew RJ, Henson MA, Roberts AC, Mishina M, Watanabe M, Lipton SA, Nakanishi N, Pérez-Otaño I, Weinberg RJ & Philpot BD (2011). NR3A-containing NMDARs promote neurotransmitter release and spike timing-dependent plasticity. Nat Neurosci 14, 338–344.

Larsen RS, Smith IT, Miriyala J, Han JE, Corlew RJ, Smith SL & Philpot BD (2014). Synapse-Specific Control of Experience-Dependent Plasticity by Presynaptic NMDA Receptors. Neuron 83, 879–893.

Lau CG & Zukin RS (2007). NMDA receptor trafficking in synaptic plasticity and neuropsychiatric disorders. Nat Rev Neurosci 8, 413–426.

Lee JH, Wei L, Deveau TC, Gu X & Yu SP (2016). Expression of the NMDA receptor subunit GluN3A (NR3A) in the olfactory system and its regulatory role on olfaction in the adult mouse. Brain Struct Funct 221, 3259–3273.

Lee JH, Zhang JY, Wei ZZ & Yu SP (2018). Impaired social behaviors and minimized oxytocin signaling of the adult mice deficient in the N-methyl-D-aspartate receptor GluN3A subunit. Exp Neurol 305, 1–12.

Liu HP, Lin WY, Liu SH, Wang WF, Tsai CH, Wu BT, Wang CK & Tsai FJ (2009). Genetic variation in N-methyl-D-aspartate receptor subunit NR3A but not NR3B influences susceptibility to Alzheimer's disease. Dement Geriatr Cogn Disord 28, 521–527.

Liu SX, Gades MS, Harris AC, Tran P V. & Gewirtz JC (2020). Repeated morphine exposure activates synaptogenesis and other neuroplasticity-related gene networks in the prefrontal cortex of male and female rats. bioRxiv; DOI: https://doi.org/10.1101/2020.02.26.966416.

Low C-M & Wee KS-L (2010). New insights into the not-so-new NR3 subunits of N-methyl-D-aspartate receptor: localization, structure, and function. Mol Pharmacol 78, 1–11.

Lyons MR, Chen L-F, Deng J V., Finn C, Pfenning AR, Sabhlok A, Wilson KM & West AE (2016). The transcription factor calcium-response factor limits NMDA receptor-dependent transcription in the developing brain. J Neurochem 137, 164–176.

Ma JZ, Payne TJ & Li MD (2010). Significant association of glutamate receptor, ionotropic N-methyl-d-aspartate 3A (GRIN3A), with nicotine dependence in European- and African-American smokers. Hum Genet 127, 503–512.

Madry C, Betz H, Geiger JRP & Laube B (2010). Potentiation of glycine-gated NR1/NR3A NMDA receptors relieves Ca2+-dependent outward rectification. Front Mol Neurosci 3, 1–8.

Madry C, Mesic I, Bartholomäus I, Nicke A, Betz H & Laube B (2007). Principal role of NR3 subunits in NR1/NR3 excitatory glycine receptor function. Biochem Biophys Res Commun 354, 102–108.

Mahfooz K, Marco S, Martínez-Turrillas R, Raja MK, Pérez-Otaño I & Wesseling JF (2016). GluN3A promotes NMDA spiking by enhancing synaptic transmission in Huntington's disease models. Neurobiol Dis 93, 47–56.

Marco S, Giralt A, Petrovic MM, Pouladi M a, Martínez-Turrillas R, Martínez-Hernández J, Kaltenbach LS, Torres-Peraza J, Graham RK, Watanabe M, Luján R, Nakanishi N, Lipton S a, Lo DC, Hayden MR, Alberch J, Wesseling JF & Pérez-Otaño I (2013). Suppressing aberrant GluN3A expression rescues synaptic and behavioral impairments in Huntington's disease models. Nat Med; DOI: 10.1038/nm.3246.

Marco S, Murillo A & Pérez-Otaño I (2018). RNAi-Based GluN3A Silencing Prevents and Reverses Disease Phenotypes Induced by Mutant huntingtin. Mol Ther 26, 1965–1972.

Martínez-Turrillas R, Puerta E, Chowdhury D, Marco S, Watanabe M, Aguirre N & Pérez-Otaño I (2012). The NMDA receptor subunit GluN3A protects against 3-nitroproprionic-induced striatal lesions via inhibition of calpain activation. Neurobiol Dis 48, 290–298.

McClymont DW, Harris J & Mellor IR (2012). Open-channel blockade is less effective on GluN3B than GluN3A subunit-containing NMDA receptors. Eur J Pharmacol 686, 22–31.

Mehra A, Guérit S, Macrez R, Gosselet F, Sevin E, Lebas H, Maubert E, De Vries HE, Bardou I, Vivien D & Docagne F (2020). Nonionotropic Action of Endothelial NMDA Receptors on Blood-Brain Barrier Permeability via Rho/ROCK-Mediated Phosphorylation of Myosin. J Neurosci 40, 1778–1787.

Mohamad O, Song M, Wei L & Yu SP (2013). Regulatory roles of the NMDA receptor GluN3A subunit in locomotion, Pain perception and cognitive functions in adult mice. J Physiol 591, 149–168.

Mueller HT & Meador-Woodruff JH (2004). NR3A NMDA receptor subunit mRNA expression in schizophrenia, depression and bipolar disorder. Schizophr Res 71, 361–370.

Murillo A, Navarro AI, Puelles E, Zhang Y, Petros TJ & Pérez-Otaño I (2021). Temporal Dynamics and Neuronal Specificity of Grin3a Expression in the Mouse Forebrain. Cereb Cortex 31, 1914–1926.

Murugan M, Sivakumar V, Lu J, Ling E-A & Kaur C (2011). Expression of N-methyl D-aspartate receptor subunits in amoeboid microglia mediates production of nitric oxide via NF-κB signaling pathway and oligodendrocyte cell death in hypoxic postnatal rats. Glia 59, 521–539.

Nilsson A, Eriksson M, Muly EC, Akesson E, Samuelsson E-B, Bogdanovic N, Benedikz E & Sundström E (2007). Analysis of NR3A receptor subunits in human native NMDA receptors. Brain Res 1186, 102–112.

Otsu Y, Darcq E, Pietrajtis K, Mátyás F, Schwartz E, Bessaih T, Abi Gerges S, Rousseau C V., Grand T, Dieudonné S, Paoletti P, Acsády L, Agulhon C, Kieffer BL & Diana MA (2019). Control of aversion by glycine-gated GluN1/GluN3A NMDA receptors in the adult medial habenula. Science (80-) 366, 250–254.

Pachernegg S, Strutz-Seebohm N & Hollmann M (2012). GluN3 subunit-containing NMDA receptors: Not just one-trick ponies. Trends Neurosci 35, 240–249.

Paoletti P, Bellone C & Zhou Q (2013). NMDA receptor subunit diversity: impact on receptor properties, synaptic plasticity and disease. Nat Rev Neurosci 14, 383–400.

Papenberg G, Li SC, Nagel IE, Nietfeld W, Schjeide BM, Schröder J, Bertram L, Heekeren HR, Lindenberger U & Bäckman L (2014). Dopamine and glutamate receptor genes interactively influence episodic memory in old age. Neurobiol Aging 35, 1213.e3-1213.e8.

Paul A, Crow M, Raudales R, He M, Gillis J & Huang ZJ (2017). Transcriptional Architecture of Synaptic Communication Delineates GABAergic Neuron Identity. Cell 171, 522-539.e20.

Peça J & Feng G (2012). Cellular and synaptic network defects in autism. Curr Opin Neurobiol 22, 866–872.

Pérez-Otaño I & Ehlers MD (2004). Learning from NMDA receptor trafficking: Clues to the development and maturation of glutamatergic synapses. NeuroSignals 13, 175–189.

Pérez-Otaño I, Larsen RS & Wesseling JF (2016). Emerging roles of GluN3-containing NMDA receptors in the CNS. Nat Publ Gr; DOI: 10.1038/nrn.2016.92.

Pérez-Otaño I, Luján R, Tavalin SJ, Plomann M, Modregger J, Liu XB, Jones EG, Heinemann SF, Lo DC & Ehlers MD (2006). Endocytosis and synaptic removal of NR3A-containing NMDA receptors by PACSIN1/syndapin1. Nat Neurosci 9, 611–621.

Perez-Otano I, Schulteis CT, Contractor A, Lipton SA, Trimmer JS, Sucher NJ & Heinemann SF (2001). Assembly with the NR1 Subunit Is Required for Surface Expression of NR3A-Containing NMDA Receptors. J Neurosci 21, 1228–1237.

Pfeffer CK, Xue M, He M, Huang ZJ & Scanziani M (2013). Inhibition of inhibition in visual cortex: The logic of connections between molecularly distinct interneurons. Nat Neurosci 16, 1068–1076.

Pfisterer U, Petukhov V, Demharter S, Meichsner J, Thompson JJ, Batiuk MY, Asenjo-Martinez A, Vasistha NA, Thakur A, Mikkelsen J, Adorjan I, Pinborg LH, Pers TH, von Engelhardt J, Kharchenko P V & Khodosevich K (2020). Identification of epilepsy-associated neuronal subtypes and gene expression underlying epileptogenesis. Nat Commun 11, 5038.

Pilli J & Kumar SS (2012). Triheteromeric N-methyl-d-aspartate receptors differentiate synaptic inputs onto pyramidal neurons in somatosensory cortex: Involvement of the GluN3A subunit. Neuroscience 222, 75–88.

Piña-Crespo JC, Talantova M, Micu I, States B, Chen HSV, Tu S, Nakanishi N, Tong G, Zhang D, Heinemann SF, Zamponi GW, Stys PK & Lipton SA (2010). Excitatory glycine responses of CNS myelin mediated by NR1/NR3 “NMDA” receptor subunits. J Neurosci 30, 11501–11505.

Rao JS, Harry GJ, Rapoport SI & Kim HW (2010). Increased excitotoxicity and neuroinflammatory markers in postmortem frontal cortex from bipolar disorder patients. Mol Psychiatry 15, 384–392.

Roberts AC, Diez-Garcia J, Rodriguiz RM, Lopez IP, Lujan R, Martinez-Turrillas R, Pico E, Henson MA, Bernardo DR, Jarrett TM, Clendeninn DJ, Lopez-Mascaraque L, Feng G, Lo DC, Wesseling JF, Wetsel WC, Philpot BD & Perez-Otaño I (2009). Downregulation of NR3A-Containing NMDARs Is Required for Synapse Maturation and Memory Consolidation. Neuron 63, 342–356.

Roozafzoon R, Goodarzi A, Vousooghi N, Sedaghati M, Yaghmaei P & Zarrindast MR (2010). Expression of NMDA receptor subunits in human peripheral blood lymphocytes in opioid addiction. Eur J Pharmacol 638, 29–32.

Rozeboom AM, Queenan BN, Partridge JG, Farnham C, Wu J young, Vicini S & Pak DTS (2015). Evidence for glycinergic GluN1/GluN3 NMDA receptors in hippocampal metaplasticity. Neurobiol Learn Mem 125, 265–273.

Sadat-Shirazi MS, Ashabi G, Hessari MB, Khalifeh S, Neirizi NM, Matloub M, Safarzadeh M, Vousooghi N & Zarrindast MR (2019). NMDA receptors of blood lymphocytes anticipate cognitive performance variations in healthy volunteers. Physiol Behav 201, 53–58.

Sadat-Shirazi MS, Vousooghi N, Alizadeh B, Makki SM, Zarei SZ, Nazari S & Zarrindast MR (2018). Expression of NMDA receptor subunits in human blood lymphocytes: A peripheral biomarker in online computer game addiction. J Behav Addict 7, 260–268.

Salter MG & Fern R (2005). NMDA receptors are expressed in developing oligodendrocyte processes and mediate injury. Nature 438, 1167–1171.

Sarker G, Sun W, Rosenkranz D, Pelczar P, Opitz L, Efthymiou V, Wolfrum C & Peleg-Raibstein D (2019). Maternal overnutrition programs hedonic and metabolic phenotypes across generations through sperm tsRNAs. Proc Natl Acad Sci U S A 116, 10547–10556.

Sasaki YF, Rothe T, Premkumar LS, Das S, Cui J, Talantova M V., Wong HK, Gong X, Chan SF, Zhang D, Nakanishi N, Sucher NJ & Lipton SA (2002). Characterization and comparison of the NR3A subunit of the NMDA receptor in recombinant systems and primary cortical neurons. J Neurophysiol 87, 2052–2063.

Savtchouk I, Di Castro MA, Ali R, Stubbe H, Luján R & Volterra A (2019). Circuit-specific control of the medial entorhinal inputs to the dentate gyrus by atypical presynaptic NMDARs activated by astrocytes. Proc Natl Acad Sci U S A 116, 13602–13610.

Schüler T, Mesic I, Madry C, Bartholomäus I & Laube B (2008). Formation of NR1/NR2 and NR1/NR3 heterodimers constitutes the initial step in N-methyl-D-aspartate receptor assembly. J Biol Chem 283, 37–46.

Shen YC, Liao DL, Chen JY, Wang YC, Lai IC, Liou YJ, Chen YJ, Luu SU & Chen CH (2009). Exomic sequencing of the glutamate receptor, ionotropic, N-methyl-d-aspartate 3A gene (GRIN3A) reveals no association with schizophrenia. Schizophr Res 114, 25–32.

Spitzer SO, Sitnikov S, Kamen Y, Evans KA, Kronenberg-Versteeg D, Dietmann S, de Faria OJ, Agathou S & Káradóttir RT (2019). Oligodendrocyte Progenitor Cells Become Regionally Diverse and Heterogeneous with Age. Neuron 101, 459-471.e5.

Sunagawa GA, Sumiyama K, Ukai-Tadenuma M, Perrin D, Fujishima H, Ukai H, Nishimura O, Shi S, Ohno R ichiro, Narumi R, Shimizu Y, Tone D, Ode KL, Kuraku S & Ueda HR (2016). Mammalian Reverse Genetics without Crossing Reveals Nr3a as a Short-Sleeper Gene. Cell Rep 14, 662–677.

Takata A et al. (2013). A population-specific uncommon variant in GRIN3A associated with schizophrenia. Biol Psychiatry 73, 532–539.

Tarabeux J et al. (2011). Rare mutations in N-methyl-D-aspartate glutamate receptors in autism spectrum disorders and schizophrenia. Transl Psychiatry; DOI: 10.1038/tp.2011.52.

Ulbrich MH & Isacoff EY (2008). Rules of engagement for NMDA receptor subunits. Proc Natl Acad Sci U S A 105, 14163–14168.

Wee KSL, Tan FCK, Cheong YP, Khanna S & Low CM (2016). Ontogenic profile and synaptic distribution of GluN3 proteins in the rat brain and hippocampal neurons. Neurochem Res 41, 290–297.

Wesseling JF & Pérez-Otaño I (2015). Modulation of GluN3A expression in huntington disease a new N-methyl-D-aspartate receptor-based therapeutic approach? JAMA Neurol 72, 468–473.

Wong HH-W, Rannio S, Jones V, Thomazeau A & Sjöström PJ (2021). NMDA receptors in axons: there's no coincidence. J Physiol 599, 367–387.

Wong HK, Liu XB, Matos MF, Chan SF, Pérez-Otaño I, Boysen M, Cui J, Nakanishi N, Trimmer JS, Jones EG, Lipton SA & Sucher NJ (2002). Temporal and regional expression of NMDA receptor subunit NR3A in the mammalian brain. J Comp Neurol 450, 303–317.

Xie X, Liu H, Zhang J, Chen W, Zhuang D, Duan S & Zhou W (2016). Association between genetic variations of NMDA receptor NR3 subfamily genes and heroin addiction in male Han Chinese. Neurosci Lett 631, 122–125.

Yang J, Wang S, Yang Z, Hodgkinson CA, Iarikova P, Ma JZ, Payne TJ, Goldman D & Li MD (2015). The contribution of rare and common variants in 30 genes to risk nicotine dependence. Mol Psychiatry 20, 1467–1478.

Yao Y & Mayer ML (2006). Characterization of a soluble ligand binding domain of the NMDA receptor regulatory subunit NR3A. J Neurosci 26, 4559–4566.

Yao Z et al. (2020). An integrated transcriptomic and epigenomic atlas of mouse primary motor cortex cell types. bioRxiv. Available at: https://doi.org/10.1101/2020.02.29.970558.

Yu Y et al. (2018). Rare loss of function mutations in N-methyl-d-aspartate glutamate receptors and their contributions to schizophrenia susceptibility. Transl Psychiatry; DOI: 10.1038/s41398-017-0061-y.

Yuan T, Mameli M, O'Connor EC, Dey P, Verpelli C, Sala C, Perez-Otano I, Lüscher C & Bellone C (2013). Expression of Cocaine-Evoked Synaptic Plasticity by GluN3A-Containing NMDA Receptors. Neuron 80, 1025–1038.

Zhu Z, Yi F, Epplin MP, Liu D, Summer SL, Mizu R, Shaulsky G, XiangWei W, Tang W, Burger PB, Menaldino DS, Myers SJ, Liotta DC, Hansen KB, Yuan H & Traynelis SF (2020). Negative allosteric modulation of GluN1/GluN3 NMDA receptors. Neuropharmacology 176, 108117.

ADDITIONAL INFORMATION

Competing interests: None declared.

Author contributions: All authors researched and wrote up their own specific sections, after which all authors edited the full document together. All authors have read and approved the final version of this manuscript and agree to be accountable for all aspects of the work in ensuring that questions related to the accuracy or integrity of any part of the work are appropriately investigated and resolved. All persons designated as authors qualify for authorship, and all those who qualify for authorship are listed.

Funding: Work in the authors´ laboratory is funded by grants from the Agencia Española de Investigación (SAF2016-80895-R, PID2019_111112RB_I00), Generalitat Valenciana (PROMETEO 2019/020) (to I.P.O.) and Severo-Ochoa Excellence Award (SEV-2017-0723). M.J.C.D. was funded by a predoctoral fellowship from the Fundación Tatiana Pérez de Guzmán el Bueno, FEBS and IBRO short-term fellowships, and O.C. by S-O and Marie Curie Postdoctoral fellowships.

Acknowledgements: The authors thank Alvaro Murillo and Ana Navarro for help with the figures.

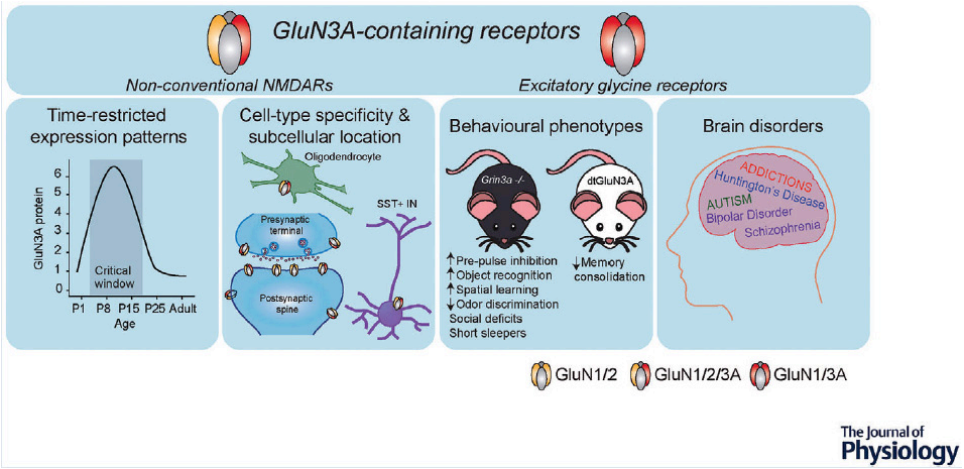

Abstract figure legend.

GluN3A (red) is known to exist in two types of receptor complexes: in non-conventional NMDARs alongside both GluN1 (grey) and GluN2 (yellow) subunits or in excitatory glycine receptors with only GluN1. Peak expression of GluN3A coincides with critical periods of postnatal development and persists through life in specific brain regions. GluN3A-containing receptors are expressed in various neuronal and non-neuronal populations, with localization observed at postsynaptic and presynaptic compartments. Genetic modulation of GluN3A expression in rodents causesmultiple behavioural phenotypes, and its dysregulation in humans is linked to a range of brain diseases.

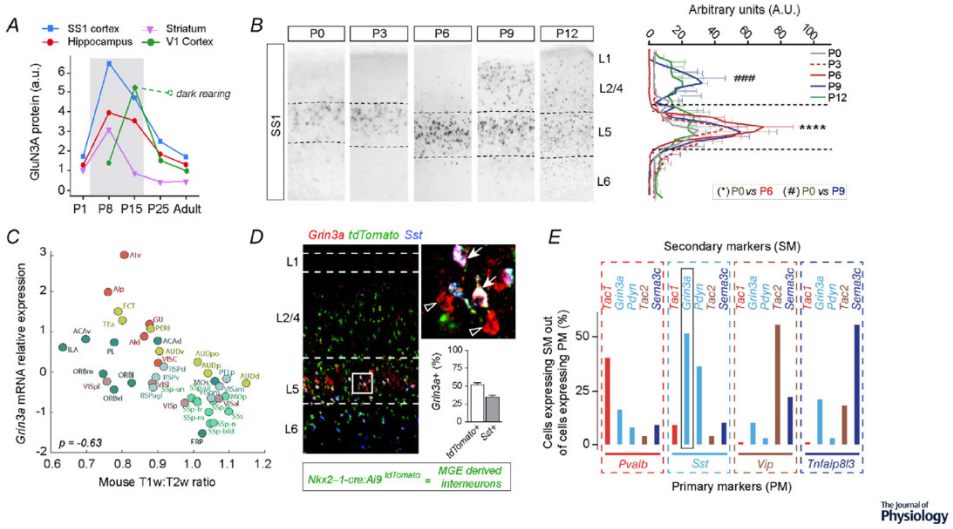

Figure 1. Temporal and regional GluN3A expression patterns in the rodent CNS

A) Regional postnatal expression profiles of GluN3A protein (shaded area = predominant expression window, adapted from (Pérez-Otaño et al., 2016)); visual deprivation (dashed green line) delays the developmental expression drop (Larsen et al., 2014). B) Time-course of Grin3a mRNA emergence and down-regulation varies across layers in primary somatosensory cortex (SS1). In situ hybridization images and quantification of Grin3a mRNA levels across layers at indicated postnatal ages are shown; dotted lines mark layer 5 (L5) boundaries. Data are mean ± S.E.M. ****P<0.0001; ### P<0.001. C) Correlation between mouse Grin3a transcription and MRI T1w:T2w ratio (for abbreviations see (Fulcher et al., 2019)). Colours represent connectivity-based area groupings; light green = somatomotor, turquoise = medial, yellow = temporal, pink = visual, red = anterolateral, dark green = prefrontal. D) RNAscope analysis of Grin3a mRNA localization in SS1 interneurons in a P6 Nkx2–1-cre:Ai9tdTomato mouse brain: Grin3a mRNA (red); tdTomato mRNA (green); somatostatin (Sst) mRNA (blue). Solid arrows = Grin3a+ MGE-derived SST interneurons. Empty arrowheads = Grin3a+ excitatoryneurons. E) Molecularly distinct interneuron categories defined by scRT-PCR (Pfeffer et al., 2013). Note high levels of Grin3a expression in SST interneurons.

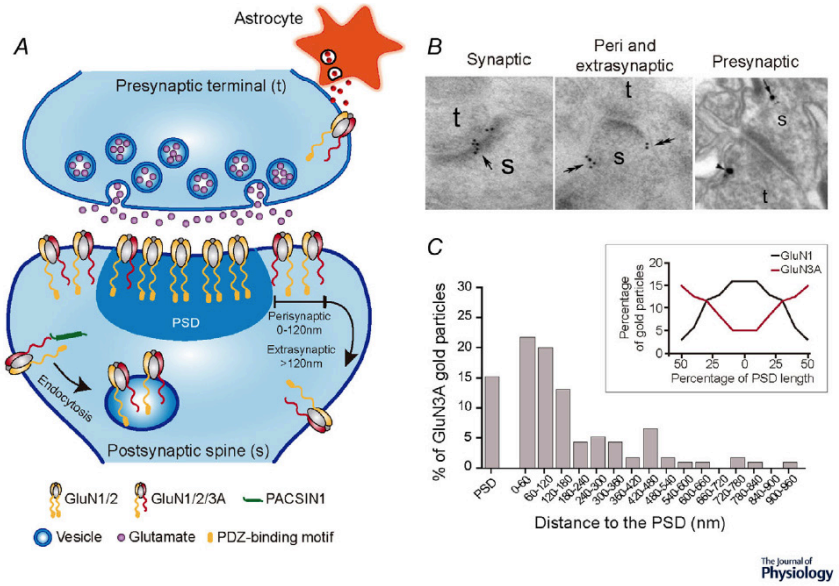

Figure 2. Subcellular distribution of GluN3A-NMDARs

A) Membrane distribution of GluN3A-containing (synaptic, peri- and extra-synaptic) and GluN3A-lacking NMDARs (mostly anchored to the PSDs via their C-terminal PDZ-binding motif). Diagram also illustrates the presence of GluN3A-NMDARs in presynaptic membranes next to astrocytes and the high rates of endocytosis driven by the adaptor PACSIN1 in mature neurons. (B) Post-embedding immunogold electron microscopy demonstrated that GluN3A is expressed at synaptic sites in CA3-CA1 hippocampus (arrows), but preferentially localizes at perisynaptic (100-120 nm from the edge of PSD) and extrasynaptic sites (>120 nm away from PSDs) (double arrows). Presynaptic GluN3A immunolabeling is also detected at MPP-GC synapses. (C) Quantification of GluN3A gold particle density as a function of distance to the PSD. Inset shows differential tangential distribution of GluN3A and GluN1 immunoparticles along the PSD of CA1 synapses. Note that labeling for GluN1 is highest at the center of the PSD while GluN3A increases towards the PSD periphery. Panels B&C are adapted from (Pérez-Otaño et al., 2006; Savtchouk et al., 2019).

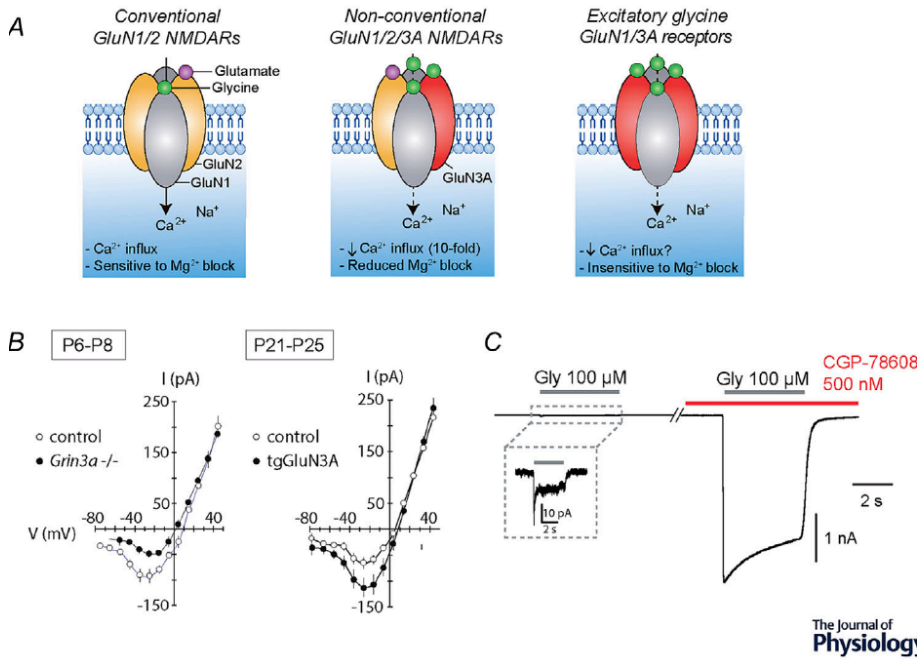

Figure 3. Unique properties of GluN3A-containing receptors

A) Cation permeabilities of different types of GluN3A-containing complexes; the calcium permeability of both GluN1/2/3A triheteromers and GluN1/3A diheteromers is lower than conventional GluN1/2 receptors but the exact value for relative permeability of GluN1/3A receptors remains less well established (see question mark). B) Mg2+ sensitivity is an electrophysiological signature of GluN1/2/3 NMDARs: at early developmental stages (P6-P8), genetic deletion of GluN3A increases NMDAR current rectification at CA1 hippocampal synapses due to loss of GluN3A-NMDARs, which exhibit reduced voltage-dependent Mg2+-block (left panel); at later stages when synaptic GluN3A is typically down-regulated, transgenically prolonging GluN3A expression (tgGluN3A) decreases NMDAR current rectification (right panel, adapted from (Roberts et al., 2009)). C) CGP-78608, an antagonist of the GluN1 glycine binding site, unmasks glycine currents mediated by GluN1/3A receptors (from (Grand et al., 2018)).

Table 1. GluN3-specific antagonists.

Inhibition measured in Xenopus oocytes expressing the indicated recombinant receptor. The compounds were co-applied with 100 μM glutamate and 0.5 μM glycine. Abbreviations: N.E, no significant effect. Maximal inhibition is 100%. IC50>300 μM indicates that the compound showed some inhibition but less than 50% at 300 μM.

Ligand	Functional property	GluN1/3A	GluN1/3B	GluN1/2A	Refs.
EU1180-438	Negative allosteric modulator	1.8μM	2.2μM	N.E.	(Zhu et al., 2020)
TK13	Non-competitive antagonist	67μM	49μM	>300μM	(Kvist et al., 2013)
TK30	Non-competitive antagonist	14μM	7.4μM	270μM	(Kvist et al., 2013)
TK80	GluN3B competitive antagonist	N.E	79μM	>300μM	(Kvist et al., 2013)

Table 2. Grin3a mutations associated with human diseases.

dbSNP is a NCBI public database for human single nucleotide polymorphisms. *non-sense mutation. Abbreviations: N-Terminal Domain (NTD); Ligand Binding Domain (LBD); C-Terminal Domain (CTD)

dbSNP ID	dbSNP allele	Amino acid change	Domain	Phenotype	Disease Related	Reference
-	G > A	Val132Leu	Extracellular (NTD)	Possibly damaging	Nicotine dependence	(Yang *et al.,* 2015)
rs556419599	C > T	Asp133Asn	Extracellular (NTD)	----	Schizophrenia (SCZ)	(Shen *et al.*, 2009)
rs769491656	G > A, C, T	Arg137Ser	Extracellular (NTD)	Disease causing	Autism Spectrum Disorder (ASD)	(Yu *et al.,* 2018)
rs773593066	G > A	Arg337Trp	Extracellular (NTD)	Possibly damaging	ASD, SCZ	(Yu *et al.,* 2018)
rs10989591	C > A, T	Val362Met	Extracellular (NTD)	Higher P300 amplitude Better associative and/ or recognition memory	Prefrontal Cortex activation	(Gallinat *et al.,* 2007; Papenberg *et al.,* 2014)
-	A > C	Val389Leu	Extracellular (NTD)	Possibly damaging	Nicotine dependence	(Yang *et al.,* 2015)
rs200120504	C > T	Val389Ile	Extracellular (NTD)	Disease causing	SCZ	(Yu *et al.,* 2018)
rs34755188	C > T	Arg480His	Extracellular (NTD)	Possibly damaging	Nicotine dependence	(Yang *et al.,* 2015)
rs149729514	G > A, C	Arg480Gly	Extracellular (NTD)	Probably damaging	SCZ	(Shen *et al.*, 2009; Takata *et al.,* 2013)
rs189425146	T > C	Lys488Glu	Extracellular (NTD)	Disease causing	ASD, SCZ	(Yu *et al.,* 2018)
-	C > T	Gln508*	Extracellular (NTD)	Patient with catatonic SCZ, inherited from mother in SCZ spectrum	SCZ	(Tarabeux *et al.*, 2011)

rs75981117	T > C	Asn549Ser	Extracellular - glycosylation site (LBD S1)	Possibly damaging	Nicotine dependence, Bipolar suicide attempting	(Yang *et al.,* 2015; Gaynor *et al.,* 2016)
rs10989563	C > T	Asp835Asn	Extracellular (LBD S2)	Susceptibility for Alzheimer's Disease (AD) pathogenesis	AD	(Liu *et al.*, 2009)
-	C > A	Gly898Trp	Extracellular (LBD S2)	Possibly damaging	ASD	(Yu *et al.,* 2018)
-	C > T	Arg1024*	Intracellular (CTD)	Possibly damaging	SCZ	(Shen *et al.*, 2009)
rs3739722	C > T	Arg1041Gln	Intracellular (CTD)	AD susceptibility, increased risk of cerebral palsy and postoperative delirium	AD, Dementia, Cerebral palsy, Non-substance-abuse delirium	(Liu *et al.*, 2009; Cacabelos *et al.,* 2012; Constantine *et al.,* 2012; Kazmierski *et al.,* 2014)
-	G > C	Gln1091His	Intracellular (CTD)	Possibly damaging	SCZ	(Shen *et al.*, 2009)
rs10121600	C > T	-	Intronic	Possibly damaging	Nicotine dependence	(Ma *et al.*, 2010)
rs11788456	G > A	-	Intronic	Possibly damaging	Nicotine dependence	(Ma *et al.*, 2010; Yang *et al.,* 2015)(Ma et al., 2010; Yang et al., 2015)
rs1323423	T > A, C, G	-	Intronic	Surrounding DNA region harbors an enhancer element	Nicotine dependence	(Chen *et al.*, 2019)
rs17189632	T > A, G	-	Intronic	Possibly damaging	Nicotine dependence, heroin addiction	(Ma *et al.*, 2010; Yang *et al.,* 2015; Xie *et al.,* 2016)(Ma et al., 2010; Xie et al., 2016; Yang et al., 2015)
rs2067056	T > C	-	5' UTR	Upstream transcript variant	Nicotine dependence	(Chen *et al.*, 2019)
rs2485530	C > G, T	-	Intronic	Possibly damaging	Bipolar suicide attempting	(Gaynor *et al.,* 2016)

rs45537432	C > G, T	-	Intronic	Possibly damaging	Bipolar suicide attempting	(Gaynor *et al.*, 2016)
rs7030238	A > C	-	3' UTR	Possibly damaging	Nicotine dependence	(Ma *et al.*, 2010)

2. CONTROL OF PROTEIN SYNTHESIS AND MEMORY BY GLUN3A-NMDA RECEPTORS THROUGH INHIBITION OF GIT1/MTORC1 ASSEMBLY

Conde-Dusman, M. J., Dey, P. N., Elía-Zudaire, Ó., G. Rabaneda, L., García-Lira, C., Grand, T., Briz, V., Velasco, E. R., Andero Galí, R., Niñerola, S., Barco, A., Paoletti, P., Wesseling, J. F., Gardoni, F., Tavalin, S. J., & Perez-Otaño, I. (2021). Control of protein synthesis and memory by GluN3A-NMDA receptors through inhibition of GIT1/mTORC1 assembly. eLife 2021;10:e71575. DOI: https://doi.org/10.7554/eLife.71575 (Accepted for publication on October 13th 2021)

Control of protein synthesis and memory by GluN3A-NMDA receptors through inhibition of GIT1/mTORC1 assembly

María J Conde-Dusman[1,2,3†], Partha N Dey[3,4†], Óscar Elía-Zudaire[1†], Luis G Rabaneda[1,3,5], Carmen García-Lira[1], Teddy Grand[6], Victor Briz[7], Eric R Velasco[8,9,10], Raül Andero Galí[8,9,10], Sergio Niñerola[1], Angel Barco[1], Pierre Paoletti[6], John F Wesseling[1], Fabrizio Gardoni[11], Steven J Tavalin[12] and Isabel Pérez-Otaño[1,3*†]

[1]Instituto de Neurociencias (UMH-CSIC), Alicante, Spain; [2]Centre for Developmental Neurobiology, Institute of Psychiatry, King's College London, London, United Kingdom; [3]Centro de Investigación Médica Aplicada (CIMA), University of Navarra, Pamplona, Spain; [4]National Eye Institute, National Institutes of Health, Bethesda, United States; [5]Institute of Science and Technology Austria, Klosterneuburg, Austria; [6]Institut de Biologie de l'Ecole Normale Supérieure/CNRS/INSERM, Paris, France; [7]Centro de Biología Molecular Severo Ochoa (UAM-CSIC), Madrid, Spain; [8]Institut de Neurociències, Departament de Psicobiologia i de Metodologia de les Ciències de la Salut, Unitat de Neurociència Traslacional, Parc Taulí Hospital Universitari, Institut d'Investigació i Innovació Parc Taulí (I3PT), Universitat Autònoma de Barcelona, Bellaterra, Spain; [9]Centro de Investigación Biomédica en Red de Salud Mental (CIBERSAM), Instituto de Salud Carlos III, Madrid, Spain; [10]ICREA, Barcelona, Spain; [11]Department of Pharmacological and Biomolecular Sciences, University of Milan, Milan, Italy; [12]Department of Pharmacology, Addiction Science, and Toxicology, University of Tennessee Health Science Center, Memphis, United States

***For correspondence**: otano@umh.es

† These authors contributed equally to this work.

Competing interest: The authors declare that no competing interests exists.

Funding: See page 25 **Received:** 23 June 2021

Preprinted: 05 September 2021 **Accepted:** 13 October 2021

Reviewing Editor: Mary B Kennedy, California Institute of Technology, United States

ABSTRACT

De novo protein synthesis is required for synapse modifications underlying stable memory encoding. Yet neurons are highly compartmentalized cells and how protein synthesis can be regulated at the synapse level is unknown. Here, we characterize neuronal signaling complexes formed by the postsynaptic scaffold GIT1, the mechanistic target of rapamycin (mTOR) kinase, and Raptor that couple synaptic stimuli to mTOR-dependent protein synthesis; and identify NMDA receptors containing GluN3A subunits as key negative regulators of GIT1 binding to mTOR. Disruption of GIT1/mTOR complexes by enhancing GluN3A expression or silencing GIT1 inhibits synaptic mTOR activation and restricts the mTOR-dependent translation of specific activity-regulated mRNAs. Conversely, GluN3A removal enables complex formation, potentiates mTOR-dependent protein synthesis, and facilitates the consolidation of associative and spatial memories in mice. The memory enhancement becomes evident with light or spaced training, can be achieved by selectively deleting GluN3A from excitatory neurons during adulthood, and does not compromise other aspects of cognition such as memory flexibility or extinction. Our findings provide mechanistic insight into synaptic translational control and reveal a potentially selective target for cognitive enhancement.

INTRODUCTION

Memories are thought to be encoded through formation and modification of the synaptic connections between neurons. Lasting memory encoding requires de novo mRNA and protein synthesis in response to neuronal activity and sensory experience. It entails the transcription of immediate-early genes (IEGs) to mRNA, and the protein products of some IEG transcripts mediate structural and functional modifications of synapses (Yap and Greenberg, 2018). However, transcription occurs in the cell body and generates a neuron-wide pool of mRNAs, whereas only a fraction of synapses of any individual neuron are modified by a given memory (Holtmaat and Caroni, 2016; Josselyn and Tonegawa, 2020). To ensure input specificity, transcription is coupled to local mechanisms that restrict the effects of activity-induced gene products to selected synapses (Wang et al., 2010).

One of these mechanisms is thought to be the local, synapse-specific translation of mRNA into protein (Holt et al., 2019; Klann and Dever, 2004; Sossin and Costa-Mattioli, 2019). The main rate-limiting step in translation is initiation, which is regulated by the phosphorylation of two separate proteins: the eukaryotic initiation factor 2α (eIF2α) and the mTOR (‘mechanistic target of rapamycin’) serine/threonine kinase. Manipulations of eIF2α phosphorylation have been implicated in synapse plasticity and memory (Costa-Mattioli et al., 2007; Sharma et al., 2020; Shrestha et al., 2020b), but evidence for a role in local translation is lacking. mTOR could in principle afford more selective translational control. mTOR forms at least two distinct multiprotein complexes, mTORC1 and mTORC2. mTORC1 is defined by the presence of Raptor, an adaptor protein which recruits mTOR substrates to promote the translation of specific mRNAs, and compartmentalized activation has been shown to be essential for mTORC1 responses to nutrients in nonneuronal cells (Liu and Sabatini, 2020). In neurons, components of mTORC1 localize to axons, dendrites, and synapses (Poulopoulos et al., 2019; Takei et al., 2004; Tang et al., 2002), and pharmacological inhibition of mTORC1 with Rapamycin blocks long-lasting synaptic plasticity and memory formation (Cammalleri et al., 2003; Hou and Klann, 2004; Stoica et al., 2011; Tang et al., 2002). Moreover, dysregulated translation is a feature in diseases of cognition, from autism to intellectual disability, and many of the mutations associated with these diseases affect genes encoding negative regulators of mTORC1 (Costa-Mattioli and Monteggia, 2013; Lipton and Sahin, 2014). However, it is currently unclear how mTOR activation might be controlled at specific synapses and linked to mechanisms that gate learning and memory.

The most intensively studied mechanism gating learning and memory involves the NMDA-type glutamate receptor (NMDAR). NMDARs contain multiple subunits, including an obligatory GluN1 subunit, various GluN2 (A–D) and, for some subtypes, one of the GluN3

(A–B) subunits (Paoletti et al., 2013). Conventional subtypes containing GluN1 and GluN2 trigger gene expression programs that mediate the strengthening and stabilization of active synapses and the persistent storage of information (Lyons and West, 2011). By contrast, nonconventional subtypes containing the GluN3A subunit (GluN3A-NMDARs) inhibit many of these synaptic modifications (Pérez-Otaño et al., 2016). Synapses that express GluN3A are resistant to the induction of long-lasting functional and structural plasticity, and memories fade more quickly in mutant mice with enhanced GluN3A expression (Kehoe et al., 2014; Roberts et al., 2009). In line with this work in mice, human genetic studies correlate enhanced cognitive performance with low GluN3A levels or variations in *GRIN3A* (human gene encoding GluN3A) (Gallinat et al., 2007; Papenberg et al., 2014; Sadat-Shirazi et al., 2019); and GluN3A dysregulation in humans is linked to cognitive impairment in schizophrenia (Greenwood et al., 2019; Mueller and Meador-Woodruff, 2004; Ohi et al., 2015; Takata et al., 2013), Huntington's disease (Marco et al., 2013; Marco et al., 2018), addiction, and other pathologies (Huang et al., 2017; Pérez-Otaño et al., 2016; Sarker et al., 2019; Yang et al., 2015; Yuan et al., 2013). We reasoned that understanding the underlying mechanisms would yield insight into the brain processes that constrain long-term memory formation and might uncover targets for therapeutic intervention.

Here, we report that GluN3A-NMDARs selectively and negatively regulate synaptic mTORC1-dependent translation without affecting neuron-wide transcriptional activation. The negative regulation is mediated by inhibition of the assembly of mTOR complexes that contain the postsynaptic adaptor GIT1 (G-protein-coupled receptor kinase-interacting protein) and Raptor. GIT1/mTORC1 complexes are located at or near synaptic sites, and couple mTORC1 kinase activity to synaptic stimulation. Through biochemical, mouse genetics, and behavioral approaches, we further show that GluN3A deletion increases the availability of GIT1/mTORC1 complexes, boosts mTORC1-dependent protein synthesis, and facilitates long-term memory formation. The advantage is selectively evident when mice are subjected to weak training behavioral paradigms; can be reversed by the mTORC1 inhibitor rapamycin; and unlike the memory enhancement seen after manipulations of general translational regulators, is not associated with deficits in memory flexibility or extinction (Shrestha et al., 2020a). Our findings identify a novel regulatory mechanism whereby GluN3A/GIT1 interactions set local modes of protein synthesis and gate memory formation, and reveal a potentially selective target for correcting cognitive impairment in pathological contexts.

RESULTS

Selective inhibition of activity-dependent gene expression by GluN3A at the post-transcriptional level

GluN3A expression is pervasive during postnatal brain development, and regulated removal allows for the activity-dependent stabilization or elimination of excess synapses (Pérez-Otaño et al., 2016). To assess whether GluN3A-NMDARs modulate activity-dependent gene expression, we expressed GluN3A in cultured cortical neurons over the stage when endogenous downregulation normally occurs (days in vitro [DIV] 9–14, ~ postnatal days P8–P16 in vivo, Figure 1A; Figure 1—figure supplement 1; Kehoe et al., 2014). We used lentiviral vectors where expression is targeted to neurons by the synapsin one promoter and induced synaptic activity with bicuculline, which inhibits ɣ-aminobutyric acid (GABA) transmission and triggers bursts of action potential firing (Hardingham et al., 2002).

As expected, bicuculline induced a robust expression of IEGs implicated in the consolidation of synaptic modifications and memories, including *Arc, Fos*, and *Zif268/Egr1* (Flavell and Greenberg, 2008; Figure 1B). Enhancing GluN3A expression largely reduced the induction of Arc and Fos proteins while Zif268 induction was unaffected, indicating that GluN3A selectively inhibits specific activity-dependent signaling pathways (Figure 1B). Analysis at the mRNA level demonstrated that modulation occurs downstream of gene transcription: *Arc, Fos*, and *Zif268* mRNA levels were strongly induced by bicuculline in both control and GluN3A-infected neurons, and no differences were observed in the time-courses or magnitude of induction (Figure 1C). Unchanged transcription was in line with intact activation of the phosphorylation of extracellular signal-regulated kinase (ERK1/2) and CREB (Figure 1—figure supplement 1B), the two major pathways for activity-dependent transcription (Flavell and Greenberg, 2008). By contrast, the general NMDAR antagonist D-2-amino-5-phosphonovaleric acid (APV) inhibited all signaling pathways analyzed and the induction of IEGs at both mRNA and protein levels (Figure 1—figure supplement 1C, D).

An analogous dissociation between protein and transcript levels of a subset of IEGs was observed when GluN3A-infected neurons were stimulated with the neurotrophin BDNF (Figure 1—figure supplement 1E, F), a potent inducer of gene expression at both transcriptional and translational levels (Rao et al., 2006). Whole transcriptome RNAseq analyses confirmed that transcriptional responses to bicuculline or BDNF were unaffected by GluN3A expression (Figure 1D; Figure 1—figure supplement 2). Together these results indicated that GluN3A-NMDARs repress the translation of specific activity-regulated mRNAs without affecting global transcriptional programs of gene expression. Inhibited induction of IEGs by GluN3A was not rescued by pretreatment with the proteasome inhibitor

MG-132 (Figure 1E), ruling out alternative mechanisms such as enhanced proteasome-dependent degradation (Rao et al., 2006).

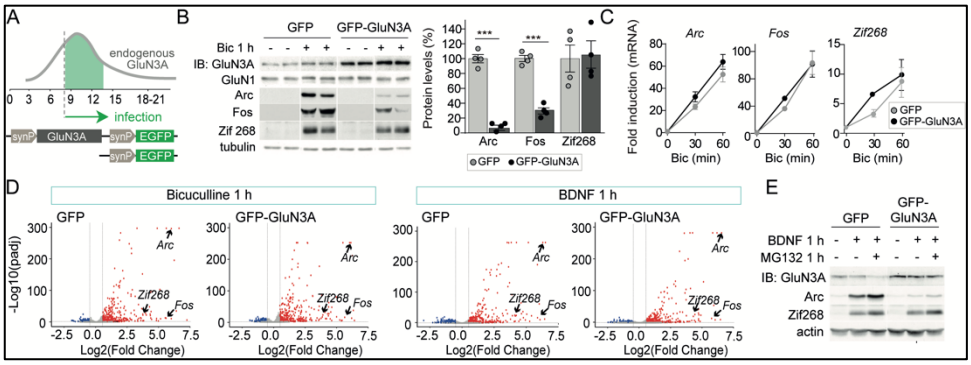

Figure 1. GluN3A inhibits the activity-dependent induction of a subset of immediate-early genes (IEGs). **(A)** Timeline of endogenous GluN3A expression and downregulation and of lentiviral infections. Rat cortical neurons in primary culture were infected on days in vitro (DIV) 9 with lentiviruses where GFP or GluN3A and GFP (GFP-GluN3A) expression is driven by the human synapsin one promoter (synP). **(B, C)** DIV14 neurons were treated with bicuculline (50 µM, 1 hr) and matching samples collected for immunoblot and mRNA analyses (n = 4 from two independent cultures; ***p < 0.001, two-tailed unpaired t-test). **(B)** Left, representative western blots show that GluN3A inhibits the induction of the IEGs Arc and Fos but not Zif268. Right, signal intensities of indicated proteins as percentage of stimulated GFP-infected neurons. **(C)** qRT-PCR analysis of IEG mRNA induction. Plotted values are fold-induction relative to non-stimulated neurons. **(D)** Volcano plots presenting the RNAseq-based differential expression analysis in DIV14 neurons treated with bicuculline or BDNF for 1 hr (n = 2–4 from two independent cultures). **(E)** DIV14 neurons were treated with MG132 (30 µM). A representative western blot probed with the indicated antibodies is shown. In immunoblot analyses, tubulin or actin was used as a loading control and GluN1 as a measure of potential effects of GluN3A on overall NMDAR numbers. Histograms in this and subsequent figures are mean ± standard error of the mean (SEM).

The online version of this article includes the following figure supplement(s) for figure 1:

Source data 1. Western blots for immediate-early gene (IEG) induction in GFP and GFP-GluN3A-infected neurons after bicuculline treatment.

Source data 2. Western blots for bicuculline induction of immediate-early genes (IEGs) in GFP and GFP-GluN3A-infected neurons in the presence of MG132.

Figure supplement 1. Selective versus global effects of GluN3A expression and general NMDAR blockade on activity-dependent signaling.

Figure supplement 1—source data 1. Annotated western blots and original scans.

Figure supplement 1—source data 2. Annotated western blots and original scans.

Figure supplement 1—source data 3. Annotated western blots and original scans.

Figure supplement 1—source data 4. Annotated western blots and original scans.

Figure supplement 2. RNAseq analysis of activity-dependent gene expression.

GluN3A inhibits mTORC1-dependent translation of IEGs

We thus turned to protein synthesis pathways to search for mechanisms underlying the selective inhibition of gene expression by GluN3A. We focused on mTORC1 because it has

been shown to couple synaptic signals including BDNF and NMDAR activation to translation of specific mRNAs in dendrites and synapses (Takei et al., 2004; Tang et al., 2002). mTORC1 signaling was strongly activated by bicuculline in DIV14 cortical neurons, as shown by phosphorylation of mTOR on Ser^{2448} (a reliable readout of mTORC1 kinase activity; see Chiang and Abraham, 2005) and of its downstream effectors, the p70-kDa ribosomal protein S6 kinase (S6K, Thr^{389}) and the ribosomal protein S6 (Ser$^{240–4}$, Figure 2A and B). The effects were blocked by APV and the NMDAR open-channel blocker MK-801, confirming NMDAR dependence in our model (Figure 2—figure supplement 1).

The phosphorylation of mTOR, S6K, and S6 following bicuculline treatment was significantly reduced in GluN3A-infected neurons, indicating that GluN3A interferes with synaptic mTORC1 activation (Figure 2B). Two experiments linked mTORC1 inhibition to the altered production of IEGs. First, low concentrations of rapamycin (100 nM) that inhibit mTORC1 but not mTORC2 (Zhu et al., 2018), blocked Arc and Fos translation in response to bicuculline without affecting Zif268, demonstrating selective mTORC1 dependence (Figure 2C). By contrast, the general protein synthesis inhibitor anisomycin fully suppressed Arc, Fos, and Zif268 induction (Figure 2—figure supplement 1B). Second, restoring mTORC1 signaling in GluN3A-infected neurons by expressing a constitutively active form of Rheb, the main upstream activator of mTORC1, was sufficient to normalize IEG induction (Figure 2D).

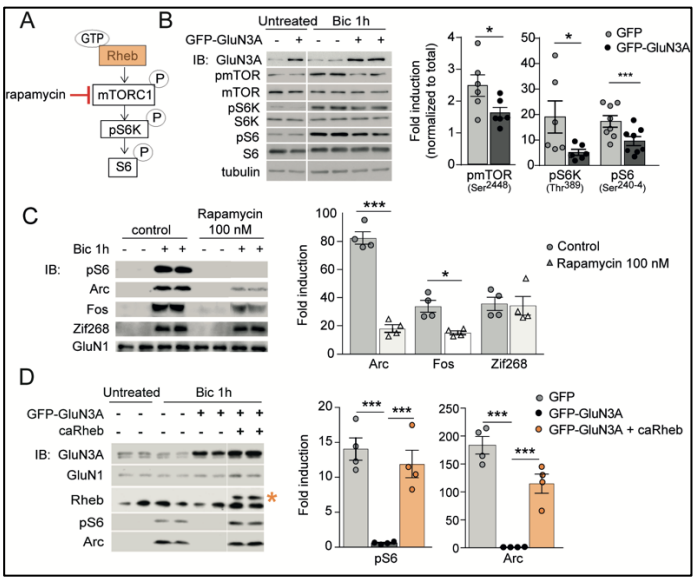

Figure 2. GluN3A expression regulates synaptic mTORC1 activation. **(A)** Schematic of the mTORC1 signaling pathway. **(B)** Left, representative western blots of primary rat cortical neurons infected with GFP and GFP-GluN3A (DIV9) and treated with bicuculline at DIV14. Right, fold-induction of phosphorylated mTOR, S6K and S6 normalized to total protein (n=6-8 from 3-4 independent cultures; *p<0.05, ***p<0.001, two-tailed paired t-test). **(C)** mTOR is required for activity-dependent induction of Arc and Fos but not Zif268. Left, representative western blots of DIV14

neurons stimulated with bicuculline after pre-incubation with rapamycin (100 nM, 1 h before and during bicuculline treatment). Right, fold-induction of IEGs in response to bicuculline (n=4 from 2 independent cultures; *p<0.05, ***p<0.001, two-tailed paired t-test). **(D)** Reactivation of mTOR in GFP-GluN3A infected neurons by AAV-driven constitutively active Rheb (caRheb) rescues Arc induction. Left, representative western blots of neurons infected with lentiviral GFP-GluN3A and AAV-caRheb and treated with bicuculline. Right, fold-induction by bicuculline of pS6 and Arc in the indicated conditions (n=4 from 2 independent cultures; ***p<0.001, one-way ANOVA followed by Tukey's test).

The online version of this article includes the following figure supplement(s) for figure 2:

Source data 1. Western blots for mTOR and downstream effector phosphorylation in GFP and GFP-GluN3A-infected cortical neurons after bicuculline treatment.

Source data 2. Western blots for rapamycin dependence of immediate-early genes (IEGs) induction in DIV14 cortical neurons by bicuculline treatment.

Source data 3. Western blots for caRheb rescue of p-S6 and Arc induction in DIV14 cortical neurons by bicuculline treatment.

Figure supplement 1. General inhibition of the activity induction of immediate-early genes (IEGs) by anisomycin.

Figure supplement 1—source data 1. Annotated western blots and original scans.

Figure supplement 1—source data 2. Annotated western blots and original scan.

Conversely, lentiviral knockdown of GluN3A in cortical neurons with a validated short hairpin RNA (Kehoe et al., 2014) enhanced mTORC1 activity (Figure 3A and B) and potentiated the induction of Arc and Fos by bicuculline or BDNF (Figure 3C and D). Increased phosphorylation of S6K and S6 was additionally detected in hippocampal lysates from mice lacking GluN3A (*Grin3a*−/−) relative to wild-type littermates (Figure 3E), confirming a role of GluN3A in limiting mTORC1 signaling in vivo.

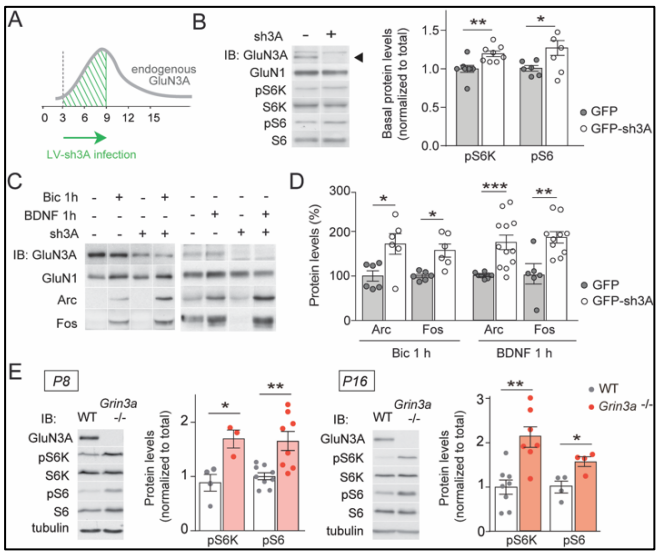

Figure 3. GluN3A deletion potentiates synaptic mTORC1 signaling. **(A)** Primary rat cortical neurons were infected on days in vitro (DIV) 3 with lentiviruses expressing GFP alone or along with a small hairpin RNA (shRNA) against GluN3A (GFP-sh3A) and collected at DIV7–9, when GluN3A expression is maximal. **(B)** Representative blots and

quantification of phosphorylated S6 kinase (S6K) and S6 normalized to total protein (n = 6–8 from three to four independent cultures; *p < 0.05, **p < 0.01 two-tailed paired t-test). Arrow marks specific GluN3A band. **(C, D)** Representative western blots and quantification of immediate-early gene (IEG) induction by bicuculline or BDNF (n = 6–12 from three independent cultures; *p < 0.05, **p < 0.01, ***p < 0.001, two-tailed paired t-test). Data plotted as percentage of stimulated control GFP-infected neurons. **(E)** Immunoblots and quantification of S6K and S6 phosphorylation in lysates from wild-type (WT) and *Grin3a*−/− hippocampi (n = 4–8 mice; *p < 0.05, **p < 0.01, two-tailed unpaired t-test).

The online version of this article includes the following figure supplement(s) for figure 3:

Source data 1. Western blots for S6 kinase (S6K) and S6 phosphorylation in control and sh3A-infected days in vitro (DIV) 7 cortical neurons.

Source data 2. Western blots for Arc and Fos induction by bicuculline and BDNF in control and sh3A-infected days in vitro (DIV) 7 cortical neurons.

Source data 3. Western blots for S6 kinase (S6K) and S6 phosphorylation in lysates from P8 and P16 wild-type and *Grin3a*−/− hippocampi.

mTORC1 inhibition requires GluN3A C-terminal domain interactions

GluN3A subunits confer unique biophysical properties to NMDARs, including reduced channel conductance and calcium permeability, and enable distinct interactions with signaling/scaffolding proteins via their intracellular C-terminal tail (Perez-Otano et al., 2016). To dissect their contribution to inhibited mTORC1 signaling, we derived primary cortical neurons from *Grin3a*-/- mice and re-expressed full-length GluN3A, a mutant where the distal 33 amino acids of the GluN3A C-terminus have been deleted and lacks synapse destabilizing activity (GluN3A1082Δ) (Fiuza et al., 2013; Kehoe et al., 2014), or GFP as a control (Figure 4A). While full-length GluN3A rescued the enhanced mTOR activation and hyper-induction of Arc and Fos proteins by bicuculline or BDNF in *Grin3a*-/- cultures, the GluN3A1082Δ mutant failed to do so (Figure 4B-E). Neither GluN3A nor GluN3A1082Δ modified the activation of other signaling pathways such as ERK1/2 phosphorylation or the induction of Zif268 in *Grin3a*-/- neurons (Figure 4D).

Since GluN3A and GluN3A1082Δ display similar distributions and cell surface targeting (Fiuza et al., 2013), the differences we observed are unlikely to stem from altered subcellular localization. We evaluated whether the deletion alters ion fluxes via GluN3A-NMDARs by analyzing electrophysiological responses to glutamate of GluN3A and GluN3A1082Δ when co-expressed with GluN1 and GluN2A in HEK293 cells. The relative calcium permeability was estimated by measuring the shift in reversal potential (ΔErev) of recombinant NMDAR currents induced by changing extracellular Ca^{2+} (Perez-Otano et al., 2001). GluN3A and GluN3A1082Δ yielded similarly reduced shifts in ΔErev relative to conventional GluN1/GluN2A NMDARs, confirming that the mutant incorporated into functional triheteromeric GluN3A-NMDARs and arguing against differences in Ca^{2+} permeability (Figure 4 - figure supplement 1A). In addition, both GluN3A versions drove comparable reductions in current densities relative to conventional NMDARs (Figure 4 -

figure supplement 1B). Along with non-conventional NMDARs, GluN3A subunits can form glycine-gated diheteromeric GluN1/GluN3 receptors (Perez-Otano et al., 2016). Thus we additionally examined whether the deletion modified responses to glycine of GluN1/GluN3 receptors taking advantage of the CGP-78608 compound (Grand et al., 2018), but no differences were found (Figure 4 - figure supplement 1C). The absence of ionotropic differences favored the hypothesis that inhibition of mTOR signaling requires metabotropic interactions of GluN3A-NMDARs, possibly modulating its association with synaptic adaptors or scaffolds.

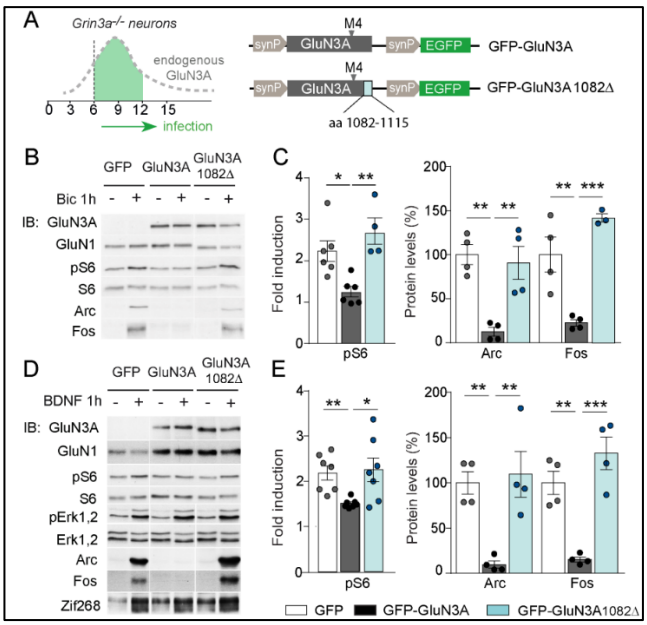

Figure 4. mTORC1 inhibition is mediated by GluN3A C-terminal domain interactions. **(A)** Cortical neurons from *Grin3a*−/− mice were infected on days in vitro (DIV) 6 with lentiviruses expressing GFP, GFP-GluN3A, or GFP-GluN3A1082Δ, and stimulated with bicuculline or BDNF at DIV12. **(B, D)** Representative western blots of lysates from bicuculline or BDNF-treated neurons probed for the indicated antibodies. **(C, E)** Induction of phosphorylated S6 (normalized to total levels), Arc and Fos by bicuculline or BDNF (n = 3–7 from two to four independent cultures, *p < 0.05, **p < 0.01, ***p < 0.001 analysis of variance [ANOVA] followed by Tukey's test).

The online version of this article includes the following figure supplement(s) for figure 4:

Source data 1. Western blots for mechanistic target of rapamycin (mTOR) effector phosphorylation and Arc and Fos induction in GFP, GFP-GluN3A, and GFP-GluN3A1082Δ-infected cortical neurons after bicuculline treatment.

Source data 2. Western blots for mechanistic target of rapamycin (mTOR) effector phosphorylation and Arc and Fos induction in GFP, GFP-GluN3A, and GFP-GluN3A1082Δ-infected cortical neurons after BDNF treatment.

Figure supplement 1. Electrophysiological properties of recombinant NMDA and excitatory glycine receptors containing full-length or truncated GluN3A.

GluN3A expression modulates the assembly of synaptic GIT1/mTORC1 complexes

A leading candidate is the multifunctional adaptor GIT1. GIT1 is enriched in postsynaptic compartments and binds the 33 amino acids of the GluN3A C-terminus that we show above are required for mTORC1 inhibition (Fiuza et al., 2013). Although best known for its role in actin signaling (Zhang et al., 2003), GIT1 has been detected in mTOR immunoprecipitates from mouse astrocytes by mass spectrometry (Smithson and Gutmann, 2016) though a function for this association could not be established. Using reciprocal immunoprecipitation with GIT1 and mTOR antibodies, we isolated GIT1/mTOR complexes from lysates of microdissected hippocampal (Figure 5A) and cortical (not shown) tissue. We chose detergent conditions that preserve mTOR interactions with Raptor and Rictor (0.3% CHAPS) to further characterize the composition of the complex, and were able to identify Raptor (but not the mTORC2 component Rictor) in GIT1 immunoprecipitates. The mTOR antibody pulled-down both, validating our assay conditions (Figure 5A). The GIT1-binding protein and Rac1 activator ßPIX was also pulled down by the mTOR antibody while the control presynaptic protein synaptophysin was not (Figure 5A). We additionally detected phosphorylated mTOR at Ser^{2448} in GIT1 immunoprecipitates, demonstrating GIT1/mTORC1 complex functionality (Figure 5B).

We then examined the subcellular localization of GIT1/mTORC1 complexes using in situ proximity-ligation assay (PLA) with antibodies against GIT1 and mTOR. PLA puncta were present along dendritic shafts often localized within or at the base of dendritic spines (Figure 5C), suggesting that GIT1 positions mTORC1 near synaptic sites to mediate dendritic translation in response to synaptic signals. To test this, we stimulated cortical neurons with bicuculline or BDNF and quantified mTOR phosphorylation in total lysates and GIT1 immunoprecipitates. Both bicuculline and BDNF induced large increases in the phosphorylation of GIT1-bound mTOR on Ser^{2448} (Figure 5D, E). Importantly, the phosphorylation of GIT1-bound mTOR was much higher than phosphorylation of the total cellular mTOR pool (BDNF: 1.98 ± 0.38-fold increase in total lysates vs 4.2 ± 1.15 in GIT1-immunoprecipates; bicuculline: 1.42 ± 0.15 vs 4.63 ± 1.24), consistent with a role for GIT1 in nucleating synaptic mTORC1 activation. Further evidence came from GIT1 loss-of-function experiments. Lentiviral knockdown of GIT1 blunted the activation of mTORC1 by BDNF, as shown by reduced phosphorylation of S6 and S6K (Figure 5F, G), and inhibited mTORC1-dependent protein synthesis assessed using a non-radioactive puromycin-labeling assay (SUnSET) (Figure 5H). Arc translation was also reduced, as judged by loss of rapamycin sensitivity relative to control neurons, while Zif268 which is mTORC1-independent was unaffected (Figure 5F, G). Collectively, these experiments demonstrated the existence of mTORC1 complexes composed of GIT1, mTOR and Raptor that mediate mTORC1 signaling in response to synaptic stimuli.

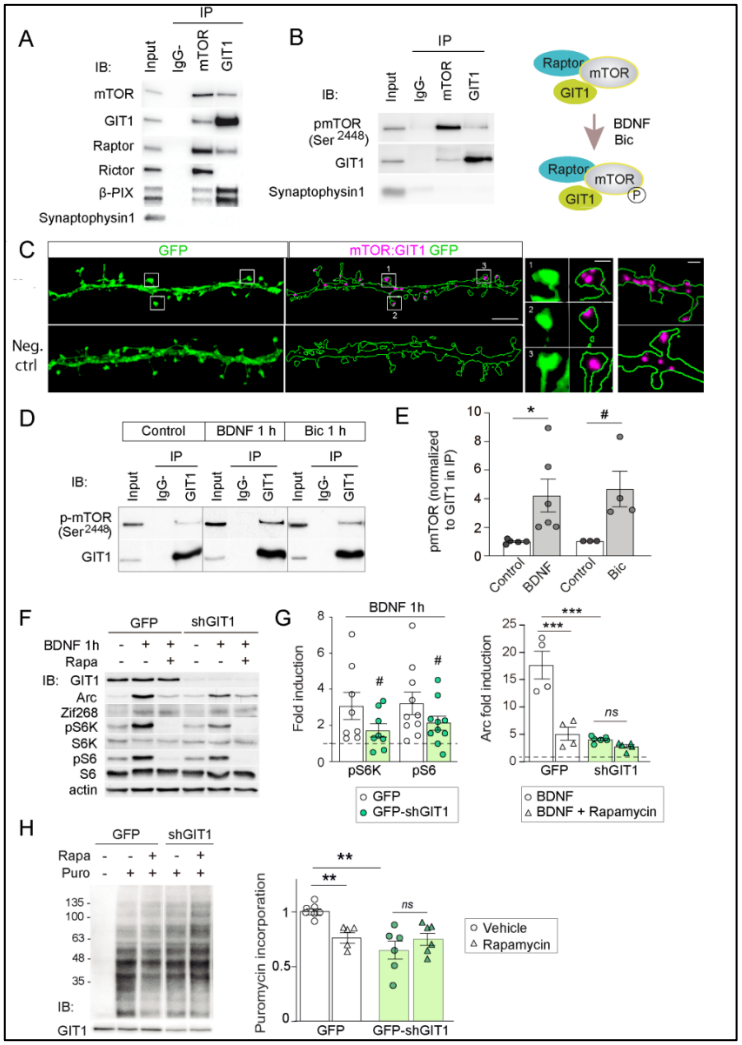

Figure 5. GIT1/mechanistic target of rapamycin (mTOR)/Raptor complexes couple synaptic activation to mTORC1-dependent protein synthesis. **(A, B)** Protein extracts from P16 mouse hippocampus were solubilized with 0.3 % CHAPS buffer, incubated with antibodies against mTOR or GIT1 (IP), and immunoprecipitated proteins analysed by immunoblot (IB). Input: 10 % of lysate used for immunoprecipitation. IgG−: no antibody control. A cartoon of the interactions and regulation by activity (see panel **D**) is shown. **(C)** Representative images of proximity ligation assay for rat mTOR: GIT1 (magenta) in days in vitro (DIV) 17 rat hippocampal neurons transfected with GFP (green) to visualize dendritic morphology (scale bar, 5 µm). High magnification examples of spines and dendrites (scale bars, 0.5 and 1 µm) are shown. As negative control, only mTOR primary antibody was used. **(D, E)** Rat cortical neurons stimulated with BDNF or bicuculline were solubilized with 0.3 % CHAPS and incubated with GIT1 antibody (IP). Representative immunoblots **(D)** and quantification of mTOR phosphorylation in GIT1 immunoprecipitates **(E)** are shown (n = 3–6 from three independent cultures; *p < 0.05, # = 0.06, two-tailed unpaired t-test). **(F–H)** Primary mouse cortical neurons were infected with lentiviruses expressing GFP or GFP-shGIT1 on DIV7. mTOR responses to BDNF **(F, G)** and puromycin incorporation **(H)** in the presence or absence of 100 nM rapamycin were analyzed at DIV14. Quantification of phosphorylated S6K and S6 and Arc induction (#pS6K: p = 0.13, #pS6: p = 0.05, two-tailed paired; ***p < 0.001, two-way analysis of variance [ANOVA] followed by Tukey's test) **(G)** and puromycin levels normalized

to Ponceau S (n = 5–7 from four independent cultures, **p < 0.01, two-way ANOVA followed by Tukey's test) **(H)** are shown.

The online version of this article includes the following figure supplement(s) for figure 5:

Source data 1. Coimmunoprecipitation assays of GIT1 with mechanistic target of rapamycin (mTOR), Raptor, and Rictor in P16 mouse hippocampus.

Source data 2. Coimmunoprecipitation of GIT1 with phosphorylated mechanistic target of rapamycin (mTOR) in Ser2448 in P16 mouse hippocampus.

Source data 3. Coimmunoprecipitaion of GIT1 and phosphorylated mechanistic target of rapamycin (mTOR) in days in vitro (DIV) 17 hippocampal neurons after bicuculline and BDNF treatment.

Source data 4. Western blots of mechanistic target of rapamycin (mTOR) effectors and immediate-early gene (IEG) induction by BDNF in the presence or absence of rapamycin in days in vitro (DIV) 14 cortical neurons infected with control or shGIT1-expressing lentiviruses.

Source data 5. Western blots of puromycin incorporation in days in vitro (DIV) 14 cortical neurons infected with control or shGIT1-expressing lentiviruses.

GluN3A/GIT1 interactions control the emergence of mTORC1-dependent protein synthesis

We further found that the abundance of GIT1/mTORC1 complexes is regulated throughout postnatal development. GIT1/mTORC1 complexes were readily observed in P16, but not P7 or P10, hippocampus or cortex of wild-type mice (Figure 6A; Figure 6 - figure supplement 1). Because this time-course matches well the timing of synaptic GluN3A down-regulation in vivo (Henson et al., 2012), we asked whether GluN3A expression influences GIT1/mTORC1 assembly. Biochemical analysis of GIT1 immunoprecipitates from hippocampi of P10 wild-type and *Grin3a*-/- showed that GluN3A removal enables the formation of GIT1/mTORC1 complexes at earlier stages, as judged by enhanced GIT1/mTOR and GIT1/Raptor binding (Figure 6B). Reciprocally, re-expression of full-length GluN3A (but not the GluN3A1082Δ mutant) in *Grin3a*-/- neurons was sufficient to prevent the GIT1/mTOR association, indicating that GluN3A-bound GIT1 cannot incorporate into the complex (Figure 6C). Taken together, the results support a model where GluN3A expression regulates the abundance of synaptic GIT1/mTORC1 complexes by directly binding GIT1, impeding its association with mTOR and limiting mTORC1 activation and downstream protein synthesis of plasticity factors. Conversely, developmental or genetic GluN3A down-regulation enables GIT1/mTORC1 formation and primes synapses for mTORC1-dependent translation (Figure 6D).

To test this model, we asked whether genetic manipulations of GluN3A/GIT1 interactions affect the timing and magnitude of mTORC1-dependent protein synthesis. A first set of experiments showed that protein synthesis in young cortical neurons (DIV7-9) is not dependent on mTORC1 activation, with strong rapamycin sensitivity emerging at later stages (DIV14) (Figure 6 - figure supplement 2). Knockdown of GluN3A resulted in a large

increase in protein synthesis in DIV7-9 neurons, which exhibited a rapamycin-dependence typical of mature neurons (Figure 6E). Robust rapamycin-dependent protein synthesis was also observed in *Grin3a*-/- neurons (Figure 6F). Re-expression of GluN3A, but not GluN3A1082Δ, reduced protein synthesis rates and was sufficient to block mTORC1-dependence, reinstating a juvenile mode of protein synthesis (Figure 6F). Thus GluN3A, via binding to GIT1, controls the age-dependent switch between mTORC1-independent and mTORC1-dependent protein synthesis.

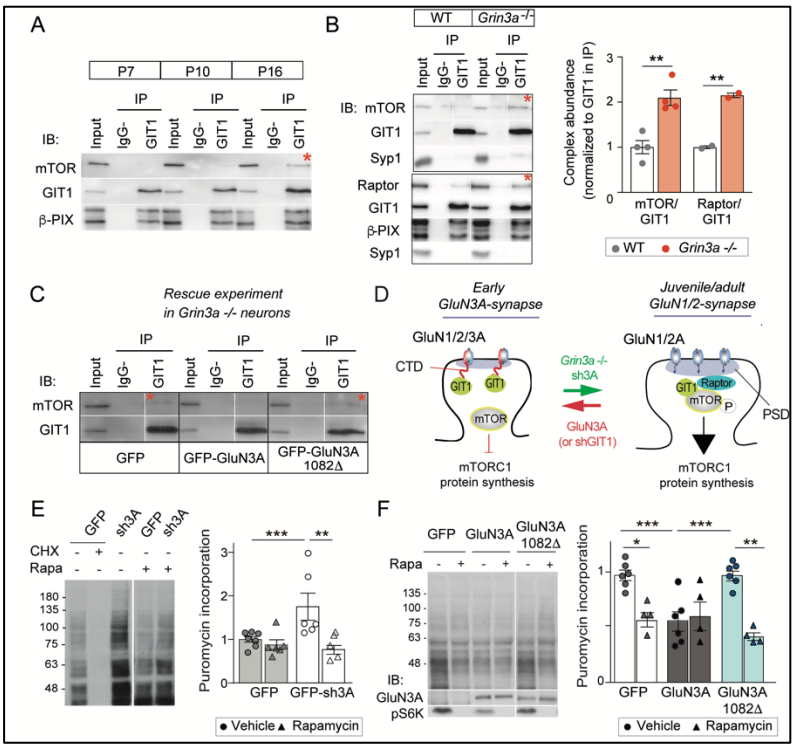

Figure 6. GluN3A/GIT1 interactions control the age-dependent onset of mTORC1-dependent protein synthesis. **(A)** Hippocampi from P7, P10, and P16 wild-type mice were lysed, immunoprecipitated with GIT1 antibody and probed for the indicated antibodies. Input: 10 % of the lysate used for immunoprecipitation. IgG−: negative control without antibody. Red asterisks here and other panels indicate mechanistic target of Rapamycin (mTOR)- and Raptor bound to GIT1. **(B)** GIT1/mTORC1 complex formation is enhanced in P10 Grin3a−/− hippocampus. Representative blots of GIT1 immunoprecipitates and quantifications are shown (n = 2–4 mice; **p < 0.01 unpaired t-test). Bound mTOR and Raptor are normalized to immunoprecipitated GIT1. Syp1: synaptophysin 1. **(C)** *Grin3a*−/− cortical neurons infected with GFP, GFP-GluN3A, or GFP-GluN3A1082Δ were solubilized and GIT1 immunoprecipitates blotted as indicated (IB). **(D)** GIT1/GluN3A control mTORC1 translation. Left: at early postnatal stages, immature synapses express GluN3A-NMDARs, which bind the postsynaptic scaffold GIT1 via their C-terminal tail preventing the nucleation of GIT1/mTORC1 and the mTORC1-mediated synthesis of plasticity proteins. Right: at juvenile/adult stages, GluN3A downregulation enables GIT1/mTOR/Raptor complex assembly and primes synapses for mTORC1 translation of mRNAs involved in synapse and memory consolidation. The genetic manipulations shown here to alter the timing of the age-dependent switch from mTORC1-independent to mTORC1-dependent modes of translation are indicated. Note that GluN3A expression is retained by subsets of synapses in adult brains and might play roles in selecting synapses that will be recruited to stably encode memory traces (see Discussion). **(E)** Mouse cortical neurons were

infected with lentiviruses expressing GFP or GFP-sh3A on days in vitro (DIV) 3 and protein synthesis analyzed at DIV7–9. Representative blots and quantification of puromycin incorporation in infected neurons treated with rapamycin (100 nM), cycloheximide (CHX, 25 μM), or vehicle. **(F)** *Grin3a*−/− cortical neurons were infected with GFP, GFP-GluN3A or GFP-GluN3A1082Δ lentiviruses, and protein synthesis analyzed at DIV12. GluN3A expression and mTOR activation were monitored with the indicated antibodies (IB). In panels D–E, n = 4–7 from three to four independent cultures (*p < 0.05, **p < 0.01, ***p < 0.001, two-way analysis of variance [ANOVA] followed by Tukey's test).

The online version of this article includes the following figure supplement(s) for figure 6:

Source data 1. Coimmunoprecipitation of GIT1 and mechanistic target of rapamycin (mTOR) in lysates from P7, P10, and P16 mouse hippocampus.

Source data 2. Coimmunoprecipitation of GIT1 with mechanistic target of rapamycin (mTOR) and Raptor in hippocampal lysates from P10 wild-type and *Grin3a*−/− mice.

Source data 3. Coimmunoprecipitation of GIT1 with mechanistic target of rapamycin (mTOR) in *Grin3a*−/− cortical neurons infected with GFP, GFP-GluN3A, and GFP-GluN3A1082Δ lentiviruses.

Source data 4. Western blots of puromycin incorporation in neurons infected with control or sh3A-expressing lentiviruses.

Source data 5. Western blots of puromycin incorporation in the presence or absence of rapamycin in *Grin3a*−/− cortical neurons infected with GFP, GFP-GluN3A, and GFP-GluN3A1082Δ.

Figure supplement 1. Postnatal regulation of GIT1/mTORC1 complexes in mouse somatosensory cortex.

Figure supplement 1—source data 1. Annotated western blots and original scans.

Figure supplement 2. Age-dependent emergence of mTORC1-dependent protein synthesis in cultured rat cortical neurons.

Figure supplement 2—source data 1. Annotated western blots and original scans.

Long-term memory formation is enhanced in *Grin3a*-deficient mice in a rapamycin-dependent manner

While GluN3A expression is typical of immature synapses at early postnatal stages as illustrated in our model, electron microscopy analyses demonstrate that subsets of synapses continue to express GluN3A into adulthood in areas such as the hippocampal CA1 (Roberts et al., 2009); and a recent mRNA expression study revealed that significant GluN3A levels are retained in a variety of brain regions (Murillo et al., 2021). Previous work showed that transgenic GluN3A overexpression impairs memory consolidation in hippocampal-dependent paradigms such as the Morris water maze (Roberts et al., 2009), but whether endogenous GluN3A expression has a physiological role in memory formation is unknown. We hypothesized that GluN3A modulation of synaptic mTORC1 signaling might provide a mechanism to set modes of translational control participating in memory encoding.

We reasoned that, if so, GluN3A deletion would create a permissive environment for stable memory formation and tested this by assessing mice learning in increasingly demanding tasks. Testing of *Grin3a*-/- mice in a standard version of the Morris water maze (4 trials per day) did not reveal differences in the latencies to reach the hidden platform relative to wild-type controls (Figure 7 - figure supplement 1). Wild-type and *Grin3a*-/- mice

displayed similar preferences for the target quadrant in probe trials where the platform was removed from the pool at the end of training, confirming that both had learnt the platform location (PT1; Figure 7 - figure supplement 1C). Differences emerged with a more demanding version of the task (2 trials per day): both male and female *Grin3a*-/- mice reached the platform significantly faster than wild-types, with shorter latencies by day 3 of training and greater preference for the target quadrant in probe trials (PT1; Figure 7A, B; Figure 7 - figure supplement 1B, D). No differences were observed in a visible version of the maze or in swim velocities, suggesting that motor or perceptual differences do not account for the phenotype (Figure 7 - figure supplement 1E, F).

Similarly reduced learning thresholds had been reported in mice with elevated activity of mTOR or other pathways controlling translation (Banko et al., 2007; Costa-Mattioli et al., 2007; Hoeffer et al., 2008; Stern et al., 2013), often at the expense of impaired ability to respond to changed environments, altered memory fidelity, or appearance of perseverant and repetitive behaviors (Banko et al., 2007; Hoeffer et al., 2008; Santini et al., 2013 ; Shrestha et al., 2020b; Trinh et al., 2012). Thus we evaluated cognitive flexibility by re-training the mice to learn a new platform location ("reversal"). *Grin3a*-/- mice were better at shifting their preference relative to wild-type controls as evident in probe trials conducted 7 days after reversal (PT2; Figure 7A, B, Figure 7 - figure supplement 1B, D). No perseverative behavior was observed either in a Y-maze spontaneous alternation task (Figure 7 - figure supplement 1G). These results showed that GluN3A deletion facilitates spatial learning and memory without the unwanted effects associated to other modulators of translation.

We then assessed associative memory formation using two tasks that depend on new protein synthesis and can be achieved with the single pairing of a conditioned (CS) and unconditioned stimulus (US): conditioned taste aversion (CTA) and contextual fear conditioning. In CTA, a novel taste (saccharin, CS) is associated with an aversive US (LiCl, which induces nausea). The LiCl dose (US) and temporal contiguity between CS-US can be regulated to evaluate standard memory (Figure 7C), or "enhanced" memory by using a weaker paradigm (Figure 7F) (Adaikkan and Rosenblum, 2015). Transgenic mice with prolonged GluN3A expression into adulthood (dt GluN3A) displayed deficits in a standard CTA paradigm (US, LiCl 0.15 M i.p.) as judged by their similar preference for saccharin 24 hours after saline or LiCl injections (Figure 7D, green bars). This result was in-line with the memory deficits reported in other behavioral paradigms (Roberts et al., 2009). Control experiments ruled out the possibility that the defect was due to insensitivity to LiCl or to defects in distinguishing flavors (Figure 7 - figure supplement 2). By contrast, *Grin3a*-/- mice did not show differences relative to wild-types in a standard paradigm of CTA memory (Figure 7E). We then used a weak CTA paradigm where the strength of the US was reduced

(LiCl 0.025 M), and US-CS were separated by 5 hours (Figure 7F). Under these conditions, only *Grin3a*-/- mice formed an association between CS-US, as shown by their significantly reduced preference for saccharin after LiCl injection but intact preference in wild-type controls. The negative association was long-lasting as it could be observed 24 (Figure 7G) and 48 hours after conditioning (data not shown). To determine whether it was mTOR-dependent, we treated mice with a subthreshold dosing regime of rapamycin (Stoica et al., 2011) that does not affect standard CTA memory (Figure 7 - figure supplement 2). Rapamycin erased the weak CTA memory in *Grin3a*-/- mice (Figure 7H), supporting the notion that disinhibited mTOR signaling causes the cognitive enhancement.

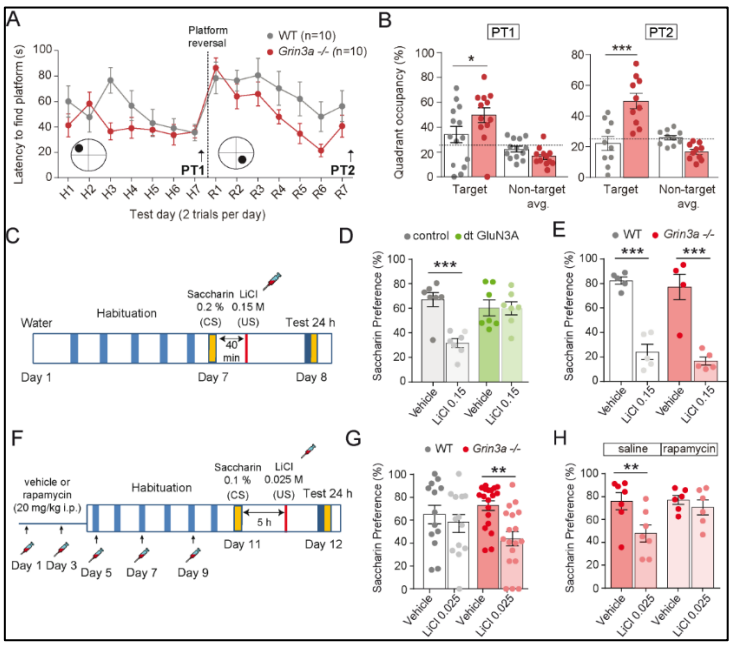

Figure 7. GluN3A deletion facilitates spatial and associative learning. **(A)** Escape latencies of male wild-type (WT) and *Grin3a*−/− mice on a weak version of the Morris water maze (two trials per day) during 7-day training and after platform reversal on day 8. **(B)** Probe trials performed 24 hr after day 7 (PT1), or 24 hr after reversal training (PT2) (n = 10–13 mice per genotype; two-way analysis of variance [ANOVA] with Bonferroni post hoc test, *p < 0.05, ***p < 0.0001). **(C)** Conditioned taste aversion (CTA) paradigm. **(D)** Saccharin preference of control and double transgenic (dt) GluN3A mice, and **(E)** WT and *Grin3a*−/− mice after vehicle or LiCl injection (n = 5–7 mice per group; ***p < 0.001, two-way ANOVA followed by Bonferroni post hoc test). **(F–H)** Weak CTA paradigm and rapamycin treatment regime. Decreased saccharin preference of *Grin3a*−/− mice on the weak CTA **(G)** was reversed by rapamycin (H) (**p < 0.01, two-way ANOVA followed by Bonferroni post hoc test).

The online version of this article includes the following figure supplement(s) for figure 7:

Figure supplement 1. Behavior of male and female *Grin3a*−/− mice in the Morris water maze.

Figure supplement 2. Controls for conditioned taste aversion (CTA) experiments.

In contextual fear conditioning, a particular environment (CS) is associated with a foot-shock (US) (Figure 8A). Wild-type and *Grin3a*-/- littermates showed similar freezing

responses before the delivery of the foot-shock (Figure 8B). However, freezing was significantly stronger in *Grin3a*-/- mice 24 and 48 hours after a weak training protocol (single pairing of a tone with a 0.3 mA foot-shock, Figure 8B, C), demonstrating enhanced and lasting memory formation. No differences were observed in short-term (1 hour) memory that is protein-synthesis independent (Figure 8B). As in CTA, rapamycin occluded the difference between wild-type and *Grin3a*-/- mice (Figure 8C). Taken together, our behavioral results demonstrate that GluN3A deletion lowers the threshold for stable memory storage and provide pharmacological evidence linking the enhanced learning to a relief of GluN3A constraints on mTORC1 signaling.

Yet the cognitive enhancement could have been due to lack of GluN3A during development rather than adult stages. Also, GluN3A is expressed by excitatory neurons and somatostatin interneurons, both recently implicated in protein-synthesis dependent memory consolidation (Sharma et al., 2020; Shrestha et al., 2020a). We therefore selectively ablated *Grin3a* from excitatory neurons or somatostatin-expressing interneurons by crossing floxed *Grin3a* mice (*Grin3a*$^{f/f}$) with mice that express Cre recombinase under the control of the Ca2+ calmodulin kinase IIα (Camk2a-Cre^{ERT2}) or somatostatin (Sst-Cre) promoter. The first strategy allowed conditional deletion of GluN3A at adult stages by injecting tamoxifen (Figure 8D). Biochemical analysis of adult hippocampal lysates confirmed effective deletion of GluN3A, and revealed that ~70% and ~20% of GluN3A protein is expressed by excitatory and somatostatin interneurons respectively (Figure 8 - figure supplement 1). We then subjected the mice to the weak fear conditioning protocol. Adult deletion of GluN3A from excitatory neurons was sufficient to enhance long-term memory, as shown by stronger freezing of *Grin3a*$^{f/f}$ x Camk2a-Cre^{ERT2} mice 24, 48 hours and even 7 days after training (Figure 8D). In contrast, *Grin3a*$^{f/f}$ x Sst-Cre and control mice exhibited similar freezing levels 24 and 48 hours after training (Figure 8E). Thus, adult GluN3A expression in excitatory neurons gates long-term memory formation.

Finally, we evaluated fear extinction, a form of memory where repeated presentation of a CS without reinforcement leads to the extinction of the acquired fear memory (Andero and Ressler, 2012). Fear extinction requires protein synthesis and is another indicator of behavioral flexibility that has been shown to be impaired after manipulation of general elements of translation. Mice were subjected to a strong auditory cued-fear conditioning protocol (5 pairings of a tone (CS) with a 0.3 mA foot-shock) followed by four cued-fear extinction sessions (15 CS alone, no foot-shock) (Figure 8F). Fear memory acquisition was similar between WT and *Grin3a*-/- littermates but fear extinction was enhanced in *Grin3a*-/- mice (Figure 8G), demonstrating that GluN3A deletion does not compromise the updating of memories but rather facilitates the extinction of fear memories.

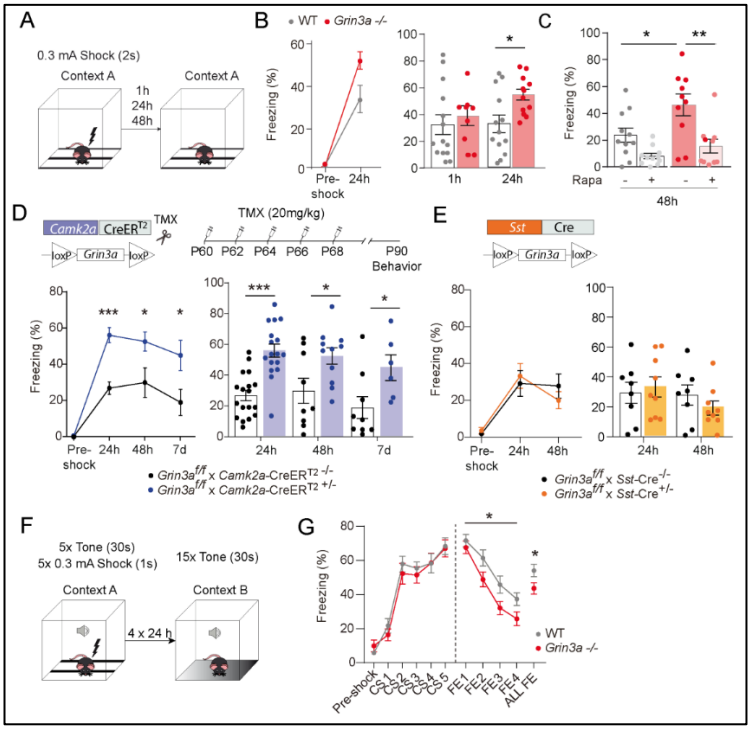

Figure 8. GluN3A deletion from excitatory neurons in adult mice is sufficient for memory enhancement. **(A)** Contextual fear conditioning test. **(B)** Enhanced contextual fear conditioning in *Grin3a*−/− mice 24 hr but not 1 hr after training (n = 9–13 mice per group; left: repeated measures two-way analysis of variance [ANOVA] with Bonferroni post hoc test, p = 0.004; right: two-tailed unpaired t-test, *p < 0.05). **(C)** Enhanced contextual fear conditioning in *Grin3a*−/− mice at 48 hr is reversed by rapamycin (2 × 20 mg/kg i.p., 24 hr apart, prior to training) (n = 10–11 mice per group; *p < 0.05; **p < 0.01, two-way ANOVA with Bonferroni post hoc test). **(D, E)** Conditional deletion of GluN3A from adult excitatory neurons, but not somatostatin (Sst) interneurons, enhances long-term contextual fear memory. The regime for tamoxifen (TMX) injection is indicated (*p < 0.05: ***p < 0.001 two-tailed unpaired t-test). **(F, G)** Cued-fear extinction in *Grin3a*−/− and wild-type littermates over a four-day fear extinction paradigm (n = 14–13 mice per group; *p = 0.0461 between-subjects effect, repeated measures ANOVA). Freezing levels were not different between phenotypes in FE1 ($t(25) = 0.760$, $p = 0.455$).

The online version of this article includes the following figure supplement(s) for figure 8:

Figure supplement 1. Expression of GluN3A and other synaptic proteins in conditional *Grin3a* knockout mice.

Figure supplement 1—source data 1. Annotated western blots and original scans.

Figure supplement 1—source data 2. Annotated western blots and original scans.

DISCUSSION

In this study we report a regulatory mechanism that affords spatiotemporal control of mTORC1-dependent translation in response to synaptic stimulation. Specifically we identify GIT1/mTORC1 complexes as key mediators of synaptic mTORC1 responses, and demonstrate that GluN3A-NMDARs, through direct association with GIT1, impede GIT1/mTORC1 assembly and negatively regulate synaptic mTORC1 activation and

mTORC1-dependent translation. Using in vitro and in vivo genetic approaches, we further show that negative regulation by GluN3A determines the emergence of mature mTORC1-dependent protein synthesis in developing brains, and continues to play a role in adult life by placing boundaries on long-term memory storage. More broadly, our findings suggest that neuronal GIT1/mTORC1 complexes might provide a central site for regulation and dysregulation of synaptic translation in other physiological and disease contexts.

Modulation by GluN3A of GIT1/mTORC1 complex assembly

mTORC1 is a ubiquitous protein kinase complex that promotes protein synthesis and cell growth in response to a variety of signals including nutrient availability, energy levels, insulin, growth factors and synaptic inputs. Coupling such diverse signals to mTORC1 activation requires the regulated targeting of mTOR to specific subcellular compartments. For instance, mTORC1 responses to amino acids require its recruitment by the Ragulator-Rag complex to lysosomal membranes, where interactions between positive (Rheb) and negative (Tsc1/2 complex) mTOR regulators take place (Benjamin and Hall, 2014; Sancak et al., 2010). Our observations suggest that GIT1 could play an analogous scaffolding role to position mTORC1 such that it senses synaptic signals, with negative regulation by GluN3A limiting mTORC1-dependent translation at specific developmental times and/or in specific subsets of synapses in adult brains.

First, GIT1/mTORC1 complexes are located at dendritic/synaptic sites and respond to synaptic stimuli, as shown by phosphorylation of GIT1-bound mTOR on Ser2448, an event that is stimulated by NMDARs (Figure 2- figure supplement 1) and is amplified by feedback from the downstream of the mTORC1 substrate S6K (Chiang and Abraham, 2005). Second, knocking-down GIT1 blunts synaptic mTORC1 signaling and mTORC1-dependent translation of specific activity-regulated genes. Third, GIT1/mTORC1 abundance increases during postnatal development and is bi-directionally modulated by GluN3A expression. Fourth, association of GIT1 with GluN3A is required for mTORC1 modulation, as demonstrated by the fact that expression in the *Grin3a* knockout of a GluN3A mutant lacking the GIT1-binding site does not rescue the increased assembly of GIT1 with mTOR (Figure 6) or the increased activation of synaptic mTORC1 (Figure 4). Given that GluN3A and mTOR bind overlapping regions in GIT1 (Fiuza et al., 2013; Smithson and Gutmann, 2016), the most parsimonious explanation is that GluN3A competes with mTOR for binding to GIT1.

We previously reported that GluN3A modulates the formation of GIT1 complexes with βPIX (Fiuza et al., 2013), and might coordinately inhibit two central mechanism in spines that are necessary for memory consolidation —actin cytoskeletal rearrangements

and protein synthesis. This action would be analogous to the translational repression by FMRP/CYFIP1 complexes (De Rubeis et al., 2013). Our results here (see Figure 6B) indicate that GluN3A exerts a more potent regulation over GIT1/mTORC1 than GIT1/βPIX complexes and suggest that mTOR modulation might be the primary event. Of note, rare coding variants in GIT1 have been identified in schizophrenic patients (Kim et al., 2017) and GIT1 knockout mice display deficits that resemble those seen in mice with elevated GluN3A expression, including reduced spine size and poor learning and memory (Martyn et al., 2018). Additional phenotypes reported in mice and flies upon GIT1 deletion, such as microcephaly, reduced neuronal size or hyperactivity, might also be related to mTOR modulation (Hong and Mah, 2015; Won et al., 2011).

Our RNAseq analyses indicate that GluN3A acts at the level of translation and would thus preserve the supply of activity-induced plasticity mRNAs but restrict their active translation to specific synapses, in contrast to classical NMDARs that work at both transcriptional and translational levels. Nevertheless, GluN3A knockdown in cultured neurons has recently been shown to enhance the transcription of a subset of mRNAs (Chen et al., 2020) upon prolonged periods of synaptic activation (6-8 hours vs 1 hour in the present study), and we cannot rule out later regulation by GluN3A of compensatory or homeostatic responses. Of note, tonic repression of mTOR-dependent protein synthesis by GluN2B-containing NMDARs has also been reported (Wang et al., 2011). However, the molecular determinants of stimulation or repression of protein synthesis were not addressed. It remains to be established whether GluN3A and GluN2B share common mechanisms.

A role for GluN3A in restricting translation for precise circuit refinements and long-term memory storage

GluN3A-NMDARs are highly expressed during critical periods of experience-dependent neural circuit refinements, when they have been proposed to determine which synapses will be maintained or eliminated, and at lower levels in specific regions of the adult brain (Murillo et al., 2021). We propose a model whereby the lack or presence of GluN3A at postsynaptic sites contributes to spine-specific translation by setting an enhanced or repressed biochemical environment for mTORC1 signaling that will depend on the stage of brain development (Figure 6D). Synaptic GluN3A levels are down-regulated by sensory experience and can be controlled at the level of individual synapses by activity-dependent endocytosis (Perez-Otano et al., 2006). Thus, regulation of mTORC1 by GluN3A may also depend on the activity history of individual synapses, which is a key aspect in theories of cellular consolidation (Redondo and Morris, 2011). Removal of GluN3A-NMDARs from active synapses would drive formation of nearby GIT1/mTORC1 complexes. This would

locally increase the potential for dendritic translation of activity-regulated mRNAs, and might give active inputs an advantage for consolidation vs less-active neighbors. Hence, competition for active mTORC1 would provide a means for selective synapse stabilization and memory storage. Defects in mTORC1 regulation might permit the consolidation of otherwise lost synaptic changes.

Such a competition-based model is supported by the localization of GluN3A to subsets of adult synapses (Roberts et al., 2009). It is also supported by the observations that in *Grin3a*-/- mice, the levels of GIT1/mTORC1 are increased and these mice exhibit enhanced capacity for memory storage, as shown by their performance in weak training protocols that are normally insufficient for stable memory formation in wild-type mice. Importantly, the restriction of dendritic translation to sites near active synapses is thought to underlie phenomena such as the competition between spines for lasting LTP expression (Fonseca et al., 2004) or the potentiation of synapses in clusters along the dendrite (Fonseca et al., 2004; Govindarajan et al., 2011). Incorporation into these models of the molecular components unveiled here might open avenues for testing how the above phenomena determine memory capacity and efficiency and for correcting cognitive dysfunction.

Our experiments using cell-type specific and inducible *Grin3a* knockout mice demonstrate a role of GluN3A in gating cognitive processing in the adult brain beyond its better recognized functions in postnatal neural circuit refinements, and identify excitatory neurons as the locus of GluN3A actions. In relation to memory, negative regulators are thought to provide an advantage by ensuring that only salient features are learnt and irrelevant events or associations are filtered out (Abel et al., 1998; Cho et al., 2015). For instance, temporal contiguity of events is required for many forms of associative learning; within the scale of seconds or minutes for classical conditioning paradigms, longer in other types of memory. In CTA the CS and US can be hours apart, with temporal boundaries set by the strength of the US (Adaikkan and Rosenblum, 2015). Our results show that the absence of GluN3A broadens this temporal limit and facilitates learning of demanding tasks, i.e. where training is spaced apart or the presented stimuli are weaker. The reversal by rapamycin is consistent with the notion that the enhanced readiness of the mTORC1 translational machinery in GluN3A-deficient mice expands the range for consolidation of memory traces. While we used a subtreshold dose of rapamycin that does not alter memory or mTOR signaling in wild-type mice (Stoica et al., 2011), we cannot rule out potential non-synaptic effects. Definitive proof will require the development of tools that directly disrupt GluN3A/GIT1 or GIT1/mTOR association or synaptic localization.

As far as tested here, GluN3A deletion does not impair other aspects of cognition such as memory flexibility or extinction. Yet significant GluN3A levels are retained in defined

areas of the mouse and human adult brain that have in common strong plasticity or functional integration needs (Fulcher et al., 2019; Murillo et al., 2021), and a recent study linked adult GluN3A expression to the control of emotional states (Otsu et al., 2019). In addition, genetic variations in *GRIN3A* have been shown to modulate prefrontal cortex activity (Gallinat et al., 2007) and episodic memory (Papenberg et al., 2014). Future investigations should determine whether domains of cognition other than the ones we tested are compromised by GluN3A deletion.

GluN3A and synaptic protein synthesis as selective therapeutic targets

The stabilization of memories requires de novo protein expression. Nevertheless, the effects on cognition of enhancing mTOR signaling or protein synthesis are perplexing. Loss of constraints on protein synthesis due to mutations in negative regulators of translation (*FMR1, MECP2*, or mTORC1 suppressors including *NF1, TSC1/2* or the phosphatase *PTEN*) are associated with cognitive impairment and high incidence of autism spectrum disorders and intellectual disability (Kelleher and Bear, 2008), although a fraction of autistic individuals exhibit enhanced cognitive skills within specific domains (Heaton and Wallace, 2004). On the other hand, inhibiting the phosphorylation of eIF2α, which generally increases translation (Costa-Mattioli et al., 2007; Stern et al., 2013), or enhancing mTORC1 activity by removal of FKBP12 (Hoeffer et al., 2008) have been reported to lower memory thresholds. However, the cognitive enhancement came at the cost of reduced memory fidelity and cognitive flexibility even when cell-type specific modulation was attempted (Santini et al., 2013; Shrestha et al., 2020a; Trinh et al., 2012), which we did not observe here. Key differences could be that other negative regulators of mTOR such as FMRP, PTEN or Tsc1/2 are expressed in multiple cell types and neuronal locations, as demonstrated by their linkage to altered cell growth and appearance of tumors (Lipton and Sahin, 2014). Also, in some of the above situations, translation is constitutively activated and responses to incoming signals might be obliterated. By contrast, lack of GluN3A does not occlude mTORC1 activation but rather seems to prime mTOR activation by synaptic stimuli. At present, the enhancement of learning and memory produced by loss of GluN3A suggests that targeting GluN3A expression or signaling functions might be of therapeutic benefit. For instance, small molecules that perturb the GluN3A/GIT1 association might work in subtler ways than general translation regulators by specifically modulating synaptic mTORC1 signaling.

MATERIAL AND METHODS

Key resources table

Reagent type (species) or resource	Designation	Source of reference	Identifiers	Additional information
Antibody	GIT-1 (mouse monoclonal, clone A-1)	Santa Cruz Biotechnology	Cat# sc-365084; RRID: AB_10850059	PLA 1:150
Antibody	Arc (mouse monoclonal, clone C-7)	Santa Cruz Biotechnology	Cat# sc-17839; RRID: AB_626696	WB 1:100
Antibody	beta-Tubulin III (mouse monoclonal)	Sigma-Aldrich	Cat# T8660; RRID: AB_477590	WB 1:20000
Antibody	NMDAR1, all splice variants (mouse monoclonal, clone R1JHL)	Millipore	Cat# MAB1586; RRID: AB_11213180	WB 1:1000
Antibody	NR2B (mouse monoclonal, clone BWJHL)	Millipore	Cat# 05-920; RRID: AB_417391	WB 1:1000
Antibody	NR3A (mouse monoclonal)	Kindly provided by Jim Trimmer	N/A	WB 1:100
Antibody	PSD-95 (mouse monoclonal, clone K28/43)	Antibodies Incorporated	Cat# 75-028 RRID: AB_10698024	WB 1:1000
Antibody	Puromycin (mouse monoclonal, clone 12D10)	Millipore	Cat# MABE343; RRID: AB_2566826	WB 1:2000
Antibody	Synapsin I (mouse monoclonal, clone 46.1)	Synaptic Systems	Cat# 106 011 RRID: AB_2619772	WB 1:5000
Antibody	Synaptophysin (mouse monoclonal, clone SY38)	Millipore	Cat# MAB5258-20UG; RRID: AB_11214133	WB 1:2000
Antibody	CREB (rabbit monoclonal, clone 48H2)	Cell Signaling Technology	Cat# 9197; RRID: AB_331277	WB 1:1000
Antibody	NR2A (rabbit monoclonal, clone A12W)	Millipore	Cat# 05-901R; RRID: AB_10805961	WB 1:1000
Antibody	Phospho-Cam Kinase II alpha (CaMKIIα) Thr286 (rabbit monoclonal, clone D21E4)	Cell Signaling Technology	Cat# 12716; RRID: AB_2713889	WB 1:1000

Antibody	Phospho-p70 S6 kinase Thr389 (rabbit monoclonal, clone 108D2)	Cell Signaling Technology	Cat# 9234; RRID: AB_2269803	WB 1:1000
Antibody	Raptor (rabbit monoclonal, clone 24C12)	Cell Signaling Technology	Cat# 2280; RRID: AB_561245	WB 1:1000
Antibody	Rheb (rabbit monoclonal, clone E1G1R)	Cell Signaling Technology	Cat# 13879; RRID: AB_2721022	WB 1:1000
Antibody	Rictor (rabbit monoclonal, clone 53A2)	Cell Signaling Technology	Cat# 2114; RRID: AB_2179963	WB 1:500
Antibody	S6 ribosomal protein (rabbit monoclonal, clone 5G10)	Cell Signaling Technology	Cat# 2217; RRID: AB_331355	WB 1:1000
Antibody	GIT1 (rabbit polyclonal)	Cell Signaling Technology	Cat# 2919; RRID: AB_2109982	IP 1:200, WB 1:1000
Antibody	Egr-1/ Zif268 (rabbit polyclonal)	Santa Cruz Biotechnology	Cat# sc-110; RRID: AB_2097174	WB 1:500
Antibody	beta-Pix, SH3 domain (rabbit polyclonal)	Millipore	Cat# 07-1450; RRID: AB_1586904	WB 1:1000
Antibody	c-Fos (rabbit polyclonal)	Santa Cruz Biotechnology	Cat# sc-52; RRID: AB_2106783	WB 1:500
Antibody	CaMKIIα (rabbit polyclonal)	Sigma-Aldrich	Cat# C6974; RRID: AB_258984	WB 1:1000
Antibody	mTOR (rabbit polyclonal)	Cell Signaling Technology	Cat# 2972; RRID: AB_330978	IP 1:100, PLA 1:150, WB 1:1000
Antibody	NMDAR2A&B, pan antibody (rabbit polyclonal)	Millipore	Cat# AB1548; RRID: AB_11212156	WB 1:1000
Antibody	NR3A (rabbit polyclonal)	Millipore	Cat# 07-356; RRID: AB_2112620	WB 1:1000
Antibody	p30alpha (rabbit polyclonal)	Santa Cruz Biotechnology	Cat# sc-535; RRID: AB_632138	WB 1:1000
Antibody	p44/42 MAPK (Erk1/2) (rabbit polyclonal)	Cell Signaling Technology	Cat# 9102; RRID: AB_330744	WB 1:1000
Antibody	p70 S6 kinase (rabbit polyclonal)	Cell Signaling Technology	Cat# 9202; RRID: AB_331676	WB 1:1000
Antibody	Phospho-CREB Ser133 (rabbit polyclonal)	Millipore	Cat# 06-519; RRID: AB_310153	WB 1:1000
Antibody	Phospho-mTOR Ser2448 (rabbit polyclonal)	Cell Signaling Technology	Cat# 2971; RRID: AB_330970	WB 1:1000
Antibody	Phospho-p38 MAPK Thr180/Tyr182 (rabbit polyclonal)	Cell Signaling Technology	Cat# 9911; RRID: AB_10695905	WB 1:1000

Antibody	Phospho-p44/42 MAPK (Erk1/2) Thr202/Tyr204 (rabbit polyclonal)	Cell Signaling Technology	Cat# 9101; RRID: AB_331646	WB 1:1000
Antibody	Phospho-S6 ribosomal protein Ser240/244 (rabbit polyclonal)	Cell Signaling Technology	Cat# 2215; RRID: AB_331682	WB 1:1000
Cell line (*Homo sapiens*)	HEK293	ATCC	Cat# CRL-1573; RRID: CVCL_0045	
Chemical compound, drug	(-)-Bicuculline methiodide	Abcam	Cat# Ab120108; CAS: 55950-07-7	
Chemical compound, drug	(D,L)-APV sodium salt	Tocris	Cat# 3693; CAS: 1303993-72-7	
Chemical compound, drug	Anisomycin	Sigma-Aldrich	Cat# A5892; CAS: 22862-76-6	
Chemical compound, drug	B27 supplement	ThermoFisher Scientific	Cat# 17504044	
Chemical compound, drug	BDNF	PeproTech	Cat# 450-02; AN: P23560	
Chemical compound, drug	CGP-78608	Tocris	Cat# 1493; CAS: 1135278-54-4	
Chemical compound, drug	cOmplete Protease Inhibitor Cocktail	Sigma-Aldrich	Cat# 04693116001	
Chemical compound, drug	Cycloheximide	Sigma-Aldrich	Cat# C7698; CAS: 66-81-9	
Chemical compound, drug	MK-801	Tocris	Cat# 0924; CAS: 77086-22-7	
Chemical compound, drug	Puromycin dihydrochloride	Sigma-Aldrich	Cat# P8833; CAS: 58-58-2	
Chemical compound, drug	Rapamycin	Alfa Aesar	Cat# J62473; CAS: 53123-88-9	
Chemical compound, drug	Tamoxifen	Sigma-Aldrich	Cat# T5648	
Chemical compound, drug	Tetrodotoxin citrate	Alomone Labs	Cat# T-550; CAS: 18660-81-6	
Commercial assay, kit	Duolink In Situ Red Starter Kit Mouse/Rabbit	Sigma-Aldrich	Cat# DUO92101	
Commercial assay, kit	MasterMix qPCR ROx PyroTaq EvaGreen	cmb	Cat# 87H24	
Commercial assay, kit	Nucleospin RNA	Macherey-Nagel	Cat# 740955.50	
Commercial assay, kit	Pierce BCA Protein Assay kit	ThermoFisher Scientific	Cat# 23227	
Commercial assay, kit	SuperScript IV First-Strand cDNA Synthesis System	Invitrogen	Cat# 18-091-050	

Genetic reagent (*Mus musculus*)	Mouse: B6;129X1-*Grin3a*$^{tm1Nnk/J}$	The Jackson Laboratory	Cat# JAX:029974; RRID: IMSR_JAX:029974	
Genetic reagent (*Mus musculus*)	Mouse: CaMKIIα-CreERT2$^{+/-}$	(Erdmann et al, 2007)		
Genetic reagent (*Mus musculus*)	Mouse: *Grin3a*$^{tm1a(EUCOMM)Hmgu/H}$	EUCOMM		
Genetic reagent (*Mus musculus*)	Mouse: Sst-IRES-Cre	The Jackson Laboratory	Stock: 018973	
Genetic reagent (virus)	LV-hSYN-WPRE-hSYN-GFP-WPRE	(Gascón *et al.*, 2008)		
Genetic reagent (virus)	LV-hSYN-GluN3A-WPRE-hSYN-GFP-WPRE	This paper		See Materials and methods; generated and stored in Perez-Otano's lab.
Genetic reagent (virus)	LV-hSYN-GluN3A1082Δ-WPRE-hSYN-GFP-WPRE	This paper		See Materials and methods; generated and stored in Perez-Otano's lab.
Genetic reagent (virus)	pLentiLox3.7-GFP (pLL3.7-GFP)	Kindly provided by Dr. Michael Ehlers	Addgene plasmid #11795; RRID: Addgene_11795	
Genetic reagent (virus)	pLL3.7-shGluN3A1185-GFP (Target sequence: CTACAGCTGAGTTTAGAAA)	(Yuan *et al.*, 2013)		
Genetic reagent (virus)	pLL3.7-shGlT1-GFP (Target sequence: TGATCACAAGAATGGGCATTA)	This paper		See Materials and methods; generated and stored in Perez-Otano's lab.
Recombinant DNA reagent (plasmid)	pcDNA1-Amp-GluN1-1A	(Perez-Otano *et al.*, 2001)		
Recombinant DNA reagent (plasmid)	pcDNA1-Amp-GluN2A	(Perez-Otano *et al.*, 2001)		
Recombinant DNA reagent (plasmid)	pCIneo-GFPGluN3A	(Perez-Otano *et al.*, 2001)		

Recombinant DNA reagent (plasmid)	pCIneo-GFPGluN3A1082Δ	This paper	See Materials and methods; generated and stored in Perez-Otano's lab.
Recombinant DNA reagent (plasmid)	pRK5-GFP	Kindly provided by Dr. Michael Ehlers	
Sequence-based reagent (oligonucleotide)	*Arc*_fwd (mouse)	This paper	GAGCCTACAGAGCCAGGAGA
Sequence-based reagent (oligonucleotide)	*Arc*_rv (mouse)	This paper	TGCCTTGAAAGTGTCTTGGA
Sequence-based reagent (oligonucleotide)	*c-Fos*_fwd (mouse/rat)	(Lyons *et al.*, 2016)	CTGCTCTACTTTGCCCCTTCT
Sequence-based reagent (oligonucleotide)	*c-Fos*_rv (mouse/rat)	(Lyons *et al.*, 2016)	TTTATCCCCACGGTGACAGC
Sequence-based reagent (oligonucleotide)	*GAPDH*_fwd (mouse/rat)	This paper	CATGGCCTTCCGTGTTCCT
Sequence-based reagent (oligonucleotide)	*GAPDH*_rv (mouse/ rat)	This paper	TGATGTCATCATACTTGGCAG GTT
Software, algorithm	ImageJ	(Schneider, Rasband and Eliceiri, 2012)	https://imagej.nih.gov/ij/
Software, algorithm	ImageQuant software version 5.2	GE Healthcare	
Software, algorithm	Prism software version 7.00	Graphpad	
Software, algorithm	QuantStudio 3 Design and Analysis software v1.5.1	ThermoFisher Scientific	
Software, algorithm	SMART software for video-tracking	PanLab S.L.	

Animals

Adult (3-6 months old) *Grin3a*-/-, *Grin3a*$^{tm1a(EUCOMM)Hmgu}$/H (*Grin3a*$^{f/f}$) and double-transgenic GFP-GluN3A (dtGluN3A) mice backcrossed for 10-12 generations into a C57Bl6/J background were used. Single transgenic mice were used as controls for dtGluN3A mice, and wild-type littermates from heterozygote crosses were controls for *Grin3a*-/- mice. Commercial C57BL6/J mice were purchased from Charles River Laboratories. For time-specific knockout of *Grin3a* in excitatory neurons, tamoxifen-inducible CaMKIIα-Cre$^{ERT2+/-}$ mice (Erdmann et al., 2007) were crossed with *Grin3a*$^{f/f}$ mice. Tamoxifen (Sigma-Aldrich T5648, 20 mg/ml dissolved in corn oil) was administered via oral gavage (5 alternate days). For inhibitory neuron-specific knockout of Grin3a, Sst-IRES-Cre$^{+/-}$ mice (JAX Stock No. 018973) were backcrossed with C57BL/6J mice for 12 generations and then bred with *Grin3a*$^{f/f}$ mice. Male mice were used for behavioral experiments unless indicated. Animals were housed four to six per cage with ad libitum access to food and water and maintained in a temperature-controlled environment on a 12 h dark/light cycle. All procedures were conducted in accordance with the European and Spanish regulations (2010/63/UE; RD 53/2013) and were approved by the Ethical Committee of the Generalitat Valenciana (2017/VSC/PEA/00196). For the cued-fear conditioning experiments, ethic protocols were approved by the Committee of Ethics of the Universitat Autònoma de Barcelona and the Generalitat de Catalunya.

Primary neuronal cultures

Cortical and hippocampal neurons in primary culture were prepared as described (Perez-Otano et al., 2006). Briefly, cortices were dissected from E19 rat pups or E17.5 mice pups and dissociated with papain (Worthington Biochemical). Mouse primary neurons were used for rescue experiments in the *Grin3a*-null background shown in Figures 4 and 6, and for shGIT1 experiments in Figure 5. Neurons were plated at 75,000 cells per well on 12-wells plates, 500,000 cells per well on 6-wells plates and 1,000,000 cells/ dish on 60mm dishes coated with laminin and poly-D-lysine and grown in Neurobasal Medium supplemented with B27 (ThermoFisher).

Neurons were infected with lentiviruses 5 days prior to collection (timing of infection is indicated in figure legends). Neurotrophic factors and other drugs were used at the following concentrations: anisomycin (0.8 μM, Sigma-Aldrich A5892), recombinant human BDNF (100 ng/ml, PeproTech 450-02), bicuculline (50 μM, Abcam Ab120108), cycloheximide (25 μM, Sigma Aldrich C7698), (D,L)-APV (50 μM, Tocris 3693), MK801 (10 μM, Tocris 0924), rapamycin (100 nM, Alfa Aesar J62473) and puromycin (10 ng/ml, Sigma Aldrich P8833).

Lentiviral vectors

For the generation of lentiviral constructs, full-length GluN3A and GluN3A1082Δ cDNAs were subcloned into a dual lentiviral vector Syn-WPRE-Syn-GFP kindly provided by Dr. Francisco G Scholl, University of Sevilla, Spain. For knockdown experiments, 19-20 base pairs (bp)-long small hairpin RNAs (shRNA) directed to GluN3A (shGluN3A1185, target sequence: CTACAGCTGAGTTTAGAAA) or GIT1 (shGIT1, target sequence: TGATCACAAGAATGGGCATTA) were cloned into the pLentilox 3.7-GFP vector downstream the U6 promoter. The AAV encoding constitutively active human Rheb (AAV-caRheb, S16H) was kindly provided by Dr. Beverly Davidson, Children´s Hospital of Philadelphia, University of Pennsylvania.

RNA isolation, qRT-PCR and RNAseq analyses

Total RNA from cultured cortical neurons was isolated using the Nucleospin RNA (Macherey-Nagel). RNA concentration and purity were assessed with NanoDrop™. RNA quality was determined by the RNA Integrity Number (RIN) algorithm using the Agilent® 2100 Bionalyzer Instrument; only samples with RIN>9 matched our standard.

For qRT-PCR experiments, first-strand cDNA was synthesized from 1 µg of total RNA using the Invitrogen SuperScript IV First-Strand cDNA Synthesis System (ThermoFisher). Quantitative real-time PCR (qPCR) was performed using the Applied Biosystems QuantStudio 3 Real-Time PCR system and analyzed with the QuantStudio 3 Design and Analysis software (v1.5.1,ThermoFisher). Briefly, real-time qPCR was assayed in a total volume of 20 µl reaction mixture containing the ready-to-use PyroTaq EvaGreen qPCR Mix Plus ROX (Cmb), 5pmol of forward and reverse (rv) primers (detailed in Table S1) and cDNA. PCR thermal conditions included an initial hold stage with 5 min at 50ºC and 15 min at 95 °C followed by 40 cycles of denaturation for 30 s at 95 °C, annealing for 32 s at 60 ºC and primer elongation for 32 s at 72 °C. All qPCR reactions were run in triplicates. Mean cycle threshold (Ct) values for each reaction were recorded and the relative RNA expression levels were calculated referring to Gapdh, encoding glyceraldehyde 3-phsophate dehydrogenase: ΔCt= 〖Ct〗_GAPDH- 〖Ct〗_(target gene). The gene expression fold change normalized to GAPDH and relative to control sample was calculated as 2^ΔCt.

For RNAseq experiments, we performed bulk mRNA sequencing single-end with a length of 50bp using the RNAseq Illumina Hiseq2500. The preparation of the polyA sequencing library, library's quality control and quantification, sequencing run and base calling data were carried out by the Genomics Core Facility of the Centre for Genomic Regulation (CRG, Barcelona). For the analysis, adapters were trimmed using trim_galore

v0.6.4_dev and reads with longer length than 40 bp were selected. Trimmed reads were aligned using star c2.6.1b to the mouse genome (mm10). Reads with mapq >30 were selected using Samtools v1.9. Mapped reads were quantified using R scripts (R version 4.0.3, 2020), Rsubread v2.4.3 and the Mus_musculus.GRCm38.99.gtf annotation data. Differential expression analysis was performed using DESeq2 1.31.1 and limma 3.46.0; genes were annotated using biomaRt v2.46.3 and Volcano plots were performed with EnhancedVolcano 1.6.0. The tracks from the samples were performed with DeepTools v3.5.0, normalized with RPKM and visualization was done in IGV v2.6.3.

Protein extraction and western blotting

Cultured neurons were collected in lysis buffer containing 50 mM Tris-HCl pH 6.8, 10% glycerol, 2% SDS, 0.1 M (D,L)-Dithiothreitol, 0.04% bromophenol blue and supplemented with protease (cOmplete Protease Inhibitor Cocktail) and phosphatase (PhosSTOP) inhibitors. Lysates were incubated for 10 min at 65 ºC, briefly centrifuged at maximum speed and proteins separated by SDS-PAGE. Proteins were transferred onto PVDF membranes (GE Healthcare). After incubation with primary antibodies, membranes were incubated with secondary HRP-conjugated secondary antibodies (1:10,000, GE Healthcare). Signals were visualized with film autoradiograpy or the Amerham 680 Blot Imager, and non-saturated immunoreactive bands were quantified using the ImageQuant 5.2 software.

For *in vivo* studies on mouse tissue, hippocampi and somatosensory cortex were dissected on ice, snapped frozen in liquid nitrogen and stored at -80ºC until processing. Tissues were homogenized in 15 (w/v) volumes of modified ice-cold RIPA buffer (50 mM Tris-HCl pH 7.5, 150 mM NaCl, 1% NP-40, 0.05% deoxycholate, 0.01% SDS) supplemented with protease and phosphatase inhibitors, sonicated and centrifuged for 20 min at 16,200 x g at 4ºC. Protein content was estimated using a Pierce BCA Assay kit (ThermoFisher) before immunoblotting.

Immunoprecipitation

Cultured cortical neurons or mouse hippocampus or somatosensory cortex were solubilized for 30 min in cold lysis buffer containing 0.1% Triton X-100, 0.1% SDS, 150 mM NaCl, 10 mM EDTA and 50 mM HEPES or 0.3% CHAPS, 150 mM NaCl, 1 mM EDTA and 40 mM HEPES, supplemented with protease and phosphatase inhibitors. Insoluble material was removed by centrifugation at 16,200 x g for 15 min and 100-150 μg of the resulting supernatants were incubated overnight at 4 °C with or without (IgG-) the immunoprecipitating antibody. Lysates were then incubated with protein A/ G magnetic beads (BioRad) for 2 h at 4 ºC. Beads were precipitated using a magnetic rack, washed

thrice in lysis buffer and immunoprecipitated proteins were eluted with SDS sample buffer and analyzed by western blotting.

Proximity Ligation Assay

Cultured neurons transfected with pRK5-GFP were fixed at DIV17 with 4% PFA, 4% sucrose in PBS (RT, 10 min), incubated with blocking solution and permeabilized. Cells were then incubated with rabbit polyclonal anti-mTOR antibody and mouse monoclonal anti-GIT1 antibody overnight at 4°C, washed with PBS, and incubated for 1 h with PLA secondary probes (anti-mouse Plus and anti-rabbit Minus, Olink Bioscience) at 37 °C. Cells were washed twice with Duolink II Wash Buffer A (Olink Bioscience) and incubated with the ligase (1:40; Olink Bioscience) in ligase buffer for 30 min at 37 °C. After additional washes with Buffer A, cells were incubated with DNA polymerase (1:80; Olink Bioscience) in amplification buffer for 100 min at 37 °C in the dark. Cells were then washed with Duolink II Wash Buffer B (Olink Bioscience) and incubated with chicken polyclonal anti-GFP for 1 h at room temperature. After washing with PBS, cells were incubated with secondary goat anti-chicken-Alexa Fluor 488 for 1 h at room temperature. Finally, cells were washed in PBS and mounted on slides with Fluoroshield mounting medium (Sigma-Aldrich). Fluorescence images were acquired by using Nikon A1 Ti2 system with a sequential acquisition setting at 1024 x 1024 pixels resolution; cells were randomly selected from different coverslips.

Protein synthesis assays

Basal protein synthesis was measured using a SUnSET (surface sensing of translation) assay. Briefly, primary cortical cultures were treated with 10 ng/ ml of puromycin for 30 min and lysed as described above. Untreated neurons and neurons preincubated with the protein synthesis inhibitor cycloheximide (15 min before puromycin) were used as controls. Proteins were resolved by SDS-PAGE and analyzed by western blotting using an anti-puromycin antibody. Ponceau S staining was used as protein loading control.

Behavioral analysis

Morris Water Maze

Mice were trained to find a submerged platform in a circular tank (190 cm diameter) filled with opaque white water in two or four trials per day with 45 min inter-trial intervals. If mice did not find the platform in 120 seconds, they were kindly guided to it. The hidden platform was relocated to the opposite quadrant after 7 days of training for the reversal training phase. 60-second-long probe tests in which platform was removed were performed at the

end of each phase (PT1, after initial hidden platform learning; PT2, after reversal learning), and time spent in the target quadrant was compared to the average time spent in all other quadrants. Mice were tracked throughout the whole protocol using the video-tracking software SMART (Panlab S. L.).

Y-maze spontaneous alternation

Mice were introduced in a three-armed Y-shaped maze and recorded for 5 minutes. Correct triad scores were noted when all three arms were sequentially entered. Alternation indices were calculated as correct triads / possible triads. Maze was cleaned between animals with a water-based soap solution.

Conditioned taste aversion

Test was adapted from (Adaikkan and Rosenblum, 2015). In brief: mice were trained to drink from two bottles of water for 6 days. On conditioning day, water was changed for 0.2% (regular CTA) or 0.1% (weak CTA) saccharin for 40 minutes (regular) or 5 hours (weak) after the exposure, mice were injected LiCl intraperitoneally at 0.15 M (regular) or 0.025 M (weak). Saccharin preference was evaluated 24 hours after injection. For unconditioned taste preference, mice were presented two drinking bottles for 48 hours: one contained water and the other one of the following solutions: Sucrose 5% (sweet), NaCl 75 mM (salty), Quinine 300 μM (bitter) and HCl 0.03 M (sour). Bottle sides were switched after 24 hours to avoid potential side bias. Solution preference was evaluated at 48 hours. For assessing sensitivity to LiCl toxicity, “lying on belly” behavior was registered after injection of LiCl (0.15 M) or saline. This behavior consists in a totally general suppression of activity, and location of the mouse in the corner of a cage. The activity was measured for 20 minutes.

Fear conditioning and extinction

Fear conditioning (FC) and extinction (FE) procedures were carried out with a computerized Fear and Startle system (Panlab-Harvard, Barcelona, Spain). Tones and shocks were delivered and controlled using Freezing v1.3.04 software (Panlab-Harvard, Barcelona, Spain). The fear chambers consisted of a black methacrylate box with a transparent front door (25x25x25cm) inside a sound-attenuating cubicle (67x53x55cm). Animals were habituated to the chambers for 5 min/day during two consecutive days prior to FC. The chambers were carefully cleaned before and after each mouse.

For contextual FC, mice were placed in the fear chambers and allowed to explore a context (CS) (metal grid floor, no light source) for 2 minutes. Mice were then presented with a tone (30s, 2.8 kHz, 85 dB tone) that co-terminated with a foot shock (US)(0.3 mA, 2s). Sixty seconds later, they were returned to their home cage. Conditioning was assessed

at 1 (short-term memory), 24 and 48 hours or 7 days (long-term memory) by re-introducing mice in the conditioning context for 5 minutes. Freezing behavior, a rodent´s natural response to fear defined as the absence of movement except respiration, was scored by a high sensitivity weight transducer system located at the bottom of the experimental chambers which records and analyses the signal generated by the movement of the animal.

For cued FC, mice were placed in the fear chambers for 5 minutes and then received 5 trials of a tone (CS) (30 s, 6 kHz, 75 dB) that co-terminated with a foot-shock (US) (0.3 mA, 1s). The intertrial interval (ITI) was of 3 minutes, and 3 additional minutes followed the last trial. The FE sessions were performed 4 times in consecutive days (FE1, FE2, FE3, FE4) starting 24h after FC. For FE, mice were placed in the fear chambers for 5 minutes and then exposed to 15 trials of the 30 s CS tone alone (cued-fear) with a 30 s of ITI interval. An additional 30 s interval followed the last trial of FE. Different contexts were used for FC and FE tests. FC context consisted of a yellow light source (~10 lux), a grid floor of 25 bars (3 mm Ø and 10 mm between bars), a background noise of 60 dB produced by a ventilation fan and soapy water in a solution of ethanol 70% was used for cleaning between sessions. FE context consisted of a red-light source (~10 lux), a grey plexiglass floor covering the bars, no background noise and soapy water in a solution of isopropyl alcohol 40% was used as cleaning agent between sessions. Different routes were used to transport animals from their home cages to testing room in FC and FE days. Freezing levels were scored and averaged in 30 second slots.

Electrophysiology

HEK293 cells were cultured, transfected, and recorded as previously described using GluN1A and GluN2A in pcDNA1/Amp and GFP-tagged GluN3A or GluN3A1082Δ subcloned in pCI-neo (Chowdhury et al., 2013). Briefly, cells were transfected with GluN1-1A, GluN2A, and either GFP-GluN3A or GFP-GluN3A1082Δ in a 1:1:3 ratio and maintained in medium with APV (250 μM). GFP was used as a transfection marker in cells where GluN3A constructs were omitted. Whole-cell recordings were made with on GFP-positive cells using a Multiclamp 700A amplifier (Molecular Devices) 24 h following transfection. Patch pipettes (2 to 4 MΩ) contained (in mM): 140 Cs methanesulfonate, 10 HEPES, 5 adenosine triphosphate (Na salt), 5 MgCl2, 0.2 $CaCl_2$, and 10 BAPTA (pH 7.4). The extracellular solution contained (in mM) 150 NaCl, 5 KCl, 2 or 10 $CaCl_2$, 10 HEPES, 10 glucose (pH 7.4) and was adjusted to 330 mOsm with sucrose. Currents were digitized at 2 kHz and filtered at 1 kHz. Series resistance (90 to 95%) and whole-cell capacitance compensation were employed. Experiments were performed at a holding potential of -80 mV with ramps (300 ms to +50 mV) elicited following a 3 s application of glutamate (1 mM) and glycine (100 μM) at 20°C. The ΔErev, was calculated by subtracting the Erev obtained in 2 mM Ca2+ from

the Erev measured in 10 mM Ca2+ and corrected for the junction potential between solutions. Initial peak currents were obtained from 1 sec agonist applications in 2 mM Ca^{2+} and used to calculate the current density. Experiments on glycine-gated diheteromeric GluN1/GluN3A receptors expressed in HEK293 cells were performed as previously described (Grand et al., 2018) using GluN1-1a and GFP-GluN3A or GFP-GluN3A1082Δ subcloned in pCI-neo (see above). HEK293 cells were obtained from ATCC. No mycoplasm contamination was detected by regular testing.

Statistical Analysis

Statistical analyses were conducted with GraphPad Prism software. Comparison of quantitative variables between two groups was performed using Student's t-test. One-way or two-way analysis of variance (ANOVA) followed by a post-hoc comparison test were used when more than two groups were compared, as indicated in the corresponding figure legend. Results are presented as mean ± standard error of the mean (SEM). Statistical methods used for behavioral studies are indicated in the corresponding figure legends.

ACKNOWLEDGEMENTS

We thank Stuart Lipton and Nobuki Nakanishi for providing the *Grin3a* knockout mice, Beverly Davidson for the AAV-caRheb, Jose Esteban for help with behavioral and biochemical experiments, and Noelia Campillo, Rebeca Martínez-Turrillas, and Ana Navarro for expert technical help. Work was funded by the UTE project CIMA; fellowships from the Fundación Tatiana Pérez de Guzmán el Bueno, FEBS, and IBRO (to M.J.C.D.), Generalitat Valenciana (to O.E.-Z.), Juan de la Cierva (to L.G.R.), FPI-MINECO (to E.R.V., to S.N.) and Intertalentum postdoctoral program (to V.B.); ANR (GluBrain3A) and ERC Advanced Grants (#693021) (to P.P.); Ramón y Cajal program RYC2014-15784, RETOS-MINECO SAF2016-76565-R, ERANET-Neuron JTC 2019 ISCIII AC19/00077 FEDER funds (to R.A.); RETOS-MINECO SAF2017-87928-R (to A.B.); an NIH grant (NS76637) and UTHSC College of Medicine funds (to S.J.T.); and NARSAD Independent Investigator Award and grants from the MINECO (CSD2008-00005, SAF2013-48983R, SAF2016-80895-R), Generalitat Valenciana (PROMETEO 2019/020)(to I.P.O.) and Severo-Ochoa Excellence Awards (SEV-2013-0317, SEV-2017-0723).

ADDITIONAL INFORMATION

Funding

Funder	Grant reference number	Author
H2020 European Research	Advanced ERC 693021	Pierre Paoletti

Council		
Ministerio de Economía, Industria y Competitividad, Gobierno de España	SAF2016-76565-R	Raül Andero Galí
Ministerio de Economía, Industria y Competitividad, Gobierno de España	SAF2017-87928-R	Angel Barco
Generalitat Valenciana	PROMETEO 2019/020	Isabel Perez-Otaño
Ministerio de Economía, Industria y Competitividad, Gobierno de España	CSD2008-00005	Isabel Perez-Otaño
Ministerio de Economía, Industria y Competitividad, Gobierno de España	SAF2013-48983R	Isabel Perez-Otaño
Ministerio de Economía, Industria y Competitividad, Gobierno de España	SAF2016-80895R	Isabel Perez-Otaño
National Institutes of Health	NS76637	Steven J Tavalin
University of Tennessee	UTHSC College of Medicine Funds	Steven J Tavalin
Agence Nationale de la Recherche	GluBrain3A	Pierre Paoletti
Instituto de Salud Carlos III	AC19/00077	Raül Andero Galí
Ministerio de Economía, Industria y Competitividad, Gobierno de España	RYC2014-15784	Raül Andero Galí
Ministerio de Economía, Industria y Competitividad, Gobierno de España	SEV-2013-0317	Isabel Perez-Otaño
Ministerio de Economía, Industria y Competitividad, Gobierno de España	SEV-2017-0723	Isabel Perez-Otaño
Brain and Behavior Research Foundation	NARSAD Independent Investigator Award	Isabel Perez-Otaño
Ministerio de Economía, Industria y Competitividad, Gobierno de España	BFU-2016-80918-R	John F Wesseling
The funders had no role in study design, data collection, and interpretation, or the decision to submit the work for publication.		

Author contributions

María Jose Conde-Dusman, Partha N Dey, Conceptualization, Investigation, Methodology, Writing – original draft, Writing – review and editing; Óscar Elía-Zudaire, Investigation, Methodology, Writing – review and editing; Luis G Rabaneda, Conceptualization, Investigation, Methodology; Carmen García-Lira, Teddy Grand, Victor Briz, Eric R Velasco, Raül Andero Galí, Sergio Niñerola, Angel Barco, Pierre Paoletti, Fabrizio Gardoni, Steven J Tavalin, Investigation; John F Wesseling, Conceptualization, Investigation, Writing – original draft, Writing – review and editing; Isabel Perez-Otaño, Conceptualization, Funding acquisition, Investigation, Methodology, Project administration, Writing – original draft, Writing – review and editing

Author ORCIDs

María J Conde-Dusman http://orcid.org/0000-0001-6841-2181

Óscar Elía-Zudaire http://orcid.org/0000-0002-1396-834X

Victor Briz http://orcid.org/0000-0001-6936-0918

Angel Barco http://orcid.org/0000-0002-0653-3751

Pierre Paoletti http://orcid.org/0000-0002-3681-4845

Fabrizio Gardoni http://orcid.org/0000-0003-4598-5563

Steven J Tavalin http://orcid.org/0000-0001-7169-0932

Isabel Perez-Otaño http://orcid.org/0000-0002-7222-8202

Ethics

All procedures were conducted in accordance with the European and Spanish regulations (2010/63/UE; RD 53/2013) and were approved by the Ethical Committee of the Generalitat Valenciana (2017/VSC/PEA/00196). For the cued-fear conditioning experiments, ethic protocols were approved by the Committee of Ethics of the Universitat ò;noma de Barcelona and the Generalitat de Catalunya.

Decission letter and Author response

Decision letter https://doi.org/10.7554/eLife.71575.sa1

Author response https://doi.org/10.7554/eLife.71575.sa2

ADDITIONAL FILES

Supplementary files

- Transparent reporting form.

Data Availability

RNAseq data have been deposited at GEO-NCBI under the access code GSE175920. The following dataset was generated:

Author(s)	Year	Dataset title	Dataset URL	Database and Identifier
Conde-Dusman MJ, Perez-Otaño I	2021	RNAseq data in cultured nerons	GEO	GSE175920

REFERENCES

Abel, T., Martin, K.C., Bartsch, D., and Kandel, E.R. (1998). Memory suppressor genes: inhibitory constraints on the storage of long-term memory. Science 279, 338-341.

Adaikkan, C., and Rosenblum, K. (2015). A molecular mechanism underlying gustatory memory trace for an association in the insular cortex. Elife 4, e07582.

Andero, R., and Ressler, K.J. (2012). Fear extinction and BDNF: translating animal models of PTSD to the clinic. Genes Brain Behav 11, 503-512.

Banko, J.L., Merhav, M., Stern, E., Sonenberg, N., Rosenblum, K., and Klann, E. (2007). Behavioral alterations in mice lacking the translation repressor 4E-BP2. Neurobiol Learn Mem 87, 248-256.

Benjamin, D., and Hall, M.N. (2014). mTORC1: turning off is just as important as turning on. Cell 156, 627-628.

Cammalleri, M., Lutjens, R., Berton, F., King, A.R., Simpson, C., Francesconi, W., and Sanna, P.P. (2003). Time-restricted role for dendritic activation of the mTOR-p70S6K pathway in the induction of late-phase long-term potentiation in the CA1. Proc Natl Acad Sci U S A 100, 14368-14373.

Costa-Mattioli, M., Gobert, D., Stern, E., Gamache, K., Colina, R., Cuello, C., Sossin, W., Kaufman, R., Pelletier, J., Rosenblum, K., et al. (2007). eIF2alpha phosphorylation bidirectionally regulates the switch from short- to long-term synaptic plasticity and memory. Cell 129, 195-206.

Costa-Mattioli, M., and Monteggia, L.M. (2013). mTOR complexes in neurodevelopmental and neuropsychiatric disorders. Nat Neurosci 16, 1537-1543.

Chen, L.F., Lyons, M.R., Liu, F., Green, M.V., Hedrick, N.G., Williams, A.B., Narayanan, A., Yasuda, R., and West, A.E. (2020). The NMDA receptor subunit GluN3A regulates synaptic activity-induced and myocyte enhancer factor 2C (MEF2C)-dependent transcription. J Biol Chem 295, 8613-8627.

Chiang, G.G., and Abraham, R.T. (2005). Phosphorylation of mammalian target of rapamycin (mTOR) at Ser-2448 is mediated by p70S6 kinase. J Biol Chem 280, 25485-25490.

Cho, J., Yu, N.K., Choi, J.H., Sim, S.E., Kang, S.J., Kwak, C., Lee, S.W., Kim, J.I., Choi, D.I., Kim, V.N., et al. (2015). Multiple repressive mechanisms in the hippocampus during memory formation. Science 350, 82-87.

Chowdhury, D., Marco, S., Brooks, I.M., Zandueta, A., Rao, Y., Haucke, V., Wesseling, J.F., Tavalin, S.J., and Perez-Otano, I. (2013). Tyrosine phosphorylation regulates the endocytosis and surface expression of GluN3A-containing NMDA receptors. J Neurosci 33, 4151-4164.

De Rubeis, S., Pasciuto, E., Li, K.W., Fernandez, E., Di Marino, D., Buzzi, A., Ostroff, L.E., Klann, E., Zwartkruis, F.J., Komiyama, N.H., et al. (2013). CYFIP1 coordinates mRNA translation and cytoskeleton remodeling to ensure proper dendritic spine formation. Neuron 79, 1169-1182.

Erdmann, G., Schutz, G., and Berger, S. (2007). Inducible gene inactivation in neurons of the adult mouse forebrain. BMC Neurosci 8, 63.

Fiuza, M., Gonzalez-Gonzalez, I., and Perez-Otano, I. (2013). GluN3A expression restricts spine maturation via inhibition of GIT1/Rac1 signaling. Proc Natl Acad Sci U S A 110, 20807-20812.

Flavell, S.W., and Greenberg, M.E. (2008). Signaling mechanisms linking neuronal activity to gene expression and plasticity of the nervous system. Annual review of neuroscience 31, 563-590.

Fonseca, R., Nagerl, U.V., Morris, R.G., and Bonhoeffer, T. (2004). Competing for memory: hippocampal LTP under regimes of reduced protein synthesis. Neuron 44, 1011-1020.

Fulcher, B.D., Murray, J.D., Zerbi, V., and Wang, X.J. (2019). Multimodal gradients across mouse cortex. Proc Natl Acad Sci U S A 116, 4689-4695.

Gallinat, J., Gotz, T., Kalus, P., Bajbouj, M., Sander, T., and Winterer, G. (2007). Genetic variations of the NR3A subunit of the NMDA receptor modulate prefrontal cerebral activity in humans. Journal of cognitive neuroscience 19, 59-68.

Govindarajan, A., Israely, I., Huang, S.Y., and Tonegawa, S. (2011). The dendritic branch is the preferred integrative unit for protein synthesis-dependent LTP. Neuron 69, 132-146.

Grand, T., Abi Gerges, S., David, M., Diana, M.A., and Paoletti, P. (2018). Unmasking GluN1/GluN3A excitatory glycine NMDA receptors. Nat Commun 9, 4769.

Greenwood, T., LC, L., AX, M., NR, S., ME, C., R, F., MF, G., GA, L., CM, N., KH, N., et al. (2019). Genome-wide Association of Endophenotypes for Schizophrenia From the Consortium on the Genetics of Schizophrenia (COGS) Study. JAMA Psychiatry 76, 1274-1284.

Hardingham, G.E., Fukunaga, Y., and Bading, H. (2002). Extrasynaptic NMDARs oppose synaptic NMDARs by triggering CREB shut-off and cell death pathways. Nat Neurosci 5, 405-414.

Heaton, P., and Wallace, G.L. (2004). Annotation: the savant syndrome. Journal of child psychology and psychiatry, and allied disciplines 45, 899-911.

Henson, M.A., Larsen, R.S., Lawson, S.N., Perez-Otano, I., Nakanishi, N., Lipton, S.A., and Philpot, B.D. (2012). Genetic deletion of NR3A accelerates glutamatergic synapse maturation. PLoS One 7, e42327.

Hoeffer, C.A., Tang, W., Wong, H., Santillan, A., Patterson, R.J., Martinez, L.A., Tejada-Simon, M.V., Paylor, R., Hamilton, S.L., and Klann, E. (2008). Removal of FKBP12 enhances mTOR-Raptor interactions, LTP, memory, and perseverative/repetitive behavior. Neuron 60, 832-845.

Holt, C.E., Martin, K.C., and Schuman, E.M. (2019). Local translation in neurons: visualization and function. Nat Struct Mol Biol 26, 557-566.

Holtmaat, A., and Caroni, P. (2016). Functional and structural underpinnings of neuronal assembly formation in learning. Nat Neurosci 19, 1553-1562.

Hong, S.T., and Mah, W. (2015). A Critical Role of GIT1 in Vertebrate and Invertebrate Brain Development. Exp Neurobiol 24, 8-16.

Hou, L., and Klann, E. (2004). Activation of the phosphoinositide 3-kinase-Akt-mammalian target of rapamycin signaling pathway is required for metabotropic glutamate receptor-dependent long-term depression. J Neurosci 24, 6352-6361.

Huang, X., Chen, Y.Y., Shen, Y., Cao, X., Li, A., Liu, Q., Li, Z., Zhang, L.B., Dai, W., Tan, T., et al. (2017). Methamphetamine abuse impairs motor cortical plasticity and function. Mol Psychiatry 22, 1274-1281.

Josselyn, S.A., and Tonegawa, S. (2020). Memory engrams: Recalling the past and imagining the future. Science 367.

Kehoe, L.A., Bellone, C., De Roo, M., Zandueta, A., Dey, P.N., Perez-Otano, I., and Muller, D. (2014). GluN3A promotes dendritic spine pruning and destabilization during postnatal development. J Neurosci 34, 9213-9221.

Kelleher, R.J., 3rd, and Bear, M.F. (2008). The autistic neuron: troubled translation? Cell 135, 401-406.

Kim, M.J., Biag, J., Fass, D.M., Lewis, M.C., Zhang, Q., Fleishman, M., Gangwar, S.P., Machius, M., Fromer, M., Purcell, S.M., et al. (2017). Functional analysis of rare variants found in schizophrenia implicates a critical role for GIT1-PAK3 signaling in neuroplasticity. Mol Psychiatry 22, 417-429.

Klann, E., and Dever, T.E. (2004). Biochemical mechanisms for translational regulation in synaptic plasticity. Nat Rev Neurosci 5, 931-942.

Lipton, J.O., and Sahin, M. (2014). The neurology of mTOR. Neuron 84, 275-291.

Liu, G.Y., and Sabatini, D.M. (2020). mTOR at the nexus of nutrition, growth, ageing and disease. Nat Rev Mol Cell Biol 21, 183-203.

Lyons, M.R., and West, A.E. (2011). Mechanisms of specificity in neuronal activity-regulated gene transcription. Prog Neurobiol 94, 259-295.

Marco, S., Giralt, A., Petrovic, M.M., Pouladi, M.A., Martinez-Turrillas, R., Martinez-Hernandez, J., Kaltenbach, L.S., Torres-Peraza, J., Graham, R.K., Watanabe, M., et al. (2013). Suppressing aberrant GluN3A expression rescues synaptic and behavioral impairments in Huntington's disease models. Nat Med 19, 1030-1038.

Martyn, A.C., Toth, K., Schmalzigaug, R., Hedrick, N.G., Rodriguiz, R.M., Yasuda, R., Wetsel, W.C., and Premont, R.T. (2018). GIT1 regulates synaptic structural plasticity underlying learning. PLoS One 13, e0194350.

Mueller, H.T., and Meador-Woodruff, J.H. (2004). NR3A NMDA receptor subunit mRNA expression in schizophrenia, depression and bipolar disorder. Schizophrenia research 71, 361-370.

Murillo, A., Navarro, A.I., Puelles, E., Zhang, Y., Petros, T.J., and Perez-Otano, I. (2021). Temporal Dynamics and Neuronal Specificity of Grin3a Expression in the Mouse Forebrain. Cerebral Cortex 31, 1914-1926.

Ohi, K., Hashimoto, R., Ikeda, M., Yamamori, H., Yasuda, Y., Fujimoto, M., Umeda-Yano, S., Fukunaga, M., Fujino, H., Watanabe, Y., et al. (2015). Glutamate Networks Implicate Cognitive Impairments in Schizophrenia: Genome-Wide Association Studies of 52 Cognitive Phenotypes. Schizophrenia bulletin 41, 909-918.

Otsu, Y., Darcq, E., Pietrajtis, K., Matyas, F., Schwartz, E., Bessaih, T., Abi Gerges, S., Rousseau, C.V., Grand, T., Dieudonne, S., et al. (2019). Control of aversion by glycine-gated GluN1/GluN3A NMDA receptors in the adult medial habenula. Science 366, 250-254.

Paoletti, P., Bellone, C., and Zhou, Q. (2013). NMDA receptor subunit diversity: impact on receptor properties, synaptic plasticity and disease. Nat Rev Neurosci 14, 383-400.

Papenberg, G., Li, S.C., Nagel, I.E., Nietfeld, W., Schjeide, B.M., Schroder, J., Bertram, L., Heekeren, H.R., Lindenberger, U., and Backman, L. (2014). Dopamine and glutamate receptor genes interactively influence episodic memory in old age. Neurobiology of aging 35, 1213 e1213-1218.

Perez-Otano, I., Larsen, R.S., and Wesseling, J.F. (2016). Emerging roles of GluN3-containing NMDA receptors in the CNS. Nat Rev Neurosci 17, 623-635.

Perez-Otano, I., Lujan, R., Tavalin, S.J., Plomann, M., Modregger, J., Liu, X.B., Jones, E.G., Heinemann, S.F., Lo, D.C., and Ehlers, M.D. (2006). Endocytosis and synaptic removal of NR3A-containing NMDA receptors by PACSIN1/syndapin1. Nat Neurosci 9, 611-621.

Perez-Otano, I., Schulteis, C.T., Contractor, A., Lipton, S.A., Trimmer, J.S., Sucher, N.J., and Heinemann, S.F. (2001). Assembly with the NR1 subunit is required for surface expression of NR3A-containing NMDA receptors. J Neurosci 21, 1228-1237.

Poulopoulos, A., Murphy, A.J., Ozkan, A., Davis, P., Hatch, J., Kirchner, R., and Macklis, J.D. (2019). Subcellular transcriptomes and proteomes of developing axon projections in the cerebral cortex. Nature 565, 356-360.

Rao, V.R., Pintchovski, S.A., Chin, J., Peebles, C.L., Mitra, S., and Finkbeiner, S. (2006). AMPA receptors regulate transcription of the plasticity-related immediate-early gene Arc. Nat Neurosci 9, 887-895.

Redondo, R.L., and Morris, R.G. (2011). Making memories last: the synaptic tagging and capture hypothesis. Nat Rev Neurosci 12, 17-30.

Roberts, A.C., Diez-Garcia, J., Rodriguiz, R.M., Lopez, I.P., Lujan, R., Martinez-Turrillas, R., Pico, E., Henson, M.A., Bernardo, D.R., Jarrett, T.M., et al. (2009). Downregulation of NR3A-containing NMDARs is required for synapse maturation and memory consolidation. Neuron 63, 342-356.

Sadat-Shirazi, M.S., Ashabi, G., Hessari, M.B., Khalifeh, S., Neirizi, N.M., Matloub, M., Safarzadeh, M., Vousooghi, N., and Zarrindast, M.R. (2019). NMDA receptors of blood lymphocytes anticipate cognitive performance variations in healthy volunteers. Physiology & behavior 201, 53-58.

Sancak, Y., Bar-Peled, L., Zoncu, R., Markhard, A.L., Nada, S., and Sabatini, D.M. (2010). Ragulator-Rag complex targets mTORC1 to the lysosomal surface and is necessary for its activation by amino acids. Cell 141, 290-303.

Santini, E., Huynh, T.N., MacAskill, A.F., Carter, A.G., Pierre, P., Ruggero, D., Kaphzan, H., and Klann, E. (2013). Exaggerated translation causes synaptic and behavioural aberrations associated with autism. Nature 493, 411-415.

Sarker, G., Sun, W., Rosenkranz, D., Pelczar, P., Opitz, L., Efthymiou, V., Wolfrum, C., and Peleg-Raibstein, D. (2019). Maternal overnutrition programs hedonic and metabolic phenotypes across generations through sperm tsRNAs. Proc Natl Acad Sci U S A 116, 10547-10556.

Sharma, V., Sood, R., Khlaifia, A., Eslamizade, M.J., Hung, T.Y., Lou, D., Asgarihafshejani, A., Lalzar, M., Kiniry, S.J., Stokes, M.P., et al. (2020). eIF2alpha controls memory consolidation via excitatory and somatostatin neurons. Nature 586, 412-416.

Shrestha, P., Ayata, P., Herrero-Vidal, P., Longo, F., Gastone, A., LeDoux, J.E., Heintz, N., and Klann, E. (2020a). Cell-type-specific drug-inducible protein synthesis inhibition demonstrates that memory consolidation requires rapid neuronal translation. Nat Neurosci 23, 281-292.

Shrestha, P., Shan, Z., Mamcarz, M., Ruiz, K.S.A., Zerihoun, A.T., Juan, C.Y., Herrero-Vidal, P.M., Pelletier, J., Heintz, N., and Klann, E. (2020b). Amygdala inhibitory neurons as loci for translation in emotional memories. Nature 586, 407-411.

Smithson, L.J., and Gutmann, D.H. (2016). Proteomic analysis reveals GIT1 as a novel mTOR complex component critical for mediating astrocyte survival. Genes & development 30, 1383-1388.

Sossin, W.S., and Costa-Mattioli, M. (2019). Translational Control in the Brain in Health and Disease. Cold Spring Harbor perspectives in biology.

Stern, E., Chinnakkaruppan, A., David, O., Sonenberg, N., and Rosenblum, K. (2013). Blocking the eIF2alpha kinase (PKR) enhances positive and negative forms of cortex-dependent taste memory. J Neurosci 33, 2517-2525.

Stoica, L., Zhu, P.J., Huang, W., Zhou, H., Kozma, S.C., and Costa-Mattioli, M. (2011). Selective pharmacogenetic inhibition of mammalian target of Rapamycin complex I (mTORC1) blocks long-term synaptic plasticity and memory storage. Proc Natl Acad Sci U S A 108, 3791-3796.

Takata, A., Iwayama, Y., Fukuo, Y., Ikeda, M., Okochi, T., Maekawa, M., Toyota, T., Yamada, K., Hattori, E., Ohnishi, T., et al. (2013). A population-specific uncommon variant in GRIN3A associated with schizophrenia. Biol Psychiatry 73, 532-539.

Takei, N., Inamura, N., Kawamura, M., Namba, H., Hara, K., Yonezawa, K., and Nawa, H. (2004). Brain-derived neurotrophic factor induces mammalian target of rapamycin-dependent local activation of translation machinery and protein synthesis in neuronal dendrites. J Neurosci 24, 9760-9769.

Tang, S.J., Reis, G., Kang, H., Gingras, A.C., Sonenberg, N., and Schuman, E.M. (2002). A rapamycin-sensitive signaling pathway contributes to long-term synaptic plasticity in the hippocampus. Proc Natl Acad Sci U S A 99, 467-472.

Trinh, M.A., Kaphzan, H., Wek, R.C., Pierre, P., Cavener, D.R., and Klann, E. (2012). Brain-specific disruption of the eIF2alpha kinase PERK decreases ATF4 expression and impairs behavioral flexibility. Cell Rep 1, 676-688.

Wang, C.C., Held, R.G., Chang, S.C., Yang, L., Delpire, E., Ghosh, A., and Hall, B.J. (2011). A critical role for GluN2B-containing NMDA receptors in cortical development and function. Neuron 72, 789-805.

Wang, D.O., Martin, K.C., and Zukin, R.S. (2010). Spatially restricting gene expression by local translation at synapses. Trends in neurosciences 33, 173-182.

Won, H., Mah, W., Kim, E., Kim, J.W., Hahm, E.K., Kim, M.H., Cho, S., Kim, J., Jang, H., Cho, S.C., et al. (2011). GIT1 is associated with ADHD in humans and ADHD-like behaviors in mice. Nat Med 17, 566-572.

Yang, J., Wang, S., Yang, Z., Hodgkinson, C.A., Iarikova, P., Ma, J.Z., Payne, T.J., Goldman, D., and Li, M.D. (2015). The contribution of rare and common variants in 30 genes to risk nicotine dependence. Mol Psychiatry 20, 1467-1478.

Yap, E.L., and Greenberg, M.E. (2018). Activity-Regulated Transcription: Bridging the Gap between Neural Activity and Behavior. Neuron 100, 330-348.

Yuan, T., Mameli, M., O'Connor, E.C., Dey, P.N., Verpelli, C., Sala, C., Perez-Otano, I., Luscher, C., and Bellone, C. (2013). Expression of cocaine-evoked synaptic plasticity by GluN3A-containing NMDA receptors. Neuron 80, 1025-1038.

Zhang, H., Webb, D.J., Asmussen, H., and Horwitz, A.F. (2003). Synapse formation is regulated by the signaling adaptor GIT1. The Journal of cell biology 161, 131-142.

Zhu, P.J., Chen, C.J., Mays, J., Stoica, L., and Costa-Mattioli, M. (2018). mTORC2, but not mTORC1, is required for hippocampal mGluR-LTD and associated behaviors. Nat Neurosci 21, 799-802.

SUPPLEMENTAL INFORMATION

Supplemental information includes ten figure supplements and two Key Resources Tables.

Supplemental Figures

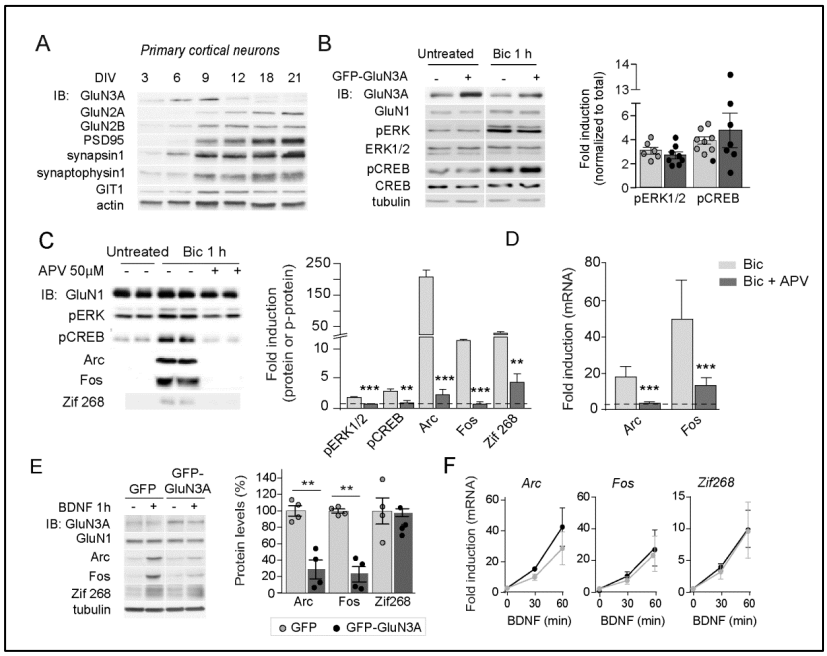

Figure 1 – figure supplement 1. Selective *versus* global effects of GluN3A expression and general NMDAR blockade on activity-dependent signaling **(A)** Immunoblot (IB) analysis of the time-course of expression of NMDAR subunits and a repertoire of synaptic proteins in cultured cortical neurons. **(B)** Immunoblot analysis of ERK1/2 and CREB phosphorylation in whole cell lysates of DIV14 cortical neurons treated with bicuculline for 1 h. Left, representative western blots probed with the indicated antibodies. Right, fold-induction by bicuculline of phosphorylated proteins normalized to their total levels (n=6-8 from 3-4 independent cultures). **(C)** Total lysates from cortical neurons pretreated with APV (50 µM, 30 min) before stimulation with bicuculline (50 µM, 1 h) were immunoblotted with the indicated antibodies. Quantification showed a general blockade of activity dependent by APV (n=4-6 samples from 2-3 independent cultures, **p<0.01, ***p<0.001 ANOVA followed by Tukey´s test). **(D)** APV blocked the increase in *Arc* and *c-Fos* mRNA induced by bicuculline (n=6-10 samples from 3 independent cultures, ***p<0.001 one-way ANOVA followed by Tukey´s test). Data are expressed as fold-induction of non-stimulated neurons. **(E, F)** Analogous experiments to the ones in Figure 1B, C were conducted upon stimulation with BDNF (100 ng/ml, 1 h).

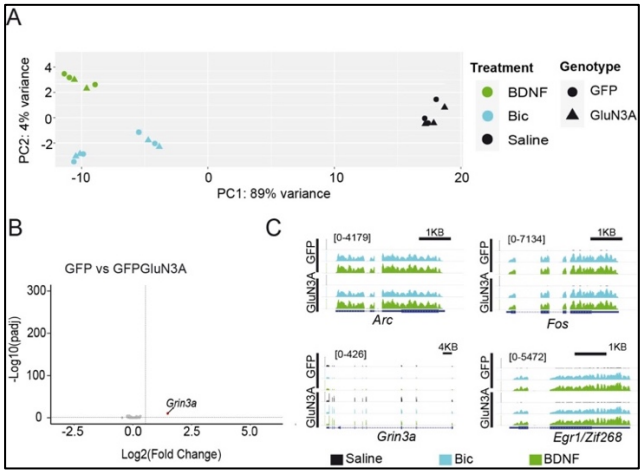

Figure 1 – figure supplement 2. RNAseq analysis of activity-dependent gene expression. **(A)** Principal Component Analysis plot representing all RNAseq samples. **(B)** Volcano plot from RNAseq analysis from gene expression in untreated DIV14 neurons infected with GFP or GFP-GluN3A. **(C)** Integrative Genome Viewer (IGV) tracks for RNAseq signal at representative genes in the different conditions. The IEGs *Arc*, *c-Fos* and *Egr1* are similarly induced by bicuculline (Bic) and BDNF treatments in GFP and GFP-GluN3a-transduced cultures. Note that levels of *Grin3a* are very much increased in GFP-GluN3A-transduced cultures compared to GFP-transduced cultures.

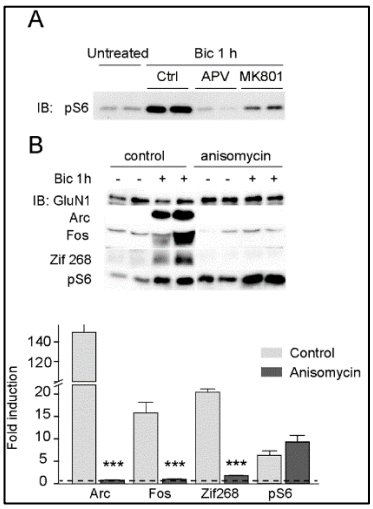

Figure 2 – figure supplement 1. General inhibition of the activity-induction of IEGs by anisomycin. **(A)** Immunoblot analysis of the phosphorylation status of the mTOR downstream effector S6 in lysates from DIV14 cortical neurons stimulated with bicuculline in the absence (Ctrl) or presence of APV (50 µM, 30 min) or MK801 (10 µM, 1 h). **(B)** General inhibition of protein synthesis blocks activity-induction of Arc, c-Fos and Zif268. Whole lysates from DIV14 cortical neurons either untreated or treated with bicuculline (50 µM, 1 h) and anisomycin (0.8 µM, 1 h) were immunoblotted with the indicated antibodies. Top, representative immunoblots and down, quantifications, show a general blockade of IEGs tested by anisomycin. Data are expressed as fold-induction of non-treated neurons (n=3-4 independent cultures, ***p<0.001 ANOVA followed by Tukey´s test).

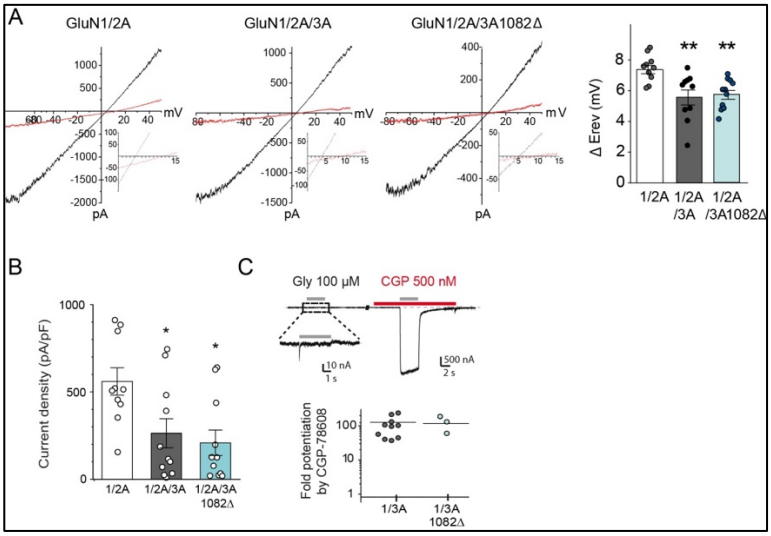

Figure 4 – figure supplement 1. Electrophysiological properties of recombinant NMDA and excitatory glycine receptors containing full-length or truncated GluN3A. **(A)** Left, representative steady-state glutamate-evoked ramp currents obtained with 2 mM (black) and 10 mM (red) extracellular Ca2+ for HEK293 cells expressing GluN1A/GluN2A alone, or with either GFP-GluN3A or GFP-GluN3A1082Δ. Insets show currents on expanded scale to highlight the Erev. Right, summary graph of the ΔErev obtained from multiple experiments is shown on right (n=10–11, **p<0.01, one-way ANOVA followed by Bonferroni post-hoc test). **(B)** Summary graph depicting current density from HEK293 cells expressing GluN1A/GluN2A alone, or with either GFP-GluN3A or GFP-GluN3A1082Δ (*p<0.05 compared to GluN1A/GluN2A, one-way ANOVA followed by Bonferroni post-hoc test). (**C**) Top, responses to glycine of HEK293 cells expressing GluN1/GluN3A receptors in absence or presence of CGP-78608 (500 nM). Bottom, quantification of fold peak current potentiation by CGP-78608 for GluN1/GluN3A and GluN1/GluN3A1082Δ receptors (n=3-11).

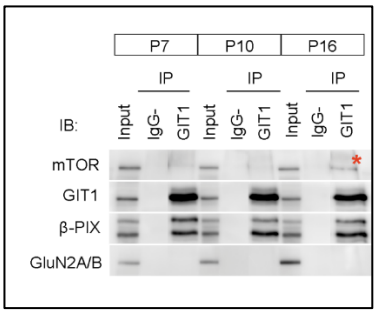

Figure 6 – figure supplement 1. Postnatal regulation of GIT1/mTOR complexes in mouse somatosensory cortex. Somatosensory cortices from P7, P10 and P16 wild-type mice were lysed, immunoprecipitated with GIT1 antibody and probed for the indicated antibodies. Input: 10% of the lysate used for immunoprecipitation. IgG- refers to a negative control without antibody. Red asterisk indicate mTOR-bound GIT1.

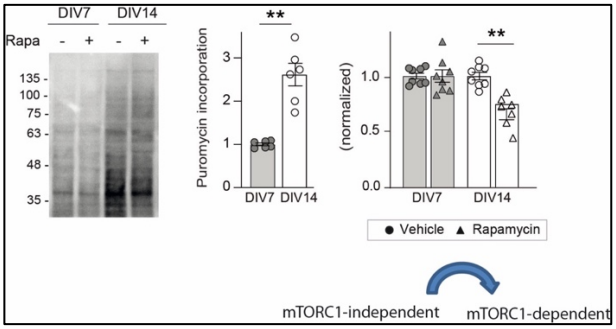

Figure 6 – figure supplement 2. Age-dependent emergence of mTORC1-dependent protein synthesis in cortical neurons. Representative blots and quantification of puromycin incorporation in the presence or absence of 100 nM rapamycin in wild-type DIV7 and DIV14 neurons. Puromycin levels were normalized to Ponceau S staining (n=6-8 samples from 3-4 independent cultures; **p<0.01, followed by Tukey's test).

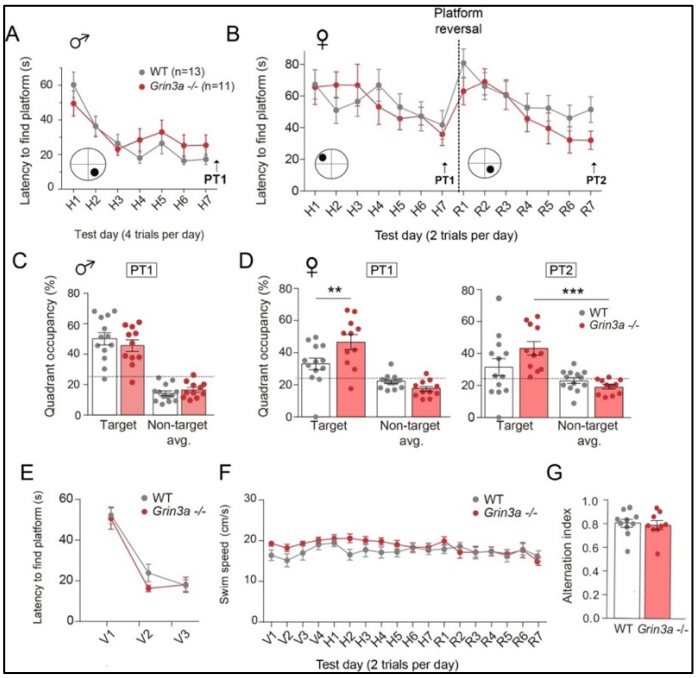

Figure 7 – figure supplement 1. Behavior of male and female Grin3a-/- mice in the Morris Water Maze. **(A)** Escape latencies of male wild-type (WT) and *Grin3a -/-* mice over the time-course of training on a standard hidden-platform version of the Morris water maze (7 days, 4 trials per day). **(B)** Escape latencies of female *Grin3a -/-* and WT mice over the course of training (2 trials per day). **(C)** On probe trials for memory acquisition performed 24 hours after day 7 (PT1), both groups showed similar preference for the target quadrant (n=11-13 mice per group). Dashed lines indicate chance levels (25%). **(D)** Left, On the probe test performed 24 hours after day 7 (PT1), female *Grin3a -/-* mice showed enhanced preference for the target quadrant relative to WT (n=11-13 mice per group; 2-way ANOVA with Bonferroni post-hoc test; p=0.0062). Right, on probe tests 24 hours after completion of reversal training (PT2), female *Grin3a-/-* showed significant preference for the target quadrant (n=11-13 mice per genotype; two-way ANOVA with Bonferroni *post-hoc* test, ***p<0.0001). **(E)** WT and *Grin3a -/-* mice showed no differences in times to reach a visible platform. **(F)** Swimming speed over the training period. Data plotted correspond to the experiment shown in Fig. 7C. **(G)** Alternation index of wild-type (WT) *and Grin3a-/-* mice in the Y-maze (n=9-10 mice per genotype).

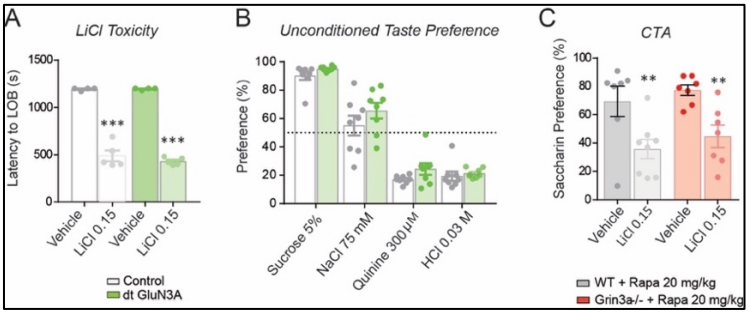

Figure 7 – figure supplement 2. Controls for conditioned taste aversion (CTA) experiments. **(A)** Double transgenic GluN3A (dtGluN3A) and WT mice showed similar "lying on belly" latencies after a 0.15 M LiCl injection (n=4-5 mice per group; unpaired two-tailed t-test, ***p<0.001). **(B)** dt-GluN3A and control mice showed similar taste preferences (n=8 mice per group). **(C)** The rapamycin treatment regime used does not impair the formation of "standard" CTA memory in WT nor *Grin3a-/-* mice (n=6-8 mice per group; 2-way ANOVA with Bonferroni post-hoc test, **p<0.01).

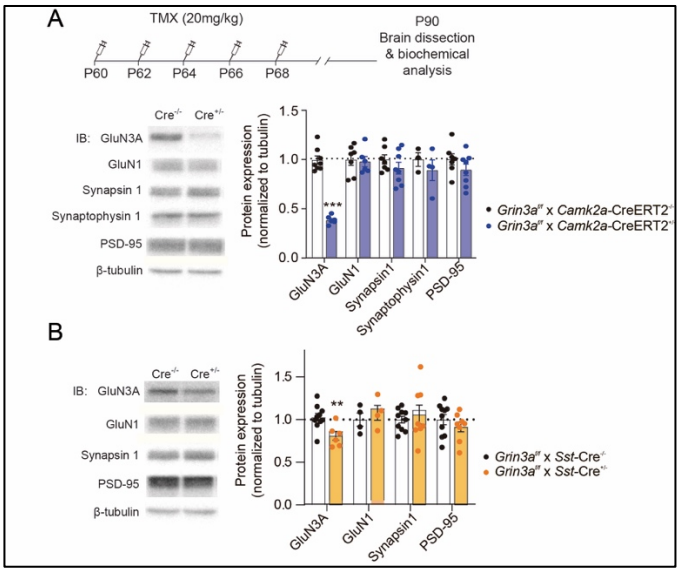

Figure 8 – figure supplement 1. Expression of GluN3A and other synaptic proteins in conditional Grin3a knockout mice. **(A)** Top, tamoxifen (TMX) administration regime to *Grin3a*$^{f/f}$ x *CamK2a*-CreER^{T2} mice. Hippocampal lysates of P90 mice were analyzed by SDS-PAGE and immunoblotted for the indicated proteins (n=4-8 mice per group; unpaired two-tailed t-test, ***p<0.0001). **(B)** Immunoblot analysis of hippocampal lysates of P90 *Grin3a*$^{f/f}$ x *Som*-Cre mice (n=4-10 mice per group; unpaired two-tailed t-test, **p<0.01). Note that conditional deletion of Grin3a decreases GluN3A expression without affecting other synaptic proteins.

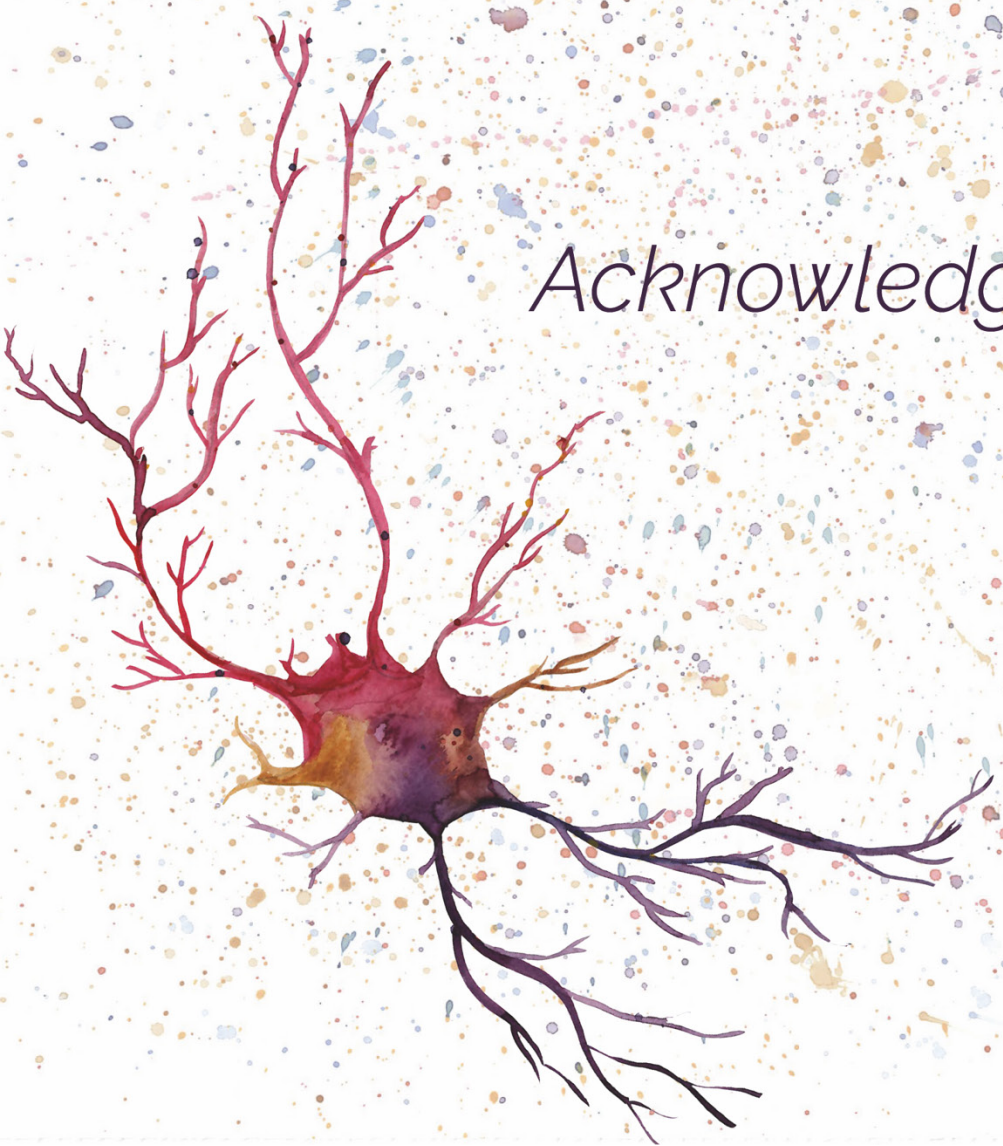

Acknowledgments

"No hay nada más honorable que un corazón agradecido"

(Séneca)

El viaje de la tesis que este libro recoge ha sido ligeramente más largo que unas 200 páginas mal contadas. Empieza allá por 2014, una época pre-pandemia en la que decidí seguir un poquito más alejada de mi tierra con la promesa del volver. De Sevilla a Pamplona. Menudo cambio… cambiar cañas por potes, reuniones por cuadrillas… todo menos el acento, claro.

En primer lugar, quiero dar las gracias a mi directora de tesis, la Prof. Isabel Perez Otaño, por confiar en mí y brindarme la oportunidad de iniciar un doctorado bajo su supervisión en el Centro de Investigación Médica Aplicada de la Universidad de Navarra. En estos 7 años juntas me has enseñado a buscar todas las posibles respuestas a una pregunta y a ser perseverante y seguir adelante aun cuando el camino se torna complicado. Te agradezco no sólo la formación que me has brindado de primera mano, sino también la posibilidad de asistir a conferencias y escuelas de verano o de realizar estancias cortas; todo ello ha enriquecido el proyecto que aquí presento y me ha empujado a seguir en esta loca carrera.

A la Fundación Tatiana Pérez de Guzmán el Bueno. Gracias por concederme una de las tres becas predoctorales en Neurociencias de la edición 2014, el home-run de las becas en palabras de Isabel, para llevar a cabo este estudio. Gracias también por vuestra comprensión y flexibilidad, extendiendo de manera extraordinaria mi financiación durante otros seis meses. Y por último, quisiera agradecerles también la organización de los encuentros anuales de becarios, eventos en los que hemos tenido la oportunidad de compartir y discutir nuestros avances.

A la International Brain Research Organization (IBRO) y la Federation of European Biochemical Societies (FEBS), gracias por premiarme con becas de

estancias cortas de investigación. Su financiación fue crucial para permitir el desarrollo de buena parte de los experimentos descritos en este trabajo.

Al laboratorio 2.04, el pre-mudanza, le agradezco toda el afecto y apoyo que me brindaron acogiéndome como la *lab baby*, apodo que me acompañó hasta dejar Pamplona. Guardo con especial cariño a Rebeca y Sonia, siempre con un buen consejo y encantadas de ayudar en lo que fuese necesario. A Partha, no por ponerme el dichoso apodo, pero sí por tu paciencia al introducirme en el mundo de los cultivos primarios e iniciar con tu tesis este proyecto. A Joao, porque en mi nevera nunca faltaron tuppers durante tu corta estancia. A Daniela, Aitor, Mathan y Kashif por vuestro apoyo técnico, las charlas de café… En definitiva, por ser grandes compañeros de equipo. Quiero aprovechar también para agradecer a la Dra. Montse Arrasate, el Dr. Tomás Aragón y sus equipos por las valiosas aportaciones que brindaron al proyecto en sus inicios.

A mi familia del norte, a mis zumberas espartanas. Quién me iba a decir que entre saunas y clases de zumba iba a conocer a gente tan importante en mi vida. Y es que, aunque muchas de nosotras llevemos ya una buena temporada lejos de Pamplona, es una alegría volver de visita o descolgar el teléfono y que todo siga como siempre. A Aintzane, la *teacher*, qué te voy a decir. En poco tiempo te convertiste en todo un pilar en mi vida, empujándome hacia delante con tus consejos y cariño. Gracias por sacar tiempo de debajo de las piedras para una videollamada o audios kilométricos… ¡Ya falta menos para que repitamos la aventura parisina con Sira! (Pero sin casi perder a nadie en el metro) A Pilar, mi madrina más guapa. A Amalia, por descubrirme la Pamplona más *chic*. A Juani y Charo, las roqueras con más marcha del grupo. A Sara, que para no ser andaluza tiene más arte que la que escribe. Y a Belén y Virginia, nuestras doctoras. Gracias. Entre planes y sorpresas conseguisteis que, aún viviendo en una ciudad de gente supuestamente fría y distante, me sintiese arropada.

Y no, no me he olvidado de ti pequeña Anais. Tú ocupas un sitio muy especial en esta historia. En uno de los momentos más complicados de salud que he tenido Iván y tú, el *pisito flow*, estuvisteis al pie del cañón. Literalmente no tengo palabras para vosotros. Anais, gracias por ser como eres. Sé que a veces incluso me enfadaba porque creía que eras demasiado buena y se aprovechaban de ti… ¡pero es que intentar cambiarte sería un delito! Me abriste las puertas de tu casa

y tu familia de par en par, ya sabes que las mías también lo están para cuando quieras (y podamos) vivir esa Feria de Abril que quedó en el tintero. Iván, otro buenazo de manual. Madre mía, quién me iba a decir que hubiese peor influencia que yo en cuanto a compras y locuras (lo del McDonald en pijama, para tus *mémoires*) Durante el tiempo que vivimos juntos hicisteis que me sintiera en casa aún a 900 kilómetros de mi familia.

Llegó el verano de 2017 y con él la mudanza del laboratorio al Instituto de Neurociencias, a Alicante. Llegaron las despedidas, mucho más amargas de lo que uno se cree pensando que sólo han pasado 3 años, pero también llegaron las nuevas incorporaciones.

Al laboratorio 013, el post-mudanza. Tengo que admitir que recién mudados la transición se me hizo bastante cuesta arriba, e incluso llegué a pensar que claudicaría y no acabaría la tesis. Pero un soplo de aire fresco (o dos) y conseguimos hacer piña de una forma que ni siquiera recordaba de Pamplona. Álvaro y Óscar fueron mis compañeros de mudanza, y ahora que Álvaro y yo ya no estamos, te toca a ti Óscar ser el último abanderado del laboratorio original como pre-doc senior. Ambos habéis sido el alma de la fiesta durante estos años. Alice, mi italiana y su bo. Gracias por haber sido toda una compañera de aventuras y frikadas dentro y fuera de Alicante. Pero aún no te libras de mí porque nos queda, como poco, ir juntas a tu tierra para ver las ATP finals. A las dos Noelias, Noelia García y Noelia Campillo, por vuestro apoyo técnico y las charletas de café en las que la primera me recomendaba vinos de la tierra (y dónde encontrarlos), y la segunda sitios increíbles a lo ancho y largo del globo. A Carmen, mi sevillana de Huelva. Por animarte a seguir con esta historia y trabajar en tu primer año de tesis como si fuera el último. A Oliver, Sara y Gloria. Porque aunque todos estuviésemos inmersos en nuestros proyectos, éramos capaces de desconectar y hacer vida fuera del laboratorio, con un arroz en la playa, un ramen en el centro o yéndonos de casa rural a una semana del estado de alarma.

Al laboratorio 014, nuestros compañeros electrofisiólogos liderados por el Dr. John Wesseling. John, muchas gracias por la ayuda que me has brindado estos años, en forma de sugerencias durante los lab meetings, ayudándome a entender el sentido biológico que aportaban los experimentos de electrofisiología o con el apoyo científico de tu laboratorio para llevar a cabo los experimentos de

late-LTP. Todo ello ha hecho enriquecido enormemente este proyecto, fomentando el dar siempre una vuelta más de pensamiento a cada cuestión y potenciando mis habilidades de presentación. A Sergio, el madrileño que más Ave coge para huir del mar, y Juanjo, mi sevillano de la otra orilla. Ambos siempre partícipes, y en la mayoría de las situaciones instigadores, de los planes del 013. Pero también por la ayuda prestada con experimentos de DHPG-LTD (Sergio) y late-LTP (Sergio y Juanjo) que seguro que pronto ven la luz. Juanjo, a ti tengo que agradecerte doblemente ya que, a falta de una, ¡me has ayudado a mudarme dos veces entre Alicante y Sevilla! A la Dra. Ana Fajardo, la valenciana que se cambió por nosotros mudándose a Pamplona, y al Dr. David Litvin. No coincidisteis en el laboratorio, pero ambos me transmitisteis importantes valores de cara al salto post-doctoral.

A mi Ana. Que no se libra de mí ni con agua caliente (ni yo de ella si nos atenemos a lo estrictamente profesional). Estoy orgullosa de haber conseguido que volvieses al ruedo por visitarme en Milano, y de que le cogieses tanto el gustillo que a comienzos del 2020 volases no una sino dos veces más. Lástima que este virus haya frenado nuestros planes como el de todos, pero para la próxima puedo ofrecerte otra ruta en carretera como la de la Toscana pero conduciendo por la izquierda. ¿Se avecina viaje en el que sujetes el bolso con una mano y te agarres al coche con la otra? Bromas a parte, dentro y fuera del laboratorio te has convertido en indispensable en mi vida y sólo espero que, aunque ya no podamos compartir un café o flashes de ventana a ventana, no perdamos la costumbre de tomarnos al menos un vermú por videollamada.

Del Instituto de Neurociencias quiero hacer especial mención al Prof. Ángel Barco y a Sergio Niñerola, por su colaboración en el análisis transcriptómico presentado en este trabajo. Y a la Dra. Sandra Jurado y la Dra. María Royo, por su ayuda en el diseño y ejecución de experimentos de DHPG-LTD y LTP.

Estoy agradecida de haber tenido la oportunidad de realizar estancias cortas de investigación en tres laboratorios distintos a lo largo de estos años. A la Prof. María de la Luz Montesinos y el Dr. Juan José Casañas, del Departamento de Fisiología Médica y Biofísica de la Universidad de Sevilla, les agradezco acogerme en su grupo y enseñarme las técnicas de marcaje metabólico por radiactividad en sinaptoneurosomas. Al Profesor José A. Esteban y el Dr. Víctor

Briz, del Centro de Biología Molecular Severo Ochoa (CSIC-UAM), por enseñarme técnicas de marcaje no radiactivo de síntesis de proteínas in vitro. Al Profesor Fabrizio Gardoni y la Profesora Monica Di Luca, del Departamento de Ciencias Farmacológicas y Biomoleculares de la Universidad de Milán, por enseñarme diversas técnicas bioquímicas y de imagen para la caracterización de interacciones proteicas, colaboración que aún sigue vigente a día de hoy. Quiero hacer especial mención a los ya doctores Nicolo Carrano y Luca Franchini, por su gran implicación en este proyecto durante mi estancia en Milán.

A mi familia española-italiana, mil gracias por estar siempre ahí para un aperitivo, una escapada o lo que hiciera falta. Vero, los Danis, Tere… pero muy en especial a Aroa; mi compañera de locuras *alla italiana*, que no permitió que se me fuese la sonrisa durante momentos muy complicados. La pandemia nos ha cortado las alas, pero en cuanto se pueda viajar sin restricciones ya sabes que las Conde te acogen con los brazos abiertos.

A la Prof. Beatriz Rico, por abrirme las puertas de su laboratorio y confiar en mí para iniciar un *postdoc sin doc* en un proyecto precioso. Gracias por haberme permitido navegar entre dos aguas durante estos meses, pero sobre todo, gracias por tus consejos. Tu trayectoria es todo un modelo a seguir.

A mis queridos BTGs. Hace ya casi diez años que no compartimos aulas y estamos bastante desperdigados, pero esto nunca ha sido un problema. Ya sea en nuestras quedadas anuales entre el Rocío y Sevilla, en encuentros fortuitos de fin de semana, por videollamadas, audios interminables… todos habéis estado ahí a lo largo de este camino. Gracias. Tengo que hacer especial mención a mis niñas: Cristina, Paula y Sofía. Cris, tan cabezota como yo (o más). Qué bien me venían (y vienen) esas conversaciones de *reseteo* en las que todo lo malo salía por la boca y nos quedábamos como nuevas. Esta tesis sin ti por no tener no tendría ni portada, y es que tu empuje almonteño ha sido indispensable en los momentos que yo flaqueaba. Pau, claramente la más sensata de las cuatro y mi fiel compañera de catas. En estos lares creo que tendremos que cambiar nuestro foco de cata, pero todo va a ir bien. Y Sofi, la serenidad personificada. Creías que exageraba cuando te decía que esta tesis iba detrás de la tuya, pero ya ves… Siempre estáis ahí, para lo bueno y para lo no tan bueno, peleando por mí y defendiéndome incluso cuando ni yo quiero. La próxima podremos celebrar que

ya somos doctoras con una jarra de rebujito y un chupito de seven-up. A Julio, o Jules para los amigos. Parece que no hacemos más que cruzarnos, o tú huyes de mí, todo depende del punto de vista. Tus consejos han sido de gran valor en estos años. A Javi, mi informático oficial, y a Antonio, el próximo Masterchef Italia. No sois BTGs de carrera pero hace ya mucho que os adoptamos en la familia. Gracias por vuestra ayuda, por vuestras visitas allá donde estuviese y sobre todo por los buenos ratos que hemos compartido. A Deivid, Marina, Paco, Dani y Tamara, por vuestro apoyo, sugerencias y, por qué no, por el pueblo duerme. A los BTGs mayores, a los papis Curro y Angie, siempre predispuestos a ayudar y a acogerme. Angie, apenas habíamos cruzado unas cuantas palabras, pero nada más saber que Cris y yo nos mudábamos a Salamanca para estudiar el máster no tardaste en escribir y ofrecer toda tu ayuda. Y ahora Curro, mi estadístico oficial, y tú habéis hecho lo mismo en UK con Luis y conmigo. ¡Gracias!

A Ana Mari, mi conexión Sevilla – el Mundo. Entre tus estudios y mis idas y venidas no podemos encontrarnos tanto como nos gustaría por nuestra tierra, pero ya sabes que “dichosos son los oídos…” cada vez que descuelgas el teléfono para charlar conmigo. Sin ser parte de esta vorágine siempre tienes el don de dar consejos alucinantes. Mil y una gracias.

A mi familia, gracias por su apoyo incondicional ya sea en lo relativo a este doctorado o cualquier aspecto de mi vida. A mi abuela Pepa, por tantas velas que pone por mí, por tener ya mareados a San Tito Antonio y San Abuelo Paco, y por tantas croquetas que me deja preparadas a buen recaudo. A mi abueli Carmen, por seguir al pie del cañón y subirme un poquito la autoestima repitiéndome en cada llamada, como buena abuela, lo mucho que valgo. A Laura, mi madrileña más internacional, porque aunque se nos dé fatal eso de ponernos al día siempre has sido mi mayor defensora. A Irene, la más reciente incorporación a las Conde viajeras, por apuntarse a un bombardeo en cuestión de segundos. Al clan de los madriles: Manolita, José Manuel padre e hijo, Fernando, Fátima, Eduardo y Cristina. Algunos ya no estáis con nosotros, pero desde muy pequeña todos me acogíais anualmente en vuestra casa a la vez que yo os liberaba de Laura durante la semana de Feria. Aún siendo la rama más norteña de la familia, siempre habéis sido los más cercanos.

A mi familia de Jaén, a Ana, Julio, Julito y Sandra. Gracias por acogerme como a una más, por llenar mi maleta de tuppers cuando iba de visita y por venir a visitarme allá donde estuviese.

A Luis, mi compañero de batallas en esta tesis. Puede que sea yo quien la escribe y defiende, pero tú la has sufrido conmigo. Gracias por estar, ya fuese a 0, 600 o 1000 kilómetros de distancia. Gracias por escucharme hasta las mil hablando de experimentos que yo intentaba entender o de técnicas que tú preferías no escuchar. Gracias por apoyarme e infundirme ánimos cuando me metía en esa espiral negativa en la que todo se me hacía cuesta arriba. Gracias por cuidar de mi, aún en la distancia, cruzándote el país ida y vuelta en un fin de semana para llevarme con mi familia cuando no podía viajar sola, o desplazándote a donde fuese necesario para acompañarme en momentos difíciles. Sé que hemos tenido ups and downs, esta tesis también. Pero aquí sigues, demostrándome lo mucho que te importo al aventurarte conmigo en esta nueva etapa. Gracias *feo*.

A mi núcleo. A mi madre María y mi padre Paco. Gracias por poner todos los medios que tuvisteis en vuestras manos para que yo pudiese llegar hasta aquí, y tan lejos como me propusiese. Gracias por la educación que me habéis regalado dentro y fuera de casa. Gracias por transmitirme desde pequeña valores tan importantes en ciencia como la disciplina, el esfuerzo y el tesón. Vuestro apoyo y comprensión hacen que no desista en perseguir este sueño, aunque suponga seguir aún una temporada lejos de vuestros abrazos. A mi hermana Carmen, *sólo* Carmen. Mi ejemplo de que todo esfuerzo da sus frutos. Gracias por haber estado ahí para cualquier cosa que haya necesitado, por escuchar mis monólogos de camino al trabajo y por no dudar un segundo en seguir a la loca de tu hermana a cualquier escapada o plan de última hora. *Mil gracias*.

Gracias a todos por vuestro tiempo e infinita paciencia. Y gracias a *ti*, que decides embarcarte en esta lectura.

María José

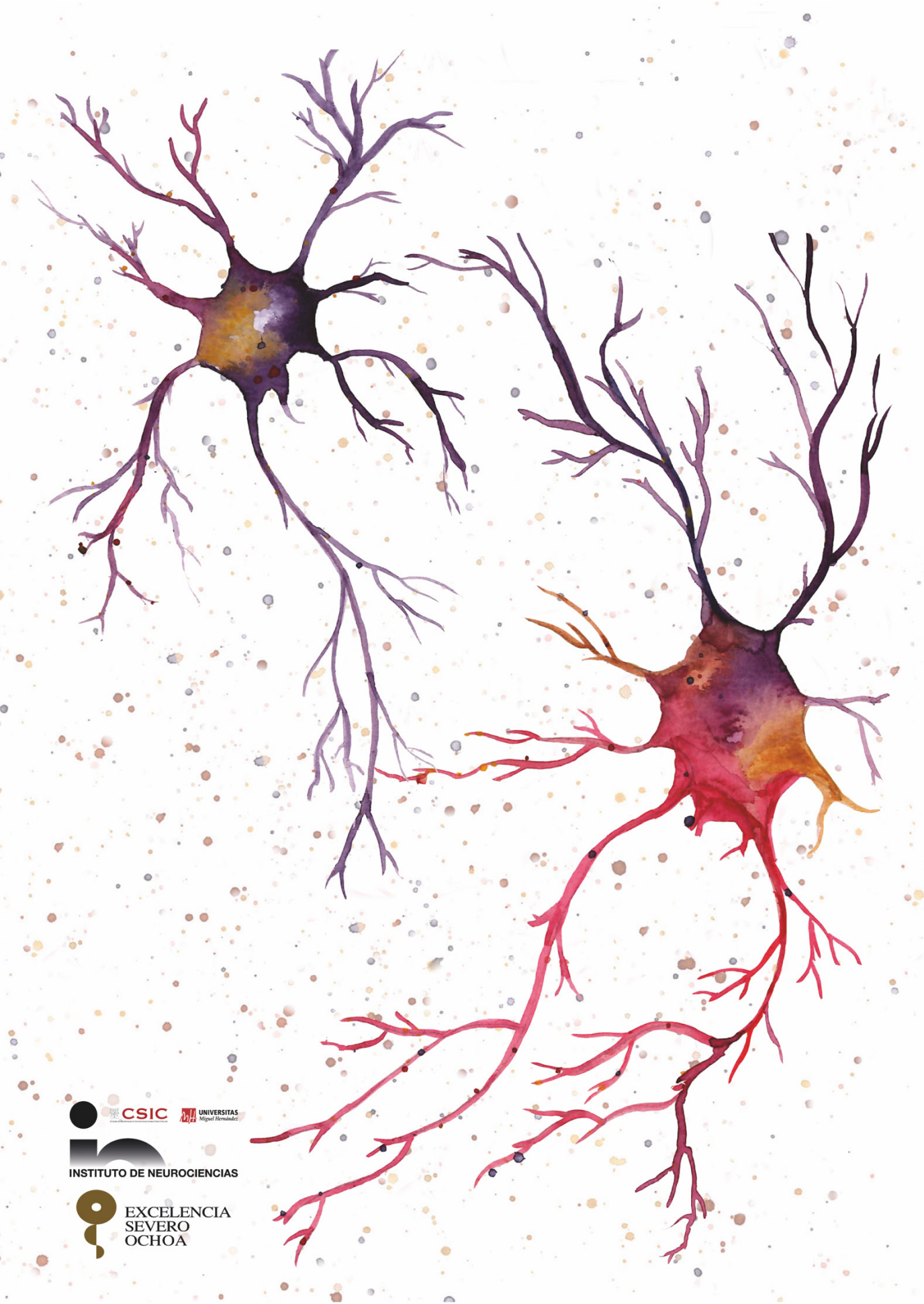

CSIC

UNIVERSITAS Miguel Hernández

INSTITUTO DE NEUROCIENCIAS

EXCELENCIA SEVERO OCHOA